NATIONAL AND KAPODISTRIAN UNIVERSITY OF ATHENS

SCHOOL OF SCIENCES

FACULTY OF GEOLOGY AND GEOENVIRONMENT

PhD THESIS

Study of the geomorphological and environmental evolution of the coastal zone of Central Cyclades

Anna Karkani

ATHENS, 2017

PhD THESIS

Study of the geomorphological and environmental evolution of the coastal zone of Central Cyclades

Anna G. Karkani

Three-Member Advisory Committee

Niki-Nikoletta Evelpidou, Associate Professor, Faculty of Geology and Geoenvironment, National and Kapodistrian University of Athens (Supervisor)

Michael Stamatakis, Professor, Faculty of Geology and Geoenvironment, National and Kapodistrian University of Athens

Hampik Maroukian, Emeritus Professor, Faculty of Geology and Geoenvironment, National and Kapodistrian University of Athens

Seven-Member Examination Committee

Niki-Nikoletta Evelpidou, Associate Professor, Faculty of Geology and Geoenvironment, National and Kapodistrian University of Athens

Michael Stamatakis, Professor, Faculty of Geology and Geoenvironment, National and Kapodistrian University of Athens

Hampik Maroukian, Emeritus Professor, Faculty of Geology and Geoenvironment, National and Kapodistrian University of Athens

Christophe Morhange, Professor, Aix-Marseille University, CEREGE

Theodoros Gournelos, Professor, Faculty of Geology and Geoenvironment, National and Kapodistrian University of Athens

Serafim Poulos, Professor, Faculty of Geology and Geoenvironment, National and Kapodistrian University of Athens

Efthimios Karymbalis, Associate Professor, Department of Geography, Harokopio University

ATHENS, 2017

Στη μητέρα μου

Abstract

The purpose of this thesis was to collect and study geomorphological, sedimentological and archaeological data in order to evaluate the evolution of sea level in Central Cyclades during the Late Holocene and assess the contribution of local tectonics. The ultimate goal was to trace the palaeoshorelines in central Cyclades, the effects of sea level changes in palaeoenvironmental evolution and to propose a reliable palaeogeographical reconstruction during the Late Holocene.

A multiproxy analysis took place through the study of submerged beachrocks, sediment corings in coastal lagoons and archaeological remains in order to accomplish the aforementioned goals. Detailed underwater surveys of Paros and Naxos beachrocks, found down to about -6 m depth, took place along with luminescence dating. The selected beachrock samples were dated by using both OSL dating of quartz and infrared stimulated luminescence (IRSL) of feldspars. Petrographic and microstratigraphic analysis of beachrock cements was accomplished in order to identify the type of cement and determine the spatial relationship between the past shoreline and beachrock formation zone. Each beachrock dated sample, showing clear intertidal formation was transformed to a relative sea level (RSL) index point. Sedimentological and paleontological data of Late Holocene coastal deposits derived from lagoonal environments of Paros Island were studied along with radiocarbon dating. Archaeological remains were revisited and evaluated in order to understand their significance in the evolution of the coastal zone of both Islands.

The west sandy beaches of Naxos are dominated by the presence of multiple submerged beachrock slabs, while for Paros only two sites were identified. In both Islands they reach a maximum depth of -6.3 m. The beachrocks in Naxos are markedly more extensive in relation to the beachrocks of Paros. Notably, in both islands the beachrock thickness ranges between 0.25-1 m. Cement examination of the dated samples has shown that bounding material between grains was mostly early intertidal cement. Shallower beachrock samples (<2 m) suggested a RSL rise of ~2 m for the last 2.0 ka. However, in the case of deeper samples (between -4 and -5.7 m), some inconsistencies were noted with expected ages and with the tectonic regime of the study area. Overall, some major palaeogeographical changes were spatially and chronologically constrained for a number of coastal sectors of the two

islands, based on the morphology of submerged beachrock slabs and luminescence dating.

The multiproxy analysis of coastal cores from Paros Island allowed to reconstruct the coastal landscape evolution of selected sites and further provided a significant collection of data for the reconstruction of relative sea-level fluctuations in Paros. New data derived from two coastal drillings in the western part of Paros allowed reconstructing the palaeogeographic evolution of Livadia for the last ~4500-4864 cal BP and of Pounta for the last ~721-986 cal BP. Sedimentological and paleontological observations have shown that a semi-enclosed lagoon existed until at least ~780-436 BC (2385-2729 cal BP) in Livadia bay that was later slowly infilled probably due to human activities. Conversely, Pounta has been primarily influenced by coastal-marine processes and the evolution of the coastal landscape is more recent.

All the data produced in this work were compiled in order to produce RSL index points and reconstruct the relative sea level changes in the study area. The resultant RSL index points were compared with RSL reconstructions from previously available data in central Cyclades. Data suggest a RSL that rose by ~2 m in the last 2000 years at an average rate of ~1.2 mm/yr. Furthermore, the new index points indicate that RSL rose at least by ~3.9 m in the last ~4500 years. A relative sea level curve has been suggested based on the compilation of data. Overall, the data indicated a slight underestimation of the RSL position in Paros and Naxos, which may reflect higher subsidence rates for the Late Holocene. This observed subsidence may be the combinatory result of eustatic sea level rise along with land subsidence. Reported submerged tidal notches suggest that subsidence is at least partly owed to coseismic events that have taken place during the last ~2800 years.

Overall, this work has contributed to the better understanding of the RSL changes in Paros and Naxos Islands and improved the chronological framework for the Late Holocene and has further shown the significance of using multiproxy investigations to better assess sea-level evolution. This study has further shown the great potential of beachrocks as a tool to track major changes in shoreline positions and to precisely assess the palaeogeographical evolution of the coastal zone, especially in the eastern Mediterranean.

Keywords: sea level changes, beachrocks, paleogeography, coastal geomorphology, geoarchaeology, Central Cyclades, luminescence dating, Holocene

Περίληψη

Ο στόχος αυτής της διατριβής ήταν η συλλογή και μελέτη γεωμορφολογικών, ιζηματολογικών και αρχαιολογικών δεδομένων προκειμένου να εκτιμηθεί η εξέλιξη της θαλάσσιας στάθμης στις κεντρικές Κυκλάδες κατά το Αν. Ολόκαινο και η συμβολή σε αυτήν της τεκτονικής. Ο απώτερος στόχος ήταν η ανασύνθεση των παλαιο-ακτών στις Κεντρικές Κυκλάδες, οι επιπτώσεις των μεταβολών της θαλάσσιας στάθμης στην παλαιοπεριβαλλοντική εξέλιξη και η παλαιογεωγραφική τους αναπαράσταση κατά το Αν. Ολόκαινο.

Πραγματοποιήθηκε ανάλυση πολλών τύπων δεδομένων (multiproxy analysis) μέσω της μελέτης βυθισμένων ακτόλιθων, πυρήνων σε παράκτιες λιμνοθάλασσες και αρχαιολογικών δεδομένων προκειμένου να επιτευχθούν οι παραπάνω στόχοι. Πραγματοποιήθηκαν αναλυτικές υποβρύχιες έρευνες στους ακτόλιθους της Πάρου και της Νάξου, οι οποίοι εντοπίστηκαν σε βάθη έως -6 m. Για την χρονολόγηση των ακτόλιθων χρησιμοποιήθηκε η μέθοδος της οπτικά διεγερμένης φωταύγειας, με τη χρήση τόσο χαλαζία όσο και άστριου. Επιπλέον πραγματοποιήθηκε πετρογραφική ανάλυση του συγκολλητικού υλικού των ακτόλιθων ώστε να χαρακτηριστεί ο τύπος του συγκολλητικού υλικού όπως και να καθοριστεί η χωρική σχέση μεταξύ της παλαιο-ακτής και της ζώνης δημιουργίας των ακτόλιθων. Όλα τα δείγματα ακτόλιθων που συσχετίστηκαν με την μεσοπαλιρροιακή ζώνη μετατράπηκαν σε σημεία-δείκτες στάθμης θάλασσας (RSL index point). Μελετήθηκαν επίσης ιζηματολογικά και παλαιοντολογικά δεδομένα από γεωτρήσεις που πραγματοποιήθηκαν σε παράκτια λιμνοθαλάσσια περιβάλλοντα και επιλεγμένα δείγματα χρονολογήθηκαν με ραδιοχρονολογήσεις. Παράλληλα επανεξετάστηκαν και αξιολογήθηκαν αρχαιολογικά ευρήματα προκειμένου να κατανοηθεί η σημασία τους στην εξέλιξη της παράκτιας ζώνης και των δύο νησιών.

Οι δυτικές ακτές της Νάξου χαρακτηρίζονται από την παρουσία πολλαπλών ακτόλιθων, ενώ στην Πάρο εντοπίστηκαν μόνο δυο θέσεις. Οι ακτόλιθοι φτάνουν σε μέγιστο βάθος -6,3 μ. Οι ακτόλιθοι στη Νάξο είναι σαφώς πιο εκτεταμένοι σε σύγκριση με την Πάρο. Αξίζει να σημειωθεί ότι, και στα δύο νησιά, το πάχος των ακτόλιθων κυμαίνεται μεταξύ 0,25-1 μ. Η μικροσκοπική εξέταση των δειγμάτων έδειξε ότι έχουν συγκολληθεί στην μεσοπαλιρροιακή ζώνη. Τα ρηχότερα δείγματα (<2 μ.) υποδηλώνουν άνοδο της θαλάσσιας στάθμης κατά ~2 m τα τελευταία 2000 χρόνια. Ωστόσο, στην περίπτωση των βαθύτερων δειγμάτων (-4 και -5.7 μ.), σημειώθηκαν ορισμένες ανακολουθίες σε ότι αφορά στις αναμενόμενες ηλικίες σε σχέση με το

τεκτονικό καθεστώς της περιοχής μελέτης. Συνολικά, μέσω της μορφολογίας των βυθισμένων ακτόλιθων και της χρονολόγησης με την μέθοδο της οπτικά διεγερμένης φωταύγειας, διαπιστώθηκαν σημαντικές παλαιογεωγραφικές αλλαγές για μια σειρά παράκτιων περιοχών στα δυο νησιά.

Η ανάλυση παράκτιων πυρήνων από επιλεγμένες θέσεις στην Πάρο έδωσε την δυνατότητα να ανακατασκευαστεί η εξέλιξη του παράκτιου περιβάλλοντος και παράλληλα συλλέχθηκαν σημαντικά δεδομένα σχετικά με τις διακυμάνσεις της θαλάσσιας στάθμης. Τα νέα δεδομένα από δύο παράκτιες γεωτρήσεις στο δυτικό τμήμα της Πάρου επέτρεψαν την ανακατασκευή της παλαιογεωγραφικής εξέλιξης στα Λιβάδια Παροικιάς για τα τελευταία ~4500-4864 cal BP και στην Πούντα για τα τελευταία ~721-986 cal BP. Οι ιζηματολογικές και παλαιοντολογικές παρατηρήσεις έδειξαν ότι μια ημίκλειστη λιμνοθάλασσα υπήρχε τουλάχιστον μέχρι ~780-436 π.Χ. (2385-2729 cal BP) στα Λιβάδια (Κόλπος Παροικιάς), η οποία επηρεαζόταν από τα ρέματα της περιοχής. Η λιμνοθάλασσα στην συνέχεια έκλεισε, πιθανώς λόγω ανθρωπογενών δραστηριοτήτων, ωστόσο είναι δύσκολο να καθοριστεί ο χρόνος,. Αντιθέτως, η Πούντα έχει επηρεαστεί κυρίως από παράκτιες-θαλάσσιες διεργασίες και η εξέλιξη του παράκτιου τοπίου είναι πιο πρόσφατη.

Όλα τα δεδομένα που προέκυψαν από αυτή τη διατριβή συγκεντρώθηκαν με σκοπό να παραχθούν σημεία-δείκτες της θαλάσσιας στάθμης (RSL index points) και να ανακατασκευαστούν οι σχετικές μεταβολές της θαλάσσιας στάθμης. Τα δεδομένα που πρόεκυψαν συγκρίθηκαν με ανακατασκευές και από άλλα διαθέσιμα δεδομένα στις κεντρικές Κυκλάδες. Η ανάλυση έδειξε ότι η σχετική θαλάσσια στάθμη αυξήθηκε κατά ~2 μ. τα τελευταία 2000 χρόνια, με μέσο ρυθμό ~1,2 χιλιοστά / έτος. Επιπλέον, τα νέα σημεία-δείκτες (RSL index points) δείχνουν ότι η σχετική θαλάσσια στάθμη αυξήθηκε τουλάχιστον κατά ~3,9 μ. τα τελευταία ~4.500 χρόνια. Μια σχετική καμπύλη στάθμης της θάλασσας προτάθηκε με βάση το σύνολο των δεδομένων. Συνολικά, τα δεδομένα έδειξαν μια μικρή υποεκτίμηση της θέσης της θαλάσσιας στάθμης στην Πάρο και τη Νάξο, η οποία μπορεί να υποδεικνύει υψηλότερους ρυθμούς βύθισης για το Αν. Ολόκαινο. Αυτή η παρατηρούμενη βύθιση μπορεί να είναι το συνδυαστικό αποτέλεσμα της ευστατικής ανόδου της θαλάσσιας στάθμης και της τεκτονικής βύθισης. Η παρουσία βυθισμένων παλιρροιακών εγκοπών δείχνει ότι τουλάχιστον ένα μέρος της βύθισης οφείλεται σε συν-σεισμικά γεγονότα που έλαβαν χώρα κατά τη διάρκεια των τελευταίων ~ 2.800 χρόνων.

Συνολικά, αυτή η διατριβή συνέβαλε στην καλύτερη κατανόηση των σχετικών μεταβολών της θαλάσσιας στάθμης στην Πάρο και τη Νάξο και βελτίωσε το χρονολογικό πλαίσιο για το Αν. Ολόκαινο. Έδειξε ακόμα τη σημασία της χρήσης

πολλών τύπων δεδομένων (multiproxy analysis) για την καλύτερη αξιολόγηση της εξέλιξης της στάθμης της θάλασσας. Επιπλέον, ανέδειξε τη μεγάλη δυνατότητα που παρέχουν οι ακτόλιθοι ως εργαλεία αφενός μεν της παρακολούθησης σημαντικών μεταβολών της ακτογραμμής, αφετέρου δε της εκτίμησης της παλαιογεωγραφικής εξέλιξης της παράκτιας ζώνης, ιδιαίτερα στην ανατολική Μεσόγειο.

Λέξεις-κλειδιά: μεταβολές στάθμης θάλασσας, ακτόλιθοι, παλαιογεωγραφία, παράκτια γεωμορφολογία, γεωαρχαιολογία, κεντρικές Κυκλάδες, Οπτικά Διεγερμένη Φωταύγεια, Ολόκαινο

Acknowledgments

I would like to thank the many people that have guided and supported me during the course of this PhD.

Assoc. Prof. Niki Evelpidou, for being such an excellent and supportive mentor. I cannot thank her enough for all her guidance and support since we first met, for all the useful discussions and brainstorming sessions during the course of this work. I could not have imagined having a better advisor and mentor for my PhD.

Prof. Michael Stamatakis, for always being available to discuss with me issues regarding this PhD and for his overall support during this work.

Emeritus Prof. Hampik Sahak Maroukian, for his scientific observations and constructive comments in all the stages of this work.

I am grateful to **Prof. Christophe Morhange**, **Prof. Theodoros Gournelos**, **Prof. Serafim Poulos** and **Assoc. Prof. Efthimios Karymbalis**, for their constructive comments and for kindly accepting to examine this PhD thesis. Their vast experience of coastal geomorphology and palaeogeography was critical in improving the quality of the final manuscript.

I would like to thank **Dr. Nick Marriner** (CNRS, Laboratoire Chrono-Environnement UMR 6249, Université de Franche-Comté) for sharing his expertise in coring analysis methods and palaeoenvironmental reconstructions as well as **Dr. Matthieu Giaime** (CEREGE, Aix-en-Provence) for fruitful discussions on palaeoenvironmental analysis of the cores.

For his assistance with submarine fieldwork and for fruitful discussions on beachrocks and sea level reconstructions, I would like to thank **Dr. Matteo Vacchi** (CEREGE, Aix-en-Provence).

The luminescence dating was accomplished through a DAAD (German Academic Exchange Service) scholarship grant ‘Research Grants for Doctoral Candidates and Young Academics and Scientists (1-6 months), 2014’, at the Leibniz Institute for Applied Geophysics. For their training and expertise, I would like to thank **Prof. Manfred Frechen** and **Dr. Sumiko Tsukamoto** and for hosting me at the Leibniz Institute for Applied Geophysics.

I would also like to thank “En Agris” and Antonis Kavadias for the aerial photography.

This project would not have been possible without the financial support of a number of funds:

- The Bilateral project Greece – France ‘Sea level changes in Cyclades’, and PHC PLATON 2014 PROJET N° 30409XH.
- DAAD (German Academic Exchange Service) scholarship grant ‘Research Grants for Doctoral Candidates and Young Academics and Scientists (1-6 months), 2014’, funded my visit to the Leibniz Institute for Applied Geophysics
- Support of the Labex OT-Med (ANR-11-LABX-0061) and of the A*MIDEX project (n° ANR-11-IDEX-0001-02), funded by the «Investissements d’Avenir» French Government program, managed by the French National Research Agency (ANR). A special thank you to **Prof. Christophe Morhange** for his kind support in radiocarbon dating and constructive comments of this research over the years.

I would like to thank colleagues and friends who helped through many adventurous and interesting fieldworks.

Finally, I would like to thank my mother for her continuous encouragement, support and personal sacrifices, through my life. I would also like to thank my friends for their love, support and patience especially during the final steps of this thesis.

Contents

Preface

This PhD thesis on the subject “Study of the geomorphological and environmental evolution of the coastal zone of central Cyclades” was assigned to me by the Faculty of Geology and Geoenvironment of the University of Athens, on 11 July 2012. The purpose of this thesis was to evaluate the evolution of sea level in Central Cyclades during the Late Holocene, assess the contribution of local tectonics with the ultimate goal to trace the palaeoshorelines in central Cyclades, the effects of sea level changes in palaeoenvironmental evolution and to propose a reliable palaeogeographical reconstruction during the Late Holocene.

The thesis is divided in four parts. **Part A – Introduction** consists of a brief introduction of sea level indicators as well as an introduction to the study area, with the following chapters:

Chapter 1 presents an introduction to the sea level indicators used and discussed in this thesis, with a particular focus on beachrocks.

Chapter 2 presents the geographical and geological context of the studied islands, Paros and Naxos.

Part B – Methodology focuses on the methodological aspects of this work and the various tools used and consists of the following chapters:

Chapter 3 presents the methodology used in this research, which includes the fieldwork and laboratory methods used for beachrocks and coastal drillings. Particular focus is given in luminescence dating that was used to date the submarine beachrocks. Theses multiple analyses were performed in order to contribute to the ongoing debate concerning the use of beachrocks as accurate proxies for past RSL.

Part C – Results and Discussion presents and discusses the results of this work. Archaeological remains, beachrocks and coastal drillings are presented in three individual chapters, respectively. Each of the chapters includes also a discussion concerning the main findings. Part C consists of the following chapters:

Chapter 4 focuses on the geoarchaeological context of the study area, with particular focus on coastal and submarine remains.

Chapter 5 discusses the results from beachrock research. Fieldwork results as well as results from luminescence dating are presented in detail and discussed. Investigation of the mid- to late Holocene shoreline evolution of two Cycladic Islands

(Paros and Naxos, Aegean Sea, eastern Mediterranean) using beachrocks was also performed. The potential of using beachrocks to track shoreline evolution in Paros and Naxos are discussed as well as their use as sea level indicators.

Chapter 6 presents and discusses two coastal drillings that were performed in the west part of Naxos Island. Two cores from Livadia and Pounta coastal zone are described and analyzed, while their potential to reconstruct RSL changes are also presented.

Chapter 7 summarizes the results produced from this research. Beachrock and drilling data are converted into RSL index points in an attempt to reconstruct the relative sea level changes in Paros and Naxos Islands. Results from this research are also compared with other researches from the study area.

Finally, **Part D – Concluding remarks**, includes the conclusions of this work and discusses the potential future research avenues and consists of C***hapter 8***.

Introduction

Coasts are amongst the most dynamic parts of the Earth's surface. The land and the sea rarely meet at the same boundary (Woodroffe, 2002). The shoreline migrates daily with the tide, the changes in atmospheric pressure, etc. It can change seasonally, and varies over longer time scales as the coast erodes or deposits, or as sea level changes (Woodroffe, 2002).

Coastal areas are one of the most rapidly evolving systems on the planet. At the same time, coastlines are the most important areas used and inhabited by humans. The population density within 100 kilometres of the coastline is nearly 3 times higher than the global average density and 10% of the human population is living less than 10 meters above sea level (especially in the tropical zones). Considering that coastal communities spread more rapidly than national populations, it is estimated that by 2020 up to 75% of the world population could be living within 60 km of the shoreline (Edgren, 1993). According to Nicholls and Mimura (1998), by 2100, 600 million people will occupy coastal flood plains below the 1.000-year flood level. There are many reasons for the increasing populations along the coastline, and these include historical colonization, commercial activities or political ties, temperate climate, availability of fertile alluvial soils, fisheries, and more recently, aesthetic and recreational reasons (Carter, 1988). For the coastal populations, the greater interest is for the current and future sea level trends.

The geomorphology and sedimentology of the coastlines today is a result of the sea level changes during the Holocene and to a lesser degree during the Pleistocene. While some coastlines haven't changed significantly over the past 6000 years, most have advanced or retreated, and some have shown alternations (Bird, 2008). When sediment deposition exceeds the rate of erosion, or when emergence occurs due to land uplift or a fall in sea level, a coastline advances while it retreats when erosion exceeds deposition, or in the case of submergence due to land subsidence or sea level rise (Bird, 2008). The response of different types of coastal systems to sea level change is often very specific to the given system (Haslett, 2000).

Environmental conditions, such as the prevailing hydrodynamics, coastal topography and sediment availability, further influence the nature of the shore and its response to sea level rise (Plater and Kirby, 2011). Environmental change may alter geomorphic process rates and process regimes in landscapes. These alterations may drive the landscape into disequilibrium, causing geomorphic activity to increase for a while or

possibly to stop. There is an overlap in the reconstruction of past coastal landscapes with reconstructing past sea levels, and the two are united in requiring a thorough understanding of the palaeoenvironment (Vis *et al.*, 2015).

The Cycladic Plateau has been subjected to successive stages of emergence and submergence due to the changing sea level during the Quaternary (Kapsimalis *et al.*, 2009). The Cycladic region has great potential in terms of sea level research, because it comprises an area of climatological interest and archaeological importance. It has been inhabited since the late Neolithic period, has provided great archaeological sites and has suffered from major palaeogeographical changes since the Last Glacial Maximum (LGM). These facts contributed in selecting the central Cyclades as the study area. For central Cyclades, the sea level record is not complete and a robust chronological framework is still poor for the Late Holocene period. At the same time the evolution of their coastline is seldom explored. Paros and Naxos Islands lie in the centre of the Cycladic region, and they formed a “mega-island” along with neighbouring islands during the LGM. The two islands separated around 8000 BP (e.g. Kapsimalis *et al.*, 2009). Naxos Island today is the largest Cycladic Island, while Paros is the 3rd largest. For these reasons, their common history, these two Islands were selected as a study area. In addition, this region is considered an area of low seismicity, characterized by the absence of large earthquakes (e.g. Papazachos, 1990; Sakellariou and Galanidou, 2016). Vertical tectonic movements have been considered of minor significance for the palaeogeographical evolution of this area (Sakellariou and Galanidou, 2016), particularly in relation to other regions in Greece, where vertical displacements are far more pronounced (e.g. Falasarna, Crete; Pirazzoli *et al.*, 1992). Therefore this area provides the opportunity to study sea level changes while minimizing the tectonic contribution to sea-level change.

In this context, the main aims of this PhD were the following:

- Understand the sea level evolution during the Late Holocene in central Cyclades. Although, it is generally acknowledged that sea level stabilized close to present levels by 6,000 years BP (Pirazzoli, 1991), the Cycladic Islands are characterized by the presence of submerged archaeological remains suggesting a continuous RSL rise during the Late Holocene.
- Place an improved chronological constrain on RSL changes in central Cyclades, and for Paros and Naxos Islands in particular.

- Reconstruct palaeoshorelines using a variety of data, such as beachrocks and drillings, and assess the impact of RSL in the evolution of the coastal zone.
- Contribute to the debate regarding the accuracy of beachrocks as sea level indicators. Some authors propose an intertidal formation (e.g. Neumeier, 1999; Vousdoukas *et al.*, 2007; Desruelles *et al.*, 2009; Mauz *et al.*, 2015a), while, on the other hand, a supratidal genesis is proposed by Kelletat (2006) in the spray zone, given the fact that beachrocks in microtidal areas often have a great thickness that does not correspond to the tidal range at the time of formation.

PART A – INTRODUCTION

Chapter 1 – Relative sea level changes and indicators

1. Relative sea level changes and indicators

1.1 Sea level changes

Sea level changes are driven by long- and short- term processes. Eustatic sea level changes are owed to variations in the mass or volume of the oceans and have a global impact, while relative sea level changes are related to changes of the land with respect to the sea surface (Rovere *et al.*, 2016a). The decay or growth of continental ice sheets is the main mechanism of eustatic sea level changes, while other processes are also involved, such as thermal expansion. Relative sea level changes may be regional and/or local and they may be owed to various processes. Glacial isostatic adjustment can bring about a RSL change on a regional scale and reflects the adjustment of the crust to redistribution of ice and ocean loads (Figure 1) (Kopp *et al.*, 2015).

Figure 1: Near Gävle (Sweden), this area was 510 m lower, during the LGM. About 9500 years BP, this area was uplifting at a rate of ~48 mm/yr. Today, this area lies at an altitude of 190 m and is still uplifting in a smaller rate of ~7.3 mm/yr.

Along tectonically active margins, RSL changes reflect vertical movements, which may differ even between adjacent areas, depending on the local tectonic regime (e.g. Corinth Gulf). In the case of the Eastern Mediterranean, the RSL changes recorded usually reflect eustatic and tectonic factors. An important feature that is commonly used to estimate the vertical stability of a particular area is the location of MIS5e palaeoshoreline (Anzidei *et al.*, 2014). Although with some spatial variability, it is

estimated that the MIS5e palaeoshoreline, in tectonically stable areas, is located between 5-7 m above the present sea level (Kopp *et al.*, 2009; Lambeck *et al.*, 2012).

The general pattern of postglacial eustatic sea-level rise is adequately known (Lambeck and Chappell 2001), even if the Mediterranean is characterized by spatial and temporal variability in land movements. Global sea-level curves, based on coral-reef data (e.g. Barbados, the Huon Peninsula, and Tahiti) show that sea level rose by 120–130 m, mainly between 16000 and 8000 years BP, and stabilized near the present level by 6000 years BP (Pirazzoli, 1991) (Figure 2). Tracking sea-level behaviour following this mid-Holocene stabilization is more difficult; however, it is important in order to separate a variety of non-eustatic dynamic factors such as isostasy, tectonics, and sea-surface topography that may bring about significant local sea-level fluctuations (e.g. Mörner, 1996). The Mediterranean coasts provide a great opportunity to establish detailed sea level histories for the late Holocene, because they are characterized by a microtidal regime and by sea-level proxies of potentially high precision (Stewart and Morhange, 2009).

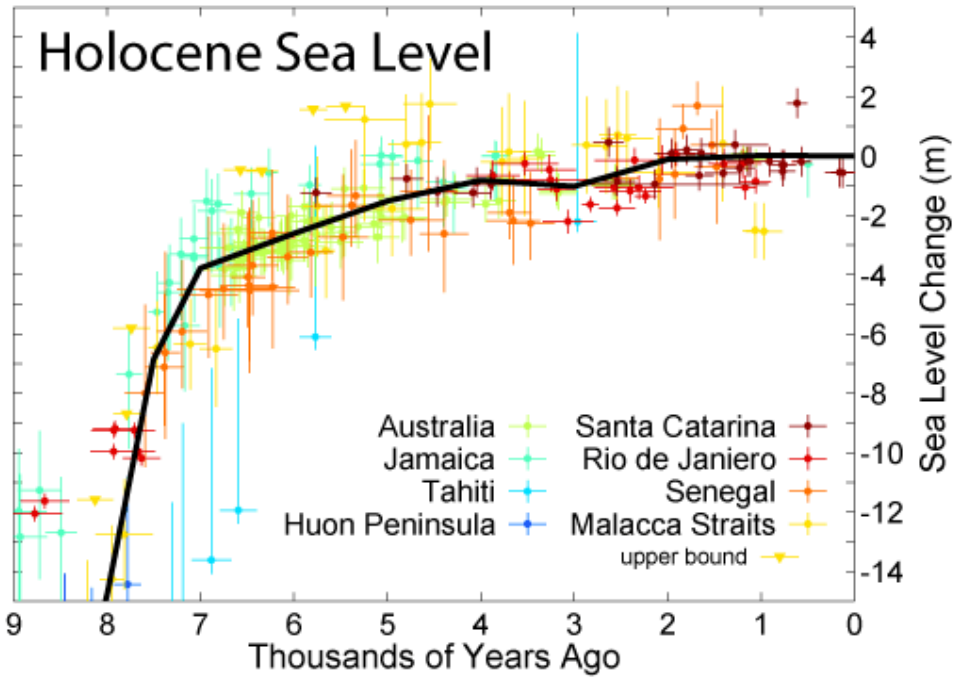

Figure 2: Holocene sea level curve for the last 9000 years, based on data from based on data from Fleming *et al.* (1998), Fleming (2000) and Milne *et al.* (2005). On average, sea level rise has been relatively slow to rise and have been fairly stable for at least the last few thousand years (source http://www.globalwarmingart.com/wiki/File:Post-Glacial_Sea_Level_png)

Fluctuations in sea level can be recorded using various techniques, depending on the desired timescale. Satellite altimetry and tide gauges are used to observe historically recent changes, of multi-decadal scale (e.g. Cazenave and Llovel, 2010). For longer timescales, various sea level markers are usually employed (e.g. Rovere *et al.*, 2016b).

1.2 Sea level markers

In the study of RSL changes, field observations on past sea level positions are a fundamental tool for pre-instrumental times. Various coastal/submarine features may prove valuable as long as we understand and interpret appropriately the information they provide. This implies understanding the original position of such a feature in relation to sea level and its interpretation with respect to sea level at the time of its formation or function.

Sea level markers may be biological, geomorphological, sedimentological or archaeological. The location of these markers to the present coastline and the determination of their relationship with sea level allow identifying sea level changes in a particular region. In the Mediterranean area, in particular, information deriving from tidal notches (e.g. Evelpidou *et al.*, 2013), beachrocks (e.g. Desruelles *et al.*, 2009), fish tanks (e.g. Lambeck *et al.*, 2004; Evelpidou *et al.*, 2012a; Morhange *et al.*, 2013), various biological indicators (e.g. Morhange *et al.*, 2001), coastal drillings (e.g. Vött *et al.*, 2006; Vacchi *et al.*, 2016a) are frequently used to deduce relative sea level changes.

Although there are a number of sea level markers, particular focus is given to the features discussed and used in this thesis.

1.2.1 Tidal notches

Notches can be divided into different types, according to their origin and shape. They include structural notches, lithological notches, abrasion (wave-cut) notches, infralittoral, supralittoral and midlittoral notches (e.g. Pirazzoli, 1986a). Amongst the various notches types, tidal notches are considered particularly reliable sea level markers (Figure 3). Tidal notches are undercut in carbonate coastal cliffs and typically have a V or U shaped profile. These markers are considered particularly

important as they provide information on both RSL changes and vertical displacements. The profile of tidal notches gives evidence regarding the duration that mean sea level (MSL) remained at the notch vertex and the mode of uplift or subsidence (Pirazzoli, 1986a, 2005; Evelpidou *et al.*, 2011). The bioerosion rate is generally higher near MSL and is gradually reduced towards the upper and lower limit of the tidal range. There are various reports regarding the bioerosion rate, ranging between 0.2 to 5 mm/yr (Pirazzoli, 1986a, Table 1; Laborel *et al.*, 1999, Table 1; Evelpidou *et al.*, 2011).

Figure 3: Tidal notch at north part of Paros Island. The notch vertex is located at -31 cm, suggesting a sea level at -35±5, according to Evelpidou *et al.* (2014a).

Fossil tidal notches have been frequently used to deduce paleo-sea levels and vertical displacements (e.g. Pirazzoli *et al.*, 1994; Stiros *et al.*, 2000; Nixon *et al.*, 2009; Faivre *et al.*, 2010a; Furlani *et al.*, 2011; Evelpidou *et al.*, 2011; 2013, 2014a, b; Mourtzas *et al.*, 2016). Difficulties however arise when trying to date this particular marker, with absolute dating methods. In the case of uplifted notches the difficulty often relates to finding datable bioindicators. In the case of submerged tidal notches, fossils are destroyed due to bioerosion after subsidence (Evelpidou and Pirazzoli, 2014). Therefore, their age is usually inferred from nearby dated sea level markers (e.g. Nixon *et al.*, 2009; Evelpidou *et al.*, 2012b; Marriner *et al.*, 2014). In any case, a well preserved tidal notch profile is an excellent criterion to determine the mode of displacement, gradual or coseismic. Notch profiles can be modified by sufficiently long enduring changes in the relative sea level, thus testifying of pre-seismic or post-seismic gradual tectonic trends.

1.2.2 Beachrocks

Beachrocks are known littoral sedimentary deposits (Figure 4) that originate from the rapid cementation of beach sediments by aragonite and High Magnesian-calcite (HMC) (Bricker, 1971). Sediments may consist of biogenic or clastic sands and pebbles (e.g. Bricker, 1971; Milliman, 1974; Vieira and Ros, 2007). Amongst the first reports of beachrocks were those by Sir Francis Beauford in 1817 (Goudie, 1969), Moresby (1835), Darwin (1841) and Dana (1849). Vousdoukas *et al.* (2007) have provided a comprehensive review for beachrock characteristics.

As beachrocks form at the sea level/intertidal zone, they have often been used to assess Holocene shoreline changes and crustally induced relative sea level (RSL) changes in the Mediterranean Sea (e.g. Desruelles *et al.*, 2009; Erginal *et al.*, 2010; Mauz *et al.*, 2015a; Kolaiti and Mourtzas, 2016; Ozturk *et al.*, 2016). Although beachrocks have received particular attention until the 80s, their research has only been “revived” during the past decade or so.

Figure 4: Submerged beachrock slabs at Glyfada beach (W Naxos Island).

The formation of beachrocks is a diachronic and widespread sedimentary process and their occurrence has been associated with various chronologies, cements and diagenetic environments (Vousdoukas *et al.*, 2007).

The cementation of coastal sediments may take place gradually as new bands may form in existing beachrocks (e.g. Neumeier, 1998). Field observations and laboratory experiments (Hanor, 1978; Hopley, 1986; Vousdoukas *et al.*, 2007) have shown that lithification can take place very quickly of the order of a few decades. In many occasions, seaward bands tend to be better cemented than the landward bands (Vousdoukas *et al.*, 2007).

Most reported beachrock occurrences come from the Mediterranean, the Caribbean Sea, the atolls of the Pacific and Indian Oceans and the tropical and subtropical Atlantic coasts (Vousdoukas *et al.*, 2007). The lack of reports in the tropical regions may be related to a lack of relevant research (Vousdoukas *et al.*, 2007). Regarding their age, most dated beachrocks are of Late Holocene, and more specifically, between 1000-5000 years old (e.g. Bernier *et al.*, 1997; Neumeier, 1998; Desruelles *et al.*, 2009).

1.2.2.1 Main characteristics

Beachrocks usually develop in bands, parallel to the beach. They may extend along a long stretch of coast, but they are also often found in patches, covering only part of the coast.

They have a small inclination seawards (up to ~15°), most commonly similar to the adjacent beach (Figure 5). When they are found differing greatly, it usually signifies their alteration due to erosion causing breaking and tilting of the beachrock slabs.

Figure 5: Underwater beachrocks at Glystra beach (E Naxos Island), with a gentle slope, similar to the beach.

The thickness of beachrocks is variable, ranging from 0.5 m to 2 m (e.g. Cooper, 1991; Vousdoukas *et al.*, 2007), even in microtidal areas. This characteristic, amongst others, lead Kelletat (2006) to suggest a supratidal genesis in the spray zone. According to Mauz *et al.* (2015b), sediment supply as well as accommodation space affect the thickness and lateral extent of beachrocks and less extensive beachrocks are formed in reflective, bedrock controlled coasts; larger occurrences are more common in intermediate, dissipative coasts.

Beachrocks may also affect beach morphodynamics. Although submerged beachrocks have been shown to mitigate beach erosion by dissipating the wave energy impinging to the coastline, modern beachrocks at the coastline may also promote offshore beach sediment loss (Vousdoukas *et al.*, 2007). According to Vousdoukas *et al.*, (2007), beach profile evolution models (Larson and Kraus, 2000; Vousdoukas *et al.*, 2005) indicate that beaches with beachrocks may show notably different morphodynamic behaviour from beaches without beachrocks under certain conditions. After the exposure of the beachrock, sediment supply from the seabed stops at the outcrop location, resulting in large spatial gradients of the sediment transport rates at the exposure limits and formation of ‘scour steps’ (Vousdoukas *et al.*, 2007). These scour steps may ‘filter’ the cross-shore sediment transport, by

blocking onshore sediment transport by the height of the step and the enhanced turbulence at its 'toe', whereas offshore sediment transport is not likewise obstructed (Vousdoukas *et al.*, 2007). According to the same authors, beach sediment erosion may take place, because the presence of these scour steps at the offshore margin of the beachrock outcrops may promote the offshore and inhibit the onshore sediment transport.

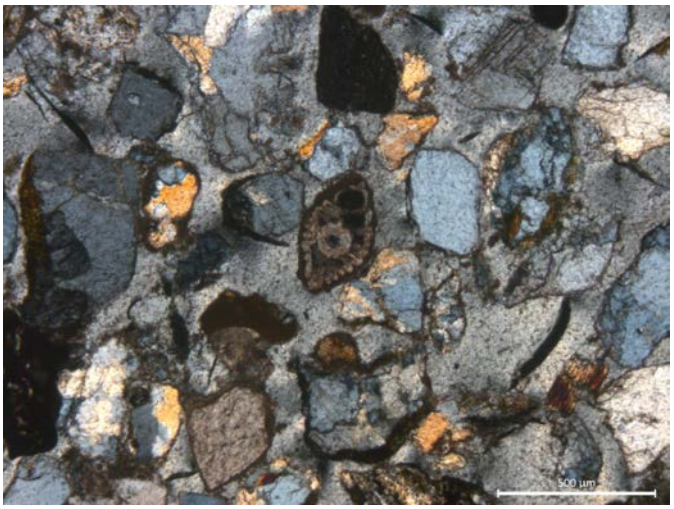

Figure 6: Gastropod at the center of the thin section, from Agios Georgios beachrocks, at a depth of -0.7 m (W Naxos Island).

1.2.2.2 Cement and sediment bedding characteristics

Beachrocks typically form in the interface between seawater and meteoric water. Beachrock cements are typically calcitic or aragonitic (Bricker, 1971), depending on the physicochemical factors of the diagenetic environment. In particular, beachrock cements consist of metastable carbonate phases (e.g. Taylor and Illing, 1969; Bathurst, 1975): High Magnesian calcite (HMC) or aragonite. The sedimentary grains of the matrix are variable, and generally reflect the nature of the surrounding sedimentary material. They may consist of quartz, chert, feldspars, heavy minerals, volcanic material, ooids, mollusc shells and skeletal fragments (Figure 6).

Earlier studies by Ranson (1955) suggested that cement may change from aragonite to calcite and amorphous CaCO3. Similarly, Taylor and Illing (1971) considered that MgCO2 may constitute an altered product of aragonite, while Stoddart and Cann (1965) suggested a two-phase cementation process, which included initially aragonite and then pore-filling by calcite. Stoddart and Cann (1965) emphasized on the identification of the cement, considering that, typically, calcite precipitates by freshwater and aragonite by seawater.

The cement mineralogy and morphology are indicative of the diagenetic environment (Tucker and Wright, 1990; Gischler, 2007). Aragonitic cements, in the marine

phreatic zone, usually form in isopachous fringes of needles, up to 100 μm long (e.g. Moore, 1973; Gischler, 2007), while HCM includes micritic cement, with crystals less than 5 μm. Cements typical of the meteoric-vadose diagenetic environment, may consist of low magnesian calcite (LMC) and exhibit e.g. equant crystals, blocky and meniscus fabrics.

The examination of cement characteristics and microstratigraphy allows identifying the type of cement and the spatial relationship between the past shoreline and beachrock formation zone (Mauz *et al.*, 2015b). Other useful tools for understating the formation environment of beachrocks are the particular bedding structures and sedimentary textures, which are indicative of the upper shoreface to beach sedimentary environment (Mauz *et al.*, 2015b) (Figure 7). Sedimentary structures and textures are often preserved in beachrocks and they are diagnostics of the depositional environment (e.g Neumeier, 1998). In some occasions beachrock bands are characterised by one lithofacies, while in other cases multiple lithofacies may be identified in one single band (e.g. Vieira and Ros, 2007).

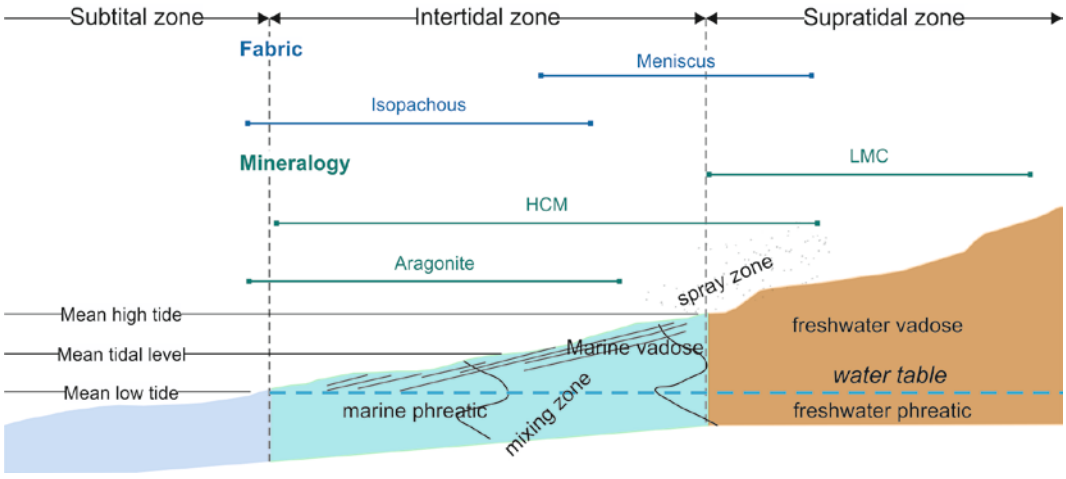

Figure 7: Characteristics of cement and sediment bedding in the tidal zone (after Mauz *et al.*, 2015b).

1.2.2.3 Age estimations

The most common methods for dating beachrocks are radiocarbon dating and Optical Luminescence dating (OSL). Obtaining a precise age for the formation of beachrocks is often a difficult task. A common method is to date the cements or shells found incorporated in the beachrock (e.g. Desruelles *et al.*, 2009; Mauz *et al.*, 2015b; Vacchi *et al.*, 2016a). However, well cemented beachrocks, however, may have undergone several diagenetic phases (Vousdoukas *et al.*, 2007), and caution is

needed in the selection of dating material, as cements from one deposit may generate different ages (Desruelles *et al.*, 2009). Furthermore, often cements are very thin, therefore the extraction of enough material is also challenging. On the other hand, dating of shells may only provide a maximum age, as they provide the age the organism died (Hopley, 1986). The time gap between the death of the organism and its incorporation into the beachrock may be small but it may also be hundreds and even thousands of years. The error may be relatively minimized, if the selected sample shows a high degree of preservation.

Luminescence dating method is increasingly used for coastal and marine sediments (e.g. Frechen *et al.*, 2004; Reimann *et al.*, 2011; Mauz *et al.*, 2010; Thiel *et al.*, 2015). The method has also been used to date beachrocks for the reconstruction of palaeoshorelines along the Brazilian coast (Barreto *et al.*, 2002; Tatumi *et al.*, 2003), India (Thomas, 2009), and the Mediterranean (Erginal *et al.*, 2010; Mauz *et al.*, 2015a; Ozturk *et al.*, 2016) and the results were also compared with absolute/independent dating such as radiocarbon dating. Bosman (2012) used both methods to date beachrocks in South Africa and concluded that OSL dating has two significant advantages in relation to radiocarbon dating: a) there is no need for marine reservoir effect correction, and b) there is no carbon contamination from other sources (e.g. bioclasts) that can greatly affect the results.

However, no dating method is flawless. Dating of beachrocks and intertidal sediments, in general, requires taking into account various environmental factors. Such sediments may exhibit changes in dose rate through time through the dissolution of carbonate cement, in concentration of radioactive elements and also in water content (Bateman, 2015). According to Bateman (2015), there is a possibility of light penetration within blocks carved for luminescence dating of submerged beachrock and aeolianite, through burrows and larger voids.

1.2.2.4 Beachrocks as proxies of coastal changes

Beachrocks have proven particularly useful in the absence of other sea level indicators or when coupled with other available sea level indicators (e.g. Erginal *et al.*, 2010; Stattegger *et al.*, 2013; Mourtzas *et al.*, 2014). In the past decades a number of studies have taken place regarding beachrocks (e.g. Guilcher, 1961; Sanlaville, 1970; Dalongeville, 1984). Hopley (1986) was the first to provide a methodological synthesis on the use of beachrocks as sea level indicators with particular guidelines, and further stated that beachrocks should be used in

conjunction with other types of evidence, particularly in macrotidal areas. Furthermore, the potential of beachrocks as a useful record of shore position has been suggested by Semeniuk and Searle (1987), while Cooper (1991) suggested they may preserve former shoreline morphology and alignment.

There has been considerable debate regarding the position of the tidal zone where beachrocks form and their use as reliable sea level indicators (e.g. Kelletat, 2006; 2007; Knight, 2007). An intertidal formation is proposed by many researchers (e.g. Neumeier, 1999; Vousdoukas *et al.et al.*, 2007; Desruelles *et al.et al.*, 2009; Mauz *et al.*, 2015b), while, a supratidal genesis was suggested by Kelletat (2006) in the spray zone, given the fact that beachrocks in micro-tidal areas often have a great vertical width that does not correspond to the tidal range at the time of formation. According to Mauz *et al.et al.* (2015a) beachrock thickness as well as lateral extent depends on sediment supply and accommodation space and the average thickness of beachrocks in microtidal areas reaches 2 m (e.g. Cooper, 1991).

However, the cement mineralogy and morphology of the beachrocks are indicative of the diagenetic environment (Gischler, 2007), therefore the examination of the cement characteristics and microstratigraphy can allow identifying the type of cement, the spatial relationship between the past shoreline and beachrock formation zone (Mauz *et al.*, 2015b). Different cement types within one formation may also indicate a sequence of diagenetic events (Tucker and Wright, 1990). In the lower intertidal zone, cement consists of acicular aragonite forming isopachous fringes (e.g. Tucker and Wright, 1990), while HMC cements form thin-bladed isopachous crusts or, dark or golden brown, pelletal and micritic, irregular grain coatings and void fillings (Alexandersson, 1972; Scholle *et al.*, 1983). The presence of sedimentary structures, such as keystone vugs, is also indicative of the intertidal zone (Dunham, 1970; Strasser and Davaud, 1986). On the other hand, cements of low-magnesium calcite with <5 mol% MgCO3 are indicative of the meteoric-vadose zone. Vadose zone is the aerial zone above the water-table and describes the supratidal environment (Scholle *et al.*, 1983; Tucker and Wright, 1990). In the vadose environment, typical meniscus, gravitational (‘dripstone’), and highly acicular ‘whisker’ type cement fabrics are observed (e.g. Land, 1970; Bricker, 1971). Examination of cement microstratigraphy allows determining a sequence of diagenetic events. A relative sea level rise or fall may result in beachrocks passing from a sequence of diagenetic environments (e.g. Beier, 1985; Tucker and Wright, 1990). For instance Vacchi *et al.* (2012), identified the progressive uplift of beachrocks in Lesvos Island by the

presence of intertidal cements followed by meteoric cements, which revealed a displacement from a former intertidal position to a supratidal one.

Based on the cement characteristics and sediment bedding information, a reliable reconstruction of RSL changes may be achieved, by defining the position of a beachrock and transforming it into a RSL index point (Mauz *et al.*, 2015b).

1.2.3 Archaeological remains

Various archaeological remains are often used to deduce RSL changes, especially in the Mediterranean area, due to its continuous human occupation (e.g. Flemming, 1969; Pirazzoli, 1976; Blackman, 1973; Raban, 1985; Galili *et al.*, 1988; Sivan *et al.*, 2004; Morhange *et al.*, 2013; Mourtzas *et al.*, 2014 amongst many others). A large number of archaeological remains do not provide indications regarding sea level and only in a few cases can be used to understand whether sea level has risen or fallen since their construction and use. Recently Auriemma and Solinas (2009) provided a comprehensive review of the various archaeological remains and their use as sea level markers. The authors highlighted the need to understand the functional height of ancient constructions and their relation with sea level. The functional height, however, corresponds to the elevation of particular architectural parts of the structure with respect to an estimated mean sea level at the time of their construction (Antonioli *et al.*, 2007). However, according to Morhange and Marriner (2015) the accurate definition of the functional height is difficult to define, because it is usually estimated based on present analogues that are not always related to past archaeological constructions. Furthermore, coastal and submerged archaeological remains are often much eroded due to wave activity.

Morhange and Marriner (2015) categorized the archaeological remains in three zones, with variable degree of accuracy: a) submerged structures including harbour foundations and wrecks, which have low accuracy and can only indicate the direction of RSL change, b) harbour installations (quays, piers, breakwaters, equipped banks, slipways, etc.) and fish tanks, which are usually quite precise RSL markers and c) emerged structures, such as buildings, pavements, roads, tombs and quarries, which also only provide information regarding the direction of RSL change.

1.2.4 Biological markers

Fossil biological remains commonly serve as datable material to chronologically constrain RSL changes and reconstruct palaeogeographic histories. Laborel and Laborel-Deguen (1994) reviewed and refined the methodology for using biological indicators to estimate RSL variations and identify slow and rapid vertical movements. The use of biological indicators in the study of Mediterranean sea level changes has gradually evolved to a multidisciplinary approach, taking into consideration morphological, sedimentary, archaeological, petrographic and biological criteria (Laborel and Laborel-Deguen, 1994).

The main principle considered when using biological indicators as sea-level index points is that, on rocky coasts, fauna and flora develop in quasi-horizontal belts parallel to the sea surface, defining the marine zonation (Pérès, 1982; Rovere *et al.*, 2015). Morhange and Marriner (2015) have distinguished two types of biological indicators: a) Sea-level indicators proper, which include organisms with a very narrow vertical life range and b) Biological indicators of submersion, which include boring species (e.g. Lithophaga lithophaga) that live down to 50 m, and subtidal builders that have a wide ecological range, but whose upper limit can yield information on RSL changes, particularly on archaeological structures.

A recent comprehensive review on the use of biological indicators is provided by Rovere *et al.* (2015), while Morhange and Marriner (2015) highlighted the usefulness of combining biological indicators with archaeological remains. Regarding the latter, RSL changes have been successfully estimated at various archaeological sites (e.g. Morhange *et al.*, 2006; Faivre *et al.*, 2010b).

1.2.5 Palaeogeographic reconstructions

Sea level fluctuations, climate changes and human interventions are well recorded in the sediments of coastal marshes and wetlands. Coastal marshes and lagoons are particularly sensitive in local and regional palaeoenvironmental changes and have proven to be a powerful tool for studying coastal changes during the Holocene (e.g. Scott and Medioli, 1978; Stanley and Warne, 1994; Cole & Liu, 1994; Vella & Provansal, 2000; Clave *et al.*, 2001; Sacchi et al., 2014; Morhange et al., 2015; Ejarque et al., 2016). Through multidisciplinary studies, it is possible to reconstruct the coastal evolution and relative sea level changes (e.g. Nixon *et al.*, 2009;

Primavera *et al.*, 2011; Ghilardi *et al.*, 2014; Marriner *et al.*, 2014; Vacchi *et al.*, 2016a).

Palaeogeographic reconstructions include a multiproxy assessment using phases analysis, dating, palaeo-bathymetry and sedimentation of deltas, estuaries and coasts. Lithological, sedimentological and ecological criteria are taken into account to understand environmental changes and result to the reconstruction of palaeoenvironmental sequences of cores and changes in sea level. Many sea-level histories have been reconstructed with stratigraphic evidence from sequences of coastal sediments. Ostracods have also been used to reconstruct Late Quaternary sea levels (e.g. Mazzini *et al.*, 1999; 2011; Primavera *et al.*, 2011). According to Cronin (2015), because of suitability for RSL reconstructions based on their ecology and preservation in coastal sediments, ostracods hold great promise in future studies of past sea-level changes.

During the last decade, many researches have produced high-resolution sea level reconstructions from saltmarsh sediment cores (e.g. Shennan and Horton, 2002; Kemp *et al.*, 2011; Engelhart and Horton, 2012). However, in the Mediterranean, salt marshes are less developed due to the microtidal regime and they usually found around large deltas and coastal lagoons (Vacchi *et al.*, 2016b).

Conversely, coastal lagoons are very common in the Mediterranean coasts (Figure 8). According to Vacchi *et al.* (2016b), two main types of lagoonal facies may be identified in the Mediterranean: a) open or marine-influenced lagoons, with sandy-silty sediments and high species diversity. Fossil assemblages include marine brackish molluscs and marine brackish or outer estuary Foraminiferal and ostracods assemblages, and b) inner or semi-enclosed lagoons, with lower species diversity in relation to the 1st type. The sedimentological and paleontological characteristics are typical of a brackish lagoonal/estuarine environment.

Figure 8: The coastal lagoon at Pounta, usually dry during the summer months (SW Paros Island). Nowadays, human activities have reduced the values and functions of this wetland.

Apart from RSL reconstructions, coastal drillings may occasionally provide with data to identify and chronologically constrain palaeoseismic events (e.g. Nixon *et al.*, 2009; Marriner *et al.*, 2014; Pilarczyk *et al.*, 2014). Pilarczyk *et al.* (2014) have discussed how microfossils (diatoms, foraminifera, and pollen) were used to reconstruct records of palaeoearthquakes from changes in microfossil assemblages, quantifying the amount of coseismic and interseismic vertical land movements along tectonically active coastlines.

1.3 Coastal evolution – impact of RSL changes

The evolution of the coastal zone is highly affected by relative sea level changes. Coastal changes significantly impact the natural and cultural resources, and the understanding of coastal evolution is important for the preservation, development and management of the coastal zone.

A number of landforms and landscapes are hosted in the coastal environment, and they have a variable sensitivity to environmental change. Particular features such as coastal dunes, marshes and lagoons as well as sandy beaches are highly sensitive to environmental changes. For the coastal system the interactions between RSL and

sediment supply are essential. The relative sea level affects the stability of coastal forms, while sediment abundance or deficit may result in either progradation sufficient to reverse transgression or erosion even when RSL is falling (Carter *et al.*, 1987; Roy *et al.*, 1994; Hansom, 2001).

Changes in sea level have always affected humans, since the evolution of *Homo sapiens*. Understanding sea level evolution and Holocene sedimentary successions is a fundamental need for not only geologists, but also for archaeologists who are required to understand and interpret their findings in a context of palaeoenvironmental changes. At the site of ancient Eretria, Ghilardi *et al.* (2014) found that a lack of human occupation in the coastal plain before 3000 cal. BC and during the 2nd millennium BC was because the area was then under seawater. Coastal palaeoenvironmental reconstructions at known archaeological sites further allows identifying ancient harbour installations (e.g. Morhange *et al.*, 2016; Giaime *et al.*, 2017).

According to Morhange and Marriner (2010), the moderate sea-level rise after 6000 years BP led to the gradual infilling of lagoons, river mouths, and marshlands. The Levantine coast lagoons and estuaries were exploited as natural harbours, during the Bronze Age. A number of factors led to the infilling of this morphology, Bronze Age sites were gradually isolated from the sea, leading human populations to new locations (Morhange and Marriner, 2010).

Chapter 2 – Study area

2. Study area

2.1 Geographical and climatological context of the study area

The study area, Paros and Naxos Islands, are located in the central Aegean, belonging to the south Cyclades complex (Figure 9). Administratively, both islands belong to the South Aegean Region, Prefecture of Cyclades. Naxos is the largest island of the Cyclades (428 km^2), while Paros is the 3rd largest (196 km^2). The two islands are separated by a narrow channel of ~5 km width.

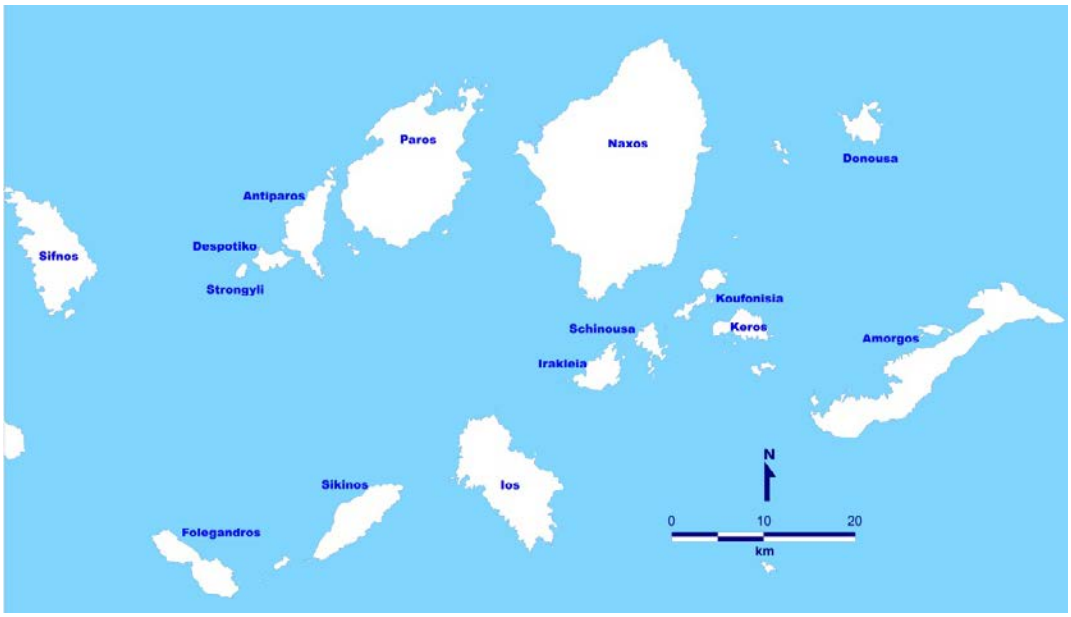

Figure 9: Paros and Naxos Islands, located at the center of the Cyclades.

The capital city of Paros is Paroikia, located at the NW part of the island, serving also as its main port. The highest peak of the island reaches 771 m, at Profitis Ilias. Antiparos lies at the SW of Paros and, near Pounta, they are separated by a narrow strip of ~1 km.

Chora is the capital city of Naxos, and its main port. Mountain Zeus is the highest peak of the island reaching an altitude of 1004 m. On its south, Naxos borders with the island of Small Cyclades (Iraklia, Schinousa, Koufonisia).

The climate in both islands is of Mediterranean type with long dry summers and mild winters. In Paros Island, the winter season is rarely characterized by frost or snow,

while storms are more common. The warm season, between May and September, is characterized by a mean temperature of ~24.45°C, due to the prevailing north and northeast winds. The mean annual temperature is 18.5°C (Table 1).

Table 1: Mean monthly temperatures in Paros (Source: Operational Programme of Rural development 2014-2020, Paros; HNMS)

	JAN	FEB	MAR	APR	MAY	JUN	JUL	AUG	SEP	OCT	NOV	DEC	AV
Mean	11.4	11.22	12.55	15.46	20.17	24.72	27.04	26.68	23.54	19.95	16.09	12.63	18.45
Mean maximum	14.04	14.08	15.61	19.08	23.91	28.48	30.36	30.23	27.07	23.41	19.21	15.38	21.74
Mean minimum	8.75	8.41	9.55	11.99	15.49	19.88	22.50	22.58	20.01	16.86	13.02	10.31	14.95

Similarly, in Naxos Island, the winter is mild, with the lowest temperature reaching 12°C, in February (Table 2). The mean annual temperature is 18.16°C. The warmest month is August with the highest mean temperature of 26.6°C.

Table 2: Mean monthly temperatures in Naxos (Source HNMS)

	JAN	FEB	MAR	APR	MAY	JUN	JUL	AUG	SEP	OCT	NOV	DEC	AV
Mean	12.1	12	13.2	16.1	19.3	23.3	24.8	24.7	23	19.8	16.1	13.5	18.16
Mean maximum	14	14.4	14.9	17.6	21.1	25.5	26.4	26.6	25.3	22.4	18.3	15.3	20.15
Mean minimum	10	9.9	10.2	13.8	17.3	21.5	23.2	23.1	20.9	17.6	13.9	10.5	15.99

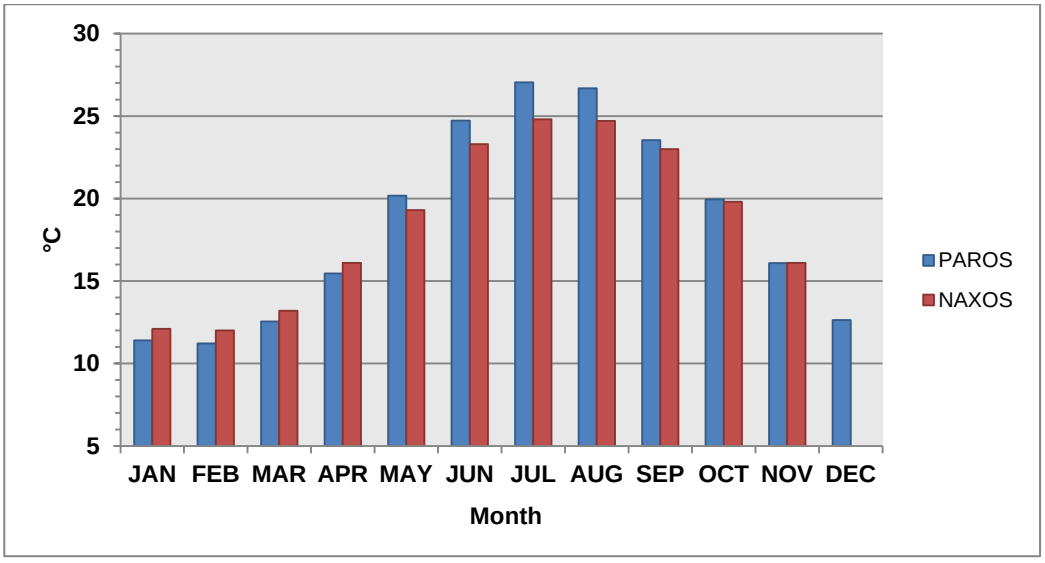

Figure 10: Mean monthly temperatures in Paros and Naxos.

Regarding the wind regime, both islands are characterized by the persistence of the northerly winds. In general, they present a double fluctuation: a primary maximum during winter (December-February), with a secondary maximum during summer

(July-August) (Table 3); the latter is also associated with the presence of the Etesians that persist for extended periods from May to September.

Table 3: Monthhly wind velocities in Paros and Naxos Islands in knots (Source: Operational Programme of Rural development 2014-2020, Paros, Naxos; HNMS)

	JAN	FEB	MAR	APR	MAY	JUN	JUL	AUG	SEP	OCT	NOV	DEC	AVER
PAROS	13.64	13.69	12.78	11.56	10.55	11.62	14.60	11.90	12.02	11.26	12.84	12.60	12.42
NAXOS	15.65	15.84	14.77	11.94	10.18	10.41	13.28	13.94	13.91	14.52	13.39	14.82	13.55

Table 4: Wave direction and height expressed in percentage of occurrence (after Athanasoulis & Skarsoulis, 1992)

Direction	**N**	**NE**	**E**	**SE**	**S**	**SW**	**W**	**NW**	**Calm**
(%)	21.8	8.2	5.7	4.7	3.3	7.6	24.7	20.0	4.0
Height (m)	0-0.5	0.5-1	1-1.5	1.5-2	2-2.5	2.5-3	3-4	4-5	>5
(%)	36.6	24.1	17.1	9.3	5.8	3.3	2.6	0.8	0.4

2.2 Coastal and submarine geomorphology

The coastal zone of Paros mainly consists of Quaternary deposits, marbles, gneiss schists and some small appearances of igneous rocks. It is mainly rocky and steep, particularly in the NE and NW part, and beaches form a smaller part. The largest plains are found in Naousa, Marmara, Drios and Pounta (Evelpidou, 2001).

The coastal zone of Naxos is diverse, mainly due to the lithological variety and tectonics that have affected the wider region. The north, east and south coasts of the island consist mainly of marbles and schists, while the west coasts are formed mainly on alluvial deposits and granodiorite. The majority of the coastal zone is characterized by low land morphology, while steeper slopes are located in the north and south part of the island (Evelpidou, 2001). Most beaches are found in the west part of the Island and are more extensive in comparison to Paros. More developed coastal dunes are also found in Naxos, often neighbouring with lagoons in the back (Figure 11).

Bathymetrically, although the relief of the Cycladic area is gentle, there is a general slope towards the west from about −100 m down to nearly −200 m. During the LGM, Paros and Naxos, along with other neighbouring islands formed a “mega-island”, 160 km long and 90 km wide (Kapsimalis *et al.*, 2009). The two islands became “autonomous” again around ~8000 BP. Today, the depth between the two islands reaches ~-40 m.

Figure 11: The western coastal zone of Naxos is characterized by the presence of many coastal wetlands. The coastal lagoon of Glyfada beach (W Naxos Island), with dunes in the front, is probably the best preserved wetland, according to WWF (2013).

2.3 Geological context of the wider area

The Aegean is a unique environment in terms of active geodynamics, plate movements, ongoing geological processes, and dynamically changing landscapes, due to the convergence between the Eurasian and African continental plates (Figure 12) (Sakellariou and Galanidou, 2016). A complicated tectonic structure has formed owing to the active subduction processes and the ongoing migration of the continental and oceanic crustal blocks (Le Pichon and Angelier 1979; Angelier *et al.* 1982; Le Pichon *et al.* 1982, 1995; Le Pichon 1982; Meulenkamp *et al.* 1988; Taymaz *et al.* 1991; Jolivet, 2001).

Cyclades, located in the center of the Aegean Sea, is an area regarded as currently seismically quiet (e.g. Bargnesi *et al.*, 2013), while an intense active seismicity characterized the surrounding areas (Jackson and McKenzie, 1984; Taymaz *et al.*, 1991; Jolivet *et al.*, 2010). The central Aegean is currently behaving rigidly, probably because of microplate locking from rotation (Taymaz *et al.*, 1991; McClusky *et al.*, 2000).

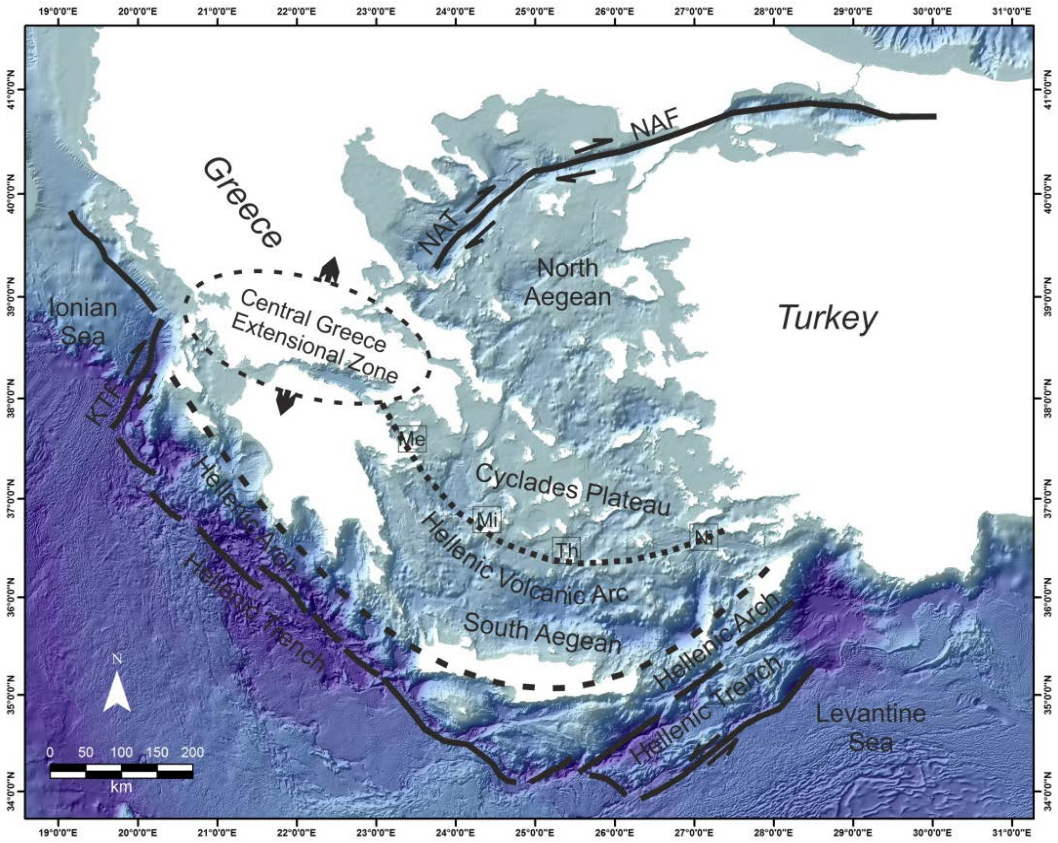

Figure 12: Main geotectonic boundaries and features of the Aegean. The Hellenic volcanic: Methana (Me), Milos (Mi); Thera (Th); Nisyros. KTF: Kephallinia Transform Fault; NAT: North Aegean Trough; NAF: North Anatolian Fault (after Sakellariou and Galanidou, 2016).

Cyclades lie on a continental crust of ~25 km thickness that occurred during the Oligocene-Miocene after the formation of the Hellenic Belt in the Eocene (Vigner, 2002; Tirel *et al.*, 2004; Karagianni *et al.*, 2005). According to Tirel *et al.* (2004), during Oligocene-middle Miocene, the gravitational collapse of the Hellenides reduced the Aegean continental crust from 50 km to ~25 km, owing to the southward retreat of the African slab. After upper Miocene, the westward extrusion of Anatolia modified the extension and associated crustal thinning in the North Aegean. During this episode, crustal thinning related to the southward retreat of the African slab, tended to be more localized in the Cretan Sea. According to Tirel *et al.* (2004), the Cyclades probably act as a rigid block translated toward the south–west with no significant deformation, in agreement with GPS velocities and lack of major earthquakes. Modern strain is partitioned into seismically active normal faults and strike-slip systems in the Northern Aegean and surrounding areas (Taymaz *et al.*, 1991)

In the central Aegean region, the extension has been continuous since late Oligocene-early Miocene (e.g. Gautier and Brun, 1994; Gautier *et al.*, 1999; Jolivet, 2001; Keay *et al.*, 2001; Brun and Faccenna, 2008; Jolivet and Brun, 2010; Jolivet *et al.*, 2010). The collapse of the Alpine Orogeny and the southward retreat of the Hellenic subduction zone (Royden, 1993; Brun and Faccenna, 2008) have resulted in back-arc extension (e.g. Fytikas *et al.*, 1984; Papanikolaou, 1993; Jolivet and Brun, 2010). The southwards migrating arc was followed with plutonism and volcanic activity (Papanikolaou, 1993; Pe-Piper and Piper, 2002).

The structure of the tectonostratigraphic units in the central Aegean is associated with the extensional reorganization of the early Cenozoic Alpine nappe stack:

1) Cycladic basement rocks: they consist of deformed gneisses and schists of Variscan age, with intrusions of various Miocene plutons (Dürr *et al.*, 1978; Altherr *et al.*, 1982; Papanikolaou, 1989; Lee and Lister, 1992; Bolhar *et al.*, 2010). U–Pb dating of gneisses basement rocks in Paros yielded ages of 315-300 Ma, suggesting that that magmatism is largely synchronous with Variscan metamorphism (Engel and Reischmann, 1998; Bargnesi *et al.*, 2013). The basement rocks are found on the islands of Paros, Naxos, Mykonos and Ios.

2) The Cycladic Blueschist Unit (CBU): it overlies the basement rocks and consists of metamorphosed early Mesozoic shelf sequences intercalated with meta-volcanic rocks (Dürr *et al.*, 1978; Negris, 1915–1919). Ages of the protolith range from the Triassic to the Cretaceous (Bröcker and Pidgeon, 2007). It is generally considered a lateral equivalent of the Pindos oceanic zone in the Hellenides (Bonneau, 1984). According to Papanikolaou (1987, 1989), this unit is divided in north and south sub-units, according to lithostratigraphic and palaeogeographic data. The CBU underwent HP–LT deformation (blueschists and eclogites) during the Middle Eocene and HT–LP overprinting in the Oligocene–Miocene (Altherr *et al.*, 1979, 1982; Wijbrans and McDougall, 1986, 1988).

3) Upper tectonic unit: In the Southern Cyclades, the Cycladic Blueschist Unit is locally overlain by the **Dryos/Messaria unit** (e.g. Papanikolaou, 2009). In Paros Island, the unit of Dryos consists of deformed metabasites, phyllites, calc-schists and low-grade marbles (Papanikolaou, 1980). According to Jolivet *et al.* (2010), this unit did not record the Eocene metamorphic event (HP–LT) and, therefore, was already in the upper crust during the formation of the Hellenides in the Eocene.

2.3.1 Geology of Paros

Paros forms a NE–SW trending dome bounded by a low-angle normal fault to the east and northeast (Bargnesi *et al.*, 2013). This low-angle detachment fault zone is visible in few areas on Paros and it is inferred that Paros and Naxos share the same detachment (Gautier *et al.*, 1993).

In Paros, the Cycladic basement rocks consist of highly deformed Carboniferous ortho- and paragneisses (Engel and Reischmann, 1998; Robert, 1982) and less-deformed, S-type granites (amphibolite facies) (Altherr *et al.*, 1982). Intercalated amphibolite-facies marbles, mica schists, and amphibolites of the Cycladic Blueschist Unit (CBU) overlie the basement rocks. The Dryos Unit overlies the Cycladic Blueschist Unit and consists of phyllites and calc-schists. The unit is characterized by lower metamorphic grade (greenschist facies) in relation to the CBU and basement rocks (Bargnesi *et al.*, 2013). According to Papanikolaou (1980), the original contact between the Dryos Unit and the underlying CBU and basement complex is likely thrust related.

A sedimentary series overlies the metamorphic rocks in tectonic contact. It is composed of an incomplete marine sequence of uncertain provenance and tectonic origin, overlain by conglomerates interbedded with sandstones (Bargnesi *et al.*, 2013). A study by Sánchez-Gómez *et al.* (2002) in the sedimentary section of Paros suggested two distinct ages, Eocene-Late Cretaceous with ages between 100 and 40 Ma and Middle-Late Miocene of 16–9 Ma.

Neogene and Quaternary formations are found above the aforementioned units. The Neogene is mostly comprised of limestone and travertine deposits of Pliocene age (Dermitzakis and Papanikolaou, 1980), while Quaternary formations mainly consist of alluvial deposits.

The structural and exhumational–erosional history of Paros and the central Cyclades, in general, is composite, characterized with repeated episodes of deformation - deposition from various perspicuous source terranes, some of which may have been completely eroded (Bargnesi *et al.*, 2013).

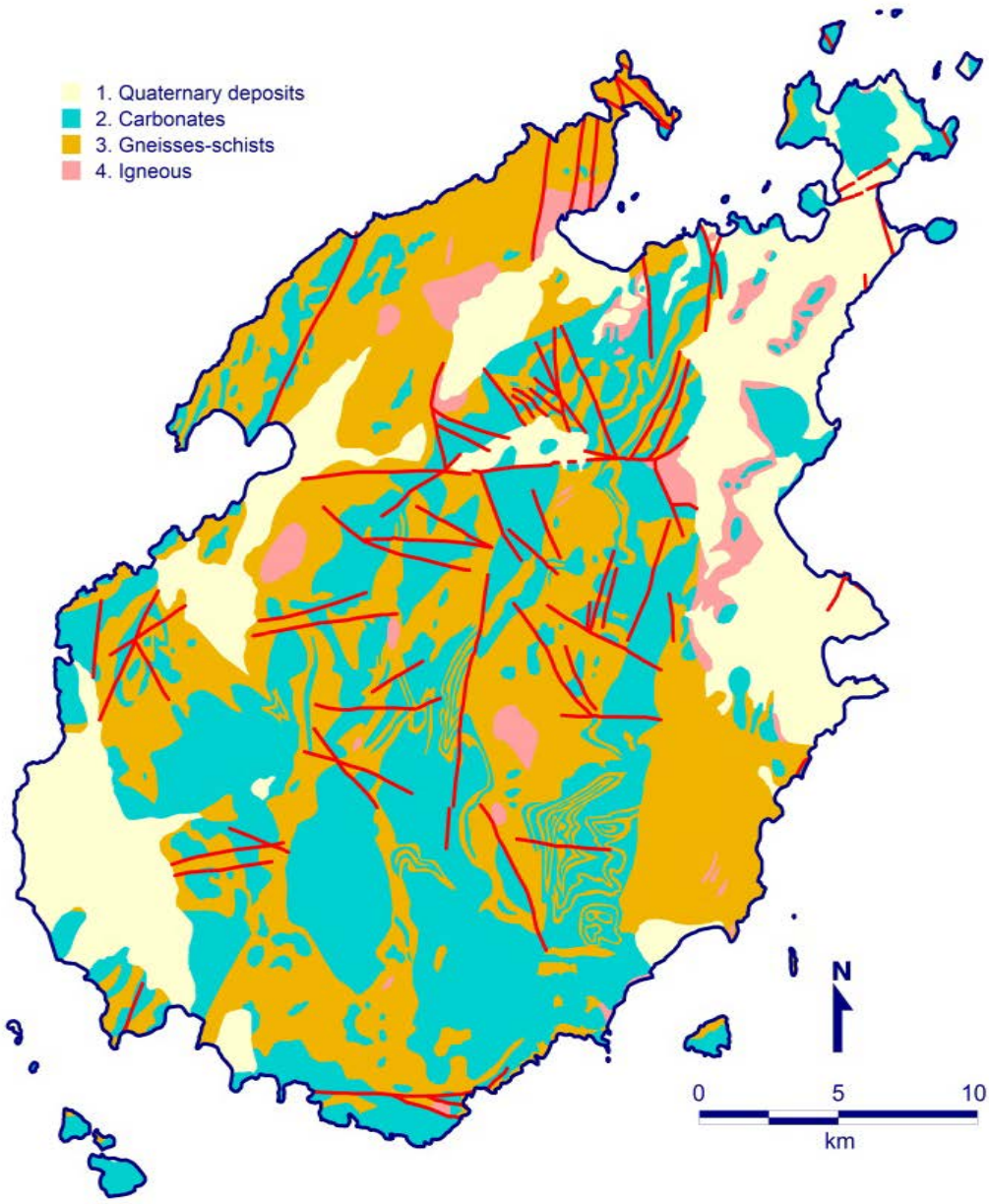

Figure 13: Simplified map with the main lithologies of Paros (after Papanikolaou, 1996).

2.3.2 Geology of Naxos

Naxos forms an N– S elongate structural dome cored by migmatite (Jansen and Schuiling, 1976; Buick, 1991). The core of the dome constitutes the lower- most structural unit, with migmatized gneissic quartzofeldspathic rocks containing marble, metapelite and amphibolite (Keay *et al.*, 2001). A series of metamorphic rocks, with marbles, schists and metavolcanics (Dürr *et al.*, 1978), surround the dome: the lower parts consist of highly metamorphosed and folded amphibolites and meta-ultrabasic rocks, while the upper parts of metaconglomerates and metabauxites (Schuiling and Kreulen, 1979). The alternation of schists and marbles is owed to the, large scale, isoclinal folding (Dürr, 1986) of Eocene age (Andriessen *et al.*, 1979).

Seven metamorphic zones have been distinguished with temperatures ranging between 300°C and more than 720°C (Wijbrans and McDougall, 1986). Above the metamorphic series, non-metamorphic rocks are found, comprising a mélange of disrupted shallow-water Mio- Pliocene sediments (Jansen, 1973; Angelier *et al.*, 1982).

The metamorphic rock series were later intruded by a range of thin leucogranite sheets and dykes and a large granodiorite body (Keay *et al.*, 2001). The timing of emplacement of the large western granodiorite on Naxos has been investigated by various researches (e.g. Dürr *et al.*, 1978; Andriessen *et al.*, 1979; Pe-Piper *et al.*, 1997). More recently, Keay *et al.* (2001) placed the timing at ~12 Ma.

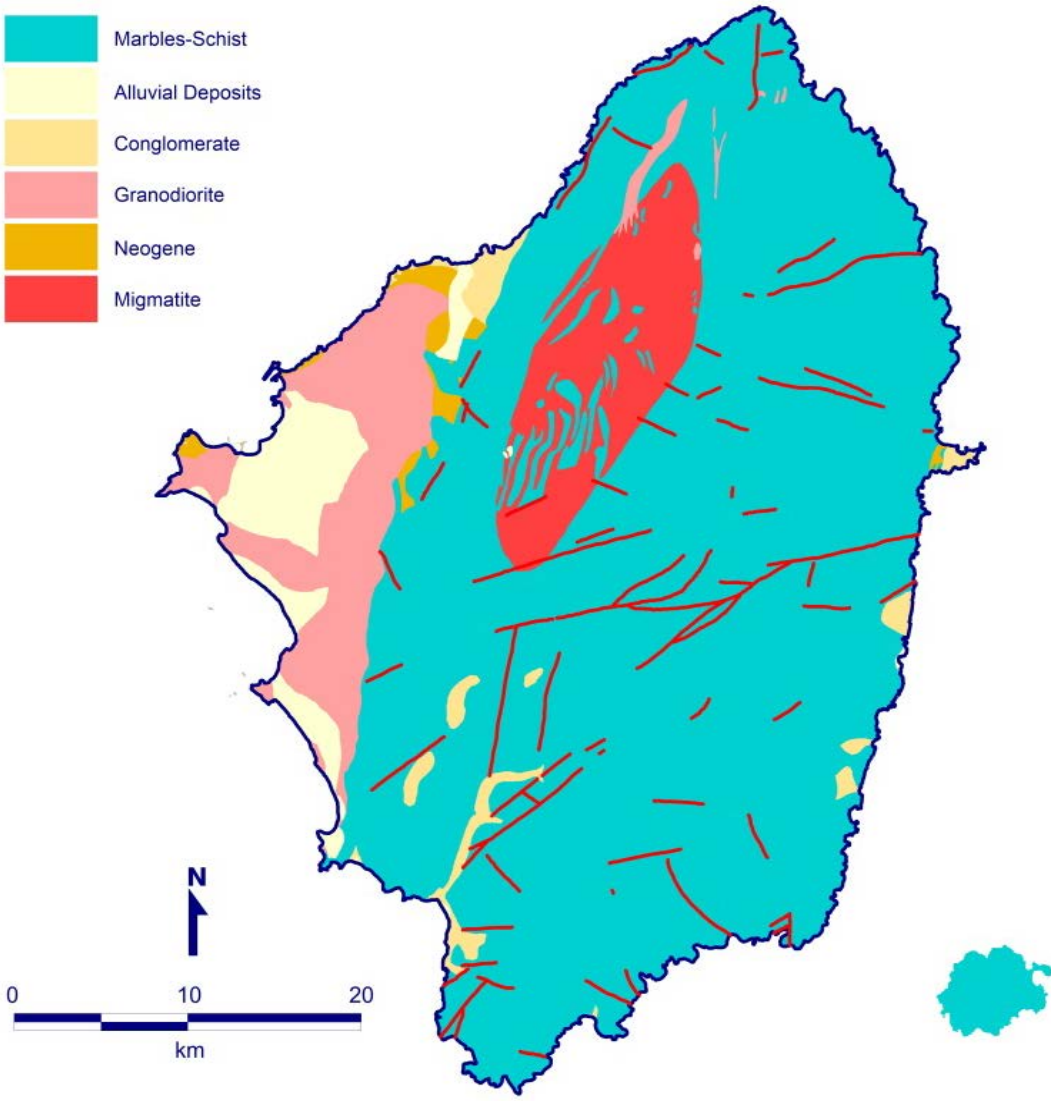

Figure 14: Simplified lithological map of Naxos with main faults.

2.4 Quaternary evolution

It is generally accepted that the tectonic regime affecting the Aegean is broadly extensional and dominated by normal faulting (e.g. McKenzie, 1978; Mercier *et al.*, 1989; Papazachos 1990). The Aegean region is characterized by intense seismic activity. However, although historical seismicity records are one of the longest and densest in the world (e.g. Galanopoulos, 1981; Guidoboni *et al.*, 1994; Papazachos and Papazachou, 1997), knowledge about co-seismic surface ruptures in the region remains limited, in particular for offshore faults, because many of the epicenters are located at sea and because instrumental data cover less than a century (Pavlidis and Caputo 2004). Where earthquake recurrence rates are smaller than 100–200 years, such information might be available; however, this may not be the case for specific active faults with an average recurrence interval longer than 500 years (Evelpidou *et al.*, 2014a).

The Cycladic region is presumed to be under an extensional tectonic regime behind the modern volcanic arc at the centre of the Aegean plate and possesses a relatively thin continental crust of about 25-26 km thickness (e.g. Tirel *et al.*, 2004; Zhu *et al.*, 2006). This is owed to the gravitational collapse of the Aegean crust due to the southward retreat of a subduction front during the Cenozoic and the westwards extrusion of the Anatolian block in the Aegean during the Neogene (Tirel *et al.*, 2004).

In recent years several major offshore faults have been identified suggesting the presence of tectonic depressions with horsts (Lykousis *et al.*, 1995, Doutsos and Kokkalas, 2001, Tirel *et al.*, 2004). According to Mascle and Martin (1990) the Central Aegean is characterized by a ‘‘puzzle-like’’ morphological and structural pattern with variously oriented normal faults. The eastern part of the Central Aegean appears to be dominated by clearer trends (NE–SW to ENE–WSW), while the western part largely displays NW–SE-oriented extensional features.

The Central Aegean is characterized by relatively low seismicity and the absence of large earthquakes (e.g. Papazachos, 1990) (Figure 15). In a recent study Vamvakaris *et al.* (2016), calculated the mean return period values for shallow earthquakes with M>6.0 in the Aegean region and suggested very long return period values (> 200 years) for the broader Cyclades Plateau, amongst other areas. The same authors also found that the most probable maximum magnitudes for a return period of 50 yr is expected to be smaller than M=5.0, for low seismicity areas, such as the Cyclades Island plateau.

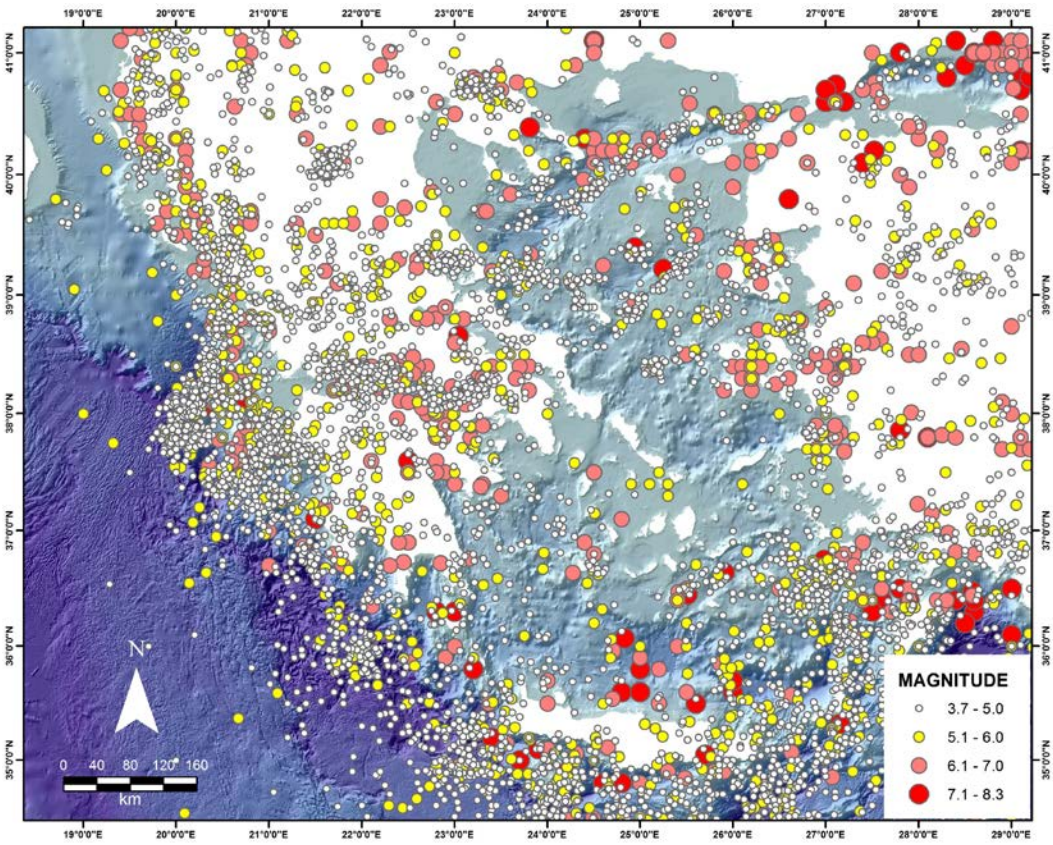

Figure 15: Seismicity in the Greek region since 550B.C. The distribution of epicenters shows that the study area is characterized by low seismicity and absence of strong earthquakes.

According to Sakellariou and Galanidou (2016), vertical tectonic movements are of minor significance and the coastal evolution of the central Aegean during Late Pleistocene-Holocene is mostly affected by eustatic sea-level fluctuations and, to a lesser degree, by isostatic movements. They do however note evidence of tectonic subsidence considering the work of Desruelles *et al.* (2009).

Lykousis (2009) noted a continuous subsidence rate during the last 400 ka, with values of 0.34–0.60 mm/yr for the Cycladic plateau, with a gradual decrease in the magnitude of the extensional tectonic regime. The relative motion of the Cyclades during the Quaternary is toward the south and south-west with a rate of about 3 cm per year (Peterek and Schwarze 2004).

2.5 Past research in the wider area

The Cycladic area has attracted many researches and several geomorphological and geoarchaeological investigations have been conducted aiming to evaluate the palaeogeographic evolution and RSL changes (e.g. Morrison 1968; Stiros *et al.*, 1994; Baika, 2008; Poulos *et al.*, 2009; Kapsimalis *et al.*, 2009; Pavlopoulos *et al.*, 2010; 2011; Mourtzas, 2010; 2012; Evelpidou *et al.*, 2012c; d; 2014a).

Morrison (1968) suggested 5-6 m of sea level rise since 5500 BC based on geomorphological and archaeological findings, at Saliagos. Baika (2008) compiled a database of archaeological remains for the Attico-Cycladic area and presented RSL estimations for different time periods since the Neolithic. Poulos *et al.* (2009), based on archaeological evidence, coastal formations, and radiocarbon-dated sedimentary units, suggested that sea level in the central Aegean region was between 4-5 around 5500 BP, and that the following sea-level rise had a steady rate of ~0.9 mm/a for the last 5000 years.

Using beachrocks in particular, the most extensive work was accomplished by Desruelles *et al.* (2009) in Mykonos, Delos and Rhenia islands. According to the authors, the sea level was located at about -3.6±0.5 m around 2000 BC, at -2.5±0.5 m around 400 BC and at -1±0.5 m at about 1000 AD. Desruelles *et al.* (2009) examined the cements and performed radiocarbon dating on the “total sample”: their beachrock samples consisted mainly of siliceous clasts (crystalline rocks, mainly granite and gneiss; low carbonate pollution possibility and re-cementation), with low proportion of bioclasts and no recrystallized micritic fillings. The authors selected the carbonate fraction below 100 μm after crushing the samples, considering that the cements were less than 100 μm thick. In general, their results present a good age-depth pattern, with the exception of 4 samples (out of 20), which yielded younger or older ages in comparison to their depth.

Further investigations were carried out in Delos Island coupling beachrocks with submerged archaeological structures, which indicated RSL rose by 2.15 m since the end of the Hellenistic period (Mourtzas, 2012).

Dalongeville and Renault-Miskovsky (1993) have reported the presence of beachrocks in Naxos Island, at Mikri Vigla and Plaka. According to Dalongeville and Renault-Miskovsky (1993), at Mikri Vigla, these beachrocks, lying partly below the current sea level, appear to have been quarried and were tentatively attributed to the Hellenistic period (323-31 BC / 2.32-2.03 ka BP). At Plaka, beachrocks are totally submerged at depths between –0.50 m and –1.20 m and three different alignments

of the beachrock are distinct. Dalongeville & Renault-Miskovsky (1993) suggest that sea level stood about 0.5 to 0.75 m below the present sea level, in recent times, prior to the Bronze Age (3300-1200 BC). Later research by Evelpidou *et al.* (2012c), revealed the presence of two beachrock benches at Mikri Vigla; the deepest is located 100 m from the coastline at depths ranging between -2.7 and -3.4 m, while the shallower one extends for about 15 m at depths between 0 m and -1.7 m. By correlating the beachrocks in Naxos with those studied in Mykonos, Delos and Rhenia (Fouache *et al.*, 2005; Desruelles *et al.*, 2009), Evelpidou *et al.* (2012c) suggest that the older submarine beachrock corresponds to the sea level stand of -3.6±0.5 m around 2000 BC.

Palaeogeographic reconstruction in Naxos Island has been performed by Evelpidou *et al.* (2012c). The authors drilled 6 boreholes in the western part of Naxos and concluded that the embayments were frequently exposed, and their communication with the sea was not perennial. Furthermore they suggested a RSL change of 1.5 – 2 m during the last 2000 years.

Recent research by Evelpidou *et al.* (2012d; 2014a) revealed the existence of seven submerged notches in SE Cyclades, suggesting the occurrence of rapid subsidence events, potentially of seismic origin. Evelpidou *et al.* (2014) placed these relative sea-level changes between about 3300 BP and very recent, by comparisons with other sea-level indicators from Naxos and Delos islands.

PART B – METHODOLOGY

Chapter 3 – Methods

3. Methods

In the investigation of sea level changes, coastal evolution and paleogeography a series of research tools are available, which could broadly be divided in field and laboratory activities.

For the purposes of this thesis, beachrocks were studied in detail, coastal archaeological remains were revisited, coastal drillings were performed in selected sites and aerial photography also took place at selected locations (Figure 16).

In order to set up a reliable chronological framework for sea level changes in the study area during the Upper Holocene, two dating methods were applied: OSL method for the submerged beachrocks and radiocarbon dating for the core samples (shells).

A comparison with already published data was also performed. The results of this research were compared with radiocarbon datings of beachrocks from Mykonos, Delos and Rhenia (Desruelles *et al.,* 2009) corings from coastal lagoons in Naxos (Evelpidou *et al.,* 2012c), as well as archaeological information.

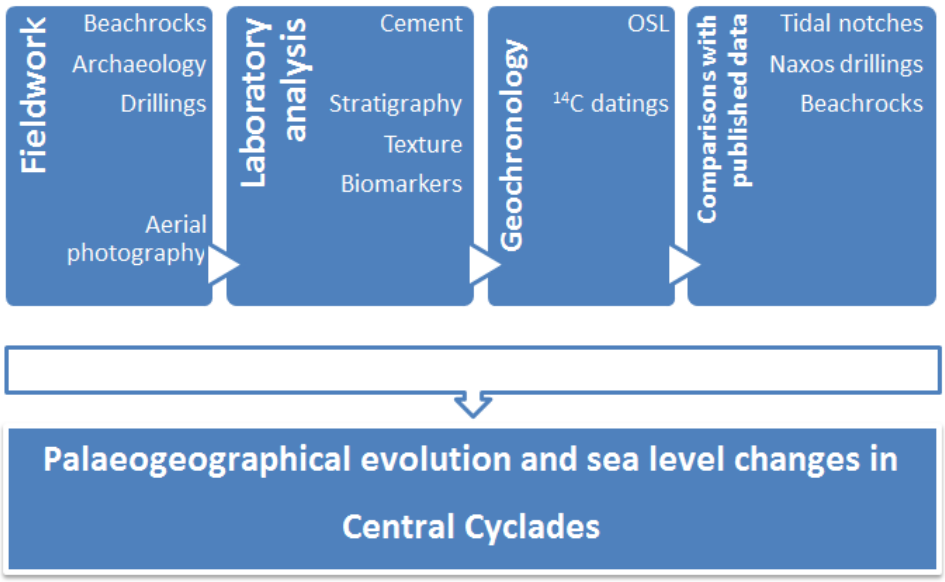

Figure 16: Diagram of methods applied for this thesis.

3.1 Beachrocks – Field and laboratory methods and techniques

3.1.1 Field methods

The coastal zone of Paros and Naxos islands was investigated in detail in order to trace beachrock remains. For each site the methodology applied included the following activities:

1) Detailed mapping of beachrock slabs (Figure 17). The mapping was mainly performed by snorkeling, as the beachrocks lay underwater. Depending on the length of the shoreline and the beachrock characteristics, one or more underwater transects were carried out. In order to record beachrock characteristics and identify different generations, the depth (from the top of the beachrock) in relation to present sea level, width and, if present, sediment bedding and architecture were recorded. The depth was recorded in the front (seaward) and end (landward) slabs of each beachrock, using hand-held sonar, with a precision of ≤0.5 m. Multiple measurements were performed for each location and the average value is provided as the depth value. Beachrock width was measured using a measuring tape and all data were recorded using a PVC slate.

For each site, a coastal transect was also accomplished. The results from the beachrock mapping are presented in sketches for each site.

2) Detailed sampling of beachrocks (Figure 18). Samples were collected from all sites in order to a) study the nature and composition of carbonate cements and b) to date them using the OSL method. Sampling took place from both the front and end slab of each beachrock band using a sledgehammer (Figure 19).

Figure 17: Beachrock mapping in (a) Glystra (E Naxos Island) and in (b) Agios Georgios (W Naxos Island).

Figure 18: Sampling of beachrock front slab in Agios Georgios (W Naxos Island), at a depth of about -6 m.

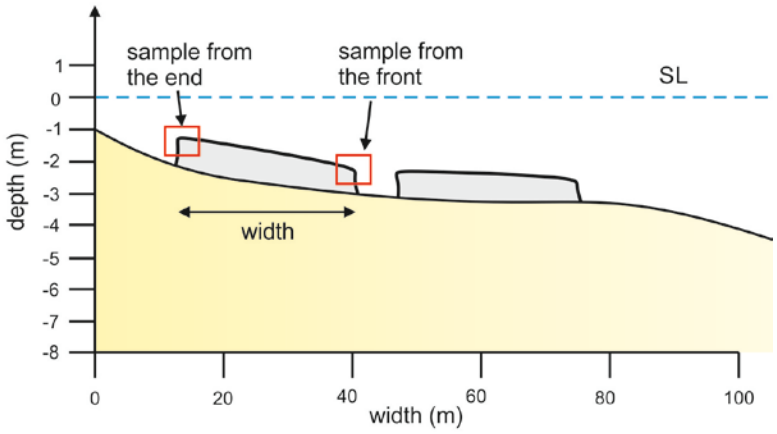

Figure 19: Beachrock sampling for dating and microscopic examination took place at the front and end beachrock slabs, at each site.

3.1.2 Laboratory analysis

An in situ beachrock is a sea-level indicator on the basis of its cement and its sediment texture and bedding structures. The clarity of its indicative meaning (its relation to the tidal range) depends mainly on the preservation of the original cement and the ability to link cement with other sedimentary information (Mauz *et al.,* 2015b). The examination of the cement is, therefore, an important phase to determine the depositional environment.

Thin sections were cut in order to perform petrographic and microstratigraphic analyses. These observations allowed the characterization of the constituents, the presence of bioclasts as well as the definition of the cements characteristics.

About 30 samples were examined under a polarizing microscope (Microscope LEICA DM RXP) at CEREGE (Centre Européen de Recherche et d'Enseignement de Géosciences de l'Environnement), in Aix-en-Provence, France (Figure 20). Observations included the recording of cement morphology, grain size and shape as well as presence of bioclasts.

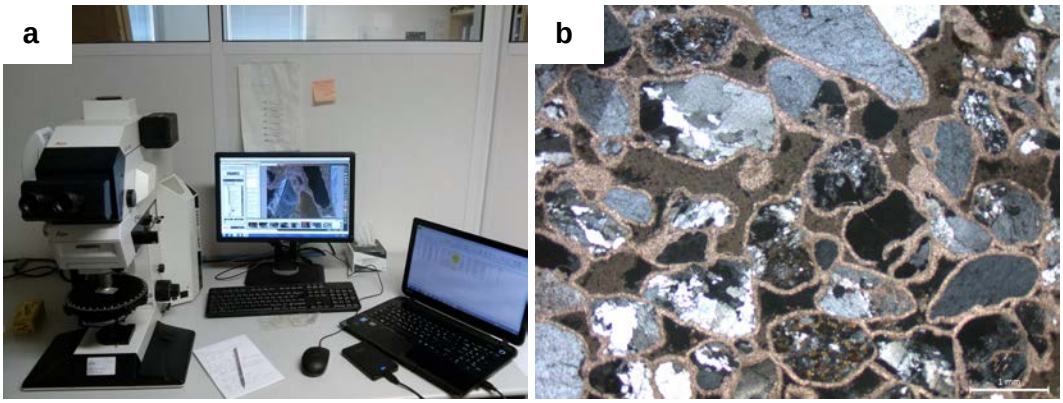

Figure 20: a) Examination of beachrock thin sections at CEREGE, b) Example of thin section from Plaka beachrocks (W Naxos Island). Sample was taken from -1.5 m depth.

3.2 Geoarchaeological methods

According to Renfrew (1976), geoarchaeology requires the skills of geology, which are focused on an archaeological site, in order to examine the predominant conditions of its location, its formation, preservation and history. Geoarchaeology is primarily concerned with the context in which archaeological remains are found.

The Mediterranean Sea, from an archaeological point of view, is a unique basin with numerous evidence from communities living on its shores and coastal plains, along with their maritime communications and their activities. Nowadays, such evidence lie emerged or submerged and can provide useful information for the reconstruction of ancient shorelines (e.g. Morhange *et al.*, 2001; 2013). Although not all archaeological proxies can allow an accurate quantification of sea level change, some are useful to constrain these changes while other archaeological records may provide evidence for palaeoseismic events.

Archaeological remains are often used in the study of sea level changes, especially when their relation to sea level is clearly defined. Apart from the obvious evidence of minimum relative sea-level rise provided by submerged structures that must have their foundations on dry land (e.g. houses, tombs, mosaic floors, passageways with a floor, storage tanks, etc.), frequent archaeologic examples refer to structures that may have been partly in the sea and may provide reliable sea-level indicators (e.g. slipways, breakwaters, jetties, quays, docks, channels, drains, salt pans, the lowest part of certain flights of steps or of coastal quarries having used a wood splitting wedge for cutting the lowest level of stones, or installations for fishing or fish farming). A recent review of criteria that might be applied for sea-level estimations from archaeological remains has been attempted by Auriemma and Solinas (2009). For a reliable estimation of the ancient sea-level height, a good understanding of the functioning of the structure and of the local hydrographic and climatic constraints is always essential.

In this context, archaeological information from the study area was studied in detail and, where possible, coastal sites were visited (Figure 21) in order to measure those features that can be useful in sea level changes.

Figure 21: Submerged remains of a Roman building in Paroikia bay, where the modern capital of Paros is located (NW Paros Island).

3.3 Aerial photography

Aerial photos are common tools for coastal geomorphology and coastal geology. The increasing use of Unmanned Aerial Vehicles (UAVs) has allowed coastal geomorphologists to obtain detailed aerial photographs of areas of geomorphological interest with high resolution. UAVs allow collecting low-altitude aerial imageries, developing Digital Surface Models (DSM) at high spatial resolution and vertical accuracy and mapping coastal and shallow submarine features.

In this context, aerial photos were obtained from selected sites in Paros and Naxos Islands, aiming to: a) study and map in detail particular submarine features and b) facilitate the reconstruction of the coastal palaeoenvironment.

The UAV (drone) used was eBee, SenseFly and its characteristics were the following:

- Height of the flights: maximum 300 m from sea level
- Aircraft: Unmanned Aerial Vehicle (UAV) with one propeller
- Wingspan: 96 cm
- Weight: 700 grams

Five locations were selected for Paros Island and three locations for Naxos Island with corresponding aerial photographs. In order to carry out the aerial photography at each site, it was necessary to locate a wide flat space for the take-off and landing of the UAV. Using special software, the desired area to cover is defined, along with required ground resolution and image overlap, and a full flight plan is generated with flight lines (Figure 22). The aerial photographs had resolution 3cm/px and the produced orthophotomaps 3 – 8 cm/px.

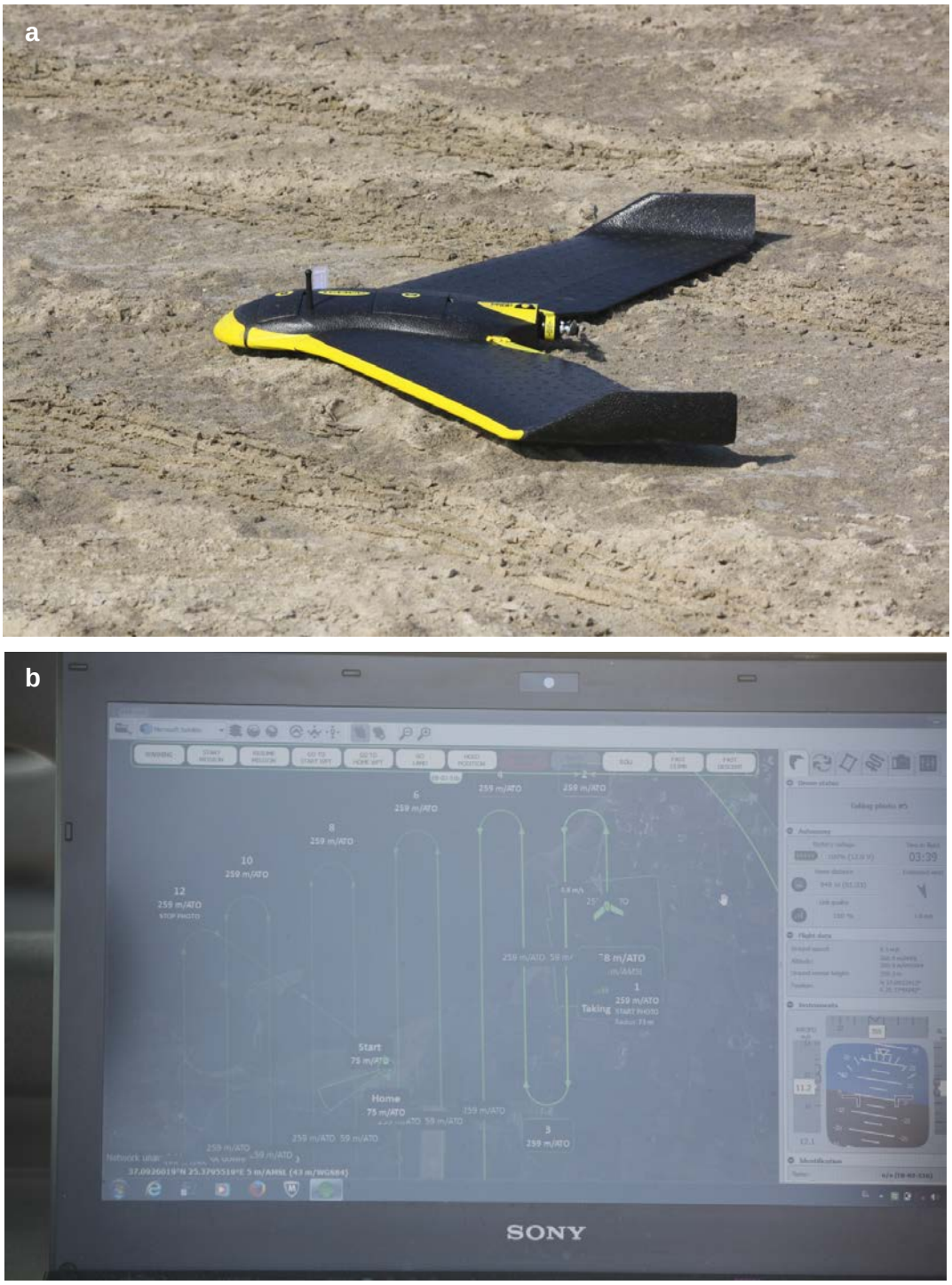

Figure 22: The UAV used for the aerial photos (a) and the software used for programming and controlling the flight (b).

3.4 Coastal corings

The relatively recent sediments, which were deposited in various geoenvironments, record a range of information that can determine the paleogeography of a region and the various changes in sea level, through datable material which is possibly found at a certain depth of the stratigraphic column.

3.4.1 Fieldwork

One of the most important steps for the coastal corings was site selection and for that purpose information for the coastal wetlands of Paros was collected beforehand and potential drilling sites were visited in order to assess their state and potential. After field investigations, six sites were selected.

The boreholes were made using a portable drilling machine (Figure 23), and 7 closed cores were obtained with a total cumulative drilling depth of 22.32 m. The location and altitude of the boreholes was recorded with GPS.

Figure 23: View of the drilling machine used, at the site of Pounta (SW Paros).

3.4.2 Laboratory analysis of coastal cores

After the drilling process, the obtained cores were maintained closed until they were transferred to the laboratory. The coastal cores obtained were processed at the CNRS laboratory, at Bensaçon, France (CNRS, Laboratoire Chrono-Environnement UMR 6249, Université de Franche-Comté). The opening of the cores is done in a specific way, so as not to disturb the stratigraphic horizons and transfer material from one layer to another. In particular, the core was placed in a horizontal position and was carefully divided in two equal parts, in order to examine the stratigraphy (Figure 24).

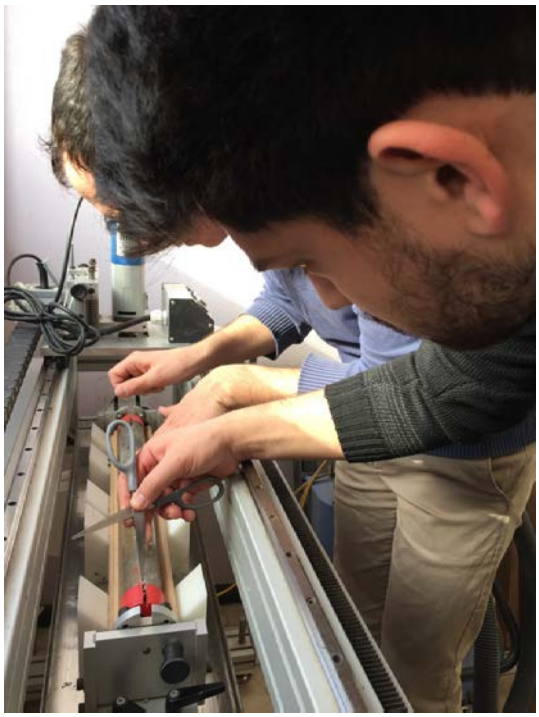

Figure 24: Opening of the cores was performed cautiously so as not to disturb the stratigraphic horizons.

3.4.2.1 Stratigraphy

Before any sampling takes place, the cores are scanned and photographed. In this way, the original cores and details are recorded, in case some information is missing or some specific details need to be re-examined. During scanning, the magnetic susceptibility along the cores is also recorded, which allows to track any changes in the nature of the sediments.

In order to examine and record the stratigraphy of the boreholes, each core is placed horizontally using a scale. By visual inspection, all changes in the stratigraphy are recorded, and their physical characteristics are also examined, i.e. color, texture, grain size. Also, the presence of archaeological remains, shells, gravels or other characteristics are recorded, i.e. characteristics suggesting changes in the deposition environment. During this phase, organic remains, shells, roots, or charcoal, may be collected for radiocarbon dating.

Figure 25: Scanning of the cores and recording of magnetic susceptibility at the CNRS laboratory, at Bensaçon, France.

3.4.2.2 Sediment texture and granulometry

Grain size analysis can provide information about sediment dynamics and coastal processes, especially if coupled with other proxies from the cores. For this purpose, each core is divided into a series of sub-samples; the interval of sub-samples mainly depends on the nature of the sediments. Smaller intervals ensure more precise reconstructions and chronology.

The samples were oven dried at 50°C and the dry sediments were weighted (Figure 26). The sediments were washed through two sieves, in order to separate gravels, sands and silts-clays. The dry fractions are afterwards weighted and the results are plotted in percentages.

Figure 26: Each core was divided into sub-samples, which were oven-dried, weighted and separated through sieving to gravels, sands and silts-clays.

3.4.2.3 Biostratigraphy

Biostratigraphy is an important tool for the reconstruction of depositional environments and the interpretation of coastal evolution (Figure 27). The most common palaeontological analysis includes mollusks, foraminifera, ostracods and diatoms. In order to reconstruct the palaeoenvironmental changes in the study area, macrofossils were recorded and identified as well as ostracods.

Figure 27: Biostratigraphic markers found in the coastal cores of Paros. From left to right: Loripes Lacteus (characteristic of lagoonal environment); Nassarius louisi (Upper-clean sand assemblage); Bittium reticulatum reticulatum (Infralittoral sand assemblage).

3.4.2.3.1 Macrofossils

The gravel fraction of the sediments was examined to record and identify mollusc shells and determine their ecology. Macrofossils were identified and assigned to assemblages based on d' Angelo and Gargiullo (1978) and Doneddu and Trainito (2005).

3.4.2.3.2 Ostracods

Ostracods are small crustaceans, consisting of soft body parts covered by a bivalve calcareous carapace, with a length of 0.3 – 30 mm (Athersuch *et al.,* 1989). They are found in any aquatic environment, from the shoreline to the deep sea and they are abundant in all Phanerozoic rocks. They are considered as important stratigraphic and environmental indicators, because their carapace has numerous morphological characteristics that allow taxonomic studies. Ostracods are excellent indicators of palaeoenvironments because of their ubiquitous presence in fresh and marine waters, their small size and their easily-preservable carapaces (e.g. Holmes and Chivas, 2002; Frenzel and Boomer, 2005; Marco-Barba *et al.*, 2013; Rossi *et al.*, 2015).

In order to record and identify ostracods on the coastal cores, the sand fraction was used. A minimum of 100 valves is preferred to ensure statistical robustness (Marriner and Morhange, 2007). The identified taxa were assigned to five assemblages on the basis of their ecological preferences: fresh water, lagoonal, marine lagoonal, coastal and marine (Breman, 1975; Bonaduce *et al.,* 1975; Carbonel, 1980, 1982, Marriner, 2007).

3.5 Geochronology

3.5.1 Optical Stimulated Luminescence

Optically Stimulated Luminescence (OSL) provides the depositional age of sediments, based on the time elapsed since the last exposure to sunlight of mineral grains (Aitken, 1998). It is based on the assumption that during sediment transport, geological luminescence is erased to a residual level by the sunlight (bleaching) and when the sediment is buried, the luminescence signal begins to grow due to the ionizing radiation present in the natural environment. The (latent) luminescence signal is zeroed by exposure to heat or light. In sediment dating, the zeroing event is the exposure to daylight during erosion, transport and deposition of the mineral grains. This zeroing is also known as bleaching.

This luminescence signal can also be released in a laboratory, using either heat or light, and the emitted luminescence signal will be recorded (Equivalent dose – De). The emitted luminescence is called Optically Stimulated Luminescence when the measured signal derives from the exposure of the mineral grains to light (Figure 28).

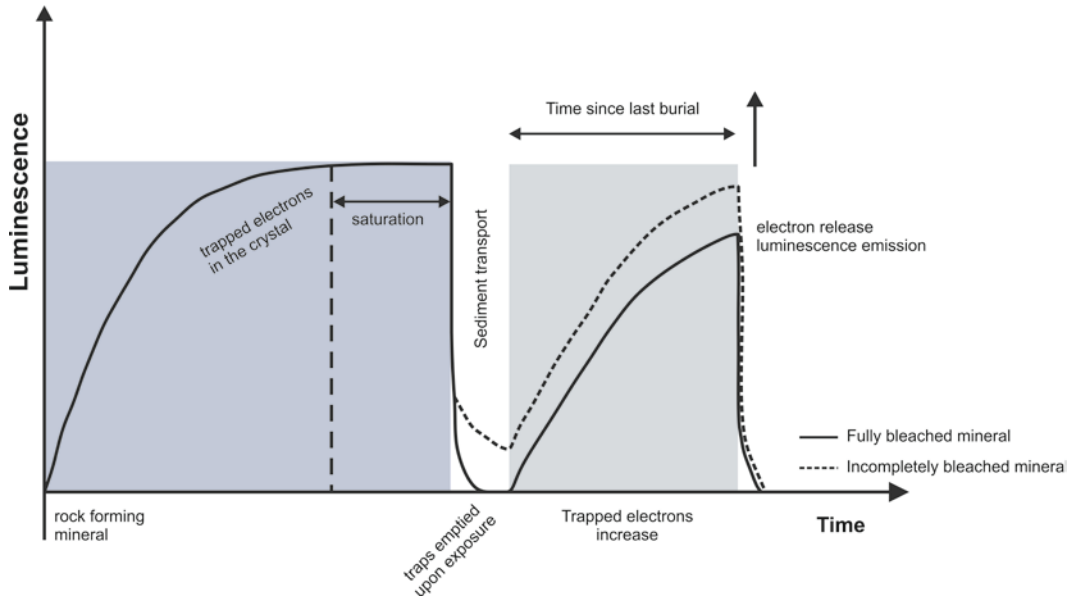

Figure 28: Schematic representation of the history of a mineral from the host-rock to the depositional event and its dating in the laboratory (after Cordier, 2010).

In the latter case, the signal recorded corresponds to the dose the mineral has received since its last exposure to light (the last zeroing event). If we can also determine the rate at which the dose was absorbed (dose rate), then it is possible to calculate an age; this age will correspond to the time elapsed between the moment

that the sediment was deposited and the moment for sampling. The age is then calculated using the following equation:

$$Age = \frac{Equivalent\ Dose\ (Gy)}{Dose\ Rate\ (Gy\ per\ year)}$$

One of the most significant advantages of luminescence dating is that the material it is applied to is found in almost all sedimentary environments. The method does not require the presence of organic material, as for radiocarbon dating, and it provides direct depositional ages for a number of different coastal features. Luminescence can be applied to quartz and feldspar minerals which are widely available both in offshore marine and onshore coastal sediments (Bateman, 2015).

One important factor is whether sand grains in the coastal zone have been sufficiently bleached. A number of recent studies (e.g., Murray and Mohanti, 2006; Thomas *et al.*, 2008) have shown that the predepositional luminescence signal is bleached to a negligible residual level in a beach environment (Huntley and Prescott, 2001). The sand grains are continuously exposed to sunlight due to the swash and backwash process, in the intertidal zone, which enables bleaching of the predepositional luminescence signal (Thomas, 2009). According to Mauz (2015), lithified coastal sediments, such as beachrocks, are usually well bleached, they may, however, present problems with dose rate. Therefore, caution is needed for changes in dose rate through time through the dissolution of carbonate cement, in concentration of radioactive elements (notably K and U), and also in water content.

In terms of age range, quartz OSL may extend up to 400,000 years (Wallinga *et al.*, 2007), while feldspar may reach up to 500,000 years (e.g. Thiel *et al.*, 2011).

During the last decade, the OSL method has also been attempted to date beachrocks for the reconstruction of palaeoshorelines along the Brazilian coast (Barreto *et al.*, 2002; Tatumi *et al.,* 2003), India (Thomas, 2009) and Turkey (Erginal *et al.*, 2010) and the results were also compared/constrained by independent dating such as radiocarbon dating.

The beachrocks were dated by using OSL dating of quartz and infrared stimulated luminescence (IRSL) of feldspar. The lithology of both islands is dominated by metamorphic and igneous rocks; therefore in the beach sands of both Islands, there is abundance in quartz and feldspar. Eight samples were selected for dating from Paros and Naxos Islands (Table 5), all showing characteristics of intertidal cement (for details see chapter 5). Because the beachrocks provided evidence of intertidal formation, the selection of samples for dating was based on depth distribution. The

samples were processed at the Leibniz Institute for Applied Geophysics (LIAG), in Hannover, Germany, through a DAAD scholarship during October – December 2014.

Table 5: Location, depth and laboratory codes of beachrock samples

Location	Longitude	Latitude	Depth (m)	Lab number
Naxos	25.3623	37.0900	-1.9	3163
Paros	25.1410	37.0969	-5.6	3164
Naxos	25.3733	37.0475	-1.5	3165
Naxos	25.3623	37.0900	-5.7	3166
Naxos	25.3916	36.9916	-4	3167
Naxos	25.3709	37.0276	-3.4	3168
Naxos	25.5852	37.0721	-3.8	3169
Naxos	25.3733	37.0475	-2	3170

3.5.1.1 Preparation for luminescence measurements

The preparation of the samples took place under subdued red light. All samples were primarily soaked with 10% HCl to remove the outer layer of the beachrock sample, which had been exposed to light. The remaining inner part of the sample was then treated with 10% hydrochloric acid (HCl) in order to remove the carbonate cement and obtain loose sediment. The samples were dry-sieved to obtain grains of 100-300 μm in size for samples 3166-3170, 200-300 μm for sample 3163, 150-200 μm for sample 3164 and 300-630 μm for sample 3165. The grain size fractions were selected according to the grain size of each sample. The selected sand portion was then treated with HCl to remove any remaining carbonates, with sodium oxalate ($C_2Na_2O_4$) to remove mineral aggregates and finally with H_2O_2 to remove any organic matter. The quartz and K-feldspar grains were isolated through density separations using Na-polytungstate. The quartz fractions were etched with HF to remove the outer part of the grains and remaining feldspar. After etching, the quartz samples were re-sieved to ensure the removal of finer grains. For sample 3165, the fraction smaller than 300 μm was used for OSL measurements of quartz after re-sieving, because larger grains are not suitable for the measurement in the luminescence reader. For the same reason K-feldspar of this sample was sieved between 300 and 355 μm for the luminescence measurement. The quartz and K-felspar grains were mounted on stainless steel discs with a diameter of 9 mm using silicone spray. All luminescence measurements were performed using a Risø TL/OSL DA-20 reader. The single-aliquot regenerative dose (SAR) protocols (Table 6; Murray and Wintle,

2000; 2003) were applied for performance tests and the measurement of the equivalent doses (De).

Table 6: SAR protocols for a) quartz (blue OSL) and b) feldspar ($pIRIR_{150}$)	
a) Quartz OSL	b) $pIRIR_{150}$
Dose	Dose
Preheat (200°C, 10 s)	Preheat (180°C, 60 s)
	IRSL (50°C, 100 s)
OSL (125°C, 40 s)	IRSL (150°C, 210 s)
Test dose	Test dose
Preheat (160°C, 0 s)	Preheat (180°C, 60 s)
	IRSL (50°C, 100 s)
OSL (125°C, 40 s)	IRSL (150°C, 210 s)

3.5.1.2 Dose rate determination

The environmental dose rates were determined in the laboratory using gamma spectrometry. Each sample was crushed and stored for one month to establish radioactive equilibrium between ^{222}Rn and ^{226}Ra. Afterwards, measurements were accomplished using a gamma-spectrometer with a high purity germanium detector. The dose rate was calculated following the dose-rate conversion factors provided by Guerin *et al.* (2011).

In order to estimate the water content, test measurements were performed on 25 beachrock samples from the study area. In particular, the samples were obtained and kept in sea water (from the same area of the sample) until they were weighted. Afterwards, they were oven-dried for three days at ~80°C and they were again dry-weighted. The minimum value measured was 6% while the maximum value was 26%, while most of the values ranged between 11% and 19%. An average value of 15±10% was therefore used for the calculation of dose rate (Table 7).

A potassium content of 12.5±0.5% was assumed for the internal dose rate of K-feldspar. The beta attenuation and the cosmic dose were calculated following Aitken (1985), Prescott and Stephan (1982) and Prescott and Hutton (1994), respectively. An a-value of 0.11 ±0.02 was used for alpha dose calculation for K-feldspar (Kreuzer *et al.,* 2014). Variations in the environmental dose rate through burial time due to the changes in water and carbonate contents for these samples would be possible,

however, due to the relatively high content of K of ~3 % (~1000 Bq/kg), which accounts for 75-80 % of the environmental radioactivity, these effects are considered to be small, except for sample 3169. For sample 3166 the sediment amount for gamma spectrometry was too little and therefore the measurement was not possible.

Table 7: Dose rate information from gamma spectrometry analysis										
Lab code	**Depth (m)**	**Water Content (%)**	**Grain size (μm)**	**^{238}U (Bq/kg)**	**^{226}Ra (Bq/kg)**	**^{210}Pb (Bq/kg)**	**^{232}Th (Bq/kg)**	**^{40}K (Bq/kg)**	**Dose rate quartz (Gy/ka)**	**Dose rate feldspar (Gy/ka)**
3163	-1.9	15±10	200-300	18.5±0.9	18.2±0.9	17.6±1.4	23.8±1.2	656±4	2.55±0.25	3.43±0.27
3164	-5.6	15±10	150-200	24.2±1.2	20.5±1.0	23.7±1.6	18.5±0.9	922±6	3.41±0.47	3.90±0.22
3165	-1.5	15±10	300-630 (300-355)[1]	14.9±0.7	12.9±0.6	16.2±2.3	16.7±0.8	1117±6	3.69±0.42	4.81±0.24
3166	-5.7	-	100-300		-	-	-	-	-	-
3167	-4	15±10	100-300	30.9±1.5	28.0±1.4	26.5±1.8	36.1±1.8	1142±6	4.16±0.49	4.95±0.41
3168	-3.4	15±10	100-300	23.1±1.2	23.8±1.2	24.1±2.0	33.7±1.7	1014±8	3.74±0.44	4.52±0.41
3169	-3.8	15±10	100-300	13.5±0.7	8.5±0.4	12.3±1.1	8.6±0.4	209±3	0.95±0.16	1.75±0.40
3170	-2	15±10	100-300	19.7±1.0	19.8±1.0	71.7±1.9	40.4±2.0	1042±5	3.88±0.45	4.67±0.41

[1] for feldspar

3.5.1.3 Quartz – Measurement performance and equivalent dose determination

In order to test the single-aliquot regenerative-dose (SAR) protocol and select the appropriate preheat temperature, dose recovery, preheat plateau and thermal transfer tests were applied at five different preheat temperatures (160-240°C). A preheat temperature of 200°C was selected for De measurements, because it yielded the dose recovery ratio close to the unity and with negligible thermal transfer (Figure 29).

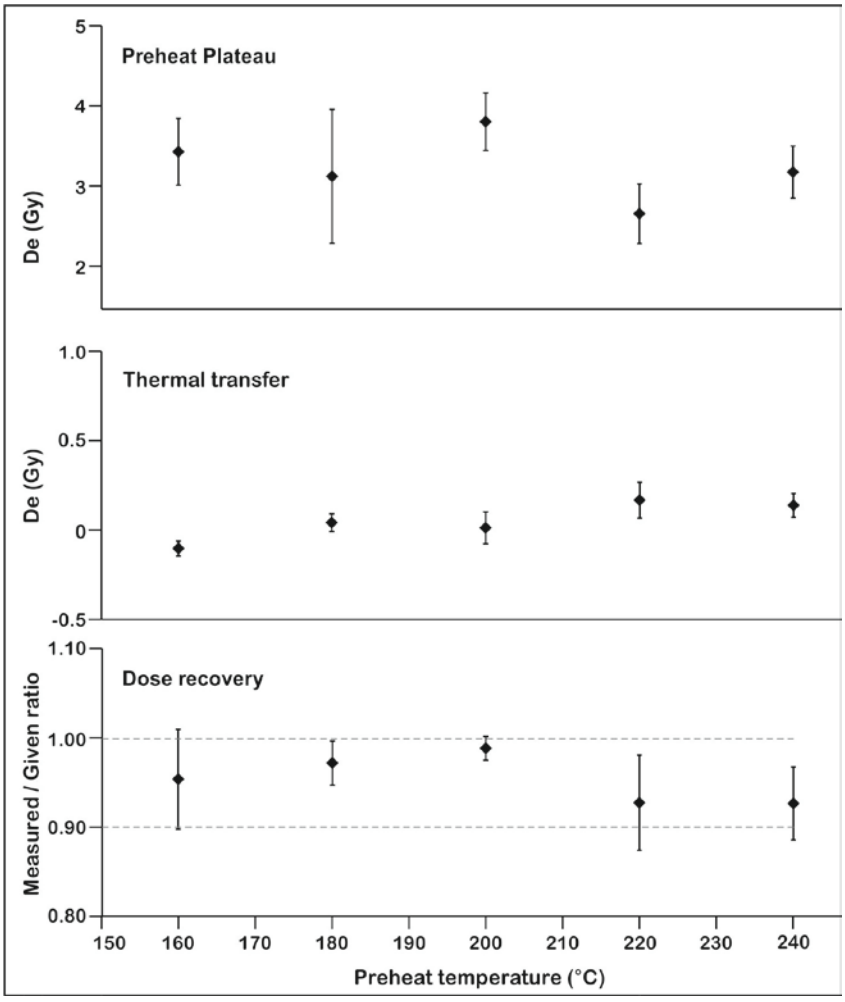

Figure 29: Preheat plateau, thermal transfer and dose recovery tests (sample 3163) were performed in order to test the single-aliquot regenerative-dose (SAR) protocol and select the appropriate preheat temperature. A preheat temperature of 200°C was selected for De measurements.

In addition, the SAR protocol was tested using a dose recovery test for each sample, which ranged between 0.86 ± 0.04 (sample 3168) and 1.06 ± 0.09 (sample 3165) with a mean of 0.97 ± 0.02 for all aliquots. For De measurements of quartz 24 aliquots per sample were used.

Aliquots with a recycling ratio >15% from unity were rejected. The mean De values and the 1-σ standard errors were calculated. The quartz OSL signals from the samples were generally very dim and not dominated by the fast component (Figure 30). For this reason, K-feldspar grains were also dated for comparison.

3.5.1.4 K-feldspar – Measurement performance and equivalent dose determination

For the tests and De measurements of feldspar the post-IR IRSL protocol with the elevated temperature stimulation at 150°C ($pIRIR_{150}$) (Reimman and Tsukamoto, 2012) was used due to the young ages of the samples The dose recovery, residual dose and anomalous fading tests were performed for three samples (3163, 3164 and 3167), using 6 aliquots per sample. The measured / given dose ratio (dose recovery ratio) was close to unity (1.01±0.01 same for all samples). The values obtained from the residual dose test after bleaching with a solar simulator for 4 hours were very small, ranging between 0.05±0.004 Gy (sample 3167) and 0.12 ±0.02 Gy (sample 3163). All measured fading rates (g-values) for the $pIRIR_{150}$ signal are very similar: 1.34±0.26 %/decade (sample 3163), 1.41±0.26 %/decade (sample 3164) and 1.36±0.07 %/decade (sample 3167). 8-10 aliquots per sample were used for the De measurements and none were rejected due to their very close to unity recycling ratio. In Figure 30, $pIRIR_{150}$ dose response curves are shown for samples 3163 and 3168, along with natural decay curves.

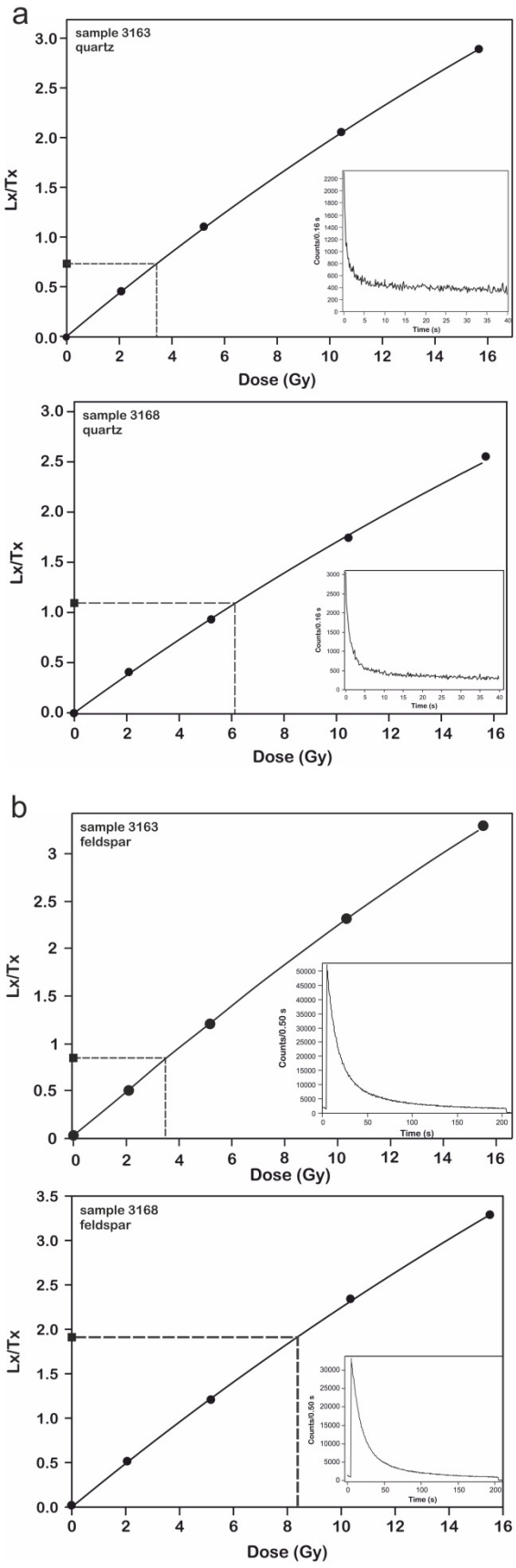

Figure 30: Quartz OSL (a) and pIRIR150 (b) dose response curves for samples 3163 and 3168. The inset shows natural decay curve for each sample.

3.5.2 Radiocarbon dating

The radiocarbon method was used for the samples deriving from coastal cores. The chronostratigraphy was determined by a series of 9 AMS radiocarbon datings on molluscan marine shells, performed at the Poznan Radiocarbon Laboratory (Poland). Further details are provided in chapter 6.

3.6 Reconstruction of relative sea level changes

The reconstruction of relative sea level (RSL) changes was accomplished following the robust methodology described by Hijma *et al.* (2015) and Vacchi *et al.* (2016b). Various sea level data are used for the production of sea level index points; however, no standardized method has been established for the Mediterranean. The database approach has been recently described in detail by Hijma *et al.* (2015) and applied for the western Mediterranean by Vacchi *et al.* (2016b). The usefulness of geological sea-level data is significantly increased if they are subjected to meticulous error analysis with well-quantified uncertainties. A sea-level index point (SLIP) estimates relative sea level (RSL) at a specified time and place, with an associated uncertainty (Hijma *et al.*, 2015).

For the production of a RSL index point the information necessary for each indicator is its location, its calibrate age and its elevation corrected for the indicative meaning (Shennan *et al.*, 2015; Hijma *et al.*, 2015; Vacchi *et al.*, 2016b). The indicative meaning describes where the sea level indicator has formed, in relation to the tidal levels (Shennan, 1982; Van de Plassche, 1986). It comprises of two parameters (Hijma *et al.*, 2015):

a) The indicative range (IR), which is the elevational range over which an indicator has formed, and

b) The reference water level (RWL), which is the midpoint of this range.

The RSL for each indicator is afterwards calculated according to RSL = E – RWL (where E is the altitude of the sample and RWL is the mid- point of the indicative range) (Hijma *et al.*, 2015).

On the occasion that a sea level indicator does not exhibit a clear, well-defined relation with MSL, it may be used as a limiting point (Shennan and Horton, 2002). Marine or terrestrial limiting points may be produced, which must fall above or below reconstructed RSL, respectively. Marine limiting points commonly correspond to

samples deposited in open marine, prodelta environments, or even lagoonal environments that do not meet the requirements to be classified as index points (Vacchi *et al.*, 2016b) , while terrestrial limiting points usually form at an elevation above HAT.

For the production of RSL index points from the cores two lagoonal facies were considered, as described by Vacchi *et al.* (2016b): a) open or marine-influenced lagoon facies samples with an indicative range from 0 to −2 m and b) Inner or semi-enclosed lagoon facies with an indicative range from 0 to−1m. Coastal lagoons are inland water bodies, separated with the open sea by a sandy barrier, and their depth seldom exceeds a few meters (Kjerfve, 1994). Although no modern analogues have been reported in the literature for the study area, the indicative ranges suggested by Vacchi *et al.* (2016b) are adopted considering the status of the coastal lagoons in Paros and Naxos. In the Cycladic area and in Paros and Naxos in particular, the contemporary coastal lagoons are usually dry during the summer, while during winter, their depths do not exceed 1-2 m.

For the beachrocks, according to the protocol recently provided by Mauz *et al.* (2015b), RSL index points (cf. Hijma *et al.*, 2015) were produced by samples showing clear intertidal formation. Cement characteristics include irregularly distributed needles or isopachous fibres of aragonitic cement or isopachous rims and micritic high-magnesium calcite (HMC) cement or HMC cement in stalactitic position and meniscus between grains) An indicative range between Mean High Water and Mean Low Water was considered for these samples.

PART C – RESULTS AND DISCUSSION

Chapter 4 – Geoarchaeological context and discussion

4. Geoarchaeological context and discussion

4.1 Geoarchaeological context of Paros Island

The archaeological remains in Paros include various constructions, such as moles, buildings, settlements and tombs, most of which are found submerged. However, not all the archaeological remains are dated, therefore, their use to constrain the relative sea level changes is limited. In the following paragraphs a brief overview of the most significant archaeological finds is attempted (Figure 31, Figure 32).

Figure 31: Paros Island is characterized by the presence of various archaeological remains. The figure summarizes the sites and locations of Paros, discussed in this text.

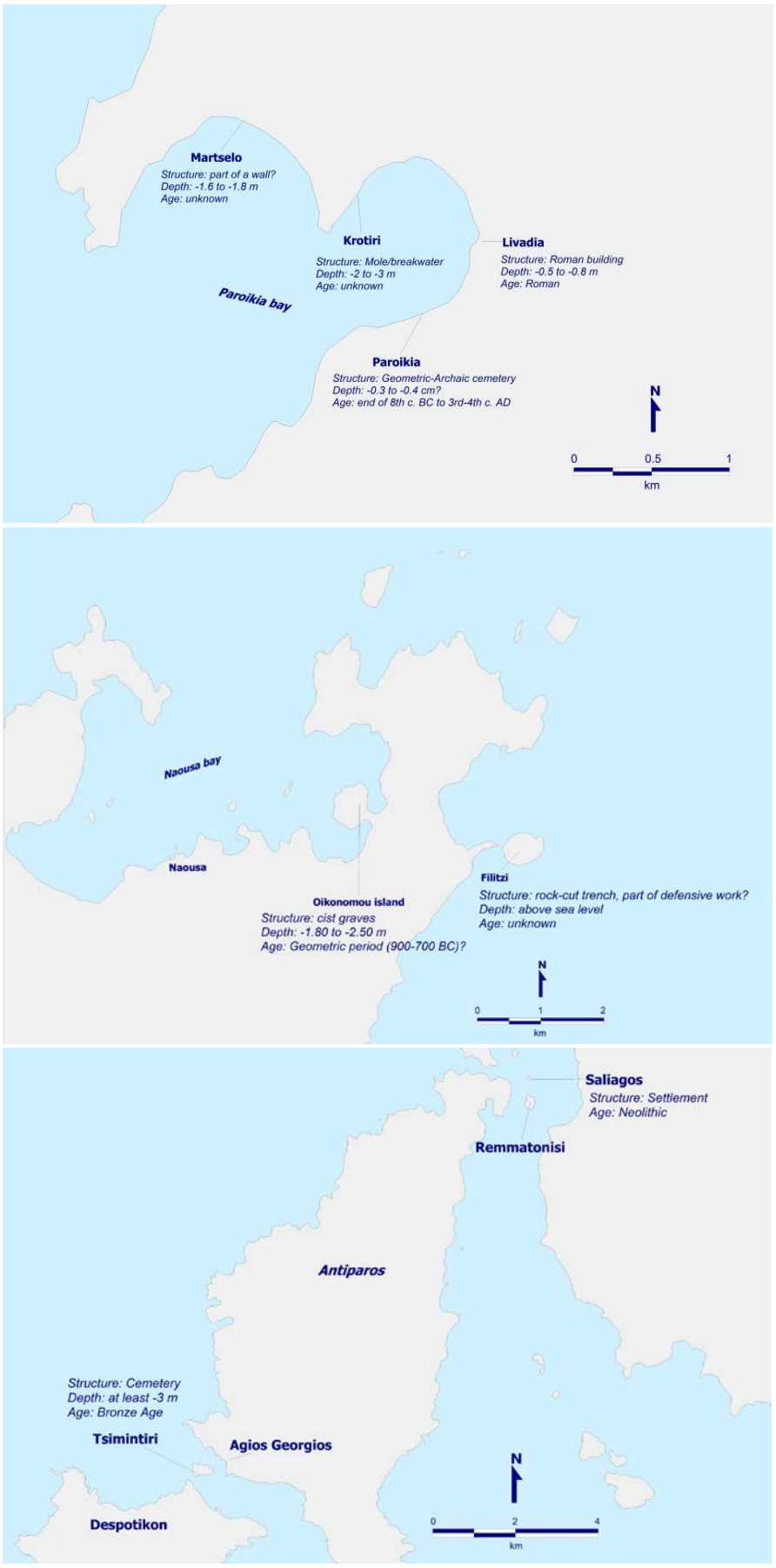

Figure 32: Overview of archaeological locations in Paros, discussed in the text.

4.1.1 Paroikia bay

In the NW part of Paros, in Paroikia, the Geometric – Archaic cemetery may be found, close to the ancient harbour (Figure 32). The cemetery was in use from the end of the 8th century BC, and its final phase dates in the 3rd-4th c. AD (Zapheiropoulou, 2000). Nowadays, the ground level of the excavation is under sea level and unless the water is strained constantly, the whole area of the excavation turns into a swamp within a few hours (Zapheiropoulou, 2000; 1990). Unfortunately the exact depth of the excavation is not mentioned in any archaeological reports or any published plans of the cemetery.

The only available datum so far is the depth of the Late Roman cemetery, which extends to the west of the Archaic and Classic one, in a neighboring plot (Zapheiropoulou, 1990). The type of graves in the Late Roman cemetery are dated to the 3rd c. AD; they were revealed in a depth of –1.50 m (below modern ground level) (Zapheiropoulou, 1990). Taking into consideration the elevation of the ground level and the depth of the sarcophagi an approximate depth of ~30-40 cm below sea level may be estimated.

In the bay of Livadia (Paroikia), Rubensohn (1949; 1901) has reported the existence of a submerged Roman building (Figure 33). Its date was deduced by the use of hard limestone bonded with mortar and puozolana in its construction (Papathanassopoulos and Schilardi, 1981; Rubensohn, 1901). According to Rubensohn (1901) the local name Ergasterakia or Magazakia indicated the original use of the building. In 1979, the remains of this construction were found 1 m offshore at a depth of 0.50 m below sea level (Papathanassopoulos and Schilardi, 1981). The upper course of the walls in the Roman building was measured at a depth of –0.80±0.1 m (Figure 34).

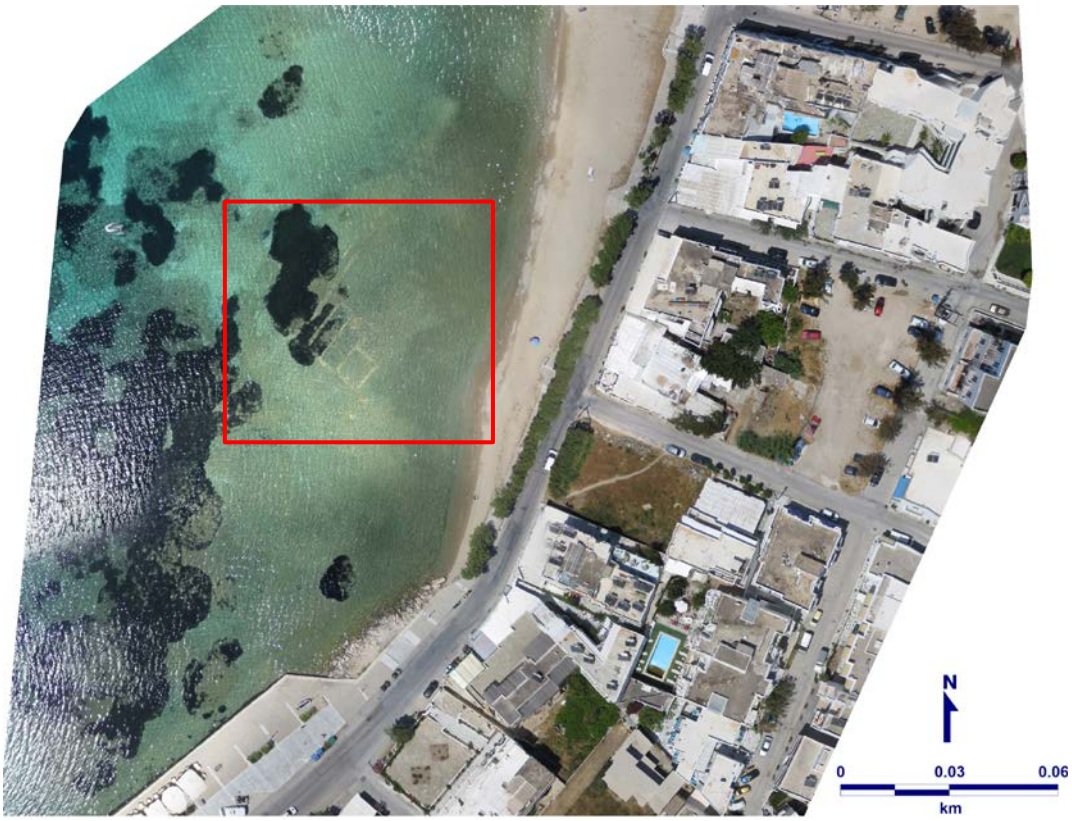

Figure 33: Remains of the submerged Roman building, in Paroikia bay (NW Paros). The local name Ergasterakia or Magazakia probably indicated the original use of the building.

Figure 34: Underwater photograph of the Roman building, in Paroika bay (NW Paros). The upper course of the walls was found at -0.8 m.

In the eastern coast of Livadia bay, during an underwater survey Papathanassopoulos and Schilardi (1981) reported the presence of an ancient mole, constructed of large sized rubble stones of schist. In 1979 the top of the mole was found at depths between -2 m and -3 m (Papathanassopoulos and Schilardi, 1981). According to Papathanassopoulos and Schilardi (1981), the mole has a length of 100 m, with a width of 9 m at its base and 6 m at the top. The satellite photographs on the other hand show that the width in the middle of the mole reaches 15 m and almost 9 m at its tongue shaped end. Although Papathanassopoulos and Schilardi (1981) do not mention the mole height, during our research, a height of 2-3 m was measured. The mole is now totally submerged, and visible to its full length only from a higher point of view (Figure 35). Measurements on the ancient mole differ from those by Papathanassopoulos and Schilardi (1981). Close to the shore the submerged mole is preserved in a low height, but approximately at the middle of its length its upper part lies at -0.80±0.2 m. The surface of the mole close to its tongue-shaped projection is located at -1.23±0.2 m.

Figure 35: The underwater construction on the eastern coast of Paroika bay (NW Paros). The mole remains undated as no evidence for dating were found by Papathanassopoulos and Schilardi (1981). (photo from https://www.tripinview.com/en?path=home)

In the NW part of Paros, Martselo beach is characterized, not only by submerged beachrocks, but also by several submarine constructions, not previously reported (Figure 36). The beachrocks may be distinguished in three slabs (see chapter 5). The first slab (shallower) is located between -0.8±0.2 and -1.8±0.2 m, the second is

found between -2±0.2 and -3.4±0.5 m and the deepest one between 3.7±0.5 and 5.6±0.5 m. All the submarine constructions are aligned parallel to the modern coast, in the East-West axis. Part of a wall was observed in a depth of -1.7±0.2 m, 1.5 m wide, built in the *emplecton* technique (i.e. two parallel lines of large rubble stones whose space in between is filled with smaller stones), a way of construction applied by the Romans (Plin. NH 36, 171. Vitr. 2.8,7). In another location of the same site, 6 large rubble stones are set in line, orientated in an East-West axis, possibly consisting part of a wall. They are located approximately 15 m from the coastline, at a depth of -1.6±0.2 m. Close to this location a construction that seems like a pavement in situ was identified, consisting of small quadrate stones. It has an East-West orientation and it is found at a depth of ~1.8±0.2 m. It cannot be observed in a great length, due to the slabs of beachrock that have covered part of it. A small part of this pavement extends a little farther to the West.

Figure 36: Part of the submerged constructions in Martselo beach (NW Paros), found at about -1.6 m depth.

4.1.2 Naoussa bay

In the east part of Naoussa bay, at Oikonomou island, an underwater survey by Papathanassopoulos and Schilardi (1981) revealed a group of three cist graves made of gneiss slabs, located in a depth of 1.80-2.50 m (Papathanassopoulos and Schilardi, 1981; Schilardi, 1973). Their distance from the shore is 15 m, and they are probably to be associated with the *peribolos* on Oikonomou Island (Papathanassopoulos and Schilardi, 1981). The evidence from the surface as well as the architecture of the settlement assigns the finds on Oikonomou Island to the Geometric period (900-700 BC) (Schilardi, 1975a). Oikonomou island nowadays forms a tombolo (Figure 37; Figure 38), which was not reported by Rubensohn (1901) but was later reported by Schilardi (1973).

Figure 37: The tombolo of Oikonomou Island, in Naousa bay (N Paros).

Figure 38: View of Oikonomou Island. The ancient settlement on the island was dated to the Geometric period (900-700 BC), while also submerged cist graves were found near the shore.

Filitzi islet is located at the northeastern part of Paros. In the SE part of Filitzi, remains of ancient buildings have been identified (Schilardi, 1975b). A 2 m wide fortification wall built in the polygonal system protected the settlement in its southern and eastern part (Schilardi, 1975b). An impressive feature is the construction of a wide trench in the outer periphery of the fortification wall, which surrounded the hill in the same parts. This trench begins in a distance of 21.50 m to the east of the fortification wall; It has a direction from North to South, then turns to the NW and ends to the sea (Schilardi, 1975b). This trench is rock-cut, covers a distance of about 400 m and has a width of 3-3.50 m (Schilardi, 1975b). According to Schilardi (1975b) this trench was part of a defensive work that needs to be studied in the future. In

Filitzi bay, three parallel trenches form a chord of a circle in relation to the curved outline of the bay (Schilardi, 1979). Their surface is now underwater, but they were probably above sea level during antiquity (Schilardi, 1979). Schilardi (1979) suggests that these rock-cut trenches belonged to huge constructions that were part of huge harbor project, perhaps docks for the exportation of marble by ships.

4.1.3 Drios

In the southeastern coast of Paros, on Drios coast, Auffray (2002) noted a group of rock-cut trenches, which lie above sea level. According to Auffray (2002), 15 rock-cut trenches are found, with a length of 40-50 m, a width of 0.80-0.90 m, and a thickness of about 0.40-0.50 m. The space between them ranges from 1.20 m to 1.30 m (Auffray, 2002). The prevailing interpretation for these trenches is that they belong to ship sheds (Auffray, 2002), while, according to Evans and Renfrew (1968) they are Hellenistic vineyards. Simosi (2009) on the other hand rejects the ancient chronology of these trenches and considers them as works of the inhabitants in an era that postdates antiquity. Whatever the case might be, the site of Drios needs further archaeological and geological investigation.

4.1.4 Antiparos

At least four underwater sites with carefully built structures that seem to be Bronze Age cists were traced around Antiparos (Evans and Renfrew, 1968). Morrison (1968) mentions that one of these underwater Bronze Age cemeteries lies in a depth of at least 3 m off a small island between Agios Georgios and Despotikon (Tsimintiri) (Figure 32); this islet bears a proved Bronze Age cemetery on its surface.

Evans and Renfrew (1968) refer to a systematic underwater topographical survey in the area of Antiparos conducted by divers from Imperial College, London, and Cambridge University, together with Mr. Ian Morrison of Edinburgh University. They also excavated a submerged system of rock-cut trenches on Antiparos in 1964. The results of this excavation and the underwater survey had not been published in 1968 (the year of the publication of the excavation of Saliagos), and they still seem to remain unpublished.

4.1.5 Saliagos

On the islet of Saliagos, Evans and Renfrew (1968) reported the existence of a Neolithic settlement. According to these findings, Morrison (1968) suggested a recent submergence for the islet of Saliagos. For a long period of time, Saliagos must have been over twice its present size, and if we take into account a rise in the sea level from at least 3.50 m (and maximum 5 to 6 m), “then it would have been possible to wade from there [Saliagos] first to a considerably larger Remmatonēsi and thence to the extended shores of either Antiparos or Paros” (Morrison, 1968).

4.2 Geoarchaeological context of Naxos

In Naxos Island, the most significant archaeological data are found in the northwestern part, where the modern capital is located (Figure 39). Most of the findings are related with archaeological excavations accomplished in Chora Naxou.

Figure 39: The archaeological sites in Naxos discussed in the text, are located on the western coast of Naxos, mostly around the modern capital.

4.2.1 Chora Naxou (modern capital)

In Grotta the floors of House B and Room A of House A were found at -0.55 m (Cosmopoulos, 1998; Kontoleon, 1967a), dating to the LH IIIA1-IIIA2 period (ca. 1400-1300 BC) (Cosmopoulos, 1998). After an earthquake demolished House B in an early phase of LH IIIA2 (ca. 1375-1350 BC), life in the settlement continued (Cosmopoulos, 1998; Kontoleon, 1967a). Room A´ was actually built in the place of House B, and became the third room of House A (Cosmopoulos, 1998; Kontoleon, 1967a). The floor of Room A´ was constructed slightly higher than that of Room A; a layer of pebbles was placed under the floor of Room A´ that stood at -0.45 m, i.e.

0.10 m higher than the rest of the floors of House A (Cosmopoulos, 1998). Room B was added later to House A, in the LH IIIC period (ca. 1190-1075 BC); its floor stood at –0.20 m to –0.10 m (Cosmopoulos, 1998).

In Plateia Metropoleos the ruins of the Mycenaean settlement were revealed in a height close to sea level (Zapheiropoulou and Lambrinoudakis, 1982). In Grotta, in a distance of 30 m from the coast, it seems that the ruins of the Mycenaean settlement were preserved at a height between +0.40 m and at least –1.20 m, in relation to the modern sea level (Lambrinoudakis, 1985). The pure Mycenaean strata were preserved up to the height of +0.20 m to +0.40 m above sea level (Lambrinoudakis, 1985). Below the level of –1.20 m the excavation could not proceed due to technical difficulties (Lambrinoudakis, 1985).

During the excavation of the Cathedral Square (Plateia Metropoleōs) it was made quite clear that a time period of abandonment intervened between the older and the younger phase of the settlement (Lambrinoudakis and Zapheiropoulou, 1985). Could this period of abandonment be explained or even attributed to certain tectonic phenomena?

The case of three Late Helladic IIIC (1190-1075 BC) chamber tombs in Aplomata provides intriguing evidence. Part of these tombs has been detached from the slopes of the coastal hills and has fallen into the sea (Kontoleon, 1958; Vlachopoulos, 2006). The findings inside these tombs revealed that the smashing of the bones and the clay vases is owed to a sudden collapse of the ceiling a little while after the use of the tomb, and definitely before the penetration of rain water and mud or the gradual detachment of parts of the ceiling (Vlachopoulos, 2006). According to Vlachopoulos (2006) the detachment of the tombs in Aplomata and the immersion of the settlement in Grotta are the combined result of an earthquake and a sea level rise.

Indeed, at Plateia Metropoleos Trench D3 (Walls 9 and 59) reached 3 m in depth (i.e. +0.30 m above sea level), due to springing water that did not allow the archaeologists to dig dipper (Chalepa-Bikake, 1983a, 1983b). Chalepa-Bikake (1983b) described a layer of pure sand at a depth of 2.40 m (i.e. at +0.90 m above sea level) at Trench D3, uncertain of its interpretation and wondering whether it is a flood.On the 23rd of August 1983 a floor is revealed at 2.78 m (i.e. +0.52 m above sea level) (Chalepa-Bikake, 1983b), on top of which lies a part of the roof. Between the pieces from the collapsed roof and the floor a very thin layer of sand was observed (Chalepa-Bikake, 1983b). The floor is made of clay and lies on top of a

thick stratum of sea sand with many stones and relics of a pre-existing Wall (Chalepa-Bikake, 1983b).

The lowest 0.70 m of this deposit consisted of pure sand with very few sherds dating to the Late Helladic IIIB2 or IIIC period (Chalepa-Bikake, 1983a, 1983b). The few sherds found on the floor (and therefore correspond to a second building phase) date the destruction to the Late Helladic IIIC period (1190-1075 BC) (Chalepa-Bikake, 1983a). This layer of destruction is overlain by a deposit (0.20 m to 0.90 m thick) with no architectural relics (Chalepa-Bikake, 1983a), which means that after the destruction of the Late Helladic IIIC period this area was abandoned (Chalepa-Bikake, 1983a).

It appears that this was not the only case of sea transgression on the north coast of Naxos. In the Hellenistic *Agora* of Naxos both Welter (Karo, 1930) and Kontoleon (1970) noticed a thick layer of sand without sherds exactly above the ruins of the *Stoas*. According to Kontoleon (1970) this suggests that the beach extended further towards the south, right after the destruction of the building.

Part of the North *stoa* was revealed close to the East one, located in the free space between the road to Eggares and the beach, in the west side of the stream running close to the city of Naxos (Kontoleon, 1967a). It was revealed in a depth of 5.40 m below modern ground surface (Kontoleon, 1967a). The foundation of the building was revealed 1 m below the modern sea level (Kontoleon, 1967a). The ruins of the North *stoa* were also covered by a modern deposit 1 m thick and a layer of sand that demonstrated the older surface of the beach (Kontoleon, 1967a).

The 1988 excavation continued in the interior of the Agora (Lambrinoudakis, 1988). The trench reached the depth of +0.85 m. The layer of sand reported by G. Welter (Karo, 1930) and Kontoleon (1967) was revealed at +0.60 m (Lambrinoudakis, 1988). The layer of destruction lies between +1.10 m and +0.60 m, consisting of a few sherds mixed with stones, mortar, pieces of lime and mosaic, as well as traces of fire (Machaira, 1988). At approximately +1.00 m the archaeologists found smoothed sherds and a large amount of pebbles (Machaira, 1988). The ruins of the *Stoa* along with the Roman structures that were built nearby seem to have been abandoned in the 2nd c. AD (Lambrinoudakis, 1988; Machaira, 1988).

4.2.2 Mikri Vigla

Mikri Vigla is characterized by the presence of submarine beachrocks; The shallower slab, located between sea level and -0.7 m or -1.7 m (Evelpidou *et al.*, 2012c), appears to have been quarried for the extraction of large thin rectangular or square slabs. It is worth noting that the beachrocks in Mikri Vigla are not well-preserved and therefore differences in depth measurements are expected. According to Dalongeville and Renault-Miskovsky (1993) the quarried beachrocks are attributed probably to the Hellenistic period.

4.3 Discussion

The mole in Livadia bay (Figure 40) bears resemblance to a tongue-shaped breakwater in Rheneia, in the area of “Lazaretto”, first published by Négris (1904). The Rheneia breakwater had posts fixed onto the surface of the quay; one of them was found *in situ*; it was roughly dressed and at least its visible part was similar to a cylindrical post (Dalongeville *et al.*, 2007; Négris, 1904). It is worth noting that the upper surface of the Roman quay at Rheneia lies at a minimum depth of -0.60 m. The breakwater that protects the quay lies a few decimeters under the modern sea level. The upper surface of the mole in Livadia bay is located at -0.80±0.2 m. They could all be contemporary. It is considered that in structures such as moles and breakwaters, marine abrasion must have lowered their surface, and the best preserved part is more reliable, since it is closer to their original height (e.g. Antonioli *et al.*, 2007; Auriemma and Solinas, 2009). Conversely, the measurement of the maximum depth can be very illusive, when used as a sea level indicator. Based on the aforementioned, it is more than likely that the protruding, perhaps well-built, part of the mole is now missing.

A recent study by de Graauw (2014), studied the relationship between the governing parameters (water depth, structure height, stone size) and the equilibrium position of the crest of rubble mound breakwaters subject to repeated wave attack in breaking wave conditions over many centuries. According to de Graauw (2014), an initially undersized emerging rubble mound breakwater will be eroded by the waves and finally reduced to a submerged breakwater whose height above the sea bed depends on its stone size and on the water depth.

Furthermore, if the submerged construction is a breakwater, then we should examine what urged the Parians to protect the coastline at a certain time period. In this case,

some parameters would have to be taken into account; a) how much has the construction been lowered due the wave action? b) the breakwater must have protruded at least 1 m above the surface of the sea; c) in which depth of the harbour could the breakwater be functional for the ships? d) When was it constructed? e) When was it abandoned? (cf. Knoblauch, 1972; Murray, 1988 for analogous discussion).

Figure 40: Inclining side of the submerged mole/breakwater in Paroikia bay (NW Paros).

A parallel to the Parian construction is provided by a manmade breakwater in the ancient harbour of Karthaia on the island of Kea (Mendoni and Mourtzas, 1985-86; 1990). Although its dimensions are much larger than the one in Livadia (it is 160 m long and 30-35 m wide), its trapezoidal section and the use of large boulders of schist could be indicative of their synchronicity. Karthaia's breakwater is now completely submerged at a minimum depth of -1.10 m according to the published plan of the breakwater (Mendoni and Mourtzas, 1985-86; 1990). Mendoni and Mourtzas (1990) consider the deepest surviving surface of Karthaia's breakwater and conclude that it is classical in date. The minimum depth of this breakwater differs from those from Paros and Rheneia and therefore places it in a much later period.

Supplementary evidence of such structures that postdate the classical period are found in Southern Italy and the Istrian coast; At Torre Saturo near Taranto a breakwater built with the technique of stone heaps without mortar was dated to the

2nd c. BC (Auriemma and Solinas, 2009). The published figure by Auriemma and Solinas (2009, fig. 9) depicts its trapezoidal section very clearly.

Naxos on the other hand provides data that may be correlated with various geomorphological indicators. For instance, a co-seismic event is represented by a tidal notch at -2.3±0.1 m on the submarine rocky coast of central Cyclades (Evelpidou *et al.*, 2014a). The inward depth of 23 cm suggests a relative sea level stability of 2.5 to 11 centuries before its rapid subsidence (see Evelpidou *et al.*, 2014a; Table 1, Tidal Notch B). This event could possibly be dated around 3100 BP based on the corresponding depth of the submerged settlement in Grotta (Evelpidou *et al.*, 2014a). This tremor is probably the reason why the roofs of the Late Helladic IIIC chamber tombs in Aplomata collapsed and part of the settlement in Grotta submerged and subsequently flooded by a tsunami (Kontoleon, 1958; Vlachopoulos, 2006). The Mycenaean settlement was abandoned for a long time period, until the new settlers of the Geometric period used the same space for the burial of their ancestors.

Below notch B, a deeper tidal notch exists at approximately -2.8±0.2 m (Evelpidou *et al.*, 2014a). The notch shape indicates a gradual subsidence followed by a co-seismic event and must have developed at least before 3350 to 4200 BP (Evelpidou *et al.*, 2014a). In this context, it is possible that the inhabitants of the coastal settlements were compelled to live with a gradual flooding and slow sea level rise. Around 3300 BP (Late Helladic IIIA2 period) an earthquake destroyed House B in Grotta (Evelpidou *et al.*, 2014a). The sea level rise caused by the earthquake at an early phase of Late Helladic IIIA2 (1350 BC) could have brought about excessive moisture. This could possibly explain the construction of the floor of Room A΄ 0.10 m higher than the earlier floors of House B and Room A of House A (Kontoleon, 1967; Cosmopoulos, 1998). The pebbles under the floor of Room A΄ may have been used as a means of drainage, a way of preventing the moisture to penetrate into the room.

According to Sample NA2/1.87 from the coastal area of St. Georgios on Naxos, the sea level around 1752±40 BP (i.e. 198±40 AD) was above -1.78±0.5 m; the age is provided by an articulated *Cerastoderma glaucum* (for more see Evelpidou *et al.*, 2012c). This result may be in agreement with the presence of the shallower quarried beachrock between 0 m and –1.70 m at Mikre Vigla (Evelpidou *et al.*, 2012c), which was partially protecting the area up to 1000 AD (Evelpidou *et al.*, 2012c). The technique of wading while quarrying, as suggested by Barber and Hadjianastasiou (1989), is not elsewhere recorded. On the contrary, coastal quarries normally have a rock strip that is not quarried, so that it forms a barrier to sea waves. That is the case

in Stavros Akroteriou and Phalasarna, both in West Crete (Kelletat, 1979; Pirazzoli, 1988; Tziligkaki, 2014). In any case, the view of the quarries in Mikre Vigla represents the last phase of its use.

Figure 41: View of the quarried beachrocks in Mikri Vigla (W Naxos). Dalongeville and Renault-Miskovsky (1993) attributed them to the Hellenistic period (323-31 BC).

The approximate depth of -1.70 m corresponds to the submerged tidal notch that is mainly confirmed on the island of Paros at a depth of 1.70±0.20 m (Evelpidou *et al.*, 2014a). The inward depth of this tidal notch measures approximately 0.37 m and indicates relative sea level stability that ranges from 2 to 10 centuries or from 3.5 to 17 centuries or even from 4.5 to 23 centuries (Evelpidou *et al.*, 2014a).

The tidal notch at -1.70±0.2 m seems to correspond to the time period that completely put out of use the breakwater in Paroikia and possibly the one at Karthaia as well. This sudden tectonic phenomenon in the 2nd c. AD recalls the Greek historian Herodian (I, 1, 4), who wrote contemporary history, and writes in his introduction, amongst others, that during his era *earthquakes* and epidemics happened with increasing frequency in comparison with the previous 200 years (Alföldy, 1976, 1971; Pirazzoli, 1986b):

«… ἐξ οὗπερ ἡ Ρωμαίων δυναστεία μετέπεσεν ἐς μοναρ χίαν, οὐκ ἂν εὕροι ἐν ἔτεσι περί που διακοσίοις μέχρι τῶν Μάρκου καιρῶν οὔτε βασιλειῶν οὕτως ἐπαλλήλους διαδοχὰς οὔτε πολέμων ἐμφυλίων τε καὶ ξένων τύχας ποικίλας ἐθνῶν τε κινήσεις καὶ πόλεων ἀλώσεις τῶν τε ἐν τῇ ἠμεδαπῇ καὶ ἐν πολλοῖς βαρβάροις, Γῆς τε σεισμοὺς καὶ ἀέρων φθορὰς τυράννων τε καὶ βασιλέων βίους παραδόξους πρότερον ἢ σπανίως ἢ μηδ΄ ὅλως μνημονευ θέντας· ὧν οἳ μὲν ἐπιμηκεστέραν ἔσχον τὴν ἀρχήν, οἳ δὲ πρόσκαιρον τὴν δυναστείαν· εἰσὶ δ΄ οἳ μέχρι προσηγο ρίας καὶ τιμῆς ἐφημέρου μόνης ἐλθόντες…»

Indeed, the co-seismic event that submerged Shoreline C covers the time span of Herodian's history; 1752±40 BP corresponds to a time period between 158 AD and 238 AD. The frequency of earthquakes during the first half of the 2nd century AD is depicted in the initiative of the Roman emperors to repair and reconstruct buildings in several cities of Asia Minor (Winter, 1996). The tsunami that hit Naxos in the middle of the 2nd c. AD seems to be contemporary with the seismic events along the coasts of Asia Minor.

Paros was very famous throughout antiquity for the good quality of its marble. Fine works of art executed in Parian marble have been exported since the 6th c. BC. During the Roman Empire, Parian marble was diffused to the most remote places (for more, see Schilardi and Katsonopoulou, 2010). In fact, during this time period Paros was never used as a place of exile like the rest of the islands, but enjoyed a certain acme (Rubensohn, 1949).

The co-seismic event of the 2nd c. AD could have affected the trade of the Parian marble, if the harbor of Paroikia suffered from subsidence and flooding, while the moles and breakwaters fell into disuse. It seems, however, that the inhabitants of Paros tried to confront the sudden and rapid sea-level rise in their city by reinforcing the old fortification harbor line with accumulated marble items from all over the island and the ancient quarries. This is deduced by the excavations during the dredging work undertaken in Paroikia in 2000 for the enlargement of the modern harbor and the construction of a new larger wharf in front of the chapel of St. Nikolaos (Kraounaki and Kourkoumelis, 2000; Schilardi, 2010). Doric column drums, marble architectural members and architraves, half-finished statues, and pottery mainly dating to the Late Roman or Early Byzantine period, were retrieved from the seabed close to the coastal wall (Kraounaki and Kourkoumelis, 2000; Schilardi, 2010).

4.4 Archaeological indicators of RSL?

All the archaeological data collected were used to compile a database of archaeological potential indicators of relative sea level change. A variety of archaeological constructions, which were originally above MSL or in contact with sea water are, nowadays, submerged and can provide information on the change between the sea level and the construction. The functional height of an archaeological sea level indicator is related to the elevation of a particular architectural part with respect to the sea level at the time of construction (Antonioli *et al.*, 2007; Auriemma and Solinas, 2009). Auriemma and Solinas (2009) have compiled a list of archaeological structures and reviewed their use as sea level indicators, according to their functional height. The most reliable sea level indicators are fish tanks (e.g. Evelpidou *et al.*, 2012a; Morhange and Marriner, 2015) and ancient port structures, such as jetties (e.g. Marriner and Morhange, 2007; Morhange and Marriner, 2015).

Following the methodology of Shennan *et al.* (2015) and Vacchi *et al.* (2016b), coastal archaeological structures, such as buildings, tombs, and breakwaters, due to difficulties in establishing a relationship with a former MSL, can only be used as terrestrial limiting points. Potential marine limiting points could be submerged structures, including harbour foundations wrecks as well as the fine-grained sediments deposited inside ancient ports (e.g. Marriner and Morhange, 2007). Reconstructed RSL points must fall below terrestrial limiting points and above marine limiting points (Vacchi *et al.*, 2016b). The resulting data were afterwards compared with the results obtained from the beachrocks and drillings of this research (see chapter 7).

Chapter 5 –Beachrocks as recorders of coastal evolution and RSL changes

5. Beachrocks as recorders of coastal evolution and RSL changes

5.1 Fieldwork results

The coastal zones of Paros and Naxos were studied in detail in order to locate, record and sample beachrocks. In Paros, two sites were found with the presence of submarine beachrocks, while in Naxos seven sites were investigated (Figure 42).

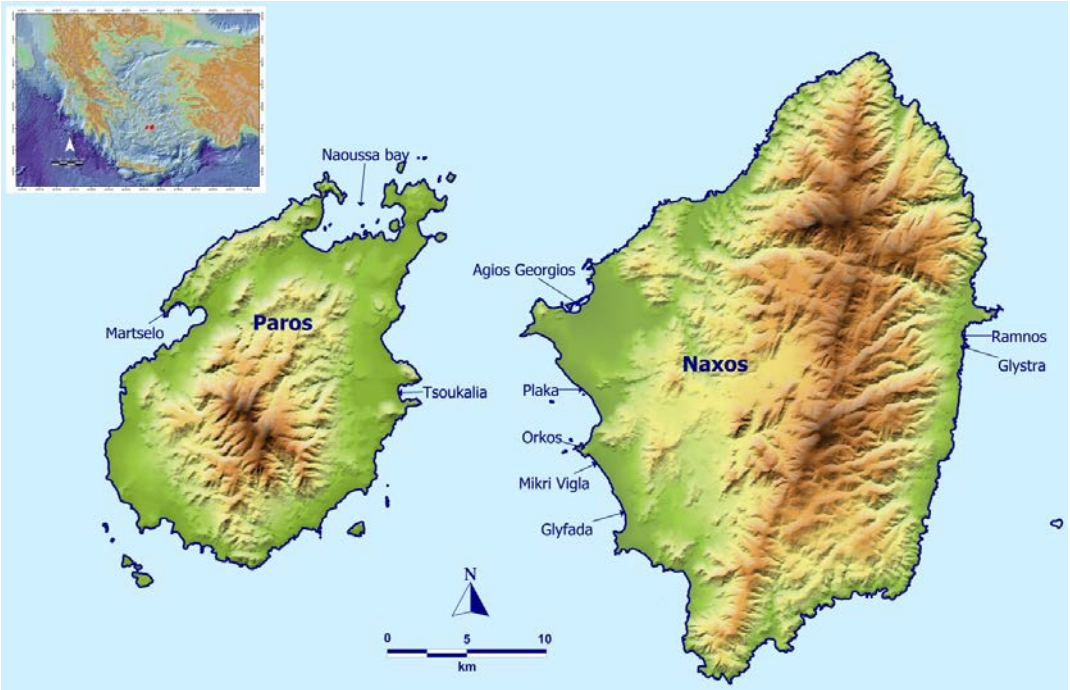

Figure 42: Investigated beachrock sites in Paros and Naxos Islands. The western coast Naxos is characterized by extensive underwater beachrock formations as opposed to Paros, where only two sites were found.

At Naxos, at Agios Georgios four beachrock slabs were identified, between the present sea level and -6.2±0.5 m. At Plaka, four slabs were identified with the deepest one at -6.3±0.5 m. At Glyfada, beachrocks extend to a depth of at least -4.4±0.5 m, while at Orkos, the deepest beachrock was found at -6.3±0.5 m. At Mikri Vigla, two beachrock slabs were identified with the shallower one at -0.7±0.2 m and the deepest at -3.1±0.5 m. On the eastern part of Naxos, at Glystra, two beachrock slabs were identified, with the shallower one reaching depths of about -1.7±0.2 m and the deeper one at -3.8±0.5 m. Lastly, at Ramnos site, the beachrocks extend from about sea level down to a depth of -1.1±0.2 m.

On Paros Island, underwater beachrocks were found at Martselo beach, in the NW of the island, with the deepest one reaching a depth of -5.6±0.5 m. At Tsoukalia beach (Molos), on the eastern part of the island, beachrocks extend to a maximum depth of -6.2±0.5 m. A summary table of depth measurements is provided below. Detailed observations are provided in the following sections.

Table 8: Summary table of depth measurements in Paros and Naxos beachrocks.

Island	Location	Latitude	Longitude	Depth in relation to SL (m) end slab; front slab
Naxos	Ag. Georgios	37° 5'24.01"	25°21'44.33"	-0.8;-0.9 -0.5;-0.7 -0.5;-2.5 -4.3;-6.2
Naxos	Plaka	37° 2'50.98"	25°22'23.78"	0;-1.6 -1.5;-2 -1.8;-4.3 -4.5;-6.3
Naxos	Orkos	37° 1'39.34"	25°22'15.16"	-3.6; -3.6 -3.9;-4.2 6.2;6.3
Naxos	Mikri Vigla	37° 1'13.96"	25°22'22.53"	0;-0.7 -2.7; -3.1
Naxos	Glyfada	36°59'29.61"	25°23'29.77"	0;-1 -1.1;-3.1 -3.6; -3.7 -3.3;-4.4
Naxos	Glystra	37° 4'19.38"	25°35'6.77"	0;-0.75 -1.5;-3.8
Naxos	Ramnos	37° 4'37.60"	25°35'10.69"	0;-1.1
Paros	Martselo	37° 5'48.68"	25° 8'27.69"	-0.8;-1.8 -2;-3.4 -3.7;-5.6
Paros	Tsoukalia	37° 4'9.33"	25°15'44.33"	0;-3.6? ? ; -4.4 -5.7;-6.2

5.1.1 Paros

Martselo beach is located in northwest Paros (Figure 42), with a length of about 450 m, composed of fine to medium sand. The western part of the beach is characterized by sand dunes, while on the submarine part beachrocks are found at depths reaching -5.6 m (Figure 43). The beachrocks can be distinguished in three slabs (Figure 44), with the shallowest between -0.8 and -1.8 m, the middle one from -2 to -3.4 m and the deepest between -3.7 to -5.6 m. Each slab has a width of about 20 m. Even macroscopically, the grain size is different among the three slabs, with the shallower one being more coarse-grained.

It is worth noting that the shallowest beachrocks are now preserved mainly on the western part of the beach, as large submarine parts have been removed from the central and eastern part, due to the touristic development of the area.

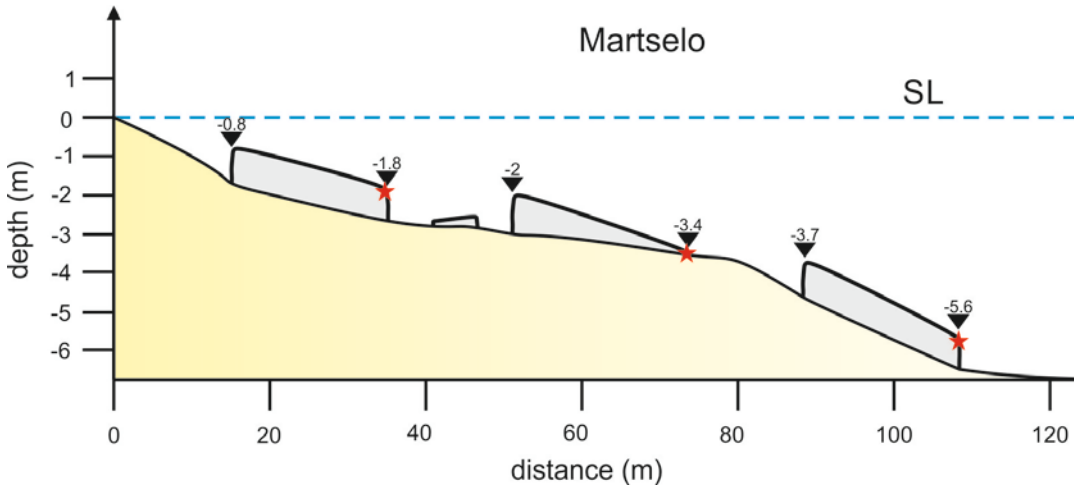

Figure 43: Submarine transect of beachrocks, in Martselo beach (NW Paros). The beachrocks are not well preserved along the coast, but only to its western part. Red stars indicate where samples were obtained.

Figure 44: The deepest beachrock slab in Martselo beach (NW Paros), located between -3.7 and -5.6 m, with a width of ~20 m.

Tsoukalia beach, in Molos area, is located in the east part of Paros Island, having a length of about 380 m (Figure 42). The southern part of the beach is characterized by the presence of small sand dunes, which are interrupted by a coastal road. The beachrocks extend from sea level to -6.2 m (Figure 45). Three beachrock slabs were identified, with the shallower one extending from sea level to -3.6 m, the intermediate one reaching -4.4 m and the deepest one lying between -5.7 to -6.2 m. The shallower slab presents the largest width reaching almost 50 m.

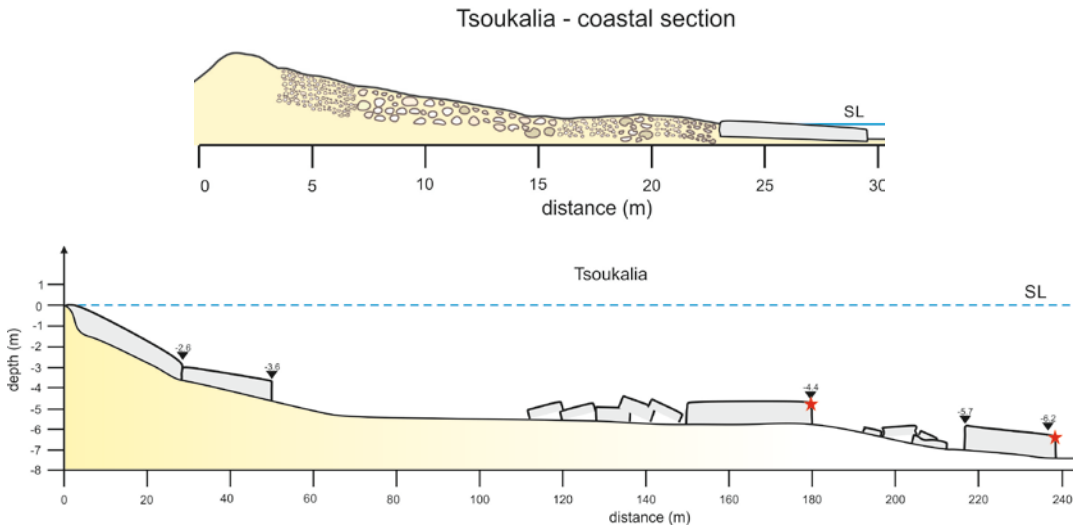

Figure 45: The coastal and submarine transect of Tsoukalia beach (E Paros). The largest width (50 m) was measured in the shallowest slab. A maximum depth of -6.2 m was recorded.

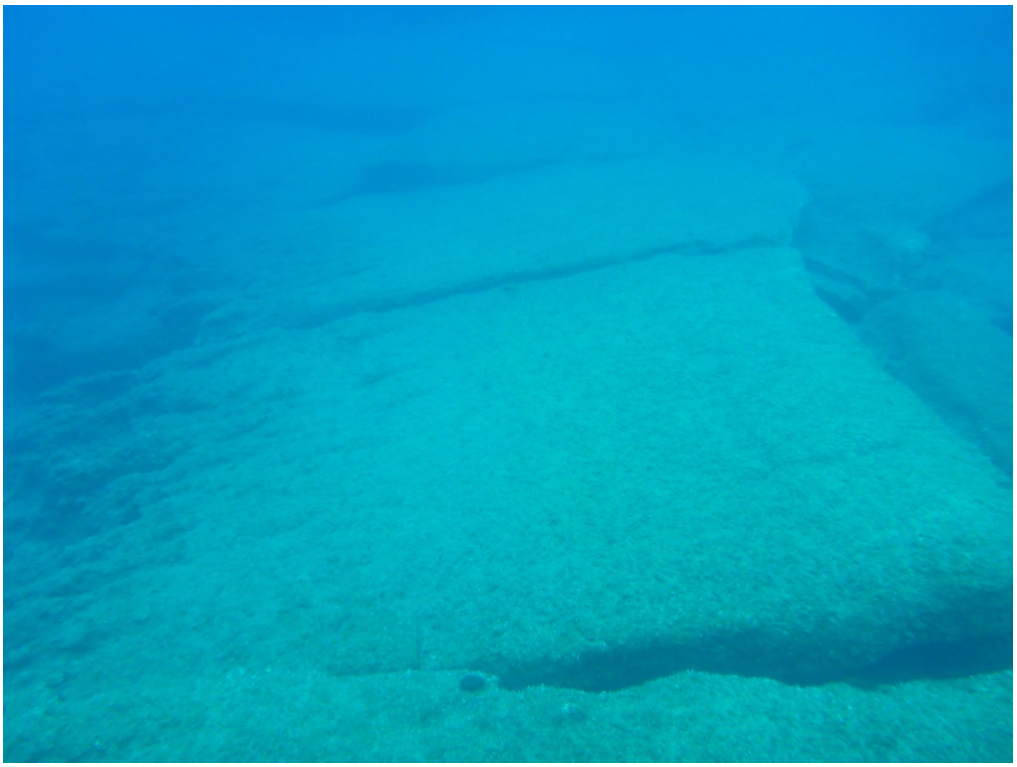

Figure 46: The deepest beachrock slab at Tsoukalia beach reached a depth of -6.2 m.

5.1.2 Naxos

Agios Georgios is located on the west part of Naxos Island, composed of a coastal lagoon in its south part, a few coastal dunes on the coastal zone and the presence of Manto Islet, which consists mainly of aeolianites. Due to the extension of beachrocks, three underwater transects were accomplished, which allowed recording their various characteristics (Figure 47). North of Manto Island, three or four beachrock slabs were found reaching depths of -6.2 m. The beachrocks extend parallel to the coast, almost continuously, for more than 1 km. Due to their extensive width, the beachrocks do not maintain the same characteristics along the coast.

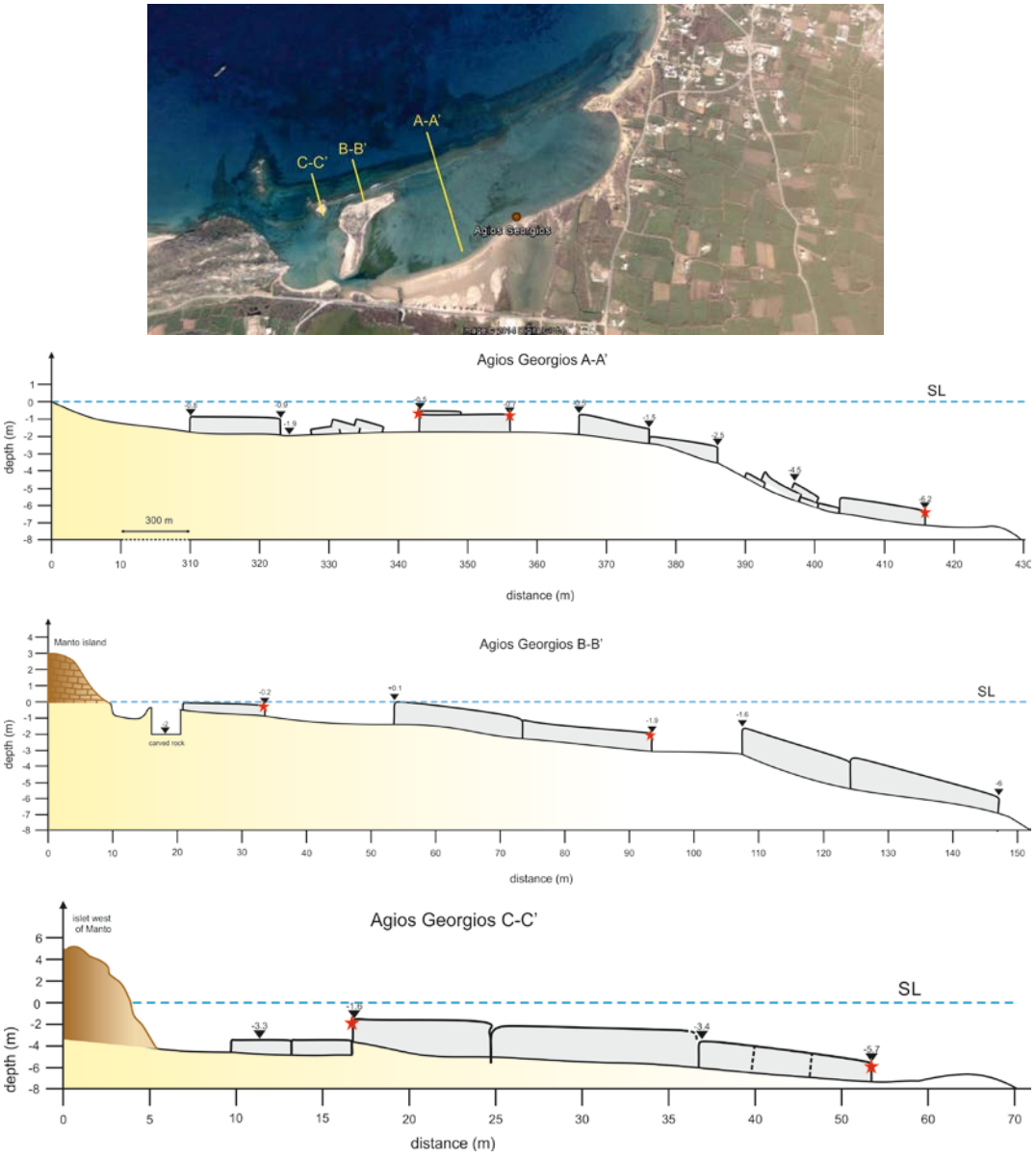

Figure 47: Three submarine transects took place at Agios Georgios (W Naxos). The beachrocks extend for more than 1 km parallel to the modern coastline reaching a maximum depth of -6.2 m.

Plaka beach is located in the western part of Naxos, south of Agios Georgios. Plaka has a length of more than 2.5 km; therefore the north and south part were mapped separately. The north part of Plaka is characterized by the presence of three submarine slabs, with the deepest one reaching -7 m. However, the orientation of one beachrock slab is not parallel to the coastline but appears to end up to a granodiorite outcrop (Figure 48). The shallowest slab is parallel to the coastline at a maximum depth of -1.5 m.

Figure 48: The submarine configuration of beachrocks on the north part of Plaka differs from the south part (W Naxos). Locally, the deepest beachrock was measured at -7 m.

The south part of Plaka is characterized by the presence of beachrocks extending from sea level to a maximum depth of -6.3 m (Figure 49). Four beachrock slabs were identified with the shallower one extending from sea level to -1.6 m, the second between -1.5 and -2 m, the third from -1.8 to -4.3 and the deepest from -4.5 m to -6.3 m. The largest width was observed at the shallowest slab reaching 20-25 m while the deeper slabs are characterized by a width of 12-15 m.

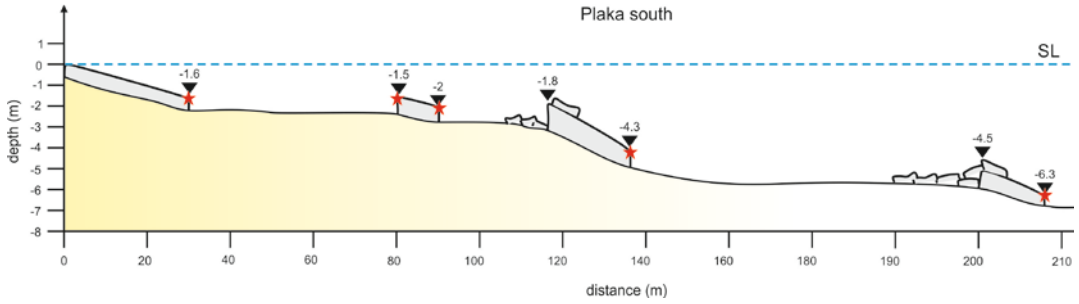

Figure 49: Submarine transect of the south part of Plaka (W Naxos). Beachrocks extend parallel to the coast for more than 1.5 km reaching a depth of -6.3 m.

Orkos beach is located in the western part of Naxos, just south of Plaka beach. Orkos has a length of about 680 m and some coastal dunes exist mainly on the west part. The submarine part of Orkos is characterized by the presence of beachrocks reaching a depth of –6.3 m (Figure 50). Four slabs were mapped, with depths between -3.4 and -3.6 for the first two, between -3.9 and -4.2 for the third and between -6.2 to -6.3 for the deepest one. The beachrocks at Orkos are not as extensive and well preserved as in other sites (e.g. Agios Georgios) and the maximum width was recorded in the deeper slab, reaching 17.8 m. The shallower slabs are less extensive, with widths between 7.8 m and 8.6 m.

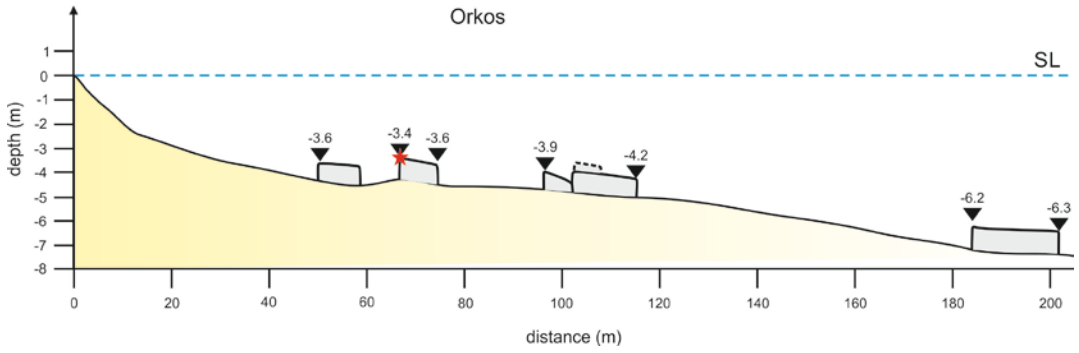

Figure 50: Submarine transect of Orkos beachrocks (W Naxos). The shallowest beachrocks were found at -3.6 m and the deepest at -6.3 m, which has the largest width of 17.8 m.

Mikri Vigla beach is also located on the western part of Naxos, south of Orkos. Mikri Vigla has a length of about 1.75 km and is characterized by the presence of coastal dunes and a coastal lagoon, in its north part. Only two beachrock slabs were identified, with the shallower one located between sea level and -0.6 m and the deeper one between -2.7 and -3.1 m (Figure 51). The shallowest slab, in particular, presents signs of quarrying (Evelpidou *et al.*, 2012c) (Figure 52). This was also noted by Dalongeville and Renault-Miskovsky (1993), who attributed them probably to the

Hellenistic period (323 B.C.-30B.C.). It is worth noting that the beachrocks of Mikri Vigla are not well preserved and they cannot be followed throughout the extent of the beach.

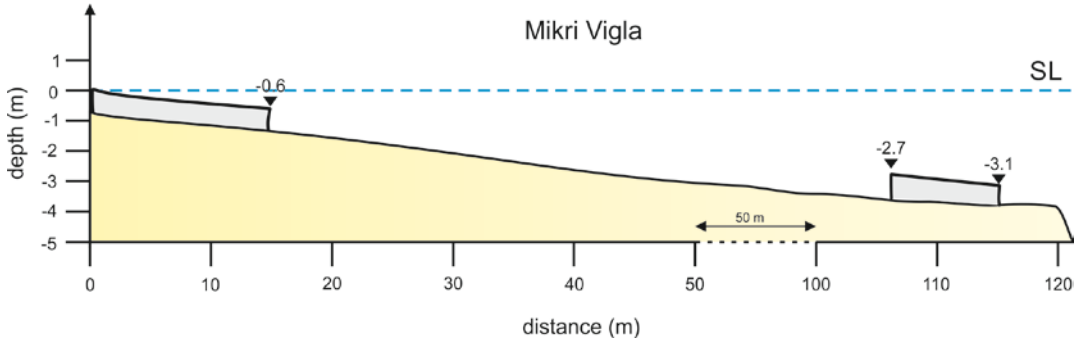

Figure 51: Submarine transect of beachrocks at Mikri Vigla (W Naxos). They reach a maximum depth of -3.1 m. Beachrocks are not well preserved and cannot be followed continuously along the submarine part of the coast.

Figure 52: Signs of quarrying (rectangular cuts) in the shallower beachrock slab, in Mikri Vigla (W Naxos).

Glyfada beach is located on the southwest part of Naxos, south of Mikri Vigla. Glyfada is also characterized by the presence of coastal dunes and a coastal lagoon, and it has a length of about 1.4 km. Beachrocks are present on the south part of the beach, extending to a depth of -4.4 m (Figure 53). Four beachrock slabs were identified with the shallower one reaching a depth of 1 m, the second lying between -1.1 and -3.1 m, the third between -3.6 and -3.7 m and the deeper one located between -3.3 and -4.4 m. The shallower slab has the largest width reaching almost 40 m, while the second slab reaches a width of 26 m, with a small interruption at 14.7 m.

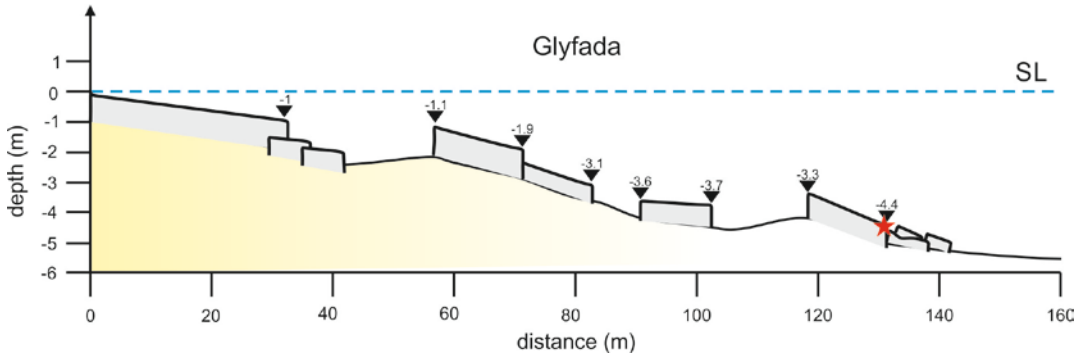

Figure 53: Submarine transect of beachrocks at Glyfada beach (W Naxos). The beachrocks extend parallel to the coast for almost 1 km and reach a depth of -4.4 m.

Glystra beach is located on the east part of Naxos. In general, the east part of Naxos is characterized by smaller coasts, in the form of pocket beaches. Glystra beach has a length of about 94 m. Two beachrock slabs were identified with the shallower one extending from sea level to a depth of -0.75 m and the deeper one from -1.5 m to -3.8 m (Figure 54). The two slabs lie next to each other, with a change in depth and their cumulative width reaches 50 m.

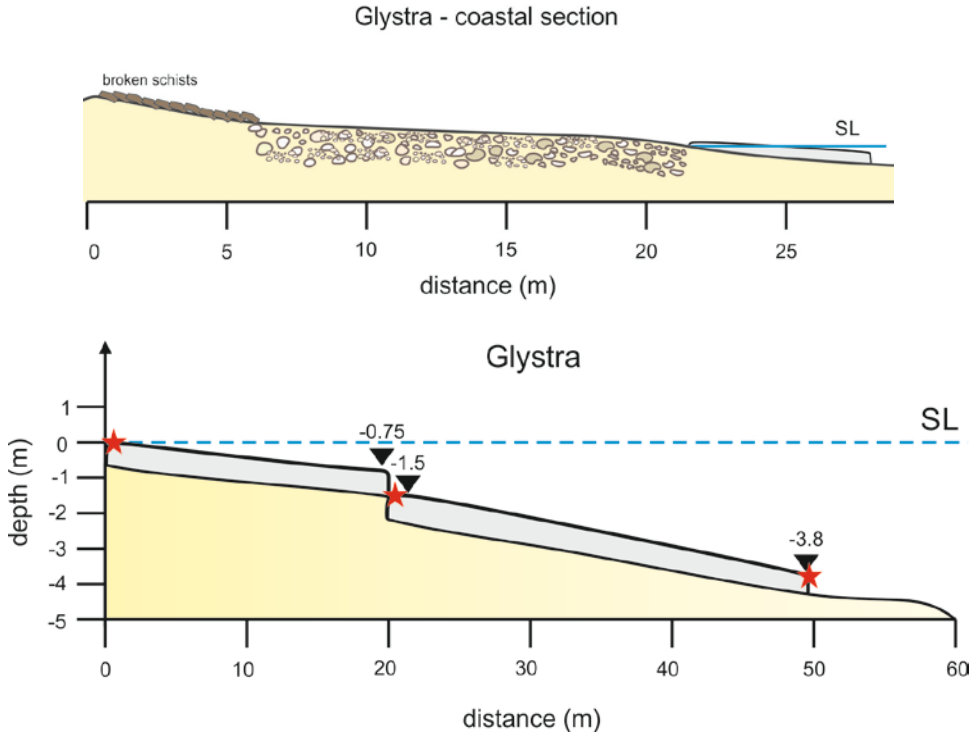

Figure 54: The coastal (top) and submarine (bottom) transect in Glystra beach (E Naxos). An almost continuous beachrock slab reaches a width of 50 m and a depth of -3.8 m.

Ramnos beach is also located on the east part of Naxos, just north of Glystra. Ramnos is also a pocket beach, with a length of about 60 m. In Ramnos, the least significant beachrock occurrence was recorded. Only one beachrock slab was found extending from sea level to a depth of about -1.1 m (Figure 55).

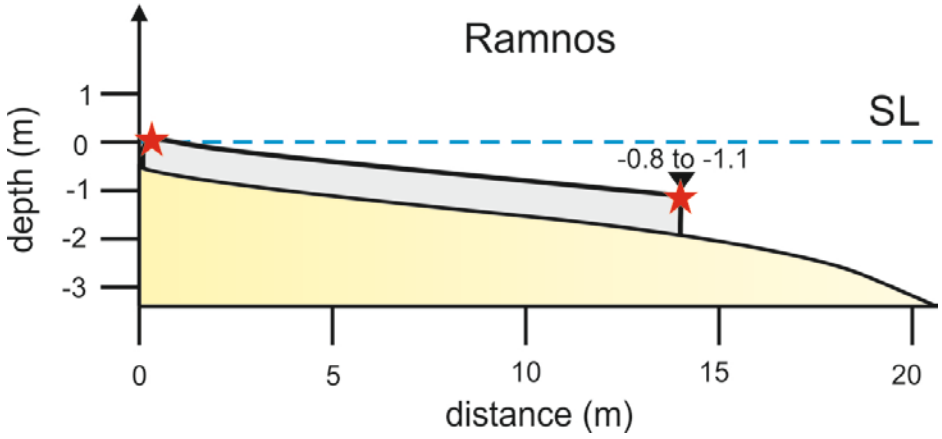

Figure 55: Submarine transect of beachrocks at Ramnos beach (E Naxos). The least extensive beachrocks were found reaching -1.1 m depth.

5.2 Mineralogical observations

About 30 samples were examined under a polarizing microscope (Microscope LEICA DM RXP) at CEREGE (Centre de Recherche et d'Enseignement de Géosciences de l'Environnement), in Aix-en-Provence, France. Observations included cement morphology, grain size and shape as well as presence of bioclasts.

In general, there is a coherent pattern in all observed samples from both islands. Grains are usually well rounded and there is a general abundance of bioclasts (mainly forams and gastropods) (Figure 56). The observed bounding material between grains is mostly early intertidal cement (Figure 61). A large abundance in quartz and feldspars was found the studied beachrocks, which were those components used for the luminescence dating.

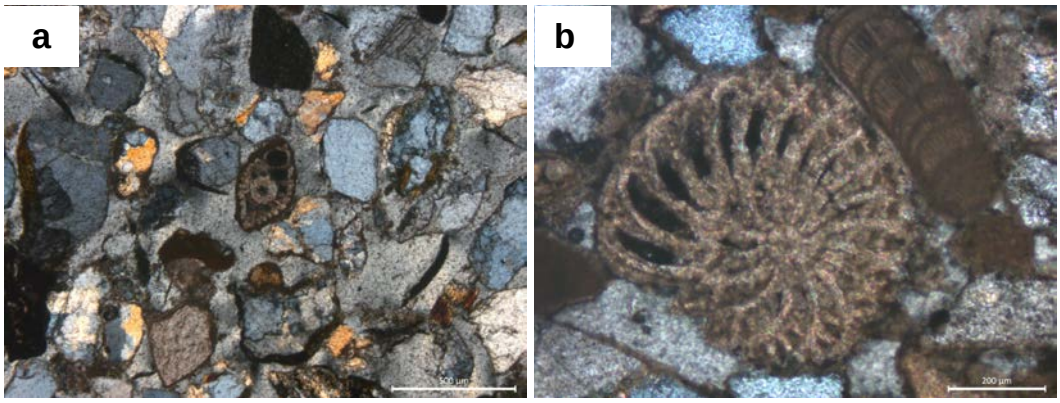

Figure 56: a) Thin section of Agios Georgios beachrocks at -0.7 m (W Naxos). A gastropod is visible at the center of the photo, and b) Thin section of Glyfada beachrock at -4m (W Naxos), showing a foraminifera.

5.2.1 Cement descriptions

Cement observations are provided in the following paragraphs, while more descriptions and photos are given in Appendix I.

5.2.1.1 Agios Georgios (Naxos)

The deepest beachrock slabs of Agios Georgios (depths of -5.7 and -6.2 m) are characterized by lithoclasts of various sizes, rounded and medium sorted (Figure 57). The cements are characterized by a well-developed isopachous radiaxial fibrous HMC followed by micritic internal sediment. Micritization has also been observed with recrystallization.

Shallower beachrocks are also characterized by well-rounded lithoclasts, with medium sorting. Cements are finer isopachous HCM, while micritic internal sediments are more developed. Micritization is also present with occasional recrystallization.

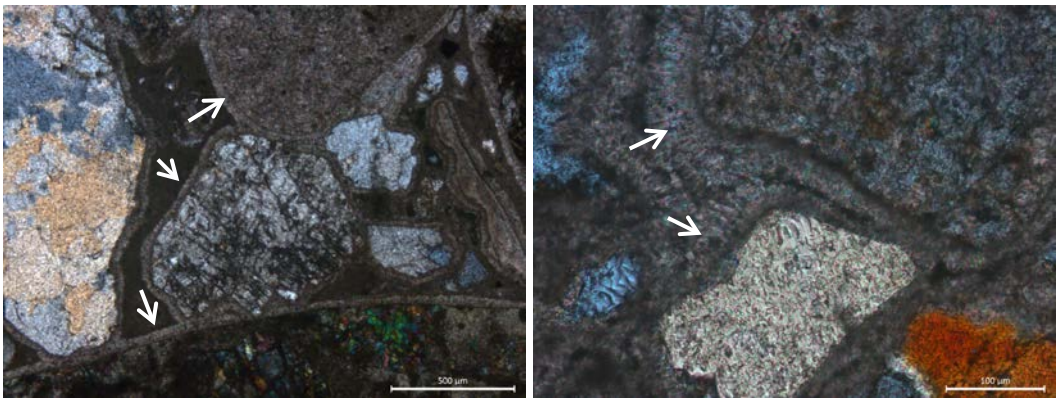

Figure 57: Cements from Agios Georgios beachrocks: left photo from -6.2 m, right photo from -5.7 m. The cements are characterized by a well-developed isopachous radiaxial fibrous HMC (white arrows).

5.2.1.2 Plaka (Naxos)

The deepest beachrocks (-6.3 m depth) are composed of sub-angular to rounded lithoclasts, medium sorted. A first generation of isopachous fine crust of HMC is observed around grains along with micritic matrix. Marine cementation of magnesium calcite around pellets (probably caused by bacterial actions) and recrystallization is also observed (Figure 58).

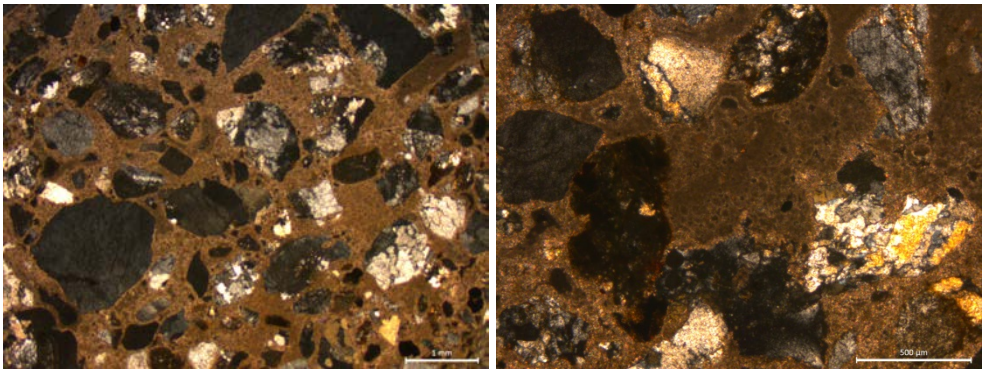

Figure 58: Plaka beachrock at -6.3 m depth. Left photo: An isopachous fringe is observed surrounding the grains and micritic matrix. Right photo (centre): micritization and recrystallization.

The shallower beachrock samples (-1.5; -2 m) are composed of well-rounded lithoclasts bounded by isopachous radiaxial fibrous HMC (Figure 59). Meniscus cement has also been observed, characteristic of vadose cementation. Evidence of

micritic filling and peloidal cement was found, generally following the first fringe of early intertidal cement. Peloidal cements are micrite partially replaced by coalescent pellet clusters. These pellets are particles agglomerates that could form within the intertidal zone during the diagenesis inside the pore space. They are probably associated to a precipitate of HCM as a result of bacterial action (Vousdoukas *et al.*, 2007).

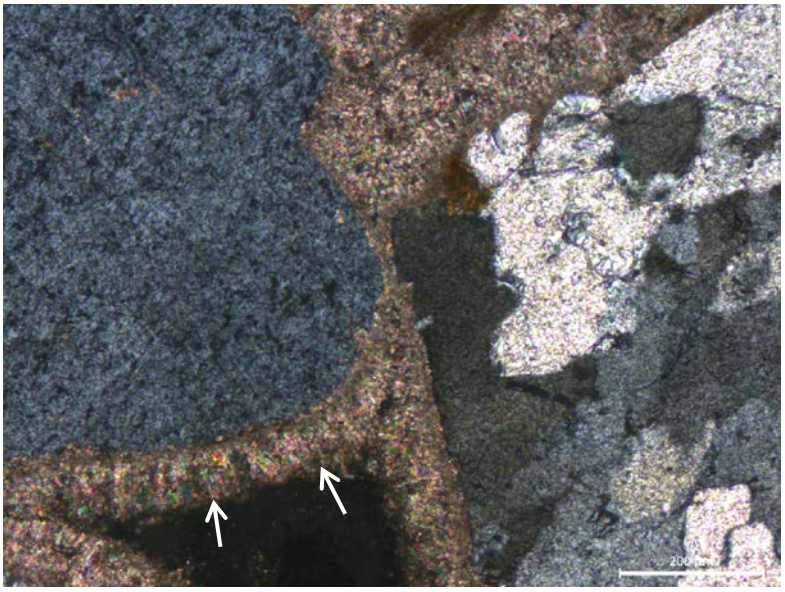

Figure 59: Beachrock sample from Plaka (W Naxos) at -1.5 m depth. Isopachous radiaxial fibrous HMC is observed around grains.

5.2.1.3 Orkos (Naxos)

Orkos beachrocks consist of rounded lithoclasts and bioclasts within the micritic cement. Cements are characterized by a fine bladed isopachous fringe of HCM, followed by micritic filling. Locally developed meniscus cement at grain contacts was also identified, which is indicative of the upper intertidal zone. Pelletization was also observed with recrystallization.

5.2.1.4 Glyfada (Naxos)

Beachrock samples are composed of sub-angular to rounded lithoclasts, with an abundance of bioclasts (mostly gastropods and foraminifera). Two cement generations are probably observed, as small bladed isopachous limpid and contiguous HMC crystals.

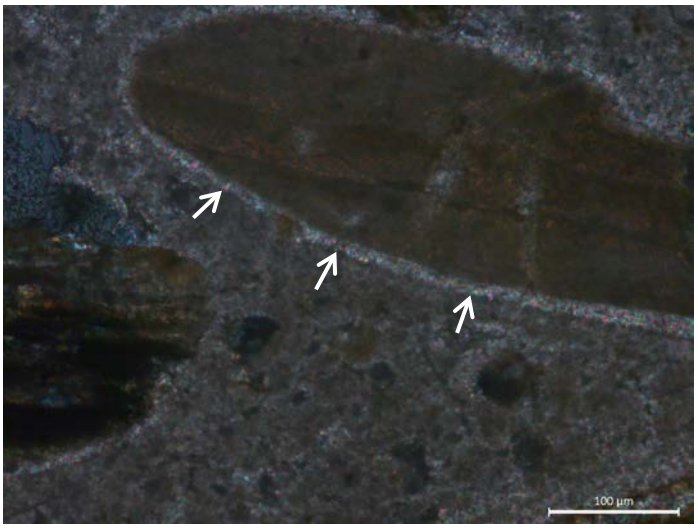

Figure 60: Beachrock from Glystra (W Naxos) (-3.8 m). A first fringe of early intertidal cement surrounding grains (white arrow) and peloidal cement with recrystallization.

5.2.1.5 Glystra (Naxos)

The deepest beachrock samples (-3.8 m) is composed of rounded lithoclasts, well sorted. A first small bladed isopachous fringe of limpid and contiguous HMC crystals has been found (~12 µm), followed by micritic internal sediment, pelletization and recrystallization (Figure 60). In the shallower samples, the first fringe forms thicker isopachous rims of HMC ~25-45µm.

5.2.1.6 Martselo (Paros)

The deepest beachrock samples are composed of fine well-rounded and well sorted lithoclasts. Bioclasts are also present, mainly foraminifera and gastropods. Cements are characterized by small bladed isopachous fringe of limpid and contiguous HMC crystals (Figure 61b). No micritic filling was observed, which probably indicates a calm protected environment.

At Martselo shallowest sample (-1.8 m), lithoclasts are well rounded and medium sorted. The first fringe of early intertidal cement is characterized by small bladed isopachous fringe of limpid and contiguous HMC crystals, followed by micritic filling (including internal sediments) and peloidal cement.

5.2.1.7 Tsoukalia

Tsoukalia beachrocks are mainly composed of sub-angular and round lithoclasts, with poor sorting. A first fringe of cement is mainly characterized by isopachous radiaxial fibrous HMC crystals, followed by micritic filling cement. Some micritization with recrystallization was also found.

5.2.2 Cement characteristics of dated samples

Diagenetic intertidal zone cements are always smaller than 100 μm and sometimes associated to detrital constituents such as bioclasts and micritic filling. Early intertidal cements were mainly characterized by isopachous radiaxial fibrous HMC crystals (e.g. sample from Plaka at -1.5 m), small bladed isopachous fringe of limpid and contiguous HMC crystals (e.g. Martselo beachrock at -5.6 m; Agios Georgios beachrocks at -1.9 m and -5.7 m), or clusters and bridges between the grains.

Evidence of micritic filling (including internal sediments) and peloidal cement was also observed, generally following a first fringe of early intertidal cement. This was mostly observed at Orkos beachrocks, with evidence of micritic cement, at Martselo shallowest slab (-1.8 m), at Molos (-3.6 m) and at the shallower slabs of Agios Georgios beachrocks.

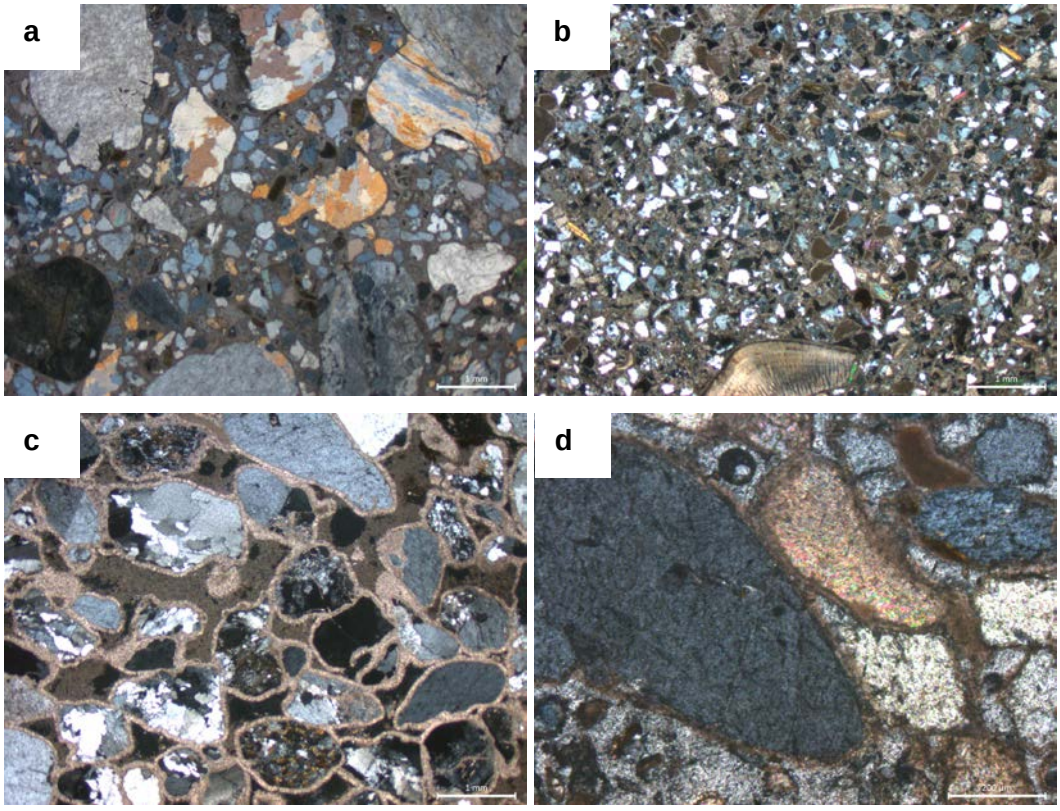

Figure 61: Thin sections from a) Agios Georgios (-6.2 m) (W Naxos), b) Martselo (-5.6 m) (NW Paros), c) Plaka (-1.5 m) (W Naxos) and d) Glyfada (-4 m) (W Naxos).

No evidence of meteoric cement was observed and the collected samples contain at least one of the calcareous constituents deposited within the intertidal zone. The microscopic analysis, together with the field observations, provides evidence that all

samples come from beachrocks. The presence of early intertidal cement with the aforementioned characteristics allowed determining the formation zone of the dated beachrocks within the intertidal zone.

The particular cement characteristics of the dated samples are summarized in Table 9 and illustrated in Figure 62.

Table 9: Cement and matrix description of dated samples

Sample	Cement type	Figure
Ag. Georgios (-1.9 m)	isopachous radiaxial fibrous HMC	Figure 62a
Ag. Georgios (-5.7 m)	isopachous radiaxial fibrous HMC→ Peloidal HMC cement → micritization	Figure 62b
Plaka (-2 m)	Micritic matrix, micritization, recrystallization	Figure 62c
Plaka (-1.5 m)	isopachous radiaxial fibrous HMC crystals→ micritic cement filling pores→ pellets with some recrystallization	Figure 62d
Orkos (-3.4 m)	Fine fringe of intertidal cement→ micritic filling cement→ micritization →recrystallization	Figure 62e
Glyfada (-4 m)	Fine fringe of isopachous HCM (two generations?)	Figure 62f
Glystra (-3.8 m)	Fine fringe of isopachous HCM (1st intertidal cement)→ micritization → recrystallization	Figure 62g
Martselo (-5.6 m)	small bladed isopachous fringe of limpid and contiguous HMC	Figure 62h

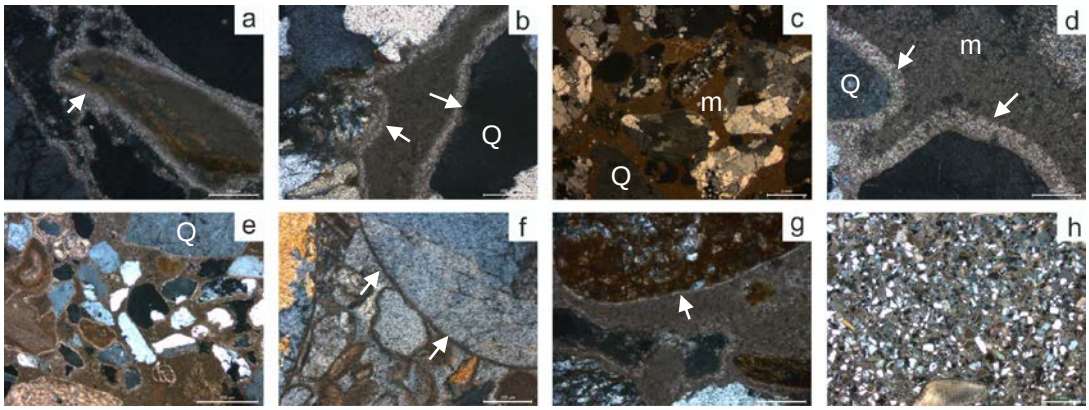

Figure 62: Cement details of the dated beachrock samples (see Table 9 for detailed description). White arrows indicate the isopachous HMC cement, m for micritic infill, Q is quartz.

5.3 Luminescence dating results

The measured equivalent dose (De) values range between 3.50±0.27 Gy (sample 3163) to 5.30±0.27 Gy (sample 3168) for quartz and 3.62±0.09 Gy (3163) to 8.23±0.19 Gy (3168) for feldspar. The ages obtained from quartz vary between 1.00±0.16 ka (sample 3170) and 4.48±0.78 ka (sample 3169), while feldspar fading uncorrected ages range between 0.86±0.08 ka (sample 3167) and 2.47±0.57 (sample 3169). The measured g-values were used to correct anomalous fading for the three samples (3163, 3164 and 3167) using the method of Huntley and Lamothe (2001). Since all measured fading rates are close to each other, the mean g-value (1.37±0.02% /decade) was applied to calculate fading corrected ages for the other samples (Table 10). The feldspar fading corrected ages range between 1.16±0.08 ka (sample 3167) and 3.39±0.57 ka (sample 3169). All ages are summarized in Table 10 and plotted in Figure 63, in order to compare the luminescence ages from both quartz and K-feldspar.

Table 10: Results of age determination from the luminescence dating of beachrocks

Site name	Laboratory code	Depth (m)	Material	No of aliquots[2]	D_e (Gy)	Age (ka)[3]
Agios Georgios (Naxos)	3163	-1.9	Quartz	17	3.50±0.27	1.38±0.17
			Feldspar	10	3.62±0.09	1.42±0.09
Martselo (Paros)	3164	-5.6	Quartz	10	4.73±0.06	1.39±0.19
			Feldspar	8	4.76±0.12	1.72±0.08
Plaka (Naxos)	3165	-1.5	Quartz	11	4.58±0.69	1.24±0.23
			Feldspar	7	5.26±0.13	1.50±0.07
Agios Georgios (Naxos)	*3166*	*-5.7*	*Quartz*	*18*	-	-
			Feldspar	*8*	-	-
Glyfada (Naxos)	3167	-4	Quartz	20	4.67±0.74	1.12±0.22
			Feldspar	10	4.24±0.13	1.16±0.08
Orkos (Naxos)	3168	-3.4	Quartz	20	5.30±0.63	1.42±0.24
			Feldspar	8	8.23±0.19	2.49±0.17
Glystra (Naxos)	3169	-3.8	Quartz	24	4.28±0.24	4.48±0.78
			Feldspar	8	4.31±0.14	3.39±0.57
Plaka (Naxos)	3170	-2	Quartz	19	3.89±0.44	1.00±0.16
			Feldspar	8	4.41±0.12	1.29±0.09

[2] number of accepted aliquots

[3] feldspar ages are fading corrected

In general, there is good agreement between the values obtained from quartz and feldspar ages, particularly for the shallower samples, while for the deeper samples, some discrepancies are observed for both minerals in age estimation (Figure 63). Deeper samples present a more complicated age-depth pattern. Sample 3168, collected at -3.4 m, yielded a quartz age of 1.42±0.24 ka while the feldspar age (2.49±0.17 ka) is greater by ~1.0 ka. Similarly, sample 3169, collected at -3.8 m, yielded a quartz age of 4.48±0.78 ka while the feldspar age (3.39±0.57 ka) was younger by ~1.0 ka.

Deeper samples (3164, 3167), collected between -4 and -5.7 m from Martselo and Glyfada correspondingly, yielded ages between 1.12±0.22 and 1.39±0.19 ka for quartz and 1.16± 0.08 and 1.72± 0.008 for feldspar (Table 10; Figure 63). These ages are similar to those yielded by the samples collected between -1.5 and -2.0 m MSL. The quartz and feldspar luminescence ages are in agreement within 2-σ uncertainty except sample 3168. However, there is a tendency that the quartz yielded younger ages than the feldspar (except sample 3169). The quartz OSL signal in this study was generally very dim and not dominated by the fast component, which is most suitable for dating. The younger quartz ages could be explained by the effects of the thermally unstable medium component (e.g. Tamura et al., 2015). Sample 3169 from the east coast of Naxos had exceptionally bright OSL signal with the clean fast component, and therefore it was possible that this sample was not affected by the thermal stability problem.

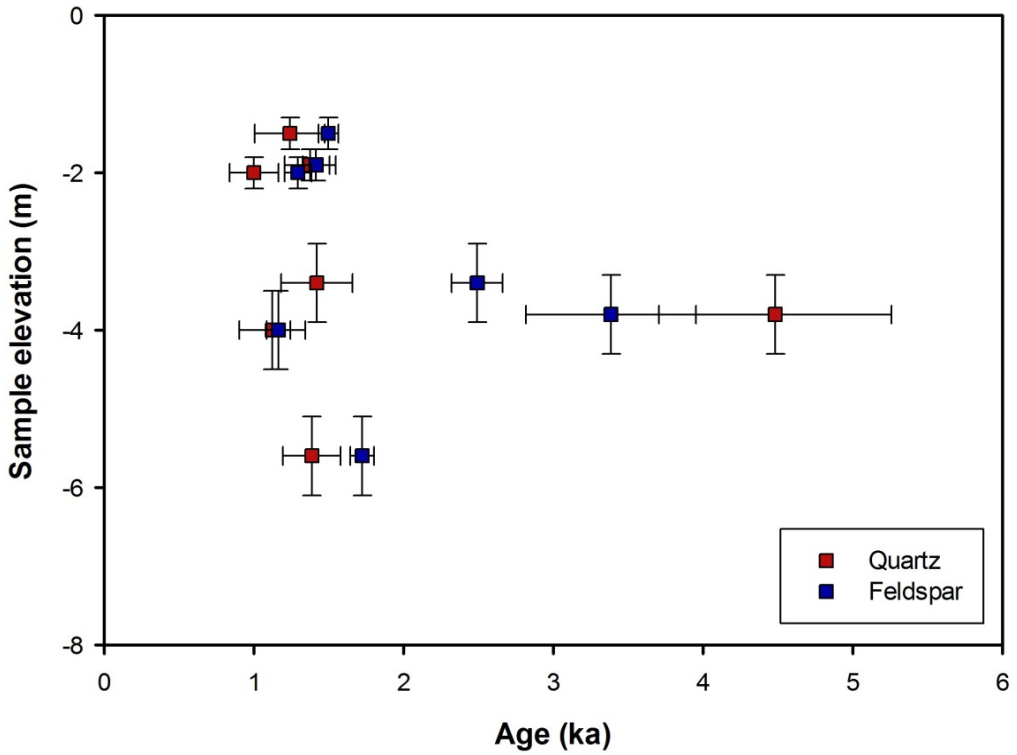

Figure 63: Comparison of luminescence dates from quartz and feldspar. Vertical error for shallow samples is 0.2 m (< 2m depth) and 0.5 m for deeper (>2 m). A good agreement between the two dosimeters is observed for shallow samples, while some discrepancies are identified for the deeper ones.

5.4 Discussion

5.4.1 Beachrock chronology

The luminescence dates present some intriguing results. It is clear from Figure 63 that the relationship between age and depth of the samples does not present a coherent pattern. In particular, the deepest beachrocks did not yield the oldest dates, as normally expected in a context of late Holocene sea level rise (e.g. De Muro and Orru, 1998; Desruelles *et al.*, 2009). The luminescence dates indicate that beachrocks with comparable ages are located between -1 m and -6 m. In order to clarify the chronological context, the luminescence dates were compared with previously published sea level data from the central Cycladic region (Figure 64). Based on submerged archaeological remains in Antiparos Island, about 5.5 m of relative sea level change since 5.5 ka has been suggested by Morrison (1968). Further archaeological evidence suggests a sea level between -2 and -3 m around 0.5 to 0.9 ka BC (2.5 – 2.9 ka) in Paros Island (Papathanassopoulos and Schilardi, 1981). Beachrocks on Mykonos, Delos and Rhenia Islands indicate that the relative sea level was at -3.6±0.5 m around ~2000 BC (4.0 ka), at -2.5±0.5 m around ~400 BC (2.4 ka), and at -1.0 ± 0.5 m around ~1000 AD (1.0 ka) (Desruelles *et al.*, 2009). According to a similar analysis by Mourtzas (2012) in Delos Island an RSL variation of ~2.1 m is estimated since the end of the Hellenistic period (100 BC or 2.1 ka).

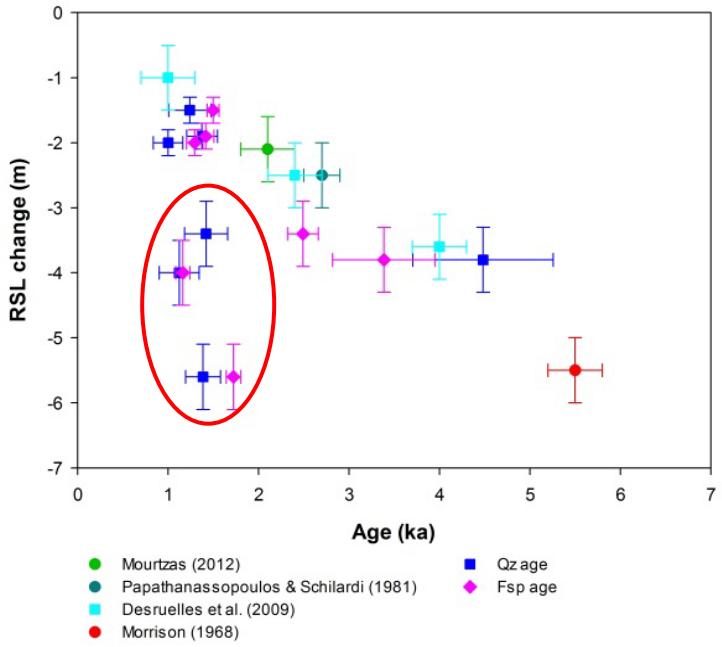

Figure 64: Luminescence results compared with published RSL data, from beachrocks and archaeological data There is a general agreement for samples shallower than 2 m, while for deeper samples the red cirle highlights age results not in agreement with the general RSL context of the area.

The ages of the shallower samples (-1.9 m; 3163, -1.5 m; 3165, -2 m; 3170) show a very good agreement with the other sea-level markers available in the area and the ages between quartz and feldspar are also in good agreement. Furthermore, the ages obtained from samples 3168 and 3169 are in general agreement with the context of relative sea level changes in the area. Quartz and feldspar ages of sample 3168 (-3.4 m MSL), from Orkos (Naxos), differ about 1.0 ka. Feldspar age (2.49±0.17 ka) seems to be more consistent with the sea-level evolution defined on the basis of previously published data. In addition, the age obtained from sample 3169 (-3.8±0.5 m MSL), from Glystra (Naxos), even with a large temporal error, is in good agreement with a RSL placed at about -3.6±0.5m by Desruelles *et al.* (2009).

There is an evident misfit between the age of the deepest beachrocks and the previously published sea-level data. Samples collected at -4 and -5.7 m (3164, 3167; Table 10) appear significantly younger than expected (e.g. Papathanassopoulos and Schilardi, 1981; Desruelles *et al.*, 2009; Evelpidou *et al.*, 2012c). Expected ages for the deepest samples should have been older than the age obtained by sample 3169 (Figure 64), while there is no evidence suggesting a tectonic regime that could explain such results (e.g. Evelpidou *et al.*, 2014a; Lykousis, 2009). Such dates appear underestimated considering the context of relative sea level changes in the area. In addition, such an age would only be explained if the area was struck by repeated earthquake events with alternations of uplift and subsidence. Such case studies are reported in the literature from Greece (e.g. Pirazzoli *et al.*, 1989; Stiros and Blackman, 2014), but this is not the case for the central Cyclades (e.g. Lykousis, 2009; Kapsimalis *et al.*, 2009; Evelpidou *et al.*, 2014). Furthermore, if there were some important earthquakes (to bring about such a relative sea level change) in the area in the last ~1500 years there would be a record in historical texts (e.g. Stiros and Blackman, 2014; Rhodes Island) and also evidence in the field. It is worth noting, however, that the luminescence ages for samples 3164 and 3167 obtained from feldspar and quartz are in very good agreement. Overall, it is clear that from a geological point of view this observed misfit is not in agreement with the tectonic regime of the area; from a geochronological point of view the luminescence ages are considered reliable because they passed all tests. Further investigations may shed some light as these two ages are not in agreement with the RSL context of the area.

5.4.2 Shoreline evolution

The beachrock outcrops in both islands allow not only to estimate the relative sea level changes in the area, but they also provide insights to the paleogeography of the coasts.

Naxos Island

In Naxos Island, two significant outcrops of beachrocks well recorded the morphological configuration of the coastline in the last ~4.5 ka. **Plaka beach** has a NW-SE orientation and submarine beachrocks can be followed for more than 2.5 km. Three palaeoshorelines can be identified, and the second shoreline in particular, appears similar to the geometric shape of the modern coastline. This second shoreline is located between -1.6 and -4.3 m and although it consists of two slabs, it should probably be considered as one paleoshoreline. In the north of Plaka coast, however, the shoreline morphology recorded by the beachrocks appears rather different. The orientation of the second shoreline in the north part is not parallel to the coastline but appears to end up to a shallow outcrop of granodiorite. This morphological configuration suggests that the geomorphology of this coastal area was different, with the presence of a paleo-tombolo and perhaps the existence of two bays, due to the presence of this granodioritic outcrop (Figure 65).

This second shoreline (shallow slab; sample depth -1.5 m) was dated to 1.50±0.07 ka from K-feldspar, and 1.24±0.23 ka from quartz as dosimeters (sample 3165), suggesting that a shoreline regression of more than 100 m has occurred in the last ~1240-1500 years. Although a sample from the deepest shoreline (depth between -4.5 and 6.3 m) was not dated, it is considered that is should be older than the age obtained from sample 3169, i.e. 4.48±0.78 ka (quartz) / 3.39±0.57 ka (feldspar), because it reaches a depth of -6.3 to the south and -7 m to the north.

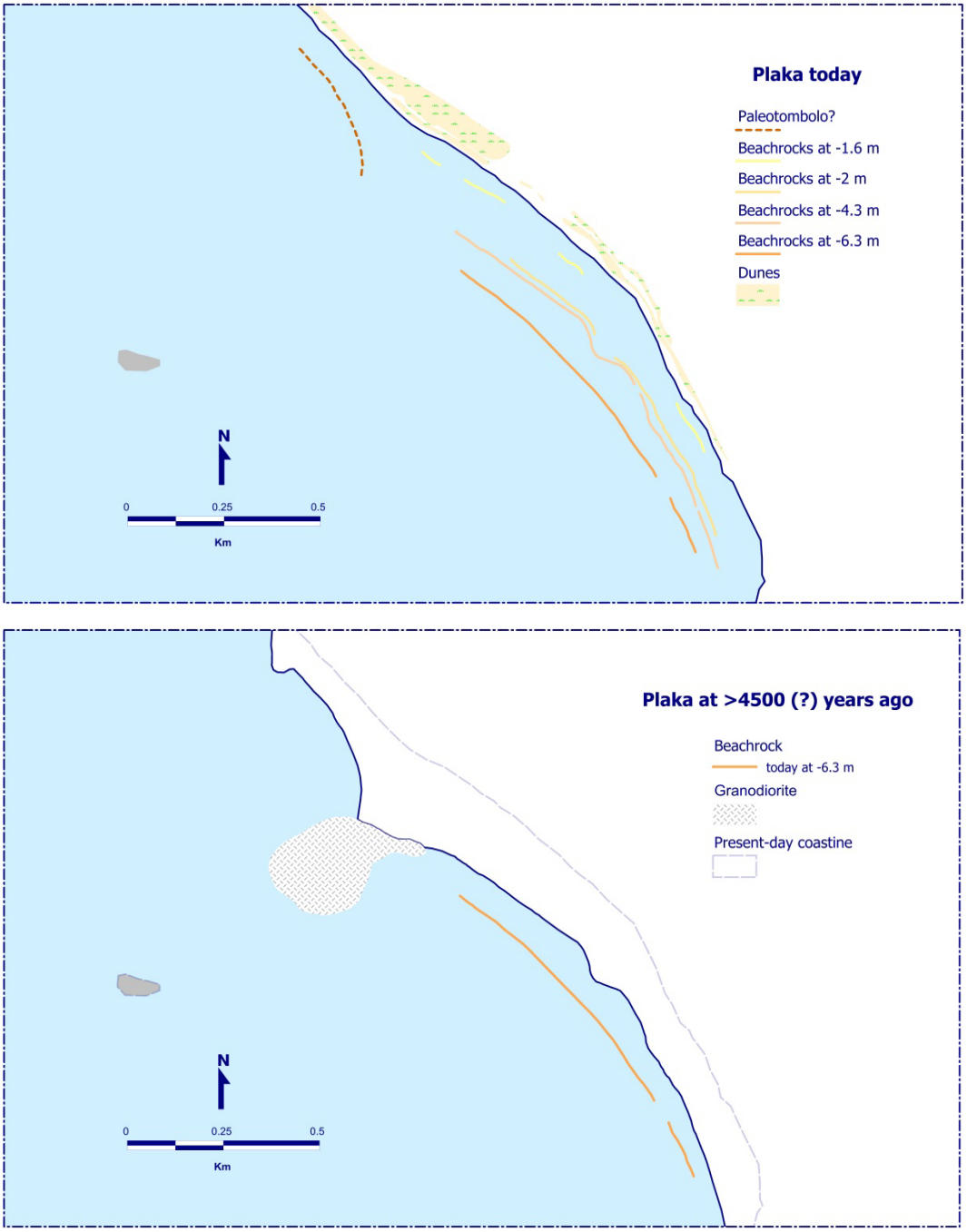

Figure 65: Shoreline evolution of Plaka (W Naxos). The submarine configuration of the beachrocks and the presence of a, nowadays, shallow granodioritic outcrop suggest that Plaka beach could have been separated in two bays with the presence of a paleo-tombolo.

Agios Georgios provides another interesting example of shoreline evolution. The submarine beachrocks could be distinguished in three shorelines (Figure 66). The second shoreline (maximum depth -1.9 m), wider than the youngest one, is dated between 1.38±0.17 ka, using quartz and 1.42±0.09 ka, using K-feldspar (sample

3163). The deepest shoreline was dated by a beachrock sample at about -5.7 m and yielded a quartz luminescence date of 1.26±0.30 ka and a K-feldspar date of 1.59±0.13 ka; as already discussed in the methodology, the dose rate was not measured for this sample and a mean value of all other samples was used to estimate the age. Even if this age is considered, such a date does not seem to be credible for such a deep sample (see also 5.4). As previously discussed, no evidence or historical records exist for such a change in relative sea level at least in the last ~1500 years and this age is not consistent with other published sea level data (e.g. Evelpidou *et al.*, 2012c; Kapsimalis *et al.*, 2009; Lykousis, 2009). This deepest shoreline reaches depths of -5.7 to -6.2 m; therefore it should have been at least older than the age obtained from sample 3169, i.e. 4.48±0.78 ka (quartz) / 3.39±0.57 (feldspar).

In Figure 66, one may observe that the beachrocks towards the NE part of the map appear shifted. This could probably be explained, at least for the deeper shorelines, from the presence of a shallower part, which, at the time of the beachrocks formation, was land. Furthermore, the bathymetry of the area suggests that the shallower beachrocks continue to the east of the bay, while the deeper shorelines were developed separately.

It is also worth noting that the second shoreline does not present the same configuration along its extent: it appears as a single slab in front of Manto island but it looks “split” towards the east.

The beachrock slabs, extending almost parallel to the present-day coastline, reveal the continuous shoreline regression in the bay of Agios Georgios. It is also worth noting that the grain size of the beachrocks is variable amongst the various palaeoshorelines, which may suggest different coastal hydrodynamic settings and the alternation of lower and higher energy coasts. In particular, the deepest shoreline appears more coarse grained and with more angular and not well rounded grains in comparison with the shallower shorelines suggesting a coast with higher energy. The second shoreline consists mainly of well-rounded mineral grains and larger lithoclasts with medium sorting. The shallower shoreline has more well sorted grains, rounded and semi-rounded suggesting a lower energy coast.

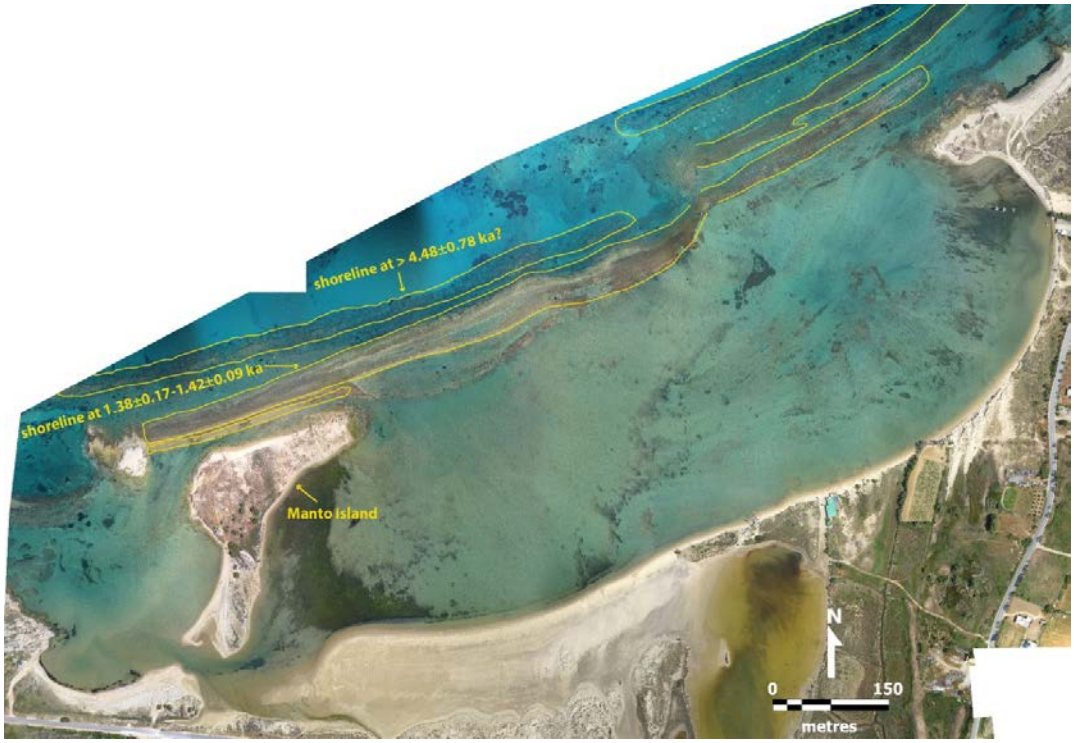

Figure 66: Palaeoshorelines deduced from submerged beachrocks in Agios Georgios (W Naxos). The beachrock slabs reveal the continuous shoreline recession in the bay of Agios Georgios.

The present configuration of the beachrocks suggests that the palaeoshorelines were more extensive, reaching probably the two edges of Agios Georgios bay. They did not however prevent the incursion of marine water into the bay, as corings from Evelpidou *et al.* (2012c) have reported that this embayment was changing from a coastal environment to a shallow marine with fresh water input and a brackish mesohaline one.

At **Orkos** beach (Naxos), three palaeoshorelines may be distinguished. The shallower one was dated between 1.42±0.24 ka (quartz) and 2.49±0.17 ka (K-feldspar). According to published sea level data (see paragraph 5.4) the age of the shoreline is probably underestimated. The second shoreline, located between -3.9 m and -4.2 m, can be correlated with the age obtained from sample 3169, and, therefore dated around 3.39±0.57 ka to 4.48±0.78 ka. The submarine configuration of the beachrocks, extending almost parallel to the contemporary coast, suggests that the morphology of the beach has not changed drastically at least in the last ~2500 years (Figure 67).

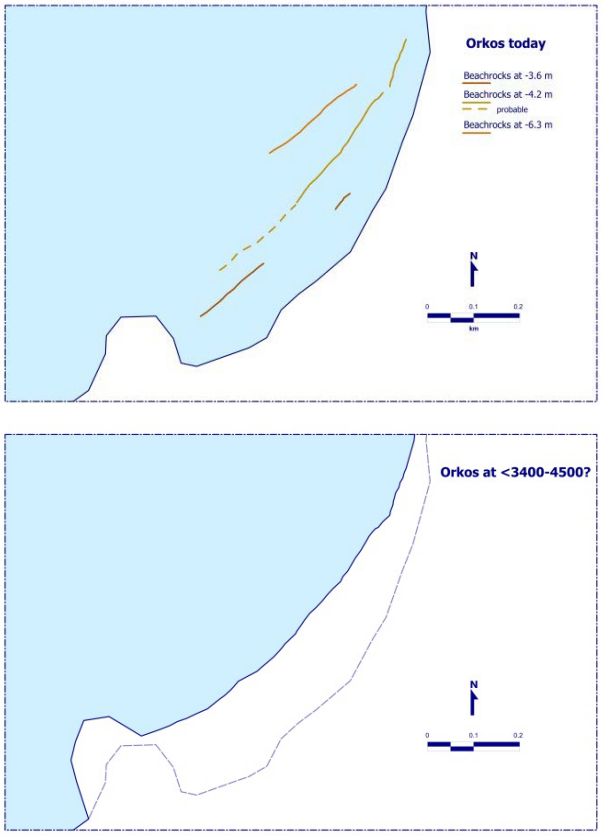

Figure 67: Palaeogeographic evolution of Orkos beach (W Naxos). The morphology of the coast does not appear to have changes drastically in the last in the last ~2500 years (dashed line represents the contemporary coastline).

Mikri Vigla is characterized by the presence of two palaeoshorelines. The shallower shoreline is better preserved and reveals a similar morphology to the contemporary one, while the deepest shoreline can be dated probably later than 2.49±0.17 ka (sample 3168). Although, the deepest shoreline is not well preserved it still provides some evidence concerning the palaeogeography of the area (Figure 68). According to Evelpidou *et al.* (2012c), during the period 3800±50 BP to 1625±45 BP, the area was an active lagoon, and the deepest beachrock was protecting the bay, acting as a

natural barrier. Similar to Agios Georgios, the beachrock was periodically submerged and allowed the connection of the lagoon with the open sea (Evelpidou *et al.*, 2012c).

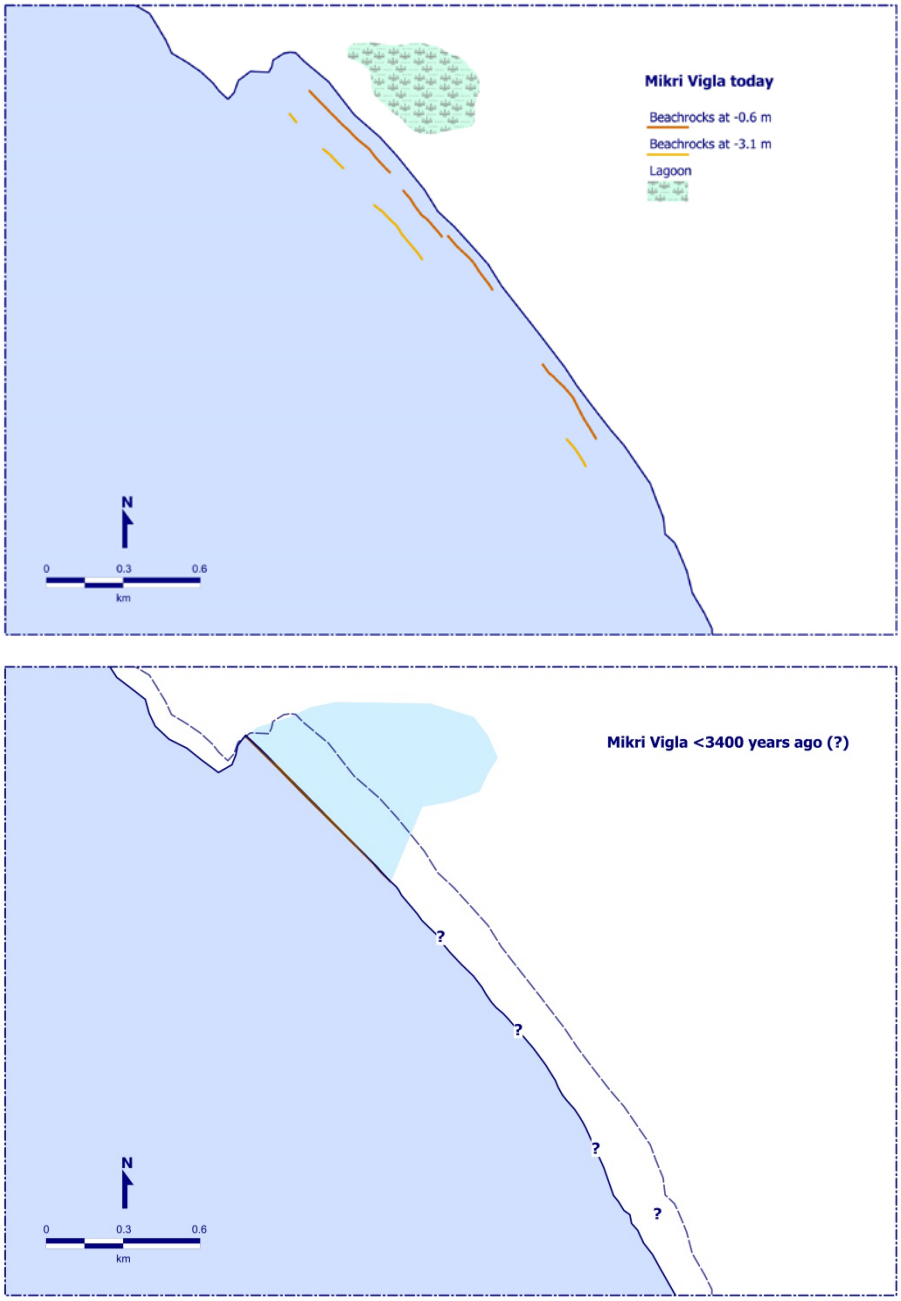

Figure 68: Palaeogeographic evolution of Mikri Vigla coast (W Naxos). The deepest submerged beachrocks probably acted as a natural barrier to the active lagoon during the period 3800±50 BP to 1625±45 BP (dashed line represents the contemporary coastline).

At **Glyfada**, the distinction to palaeoshorelines is not as clear as in other cases. Three palaeoshorelines may be distinguished that are almost parallel to the contemporary one. The deepest one, reaching -4.4 m was dated between 1.12±0.22

ka (quartz) and 1.16±0.08 ka (K-feldspar), however this age is considered too young for such a depth. It can be correlated with the age obtained from sample 3169, and, therefore dated around 3.39±0.57 ka to 4.48±0.78 ka (Figure 69). In any case, the submarine configuration of the beachrocks suggests that the coast has not changed greatly in terms of morphology, and reveal the shoreline recession for the last ~4500 years.

Figure 69: Palaeogeographic evolution of Glyfada beach (W Naxos). Although the submerged beachrocks are not as well preserved as in other sites, the continuous recession of the coast is well demonstrated during the last ~4500 years (dashed line represents the contemporary coastline).

Glystra beach, although not extensive, is characterized by the presence of probably two extensive palaeoshorelines, almost continuous. The deepest one was dated

between 3.39±0.57 ka and 4.48±0.78 ka, suggesting a shoreline recession of about 50 m in the last ~ 3400-4500 years (Figure 70).

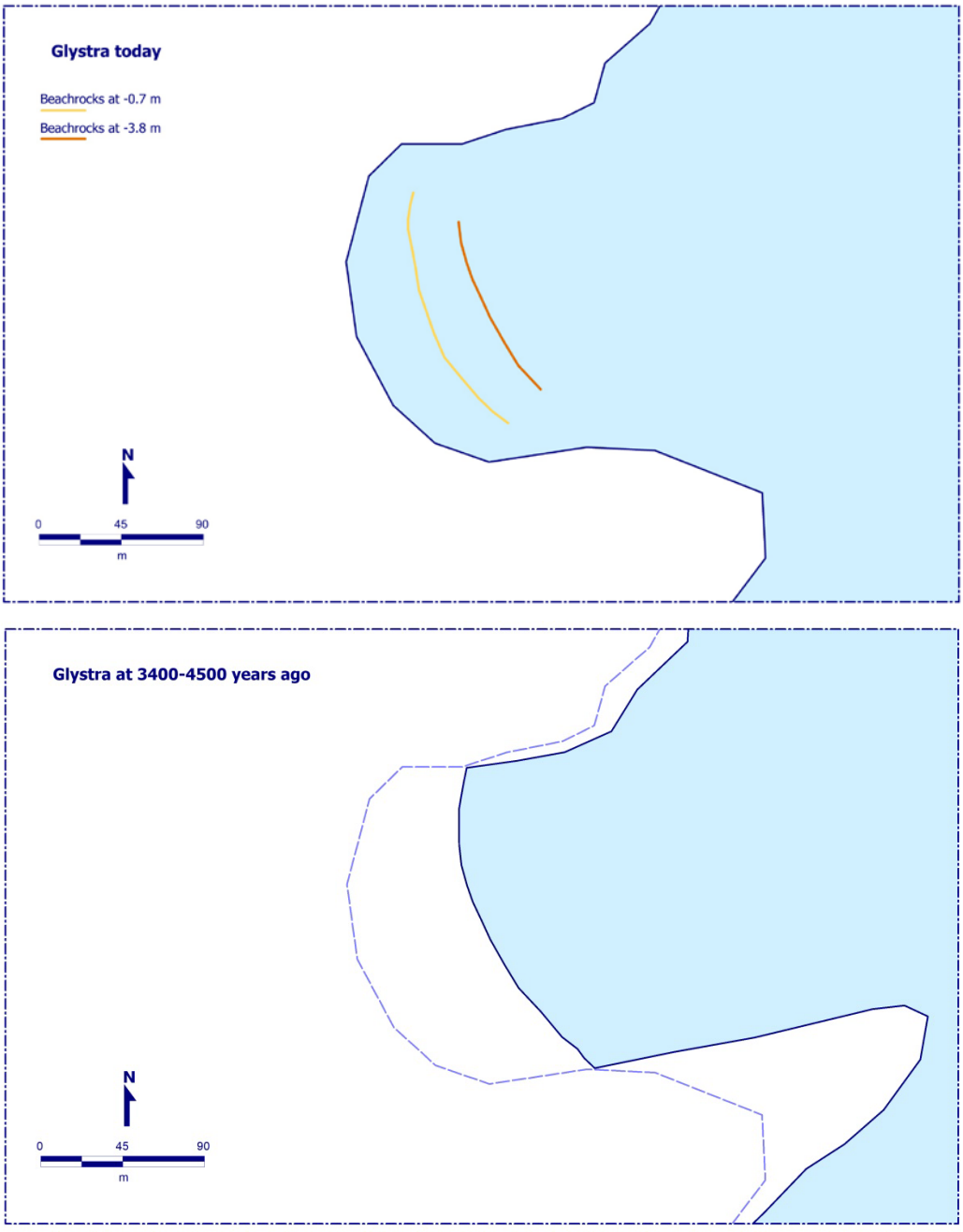

Figure 70: Palaeogeographic evolution of Glystra coast (E Naxos). The morphology of the coast has not changed significantly. On the basis of the submerged beachrock slabs a shoreline recession of about 50 m in the last ~ 3400-4500 years is suggested.

Paros Island

In Paros Island, the most significant beachrock outcrop is at **Martselo** beach. The submarine beachrocks could be distinguished in three shorelines, each one characterized by different grain sizes, with the shallower one being the most coarse-grained. This probably indicates that there was an alteration of hydrodynamic settings, of lower and higher energy. In particular, during the time of the shallower shoreline, the hydrodynamic setting was probably higher than today. Past aerial photographs reveal that the shallower shoreline was more extensive; nowadays significant parts have been removed however it is clear that this paleoshoreline is parallel to the contemporary one. Although this shoreline was not dated, if correlated with the results from Naxos, it probably corresponds to the age obtained by sample 3165, from Plaka, having an age between 1.24±0.23 ka and 1.50±0.07 ka. It should also be noted that this shoreline lies next to archaeological remains, probably dating to the Roman period (see also chapter 5).

The second shoreline is not well preserved and is partly buried, while the third shoreline can be followed mainly along the central part of the beach. The third shoreline was dated (sample 3164) between 1.39±0.19 ka (quartz) and 1.72±0.08 ka (feldspar), however this age does not seem credible for such a deep shoreline, reaching a depth of -5.6 m. It is more likely that this shoreline is dated probably closer to sample 3169, i.e. 4.48±0.78 ka (Figure 71).

In any case, the submarine configuration of the beachrocks reveals that the general morphology of the coast has not changed at least in the last 1500 years and suggests a shoreline regression of about 35-40 during this period.

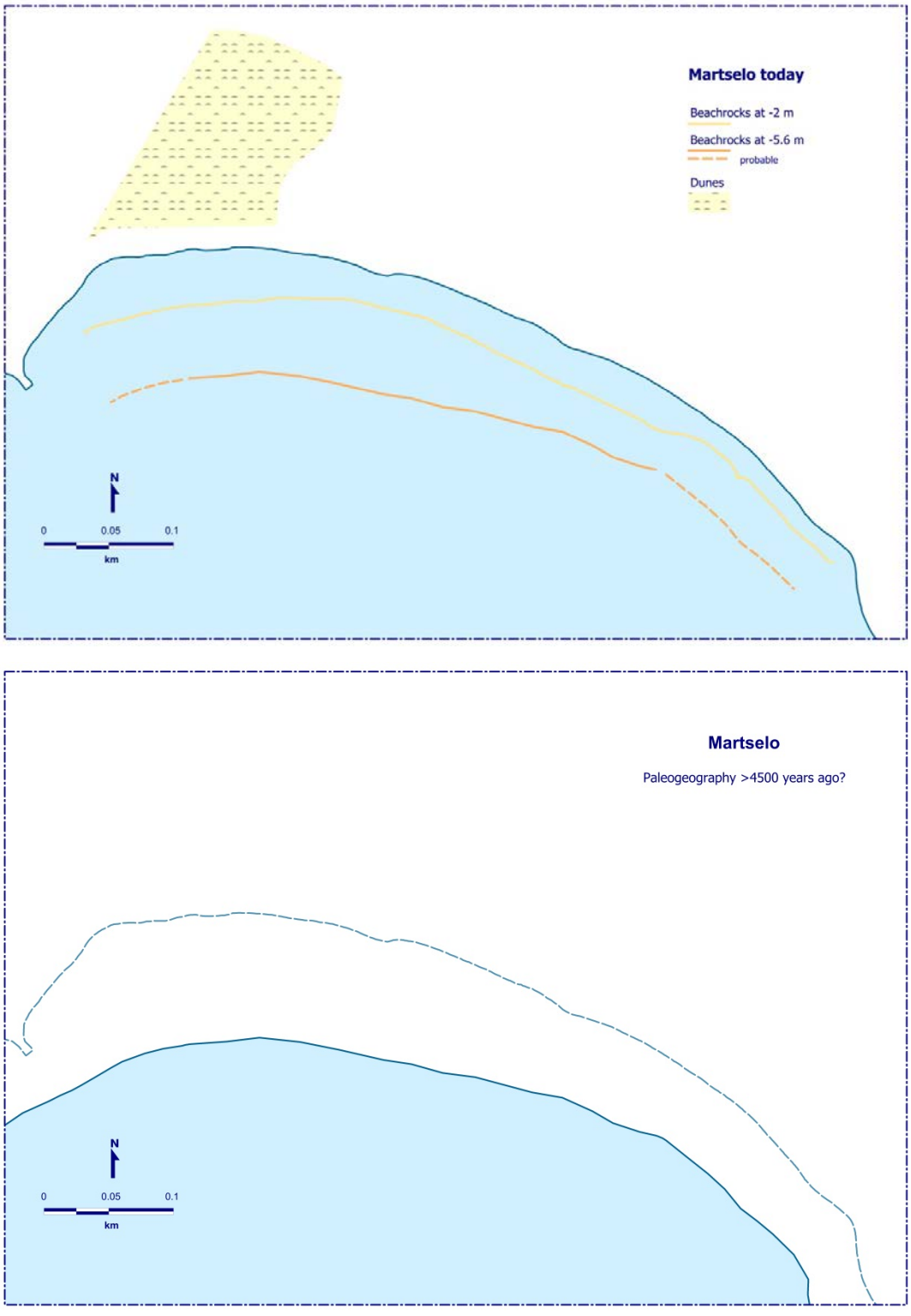

Figure 71: Palaeogeographic evolution of Martselo beach (NW Paros): a) present configuration, b) shoreline position before ~4500 years (?), with the dashed line representing the contemporary shoreline. The submerged beachrocks at a maximum depth of -1.8 m, if correlated with the nearby archaeological remains are probably older than Roman times.

Tsoukalia beach, at the east part of Paros, is characterized also by the presence of three paleoshorelines. The shallower shoreline is the most well-preserved with a width of about 45 m. The deepest shoreline reaches a depth of -6.2 m and suggests that the paleogeography of the coast was different. In particular, the beachrocks extend to the NNW of the beach and suggest that, during that time, Tsoukalia beach was united with Glifades beach (Figure 72), probably forming a longer coast. Similar to the previous cases, this paleoshoreline is dated probably closer to sample 3169, i.e. 4.48±0.78 ka.

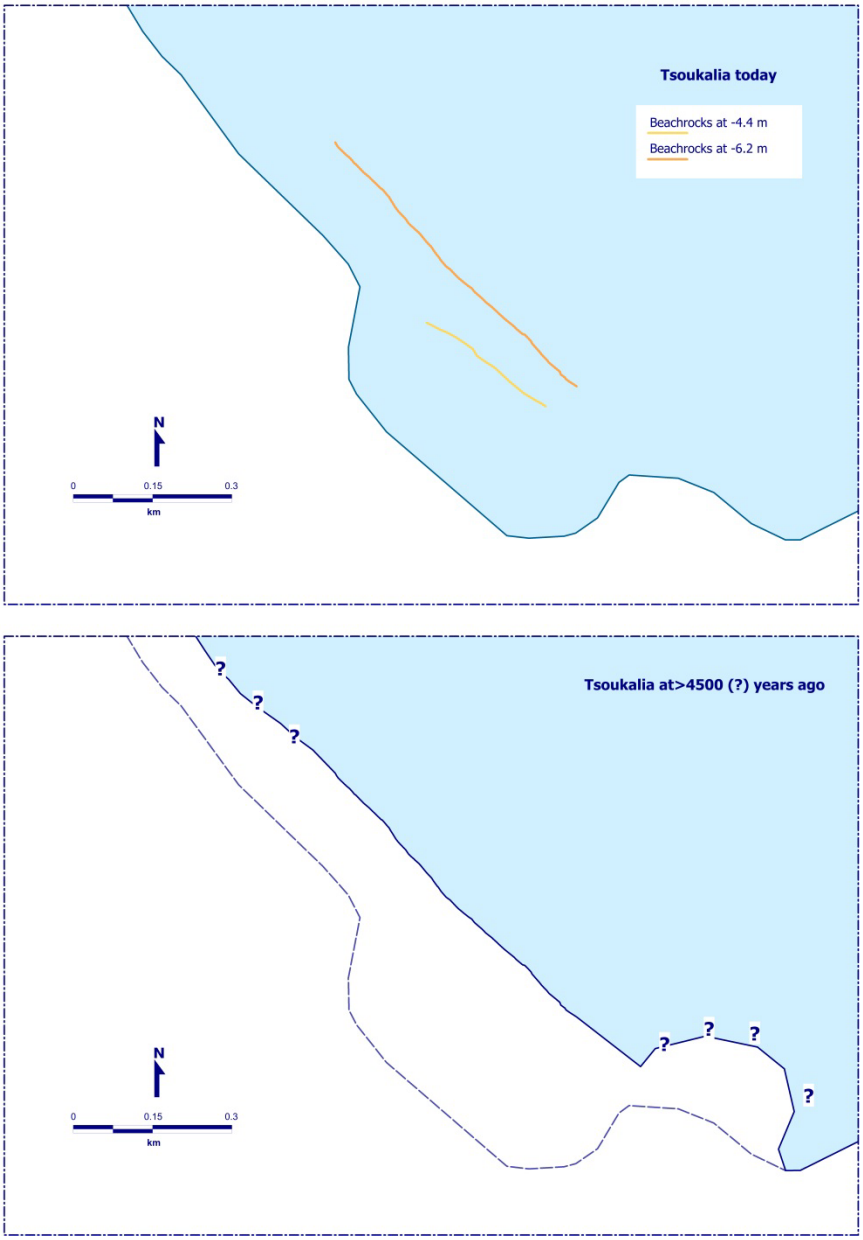

Figure 72: Palaeogeographic evolution of Tsoukalia beach (E Paros). The morphology of the deepest beachrocks suggests that the coast was more extensive and continued towards the NNW part, and Tsoukalia beach was probably united Glifades beach (dashed line corresponds to the contemporary coast).

Chapter 6 – Drillings

6. Drillings – results and discussion

6.1 Introduction

For the purposes of this study a multiproxy analysis took place, which included sedimentological analysis of the cores, biostratigraphy through macrofauna and ostracods and radiocarbon dating. The boreholes were drilled with a portable drilling sampler, 35 mm in diameter. Three cores are analysed (Figure 73): one from Livadia coastal zone (LIV1), depth 4.46 m, one from Pounta coastal zone (POU2), depth 3.96 m and one from Kolymbithres (KOL1), with depth 4.20 m. The scanned cores are provided in Appendix II.

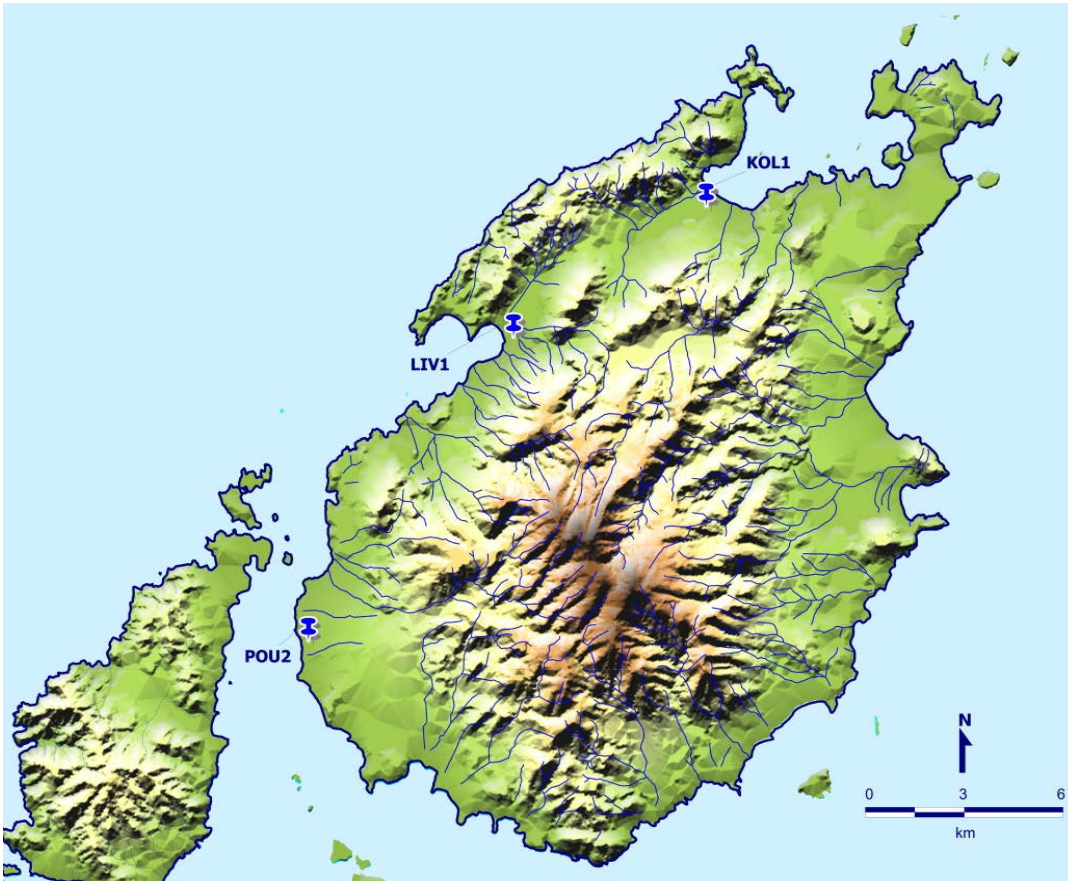

Figure 73: Location of the boreholes discusses in this chapter in Paros Island. POU2 was drilled at Pounta (SW Paros) while LIV1 took place at the bay of Paroikia (NW Paros).

6.2 Dating results

The chronostratigraphy of the cores was determined by a series of 9 AMS radiocarbon datings undertaken on marine shells, performed at the Poznan Radiocarbon Laboratory (Poland). No suitable material for dating was found in KOL1 borehole. The samples were corrected for the local marine reservoir effect according to Reimer and McCormac (2002), using a using a ΔR value of 154±52 for the Aegean Sea. The conventional radiocarbon ages of the samples were converted into calendar years by using the online software Calib 7.10 (Stuiver *et al.*, 2016), using the Marine13 curve (Reimer *et al.*, 2013). It should, however, be noted that two samples (Poz-81140, Poz-81147) were not possible to calibrate as post ad 1950 calibration for marine or mixed samples cannot be made (bomb 14-c). Thus, for samples Poz-81140 and Poz-81147, only the ^{14}C ages are provided.

Table 11 presents the results of the radiocarbon dating. One sample from POU2 core (Poz-81140) provided an age that is inconsistent with the stratigraphic order and the ages of the rest of the samples. In the same manner, sample Poz-81150 from LIV1 core is an outlier, as well as probably Poz-81151, as they provide older dates than the next deeper samples in the same borehole.

Table 11: Radiocarbon ages for dated samples from Paros cores.

Sample code	Lab code	Depth (m)	Material	$\delta^{13}C$	^{14}C BP	Age Cal. BP	Cal. BC/AD (2σ)
POU2-1	Poz-81147	85	Conus mediterraneus	2.8	520±30	-	-
POU2-2	Poz-81148	186-196	Loripes lacteus	0.3	715±30	40-298	1652-1910 AD
POU2-3	Poz-81354	260-270	Cerithium vulgatum	-3.9	1475±30	721-986	964-1229 AD
POU2-4*	Poz-81140	337-346	Nassarius louisi	4.9	490±30	-	-
LIV1-1*	Poz-81150	150-160	Cerithium vulgatum	4.3	3630±30	3193-3508	1559-1244 BC
LIV1-2*	Poz-81151	235-245	Bittium reticulatum reticulatum	-1.4	3470±30	2985-3330	1381-1036 BC
LIV1-3	Poz-81156	284-296	Pirinella conica	-7	2985±35	2385-2729	780-436 BC
LIV1-4	Poz-81157	360-370	Pirinella conica	2.7	3110±30	2559-2872	923-610 BC
LIV1-5	Poz-81192	420-430	Hydrobia	-5.9	4670±50	4500-4864	2915-2551 BC

6.3 Lithology – faunal evidence – depositional environment

6.3.1 POU2 core

POU2 core was drilled in the southwest part of Paros Island, 1 km south of Pounta. The area today is characterized by the presence of small coastal dunes, forming a sandy spit/barrier and a lagoon in the back (Figure 74). The site is an extensive seasonal salty pond (water salinity salty: >18.0 g/l; WWF, 2013) that has received major anthropogenic pressures. Human activities that have reduced the values and functions of this wetland mainly include: earthworks, land reclamation, construction, road building and heavy touristic activities such as water sports. The supply of fresh water occurs via runoff while it is also connected seasonally with the sea (surficial and underground).

Figure 74: Aerial photo of Pounta site (SW Paros). The yellow arrow shows the location of the borehole. Nowadays, the value of this wetland is significantly reduced due to heavy touristic activities.

The core is mainly characterized by sand deposits (Figure 75). Figure 76 presents the distribution of macrofauna in POU2 core, while Figure 77 presents the ostracods distribution. Three units were distinguished.

In particular, Unit A, from the bottom of the core up to 2.6 m is dominated by medium to coarse sand with shell fragments. In fact, the sand fraction comprises more than 87% of the total sediment texture. The macrofauna are dominated by infralittoral sand assemblages, hard substrate assemblages and algae (Figure 76). In particular, infralittoral sand assemblages consist mainly of *Truncatella subcylindrica*, *Rissoa lineolate*, *Rissoa monodonta*, *Tricolia pullus*, while hard substrate assemblages are

represented by *Conus mediterraneus, Cardita calyculata, Gibbula spp., Jujubinus sp., Columbella rustica, Cantharus pictus, Gibberula miliaria, Gibbula varia, Cythara paciniana and Vermetide*. Algae are represented by *Alvania cimex* and *Alvania montagui*. Smaller peaks represent lagoonal species (*Loripes lacteus*), upper muddy sand assemblages (*Acanthocardia echinata, Cerithium vulgatum*) in sheltered areas and upper-clean sand assemblages (*Pirenella conica, Nassarius pygmaeus, Nassarius mutabilis, Nassarius reticulate, Nassarius louisi*). Ostracods are almost absent with the exception of a few coastal (54.3%) (*Aurila convexa, Aurila woodwardii, Cytherelloidea sordida, Hiltermannicythere cf., Urocythereis oblonga, Cytherois frequens, Neocytherideis fasciata, Costa edwardsii*) and marine lagoonal species (45.7%) (*Loxoconcha stellifera*) at ~3.3 m depth (Figure 77). This unit is therefore representative of a marine – shallow marine environment. Two marine shells were dated from the middle and the top of this unit, however, the deeper sample yielded an age (490±30 BP) younger than the rest shallowest samples. The top was dated at 964-1229 cal AD (721-986 cal BP).

Unit B is found from 2.46 m up to 1.18 m the stratigraphy consists of silty sand to sandy silt with posidonia and shell fragments. Sands represent 71.6% of the total sediment texture and silts-clays 26.3%. The macrofauna is dominated by lagoonal (*Loripes lacteus, Abra segmentum*), upper muddy sand assemblages in sheltered areas (*Acanthocardia echinata, Cerithium vulgatum*), and infralittoral sand assemblages (*Tricolia pullus, Tricolia tenius, Rissoa lineolate, Rissoa guerini, Mitra ebenus*). Smaller peaks in this unit consist of hard substrate assemblages (*Conus mediterraneus*, *Jujubinus sp.*, *Columbella rustica*) and algae (*Alvania cimex*, *Alvania sp.*). Microfossil analysis indicates that assemblages are dominated by marine lagoonal (*Loxoconcha stellifera*, *Xestoleberis communis, Xestoleberis sp., Loxoconcha rhomboidea*) and coastal species (*Cytherelloidea sordida, Aurila convexa, Aurila woodwardii, Urocythereis oblonga, Cytherois frequens, Leptocythere lacertosa*). Marine species are represented by some individuals of *Bassleristes berchoni* and *Paradoxostoma planum*. The middle of this unit was dated at 1652-1910 AD (40-298 cal BP). This unit can be considered as representative of an open lagoon largely open to the sea.

Unit C is found from 1.18 m until the top of the core consists of coarse to medium sand, which becomes siltier towards the top. Sands represent 91% of the total sediment texture up to 50 cm and silts-clays are increased on the last 50 cm reaching 25.4%.Macrofauna analysis indicates that assemblages are poorer in species diversity and mainly consist of upper muddy sand assemblages in sheltered

areas (*Cerithium vulgatum*), upper-clean sand (*Pirenella conica, Nassarius pygmaeus*) and hard substrate assemblages (*Conus mediterraneus, Cardita calyculata, Gibbula spp.*) and algae (*Alvania sp.*, *Alvania cimex Alvania montagui*). Ostracods are characterized by the presence of mainly marine lagoonal species (*Loxoconcha stellifera*, *Xestoleberis communis, Loxoconcha rhomboidea, Xestoleberis sp., Loxoconcha sp.*), lagoonal species are represented by few individuals of *Cyprideis torosa*, and coastal species (*Aurila convexa, Cytherelloidea sordida, Urocythereis oblonga, Cytherois frequens, Neocytherideis fasciata, Procytherideis foveolata*). The middle of this unit (85 cm depth) was dated at about 520±30 BP. This unit is probably representative of a leaky lagoon (Kjerfve, 1994).

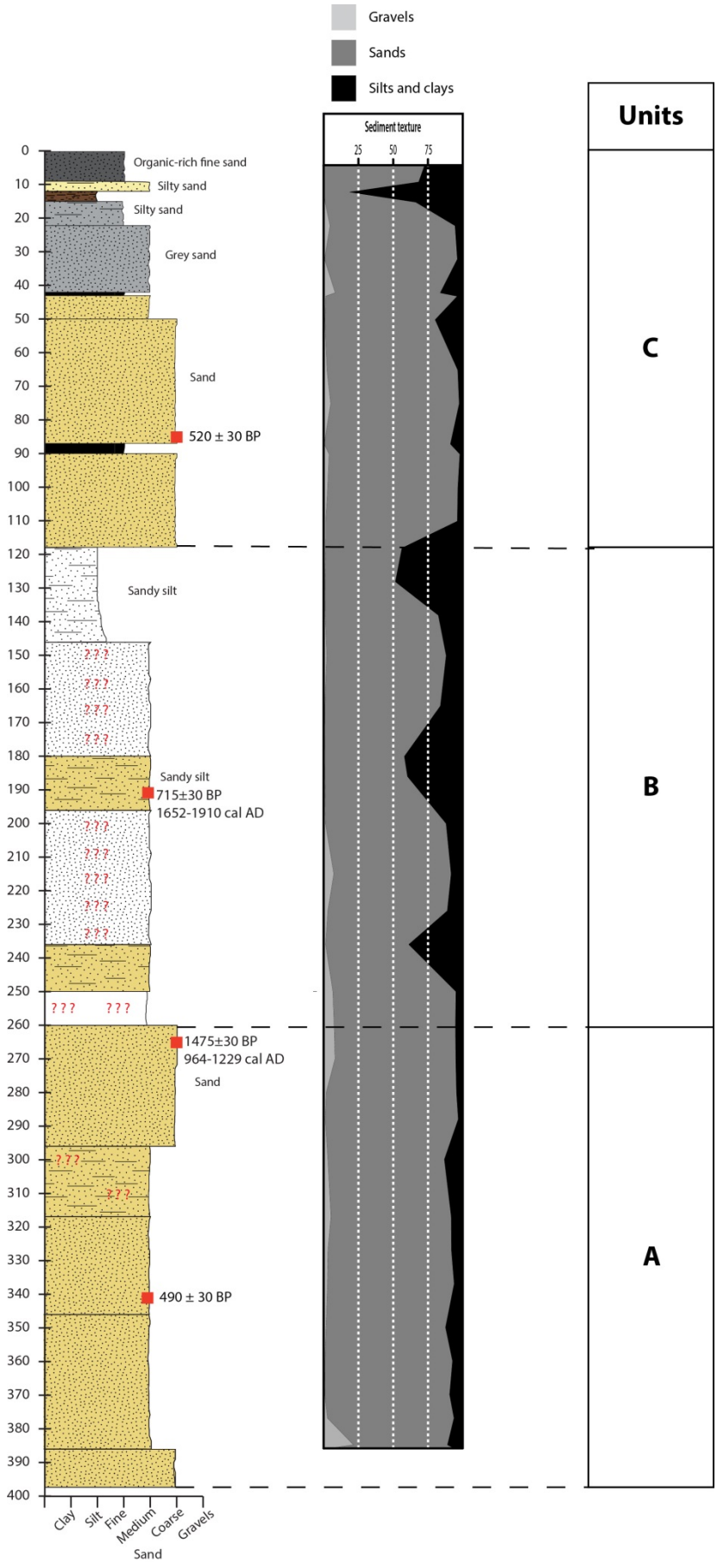

Figure 75: The lithostratigraphy of core POU2. The majority of the core is dominated by medium to coarse sands.

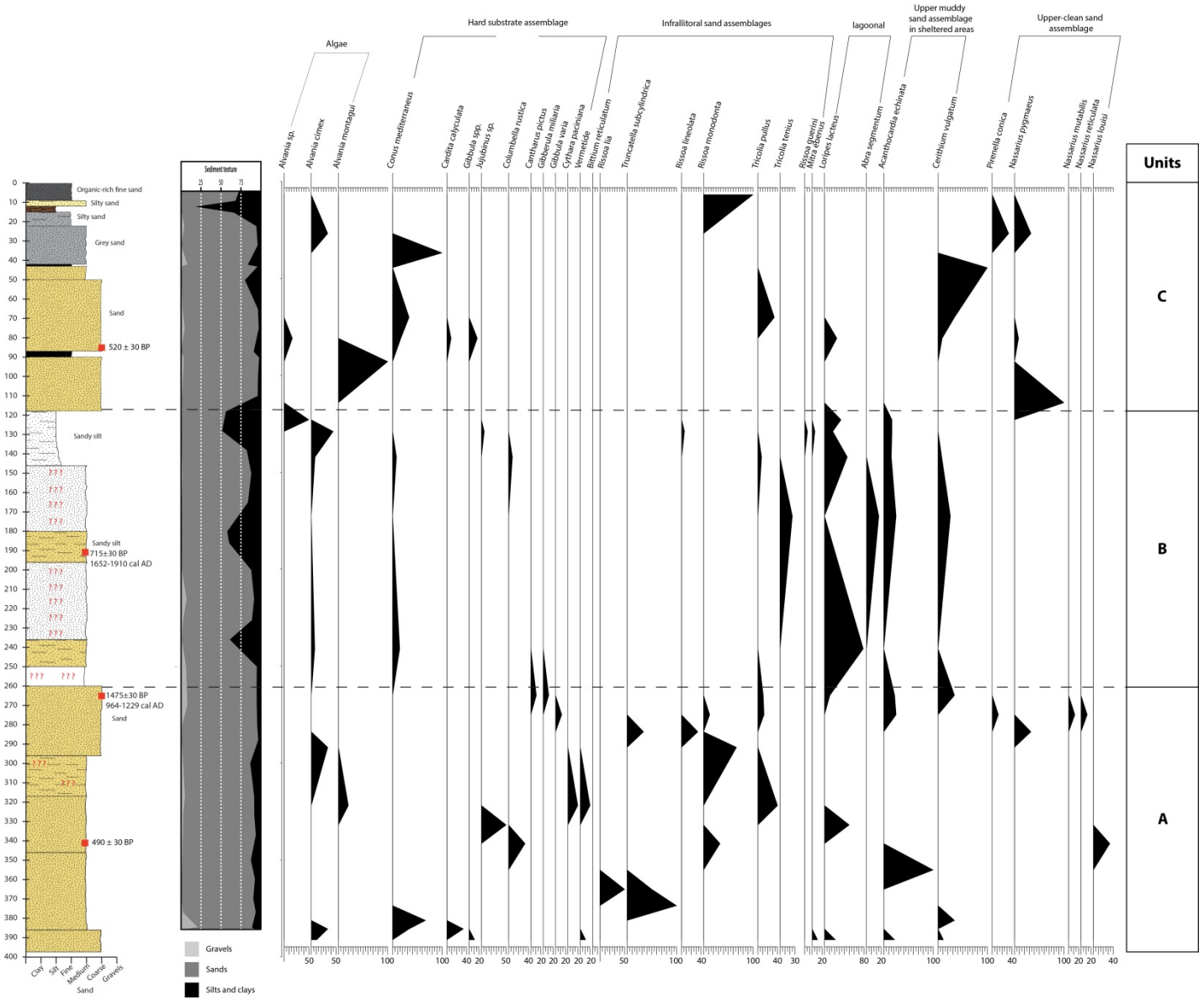

Figure 76: The macrofauna of core POU2, along with the stratigraphy. Macrofossils were identified and assigned to assemblages based on d' Angelo and Gargiullo (1978) and Doneddu and Trainito (2005).

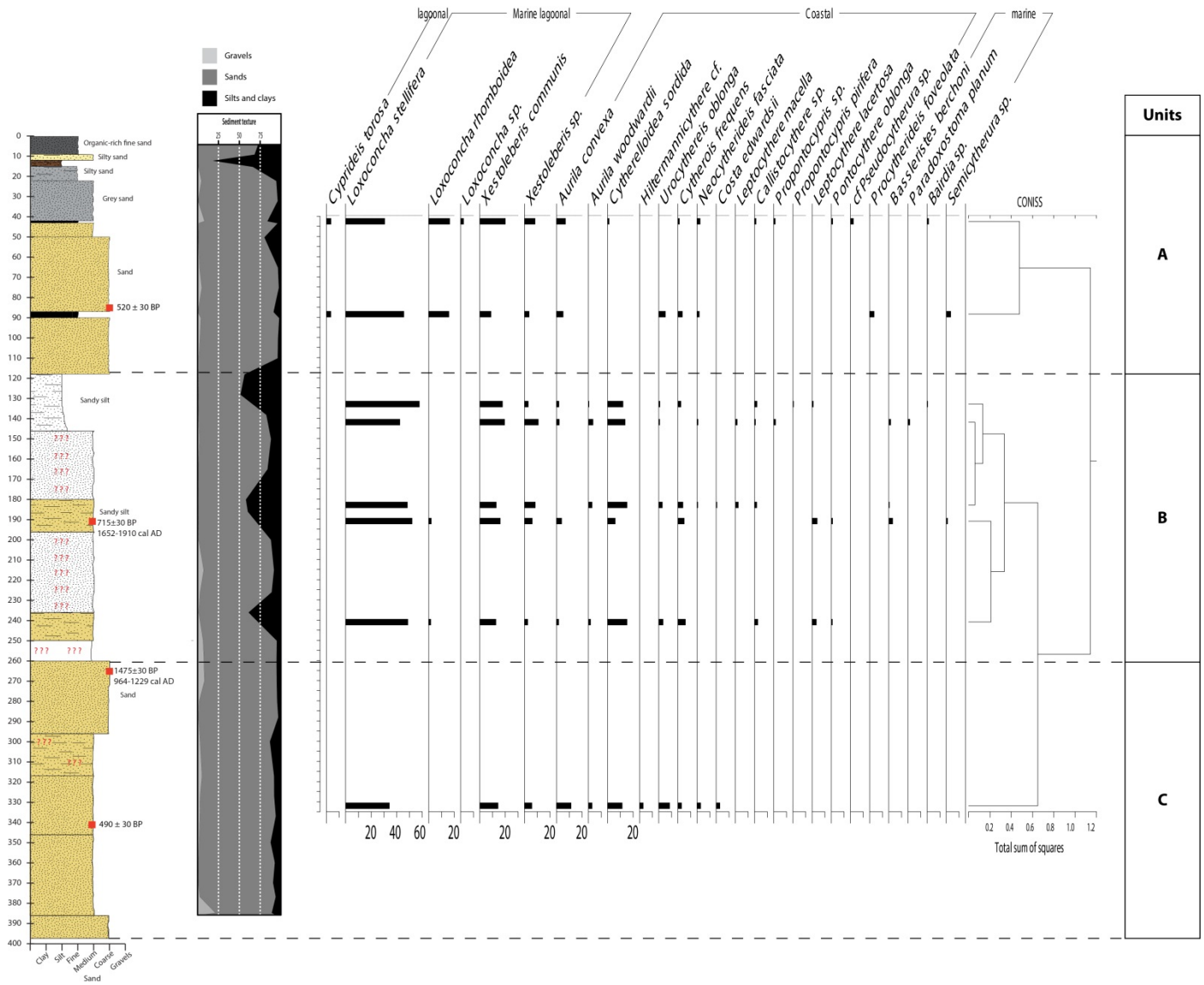

Figure 77: The ostracods of core POU2. Ostracods were assigned to four assemblages: lagoonal, marine lagoonal, coastal and marine.

6.3.2 LIV1 core

LIV1 core was drilled in the west-northwest part of Paros Island, 1.2 km to the north-northeast of Paroikia (Figure 78). The site today is a coastal marsh of brackish water (water salinity brackish: 5.0-18.0 g/l; WWF, 2013). It is supplied with fresh water from the discharge of the aquifer and from small amounts of fresh water through an intermittent stream, separated in drainage channels that have been created in the upstream region.

Figure 78: Aerial photo of Livadia site (NW Paros). The yellow arrow shows the location of the borehole. Today the site is today is a coastal marsh of brackish water.

According to sedimentological and faunal analysis, 4 units were distinguished.

Unit A1, from the bottom of the core up to 2.84 m, the core is dominated by grey silt (Figure 79). In fact, the silt/clay fraction represents almost 77% of the total sediment texture up to 3.85 cm, and between 3.75-2.84 m they are reduced to 45%. Lagoonal (*Cyprideis torosa*) and freshwater ostracods (*Illyocypris gibba, Heterocypris salina, Darwinula stevensoni, Candona lacteal, Potamocypris variegate, Potamocypris similis, Heterocypris salina*) are characteristic of this unit. Small peaks of marine lagoonal (*Loxoconcha rhomboidea*) and coastal ostracods (*Urocythereis oblonga, Pontocythere elongate, Aurila convexa, Aurila woodwardii*) were only observed in the upper part of the unit. The molluscan fauna is poor with the presence of the lagoonal *Loripes lacteus*, upper clean sand assemblages (*Pirinella conica, Nassarius sp.*) and few hard substrate (*Gibbula varia, Gibbula sp.*) and upper muddy sand assemblage in sheltered areas, represented by *Cerithium vulgatum*, in the upper part of the unit. The age of this unit was determined through three radiocarbon dates of marine shells. They indicated an age of 2915-2551 cal BC (4500-4864 cal BP) for the lowermost part, and 780-436 cal BC (2385-2729 cal BP) for the uppermost part. The middle part was dated at 923-610 cal BC (2559-2872 cal BP). The relative low species diversity along with the presence of typical lagoonal *Cyprideis torosa* and *Loripes lacteus* suggests this unit is representative of a semi-enclosed lagoon. The presence of freshwater ostracods (*Illyocypris gibba*) further suggests a freshwater influence.

Unit A2 is an intermediate unit consisting of a 10 cm layer (3.75-3.85 m) of coarse sand with some gravels. The sand fraction represents 54.8%, gravels 14.4% and silt/clays 30.8% of the total sediment texture. This unit is barren of any molluscan fauna, while ostracod fauna are characterized by a peak in the coastal *Pontocythere elongata* (17%), a decrease in freshwater species (8%) and an increase in *Cyprideis torosa* (75%). Considering the chronostratigraphy of Unit A1, this unit is older than ~923-610 cal BC (2559-2872 cal BP). The transition from fine deposits of unit A1 to coarser deposits (unit A2), correlated with the increase in the proportion of coastal ostracods in A1, may indicate a reshuffle during a storm episode.

Unit B was found from 2.84 m until 2.35 m. It consists of coarse-medium sands. Sands represent 54.4% and silt/clays 38.9 % of the total sediment texture. It is barren of molluscan fauna except at the top of the unit where a peak of an infralittoral sand species (Bittium reticulatum reticulatum) is identified. The ostracods are dominated by freshwater (*Illyocypris gibba, Heterocypris salina, Potamocypris variegate*) (82.2%) and lagoonal species (*Cyprideis torosa*) (17.8%), with the

absence of any marine lagoonal or coastal species. Towards the top of the unit, *Cyprideis toros*a is decreased and *Heterocypris salina* is increased. The abundance in freshwater ostracods, along with the lagoonal *Cyprideis torosa* is probably indicative of a local stream/river influence into the lagoon. The top of this layer was dated through a marine shell at 1381-1036 cal BC (2985-3330 cal BP). However, this date is older than the ages obtained in Unit A and appears inconsistent with the stratigraphic order.

Unit C was found between 2.35 and 1.5 m, dominated by sandy silts with charcoal that turn to silty sands with traces of oxidation. Ostracods are only present in the sandy silt layer. The lagoonal species, *Cyprideis torosa* (83%), is dominant but freshwater species were also identified, such as *Potamocypris variegata* (17%). Infralittoral sand assemblages (*Bittium reticulatum reticulatum*) are only present in the lower part of the unit and the rest is characterised by few individuals of hard substrate assemblages (*Murex, Gibbula sp.*). The top of the unit was dated at 1559-1244 BC (3193-3508 cal BP). However, this date also appears inconsistent with the stratigraphic order and the ages of the rest of the samples. The presence of the lagoonal *Cyprideis torosa* only to the lower part of the unit, the absence thereafter of any ostracods and the presence of only few hard substrate assemblages may reflect the gradual infill of the lagoon.

The top 1.5 m of the core corresponds to a modern manmade artificial infill.

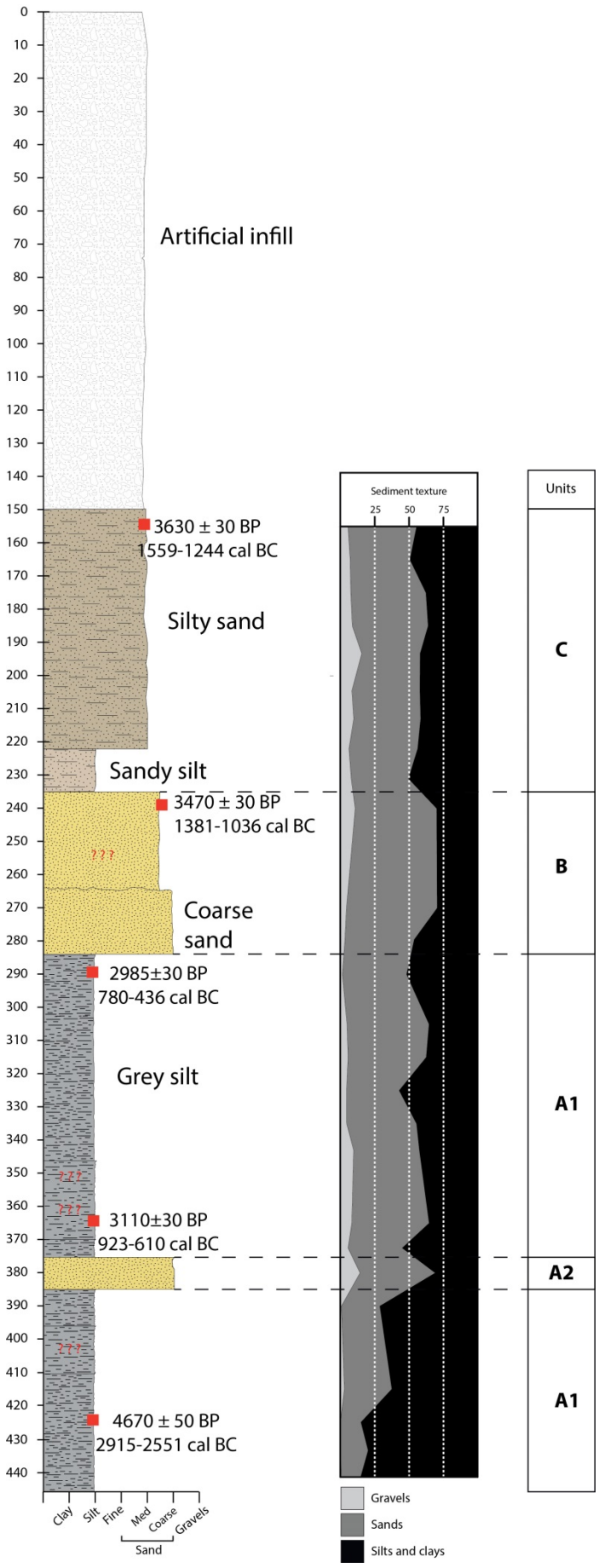

Figure 79: The lithostratigraphy of core LIV1. Five units were identified based on sedimentological and paleontological data.

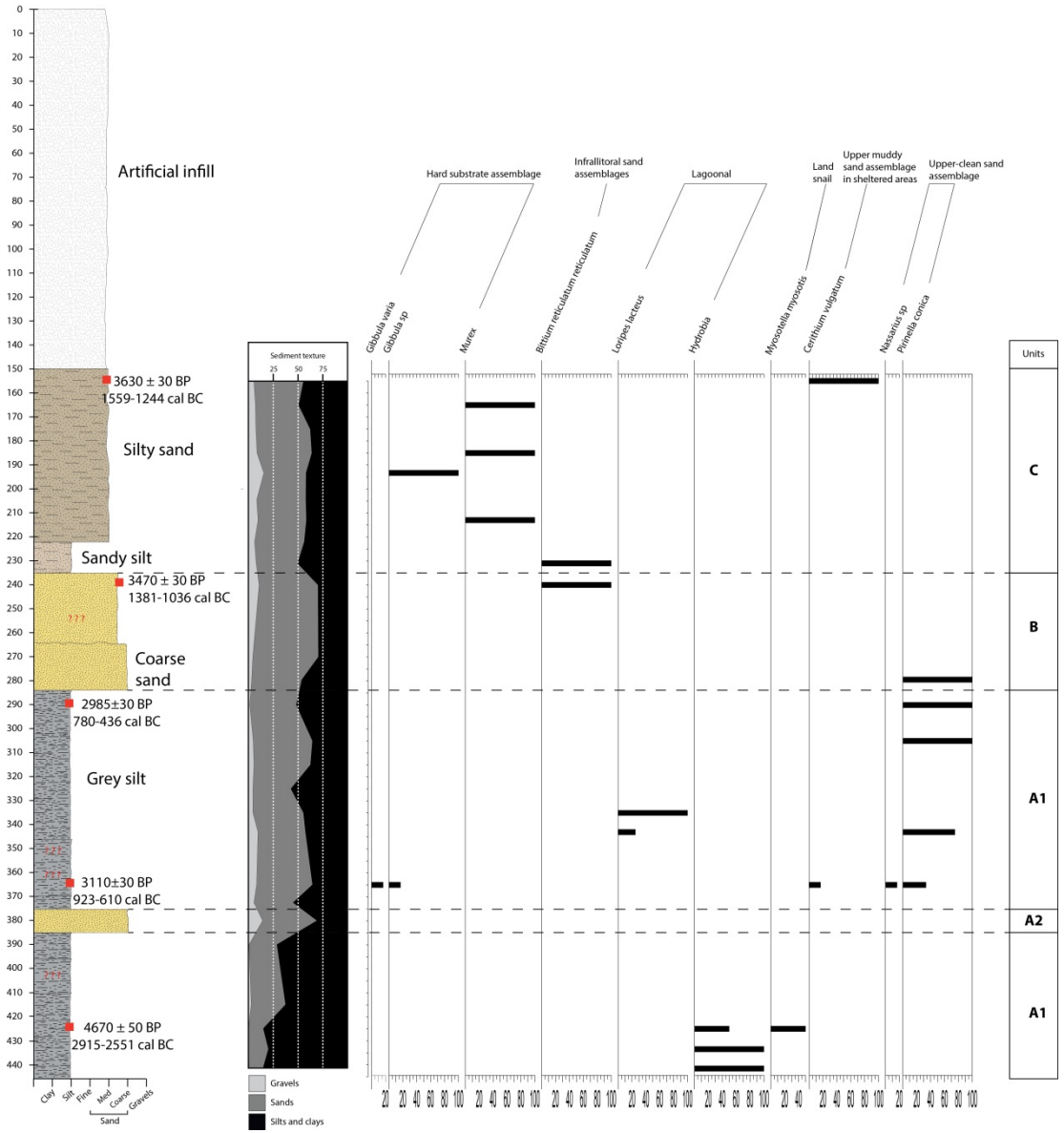

Figure 80: The macrofauna of core LIV1. Overall, the molluscan fauna of LIV1 is poor, both in species diversity and quantity.

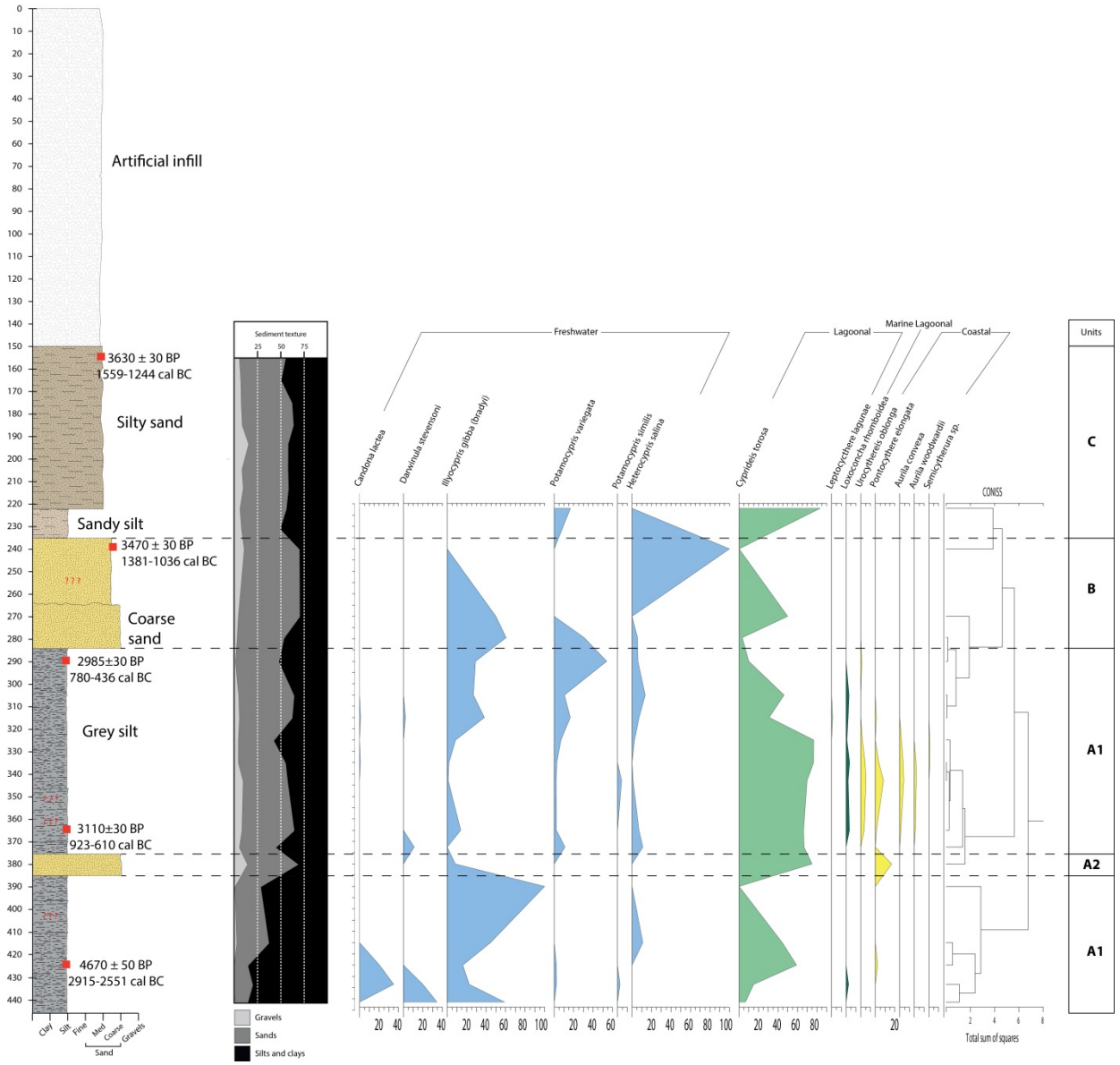

Figure 81: The ostracods of core LIV1. Ostracods were assigned to four assemblages: freshwater, lagoonal, marine lagoonal and coastal.

6.3.3 KOL1 core

KOL1 core was drilled in the north part of Paros, 2 km west of Naousa. Today the wetland of Kolymbithres consists, in the south, by the mouth of two streams hat drain the same, relatively large, basin (water salinity brackish: 5.0-18.0 g/l; WWF, 2013).

From the bottom of the core (4.20 m) up to 3.89 m, the stratigraphy consists of silt with some charcoal, along with the presence of terrestrial snails. Between 3.89 – 3.59 m, a layer of sand was recorded, which gets finer towards the top with traces of oxidation. From 3.59 m up to 2.37 m, silt to sandy silt was observed, with some roots between 3.59 – 3.51 m. Alterations with silt and sandy silt was also recorded between 2.37 – 1.87 m. Between 1.87 m and 1.00 m yellowish sandy silt with some gravels, roots and traces of oxidation were observed. Fine sand, of maybe aeolian origin, was recorded between 0.96 – 0.77 m followed by silty sand (0.77 – 0.50 m). The last 0.50 m of the core consists of soil, light brown silty sand with roots. It should be noted that no appropriate dating material was found in this core. In total, KOL1 core appears to be dominated by terrestrial processes, as indicated by the occasional presence of terrestrial snails. Furthermore, no molluscan fauna were found.

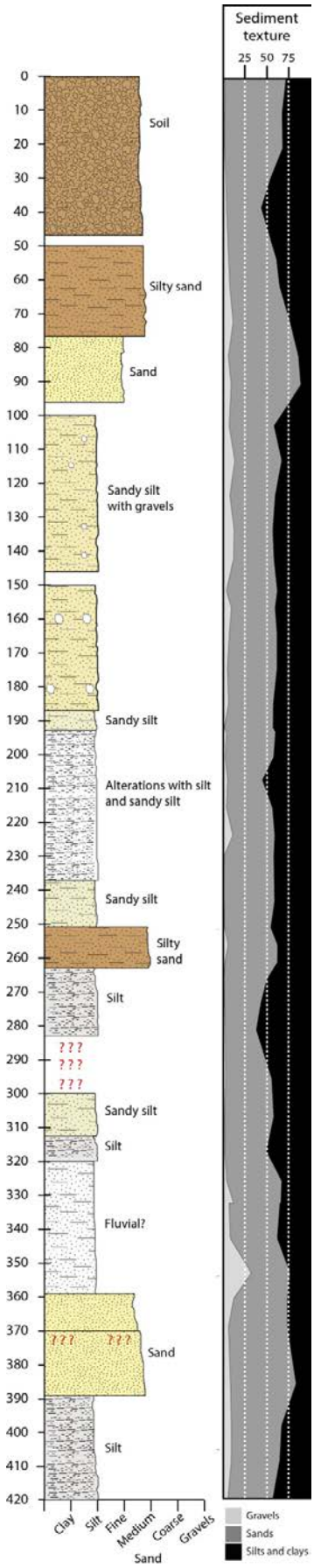

Figure 82: The lithostratigraphy of core KOL1.

6.4 Discussion

The studied cores from Livadia and Pounta reveal different palaeogeographical histories for the sites.

6.4.1 Pounta

The area of Pounta appears to be influenced by coastal-marine processes. Today, the dominant features of the area are the coastal lagoon in the back and low-lying sand dunes in the front, forming a beach spit/barrier.

In particular, until ~964-1229 AD (721-986 cal BP), the area was a shallow marine environment, as evidenced by the medium-coarse sand deposits and the presence of marine molluscan fauna (infralittoral sand assemblages, hard substrate assemblages and algae). A little after 964-1229 AD (721-986 cal BP), the area turned into a coastal lagoon open to the sea. A growing coastal spit progressed and gradually isolated a lagoon from the sea (Figure 83). This lagoon however remained constantly connected to the sea. The increase in molluscan fauna characteristic of sheltered areas suggests that the environment becomes more protected, indicating that this is most likely the timing of the formation of the sandy spit. According to the river network of the area, a 1st order stream discharges close to this area, while a 4th order river branch discharges north of the drilling site. A combination of sediment supply from the river network and the coastal currents provided the material for the coastal spit to develop. In fact, observation of satellite images suggests coastal currents run from south to north, continuously modifying the spit shape.

After the development of the coastal spit, a protected coastal environment may be deduced, based on sedimentological and faunal evidence. The top 0.43 m of the core, suggest a relatively calm coastal environment that becomes marshier towards the top, consistent with the present day geography of the area.

Although the core reached a depth of ~4 m, the dating results suggest that the coastal landscape of Pounta is very recent. It seems that sediment accumulation was relatively rapid, with a sediment thickness of ~270 cm since 964-1229 AD (721-986 cal BP) (rates of ~0.11 cm per year between 964-1229 AD and 1652-1910 AD). It is worth noting that satellite images suggest the area is characterized by shallow depths, the sediment supply is quite high and the coastal currents reshape the coastal zone frequently.

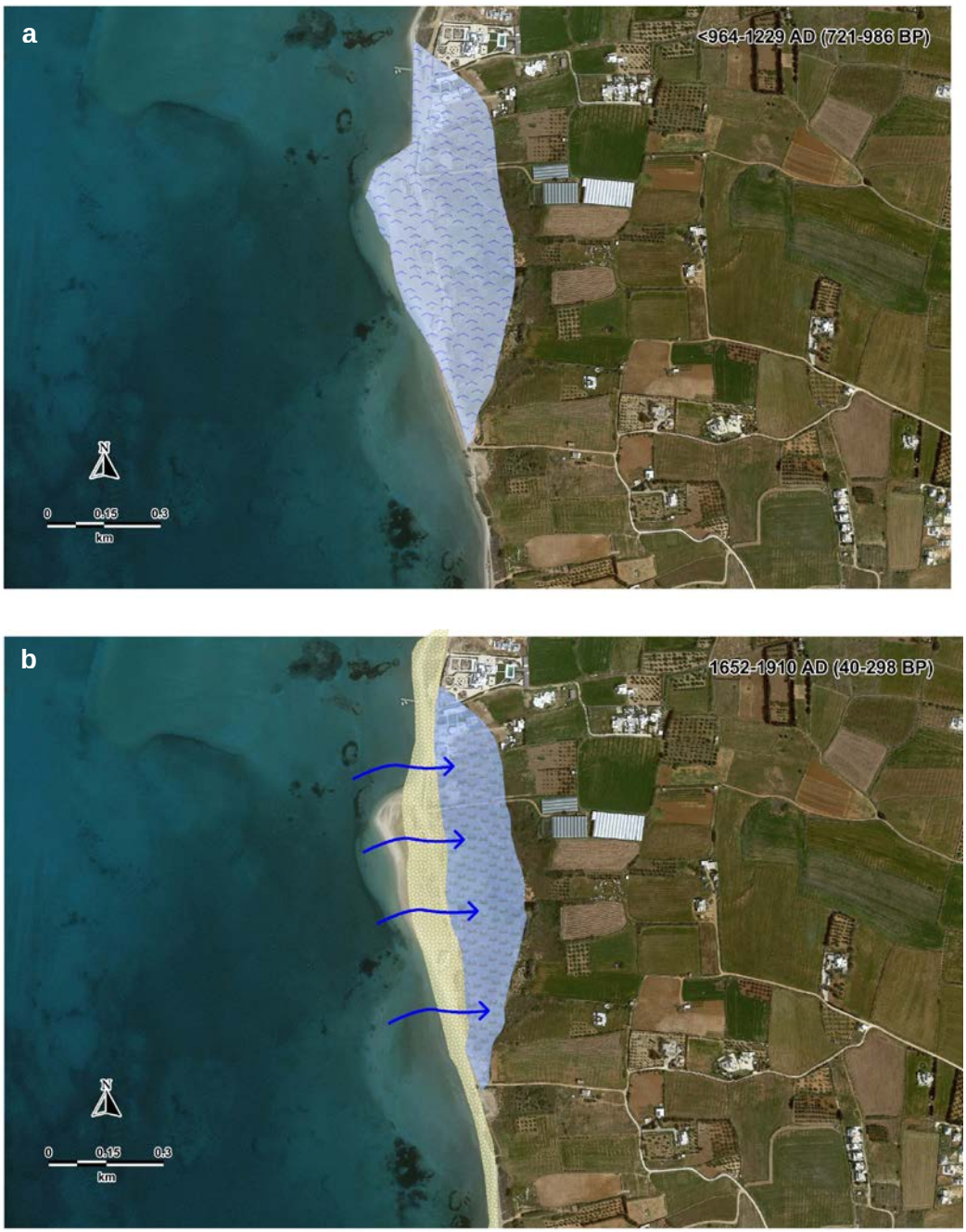

Figure 83: The paleogeography evolution of Pounta coastal zone since 964-1229 AD. (a) The area used to be a shallow marine environment at least before 964-1229 AD, which later turned into a coastal lagoon largely open to the sea (b). Earlier than 1652-1910 AD a growing coastal spit progressed and gradually isolated a lagoon from the sea. This lagoon however remained constantly connected to the sea.

6.4.2 Livadia

The drilling site at Livadia is located a few hundred meters from the remains of a submerged Roman building (Rubensohn 1901; Papathanassopoulos & Schilardi, 1981) and a Geometric – Archaic cemetery (Zapheiropoulou, 2000). In the eastern coast of Livadia bay, Papathanassopoulos and Schilardi (1981) have also reported the presence of an ancient mole, constructed of large sized rubble stones of schist (Figure 84). Both the submerged Roman building and the Geometric – Archaic cemetery give information only on the direction of sea level change.

Figure 84: Location of LIV1 core and archaeological remains discussed in the text. All the archaeological remains lie below the present sea level.

The results from the Livadia core offer new elements for reconstructing the main phases of shoreline development in the north part of Paroikia. From about 2915-2551 BC (4500-4864 cal BP) until ~780-436 BC (2385-2729 cal BP), the area was a semi-closed lagoon, as suggested by relative low species diversity along with the presence of typical lagoonal *Cyprideis torosa* and *Loripes lacteus.* The presence of freshwater ostracods (Illyocypris gibba), suggests that this lagoon must have been affected also by the presence of a local stream. In fact, a closer examination of the river network of the area shows that two 3rd class streams discharge in the bay of Livadia.

This lagoonal environment appears to be interrupted by a 10 cm coarse layer. This event is probably dated before 923-610 BC (2559-2872 cal BP). The coarse sand layer bears no evidence of molluscan fauna. However, ostracod fauna are characterized by a peak in the coastal Pontocythere elongata and freshwater

ostracods are poorly represented in comparison to Unit A1. This sudden transition from lagoonal deposits to coarser deposits correlated with increased presence of coastal ostracods may indicate a reshuffle during a storm episode. The coastal zone of the wider area, nowadays, is characterized mainly sandy, with the presence of pebbles.

Following this event, the lagoon is characterized by the presence of coastal macrofauna and marine lagoonal and coastal ostracods, which may suggest the lagoon barrier is more frequently breached.

After ~780-436 BC (2385-2729 cal BP), the absence of any coastal-marine mollusks and the presence of the lagoonal *Cyprideis torosa* along with freshwater ostracods, suggests that the lagoon is primarily affected by fluvial processes. These fluvial processes are not evidenced in the last unit of the core (Unit C). Although it is not possible to chronologically constrain the timing of this change, it may be relative young indicating manmade activities that have altered the discharge of the streams.

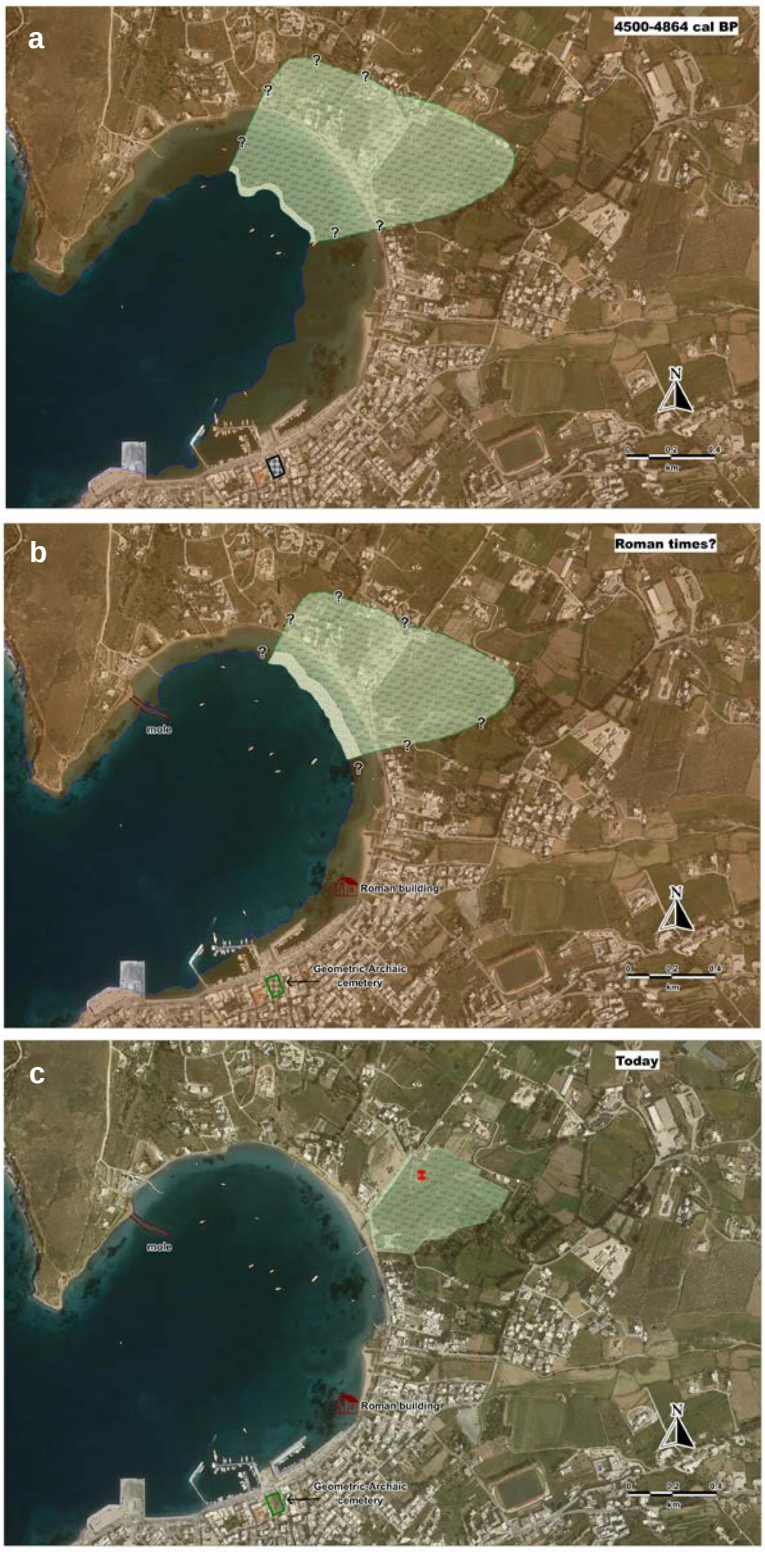

Figure 85: The palaeogeographic evolution of Livadia in Paroikia bay. (a) The site used to be a semi-enclosed lagoon from 4500-4864 cal BP until ~2385-2729 cal BP, occasionally influenced by a local stream. Considering a sea level of ~-4.5 m, the bay of Livadia was narrower. (b) Considering a sea level of ~-2 m during the Roman period, the Livadia bay slowly approaches its present shape. Later the lagoon is slowly infilled. Although it is not possible to chronologically constrain the timing of this change, it may be relative young indicating manmade activities that have altered the discharge of the streams, c) the site of Livadia today.

6.4.3 Relative sea level changes

The radiocarbon ages of marine shells in this study provide a significant collection of data for the reconstruction of the coastal evolution and the relative sea-level fluctuations in Paros since ~2915-2551 BC (4500-4864 cal BP). In order to use the dated material to reconstruct the relative sea level changes, the indicative meaning of each sample was taken into account (for details, see section 3.6 and 7.2), in order to be afterwards converted to a RSL index point. For samples deposited in an open or marine influenced lagoon, such as *Bittium reticulatum*, *Cerithium vulgatum* and *Loripes lacteus*, an indicative range from 0 to −2 MSL was considered according to the methodology of Vacchi *et al.* (2016b). Likewise, for samples from semi-enclosed lagoons an indicative range from 0 to−1 m is taken into account (see chapter 3.6, for details). The produced index points derived from taking into account their indicative range and the associated error. Figure 86 shows the index points produced from cores POU2 and LIV1 in relation to the sea level curve predicted by the glacio-hydro-isostatic model (Lambeck and Purcell, 2005). Although some outliers may be observed the general trend suggests that the sea level in Paros Island may have been lower than the predicted. Implications and further discussions regarding this observation are further analysed in detail, in chapter 7.2. In particular, three samples were rejected (Poz-81140, Poz-81150, Poz-81151) from palaeogeographic interpretations because they provided ages, inconsistent with the stratigraphic order and the ages of the rest of the samples.

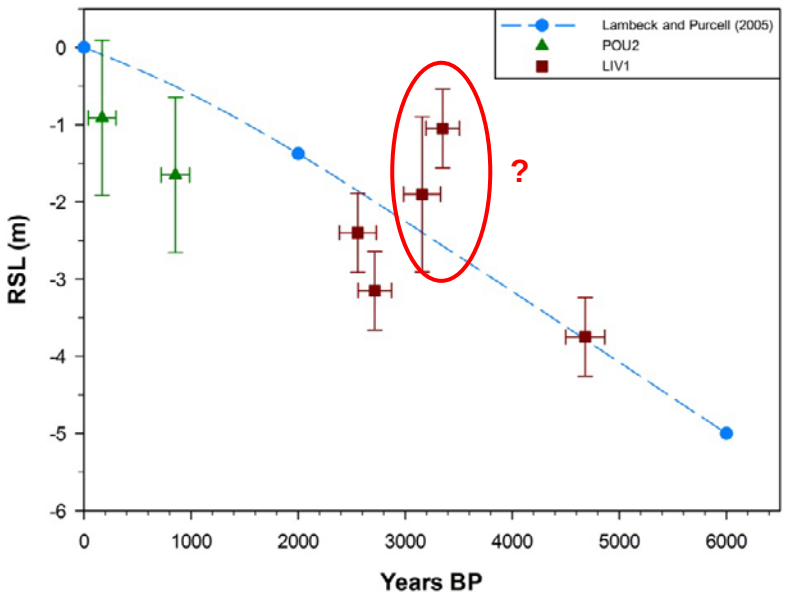

Figure 86: Relative sea level changes in Paros Island. Samples from LIV1 and POU2 cores are plotted against the sea level curve by Lambeck and Purcell (2005). Two samples, in the red circle, lie well above the sea level curve and they were found not in stratigraphic order in the cores.

Chapter 7 – Coastal evolution of the study area

7. Coastal evolution of the study area

This chapter is devoted to the combinatory discussion of the results of this research. In order to have a better understanding of the coastal evolution of Paros and Naxos Islands, a multiproxy approach was attempted through the use of geomorphological and archaeological data. The combinatory results are discussed and evaluated here, from the study of beachrocks, drillings and archaeological remains from Paros and Naxos Islands. The compilation of these data and their comparison allows estimating the overall accuracy and validity of the results and a better understanding of the coastal evolution and history of relative sea level changes. The results of this work are further compared with data produced from past researches in the study area.

7.1 Past research on relative sea level changes and coastal evolution

The Cycladic region is presumed to be under an extensional tectonic regime behind the modern volcanic arc at the centre of the Aegean plate and possesses a relatively thin continental crust of about 25-26 km thickness (e.g. Tirel *et al.*, 2004; Zhu *et al.*, 2006). It is generally assumed that most Cycladic islands are affected by a gradual subsidence that is ascribed to the thinning of the local earth crust and to isostatic processes that accompanied the post-glacial rise in sea level. The absence of morphological coastal features indicative of uplift, such as marine terraces or benches, elevated beachrocks, marine notches, or raised Quaternary coastal deposits, are often interpreted as an absence of local uplift tectonism, at least during the Holocene. The Cycladic region has been regarded in the past as a relatively aseismic plateau (McKenzie, 1972; Morelli *et al.*, 1975; Papazachos, 1990), characterized by the relative absence of earthquakes and by limited neotectonic activity.

The Cycladic region has attracted many researchers and a number of geomorphological and archaeological studies have taken place (e.g. Baika, 2008; Poulos *et al.*, 2009; Kapsimalis *et al.*, 2009; Pavlopoulos *et al.*, 2011; Mourtzas, 2012; Evelpidou *et al.*, 2012c; d; 2014a). Using beachrocks in particular, the most extensive work was accomplished by Desruelles *et al.* (2009) in Mykonos, Delos and Rhenia islands. The authors suggested 3 separate sea level stands: at about -3.6

m±0.5 m around 2000 BC, at about -2.5 m±0.5 m around 400 BC and finally at about -1 m±0.5 m around 1000 AD. In a more recent paper, Pavlopoulos *et al.* (2011) compiled a database of published geomorphological (with associated biological material) and archaeological sea level markers, in an attempt to estimate the trends of the vertical displacement of the Aegean coastal zone by comparing observational data with those derived from the predictive glacio-hydro-isostatic model of Lambeck and Purcell (2005) for a period between the Mesolithic to the late Roman times. According to the authors, Saliagos (Antiparos) and part of the Mykonos-Rhenia-Delos district in Cyclades did not reveal any vertical trends, while the rest of the data regarding Cyclades did not support that concept since uplifting (e.g. Naxos) and subsiding trends were quite evident. They suggested that this 'stability' has resulted from a dynamic equilibrium between uplift and subsidence in a tectonically active area.

Recent research by Evelpidou *et al* (2014a) has shown that various Cycladic Islands are characterized by the presence of a series of submerged tidal notches. In particular, at least seven former shorelines were identified at depths between 280±20 and 30±5 cm below modern sea level. In Paros Island, four paleoshorelines were identified by Evelpidou *et al.* (2014a), at -35 ± 5 (G), -170 ± 20 (C) and -230 ± 10 (B) cm. In Naxos Island, the following shorelines were identified at -35 ± 5 (G), -75 ± 10 (F), -100 ± 10 (E), -120 ± 10 (D), and -280 ± 20 (A) cm. According to Evelpidou *et al.* (2014a) the relative sea level changes suggested by these paleoshorelines took place after 3300 BP and concluded that the amplitude of submergence is too large to be explained only in terms of glacio-hydro-isostatic effects, so that also vertical crustal movements have contributed to the submergence and that the Cycladic region has undergone, during the observation time window, a series of strong seismic events and/or short-timescale tectonic subsidence trends.

Poulos *et al* (2009) have published a relative sea level curve for the Attico-Cycladic region for the last 5000 years based on published archaeological and geomorphological data. The authors concluded that the rapid increase of sea level ended prior to 5.5 ka and was followed by a slow steady rise at a rate of 0.9 mm/a up to its present stage (Figure 87). Lambeck and Purcell (2005) modelled the sea level changes for the whole Mediterranean Sea since the LGM, considering tectonically stable areas. For the Cycladic area, the predicted sea level evolution is illustrated in Figure 87.

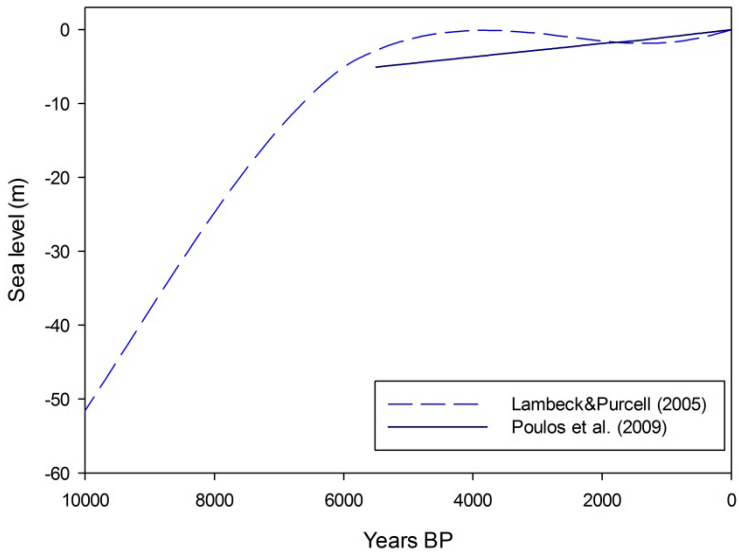

Figure 87: Sea level reconstructions of the Cycladic area. The dashed line represents the sea level curve by Lambeck and Purcell (2005) and the continuous line was suggested by Poulos *et al.* (2009) based on published archaeological and geomorphological data.

7.2 Relative sea level changes during Late Holocene

The coupled analysis of beachrock samples along with the cores of Paros allowed to improve our understanding on the RSL changes in this sector of central Cyclades. RSL index points (Hijma *et al.*, 2015) were produced by taking into account the methodology proposed by Shennan *et al.* (2015) and Vacchi *et al.* (2016b). The indicative meaning[4] was evaluated for each dated sample and the elevation of each indicator was corrected for the indicative meaning. The RSL for each sample is calculated according to RSL = E – RWL (where E is the altitude of the sample and RWL is the mid- point of the indicative range) (Hijma *et al.*, 2015).

Beachrocks are considered as reliable sea level indicators, particularly in the Mediterranean area, due to the microtidal setting. In particular, Mauz *et al.* (2015b) recently defined how the position of a beachrock can be transformed into a RSL index point (cf. Shennan *et al.*, 2015) according to the cement characteristics and the sediment bedding information. Following the protocol recently provided by Mauz *et al.* (2015b), only samples showing clear intertidal formation were converted into RSL

[4] The indicative meaning consists of the indicative range (IR) and the reference water level (RWL). The IR is the elevational range over which an indicator forms and the RWL is the midpoint of this range.

index points (cf. Hijma *et al.*, 2015). Samples showing irregularly distributed needles or isopachous fibres of aragonitic cement or isopachous rims and micritic high-magnesium calcite (HMC) cement or HMC cement in stalactitic position and meniscus between grains, are indicative of beachrock formation in the intertidal zone (e.g. Tucker and Wright, 1990; Desruelles *et al.*, 2009). For these samples an indicative range between the Mean High Tide (MHT) and Mean Low Tide (MLT) was considered. The associated vertical error was obtained by adding in quadratic individual errors both the indicative range (0.14 m, Mean High Tide to Mean Low Tide in Paros; HNHS, 2012) and the sampling error (0.2 m for shallow beachrocks and 0.5 for the deepest ones).

For the samples deriving from Paros drillings, the same methodology was applied. In particular, for samples deposited in an open or marine-influenced lagoon an indicative range from 0 to -2 m was considered, while for samples deposited in a semi-enclosed lagoon an indicative range between 0 and -1 m was taken into account.

In Figure 88, the resultant index points from the beachrock samples and the drillings are presented. A general good agreement between these data is observed for the last ~2000 years and the same applies for around ~4500-5000 years BP. Discrepancies concerning the beachrock age results have already been discussed in chapter 5, therefore the index points that suggest a RSL between -4 and -6 m between 1000-2000 years BP are clearly misleading. A large cluster of proxies indicate that RSL variation did not exceed ~2 m in the last 2.0 ka, whilst there is a good agreement between beachrocks and drillings about a relative sea level at about ~-4 m at about 4500 years BP.

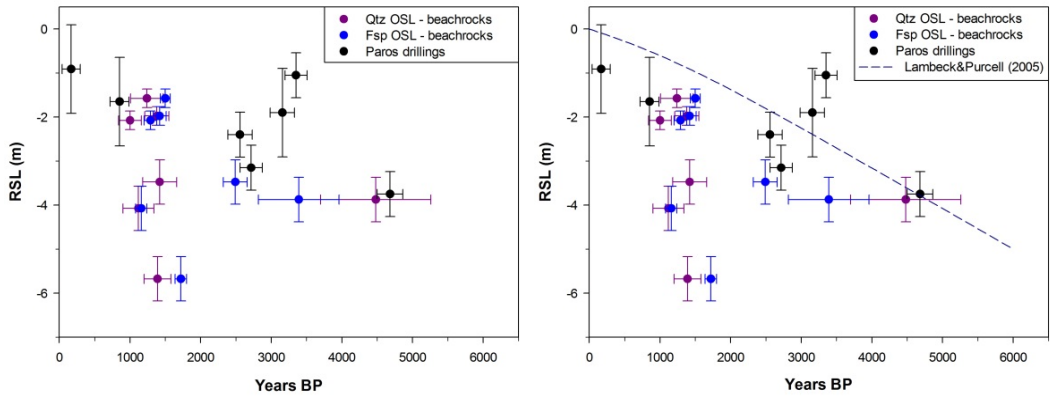

Figure 88: RSL index points produced from the studied beachrocks and drillings of Paros and Naxos Islands plotted with and without the Lambeck & Purcell (2005) curve. Most RSL index points lie below the sea level curve.

In order to evaluate the results at a broader scale, the index points from Paros and Naxos were plotted against RSL reconstructions derived from previously available data in central Cyclades (e.g. Morrison, 1968; Desruelles *et al.*, 2009; Evelpidou *et al.*, 2012c; Mourtzas, 2012). The coupled analysis of available data allowed improving our understanding on the RSL changes in this sector of the central Aegean (Figure 89). RSL index points were produced using samples deposited in semi-enclosed lagoon facies from Evelpidou *et al.* (2012c), and from samples found in a brackish environment, most likely deposited ±0.5 m within former MSL (Pavlopoulos *et al.*, 2011; Evelpidou *et al.*, 2012c).

Based on submerged archaeological remains, about 5.5 m of RSL variation since ~5.5 ka has been quantified in Antiparos Island (Morrison, 1968). According to Papathanassopoulos and Schilardi (1981), archaeological evidence suggests a sea level between -2 and -3 m around 2.5 – 2.9 ka BP (500-900 BC) in Paros Island. The coupled analysis of beachrocks and archaeological remains on Mykonos and Rhenia Islands indicates RSL was at -3.6±0.5 m at ~4.0 ka BP (2000 BC), at -2.5±0.5 m at ~2.4 ka (400 BC), and at -1.0 ± 0.5 m at ~1.0 ka BP (1000 AD) (Desruelles *et al.*, 2009). A similar analysis in Delos Island quantified a RSL variation of ~2.15 m since the end of the Hellenistic period (~100 BC or ~2.1 ka BP, Mourtzas, 2012).

Overall, there is good agreement for a RSL that rose by ~2 m in the last 2000 years. Furthermore, the new index points indicate that RSL rose at least by ~3.9 m in the last ~4500 years. The data (with errors) are in general agreement with the corings, at least in the last 3000 years. Conversely, two brackish samples from a core in Mikri Vigla (Naxos Island, Evelpidou *et al.*, 2012c), indicate that the RSL reached ~-2 m at about ~4.0 ka. Similarly, two lagoonal samples from Livadia core suggest a sea level between -1 and -2 m around 3100-3300 years BP. In both cases, the samples were rejected as they provided ages inconsistent with the stratigraphic order and the ages of the rest of the samples.

New data generally indicate a slight underestimation of the RSL position in Paros and Naxos with respect to the other data. It may suggest higher subsidence rates in the two Islands, at least in late Holocene. Such continuous subsidence is consistent with the constant shoreline recession recorded by the submerged beachrocks, notably in Agios Georgios (see chapter 5). Beachrock formation does not require a RSL standstill (Mauz *et al.*, 2015b), and the presence of continuous beachrock slabs in several coasts of Paros and Naxos may indicate a continuous gradual relative sea level rise.

A comparison of the results with the curve predicted by the glacio-hydro-isostatic model clearly shows that sea level in Paros and Naxos Islands is lower than the predicted (Figure 89). This is particularly true for the last 3000 years, where a large cluster of proxies lies well below the curve. Conversely, sea level appears closer to the predicted around ~4000-4500 years BP. It should, however, be noted that the new data do not support the possibility of uplift in Naxos Island, as suggested by Pavlopoulos *et al.* (2011); on the contrary both islands suggest a subsidence regime.

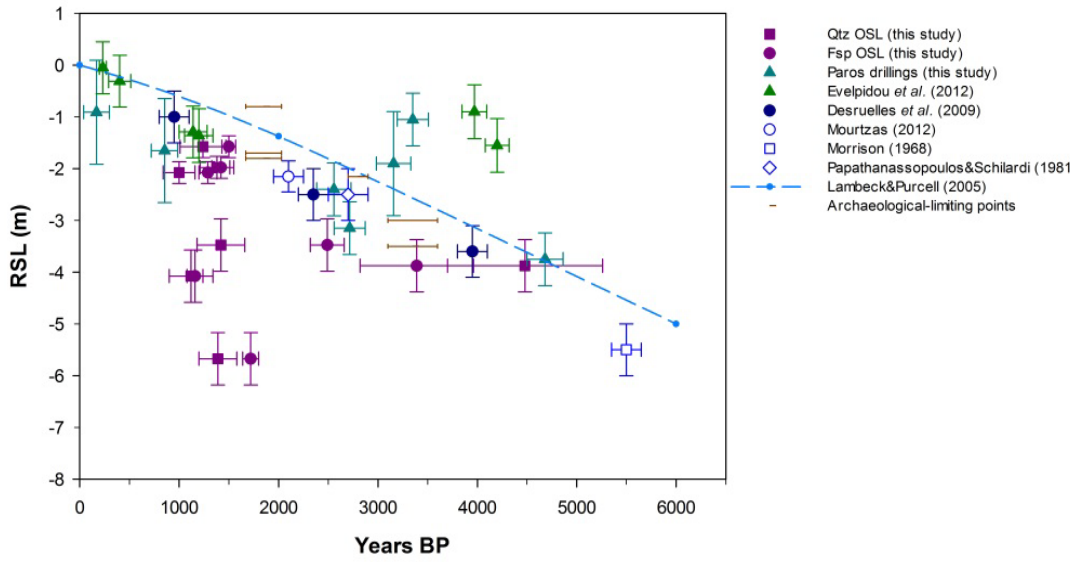

Figure 89: Plot of published sea level data in central Cyclades, derived from coastal drillings, beachrocks and archaeological remains, along with the data produced in this work. Archaeological remains not directly related to sea level are plotted as limiting points. The index points are plotted against the curve predicted by the glacio-hydro-isostatic model of Lambeck and Purcell (2005). The majority of RSL index points lie below the predicted curve suggesting continuous subsidence for the study area. A very good agreement is noted for the last ~2000 years.

The combined analysis of the different proxies indicates that RSL rose by an average rate of ~1.1 m/yr since about ~5.5 ka. During the last ~2.0 ka, where a large cluster of proxies is available, an average rate of ~1.2 mm/yr may be deduced, while for the period between 2.0 ka and 5.5 ka an average rate of ~1 mm/yr is indicated. The overall trend suggests an increasing rate.

The observed subsidence may be the combinatory result of eustatic sea level rise along with land subsidence. However, most of the available proxies are not able to provide information on whether the subsidence was gradual or rapid. Beachrocks are not capable of indicating whether the relative sea level change was gradual or rapid, although cement microstratigraphy may occasionally elucidate a progressive uplift (e.g. Vacchi *et al.*, 2012). Coastal drillings on the other hand may occasionally provide with data to identify palaeoseismic events. In a recent work Pilarczyk *et al.*

(2014) have discussed how microfossils (diatoms, foraminifera, and pollen) were used to reconstruct records of palaeoearthquakes from changes in microfossil assemblages, quantifying the amount of coseismic and interseismic vertical land movements along tectonically active coastlines.

Although the studied cores did not provide such information, the presence of submerged tidal notches, investigated by Evelpidou *et al.* (2014a), suggest that the observed subsidence in Paros and Naxos Islands is at least partly owed to coseismic events. A tentative correlation of the submerged notches with the results of this study suggests that these co-seismic displacements have occurred during the last ~3000 years. For instance, the tidal notch at about -2.3±0.1 m may be correlated with a sample from LIV1 core indicating a sea level at -2.4±0.5 m and may be tentatively dated at about ~2559-2872 BP. The tidal notch found at -1.7±0.2 m may be dated at about ~1230-1500 BP based on the luminescence ages of a beachrock sample from Plaka (sample depth -1.5 m). Overall, the study area appears to be subjected to short–term coseismic displacements in combination with a long-term subsidence trend. This possible combination of abrupt and gradual relative sea level rise appears to have impacted the lives of ancient inhabitants of coastal settlements, forcing them to adjust their houses by placing pebbles under floors, as a means of drainage and moisture prevention or even abandoning settlements, as in the case of the Mycenaean settlement in Naxos.

Based on the RSL index points produced in this study the suggested evolution of sea level for the last 5000 years is presented in Figure 90.

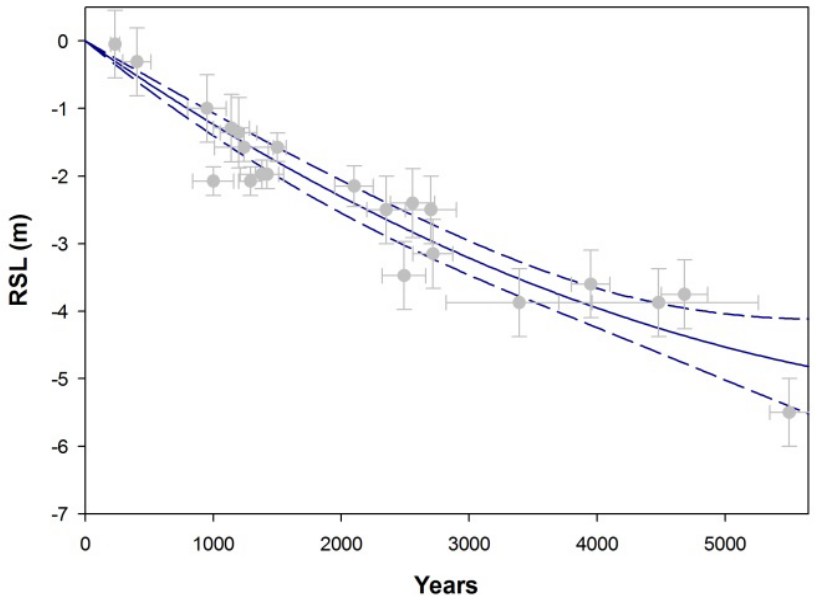

Figure 90: Evolution of sea level for the last 5000 years in central Cyclades (95% with confidence intervals).

PART D – CONCLUDING REMARKS

Chapter 8 – Conclusions

8. Conclusions

An important focus of this thesis was the study of beachrocks in Paros and Naxos Islands. In the literature, there is an ongoing debate regarding the accuracy of beachrocks as sea level indicators. This study has shown the great potential of using beachrocks as accurate sea level indicators when following updated protocols (e.g. Mauz *et al.*, 2015b). Beachrocks are also a powerful tool to track major changes in shoreline positions and to precisely assess the palaeogeographical evolution of the coastal zone, especially in the eastern Mediterranean.

The study of submerged beachrocks slabs has provided new insights on the millennial shoreline evolution of Paros and Naxos Islands as well as on the RSL evolution in the late Holocene. This allowed to chronologically constrain some major palaeogeographical changes recorded by the beachrocks morphology and to track the shoreline recession at least for the last ~4 ka.

Luminescence dating method is increasingly used for coastal and marine sediments and it has also been used successfully to date beachrocks for the reconstruction of palaeoshorelines along the Brazilian coast, India, and the Mediterranean. So far, it hasn't been used to date the Aegean submerged beachrocks. In this work, submerged beachrock samples were dated by using OSL dating of quartz and infrared stimulated luminescence (IRSL) of feldspar. The ages obtained from quartz varied between 1.00±0.16 ka (sample 3170) and 4.48±0.78 ka (sample 3169), while feldspar fading corrected ages ranged between 1.16±0.08 ka (sample 3167) and 3.39±0.57 ka (sample 3169). RSL index points produced from beachrocks suggest a RSL rise of ~2 m for the last 2.0 ka.

The multiproxy analysis of two coastal cores from Paros Island allowed to reconstruct the coastal landscape of selected sites and further provided a significant collection of data for the reconstruction of relative sea-level fluctuations in Paros since ~2915-2551 BC (4500-4864 cal BP). In particular, in Livadia bay a semi-enclosed lagoon existed from at least 2915-2551 BC (4500-4864 cal BP) until ~780-436 BC (2385-2729 cal BP). The final infilling of this lagoon is probably related to manmade activities that have altered the discharge of the local streams. A more recent landscape evolution was investigated at Pounta (W Paros), which has been affected by coastal and marine processes. A marine – shallow marine environment existed until ~964-1229 AD (721-986 cal BP), which later turned to a coastal lagoon largely open to the sea.

A coupled analysis of the results of this study with published sea level data from the study area also took place. Using multiproxy investigations and updated methodologies is a powerful tool for better assessing sea-level evolution. RSL index points were produced from the studied beachrocks and cores of this work and were compared with RSL reconstructions derived from previously available data in central Cyclades. Data suggest a RSL that rose by ~2 m in the last 2000 years. Furthermore, the new index points indicate that RSL rose at least by ~3.9 m in the last ~4500 years.

A slight underestimation of the RSL position in Paros and Naxos has been deduced, which may reflect higher subsidence rates at least for the Late Holocene. Such continuous subsidence is consistent with the constant shoreline recession recorded by the submerged beachrocks at various sites on both Islands (e.g. Agios Georgios, W Naxos). This observed subsidence may be the combinatory result of eustatic sea level rise along with land subsidence. Reported submerged tidal notches suggest that subsidence is at least partly owed to coseismic events that have occurred since ~3000 BP.

The combined analysis of different proxies (beachrocks, drillings and archaeological data) indicates that RSL rose by an average rate of ~1.1 m/yr since about ~5.5 ka. During the last ~2.0 ka, where a large cluster of proxies is available, an average rate of ~1.2 mm/yr may be deduced, while for the period between 2.0 ka and 5.5 ka an average rate of ~1 mm/yr is suggested by the data.

8.1 Future research

This work has shown the significance of using multiproxy investigations to better assess sea-level evolution. The variability of RSL appears better constrained for the last ~2000 years, but for the period 3000-6000 years BP more data are needed.

The results of this work call for further investigations using multiproxy analyses with sediment coring, beachrocks, archaeological data, etc. that will allow to more robustly constrain temporally and spatially the RSL changes during the last 6000 years and the role of tectonic subsidence on the RSL evolution of this sector of the Aegean Sea. Such information has implications in the environmental changes of the coastal zone during the late Holocene and the evolution of the Cycladic coastal landscape.

The Cycladic region is rich in archaeological remains dating as early as the Neolithic period (e.g. Saliagos, SW of Paros Island). Palaeogeographical reconstructions are fundamental to improve our understanding for the past human-environment in the Cycladic region.

References

References

Aitken, M.J., 1985. Thermoluminescence Dating. Academic, New York.

Aitken, M.J., 1998. An Introduction to Optical Dating. Oxford University Press, Oxford.

Alexandersson, T., 1972. Intragranular Growth of Marine Aragonite and Mg-Calcite: Evidence of Precipitation from Supersaturated Seawater. Journal of Sedimentary Research 42(2), 441–460.

Alföldy, G., 1971. Zeitgeschichte und Krisenempfindung bei Herodian. Hermes (Wiesb). 99, 429–449.

Alföldy, G., 1976. The crisis of the 3rd c. AD (235 – 284 AD). Hist. Greek Nation, Hell. Rome 6, 584–614.

Altherr, R., Schliestedt, M., Okrusch, M., Seidel, E., Kreuzer, H., Harre, W., Lenz, H., Wendt, I., Wagner, G.A., 1979. Geochronology of high-pressure rocks on Sifnos (Cyclades, Greece). Contributions to Mineralogy and Petrology 70, 245–255.

Altherr, R., Kreuzer, H., Wendt, I., Lenz, H., Wagner, G.A., Keller, J., Harre, W., Hohndorf, A., 1982. A Late Oligocene/Early Miocene high temperature belt in the anti-cycladic crystalline complex (SE Pelagonian, Greece). Geologisch Jahrbuch 23, 97–164.

Andriessen, P.A.M., Boelrijk, N.A.I.M., Hebeda, E.H., Priem, H.N.A., Verdurmen, E.A.T., Verschure, R.H., 1979. Dating the events of metamorphism and granite magmatism in the Alpine orogen of Naxos (Cyclades, Greece). Contributions to Mineralogy and Petrology 69, 215– 225.

Angelier, J., Lyberis, N., Le Pichon, X., Barrier, E., Huchon, P., 1982. The tectonic development of the Hellenic arc and the Sea of the Crete: a synthesis (Mediterranean). Tectonophysics 86, 159–196.

Antonioli, F., Anzidei, M., Lambeck, K., Auriemma, R., Gaddi, D., Furlani, S., Orrù, P., Solinas, E., Gaspari, A., Karinja, S., Kovačić, V., Surace, L., 2007. Sea-level change during the Holocene in Sardinia and in the northeastern Adriatic (central Mediterranean Sea) from archaeological and geomorphological data. Quaternary Science Reviews, 26(19–21), 2463–2486.

Anzidei, M., Lambeck, K., Antonioli, F., Furlani, S., Mastronuzzi, G., Serpelloni, E., Vannucci, G., 2014. Coastal structure, sea-level changes and vertical motion of the

land in the Mediterranean. Geological Society of London, Special Publications, 388(1), 453–479. https://doi.org/10.1144/SP388.20

Athanasoulis, G.A., Skarsoulis, E.K., 1992. Wind and Wave Atlas of north-east Mediterranean Sea, 1992. Laboratory of Nautical and Marine Hydrodynamics, NTUA, Athens.

Athersuch, J., Horne, D.J., Whittaker, J.E., 1989. Marine and Brackish Water Ostracods (Superfamilies Cypridacea and Cytheracea: Keys and Notes for the Identification of the Species). Brill Academic Publishers, Leiden.

Auffray, D., 2002. Recherches sur les entailles creusées dans le roc sur les îles Paros, Antiparos et Remmatonisi. Proceedings of 7th International Symposium on Ship Construction in Antiquity, Tropis VII.

Auriemma, R., Solinas, E., 2009. Archaeological remains as sea level change markers: A review. Quaternary International 206, 134–146.

Baika, K., 2008. Archaeological indicators of relative sea-level changes in the Attico-Cycladic massif: preliminary results. Bulletin of the Geological Society of Greece XLII/II, 33-48.

Barber, R.L.N., Hadjianastasiou, O., 1989. Mikre Vigla: A Bronze Age Settlement on Naxos. The annual of the British School of Athens 84, 63–162.

Bargnesi, E.A., Stockli, D.F.,Mancktelow, N., Soukis, K., 2013. Miocene core complex development and coeval supradetachment basin evolution of Paros, Greece, insights from (U–Th)/He thermochronometry. Tectonophysics 595-596, 165–182.

Barreto, A.M.F., Bezerra, F.H.R., Suguio, K., Tatumi, S.H., Yee, M., Paiva, R.P., Munita, C.S., 2002. Late Pleistocene marine terrace deposits in northeastern Brazil: sea-level changes and tectonic implications. Palaeogeography, Palaeoclimatology, Palaeoecology 179, 57–69.

Bateman, M.D., 2015. The application of luminescence dating in sea-level studies. In: Shennan, I., Long, A.J., Horton, B.P., Handbook of Sea-Level Research, pp. 404-417. John Wiley & Sons, Ltd.

Bathurst, R.G.C., 1975. Carbonate Sediments and their Diagenesis. Developments in Sedimentology vol. 12. Elsevier, 658 pp.

Beier, J. A., 1985. Diagenesis of Quaternary Bahamian beachrock; petrographic and isotopic evidence. Journal of Sedimentary Research 55(5), 755-761.

Bernier, P., Guidi, J.-B., Bottcher, M.E., 1997. Coastal progradation and very early diagenesis of ultramafic sands as a result of rubble discharge from asbestos excavations (northern Corsica, western Mediterranean). Marine Geology 144 (13), 163–175.

Blackman, D.J., 1973. Evidence of sea level change in ancient harbours and coastal installations. In: Blackman, D.J. (Ed.), Marine Archaeology, pp. 115–139. Colston Papers, 23.Butterworth, London.

Bird, E., 2008. Coastal Geomorphology: An Introduction, 2nd edition. John Wiley & Sons Ltd, Chichester

Bolhar, R., Ring, U., Allen, C.M., 2010. An integrated zircon geochronological and geo- chemical investigation into the Miocene plutonic evolution of the Cyclades, Aegean Sea, Greece: part 1: geochronology. Contributions to Mineralogy and Petrology 160, 719–742.

Bonaduce, G., Ciampo, G., Masoli, M., 1975. Distribution of Ostracoda in the Adriatic sea. Pubblicazioni della Stazione zoologica di Napoli, Napoli, 40, 1-304.

Bonneau, M., 1984. Correlation of the Hellenic nappes in the south-east Aegean and their tectonic reconstruction. In: Dixon, J.E., Robertson, A.H.F. (Eds.), The Geological Evolution of the Eastern Mediterranean, pp. 517–527. Special Publication of the Geological Society of London. Blackwell Scientific Publications, Oxford.

Bosman, C., 2012. The marine geology of the Aliwal Shoal, Scottburgh, South Africa. PhD thesis, University of KwaZulu-Natal, Durban, 581 pp.

Breman, E., 1975. The distribution of Ostracodes in the bottom sediments of the Adriatic sea. Dissertation, Vrije Universiteit, Amsterdam

Bricker, O.P., 1971. Introduction: beachrock and intertidal cement. In: Bricker, O.P. (Ed.), Carbonate Cements, pp. 1–13. Johns Hopkins Press, Baltimore.

Bröcker, M., Pidgeon, R.T., 2007. Protolith ages of meta-igneous and metatuffaceous rocks from the Cycladic blueschist unit, Greece: results of a reconnaissance U–Pb zircon study. Journal of Geology 115, 83–98.

Brun, J.-P., Faccenna, C., 2008. Exhumation of high-pressure rocks driven by slab roll- back. Earth and Planetary Science Letters 272, 1–7.

Buick, I.S., 1991. The late Alpine evolution of an extensional shear zone, Naxos, Greece. Journal of the Geological Society of London 148, 93– 103.

Carbonel, P., 1980. Les ostracodes et leur interêt dans la définition des écosystèmes estuariens et de plateforme continentale. Essais d'application à des domaines anciens. Mém. Inst. Géol. Bassin d'Aquitaine, 11, 1-378.

Carbonel, P., 1982. Les ostracodes, traceurs des variations hydrologiques dans les systems de transition eaux douces-eaux salées. Mémoires de la Société Géologique de France N.S. 144, 117-128.

Carter, R.W. 1988. Coastal Environments. Academic Press Limited, London.

Cazenave, A., Llovel, W., 2010. Contemporary sea level rise. Annual Review of Marine Science, 2, 145–73. https://doi.org/10.1146/annurev-marine-120308-081105

Chalepa-Bikake, A., 1983a. Trenches D3 and E3, in: Lambrinoudakis, V.K., Zapheiropoulou, P. (Eds.), Excavation of the Cathedral Square (Plateia Metropoleōs) on Naxos. pp. 299–304.

Chalepa-Bikake, A., 1983b. Excavation Notebook 1983, Trench D3, 22-08-1983; 23-08-1983; 24-08-1983.

Clave, B., Masse, L., Carbonel, P., Tastet, J.-P., 2001. Holocene coastal changes and infilling of the La Perroche marsh (French Atlantic coast). Oceanologica Acta 24, 377-389.

Cole, K.L., Liu, G., 1994. Holocene paleoecology of an estuary on Santa Rosa Island, California. Quaternary Research 41, 326–335.

Cooper, J.A.G., 1991. Beachrock formation in low latitudes: implications for coastal evolutionary models. Marine Geology 98 (1), 145–154.

Cordier, S., 2010. Optically stimulated luminescence dating: procedures and applications to geomorphological research in France. Géomorphologie: relief, processus, environnement 1, 21-40.

Cosmopoulos, M.B., 1998. Reconstructing Cycladic Prehistory: Naxos in the Early and Middle Late Bronze Age. Oxford Journal of Archaeology 17, 127–148. doi:10.1111/1468-0092.00055

Cronin, T.M., 2015. Ostracods and sea level. In: Shennan, I., Long, A.J., Horton, B.P. (Eds.), Handbook of Sea-Level Research, pp. 249-257. John Wiley & Sons Ltd.

d' Angelo, G., Gargiullo, S., 1978. Guida alle conchiglie Mediterranee. Fabbri Editori, Milano.

Dalongeville, R. (Ed.), 1984. Le Beach-rock. Colloque tenu à Lyon les 28 et 29 novembre 1983. Maison de l'Orient et de la Méditerranée Jean Pouilloux, Lyon, 202 p.

Dalongeville, R., Renault-Miskovsky, J., 1993. Paysages passés et actuels de l'île de Naxos, in: Dalongeville R.; Rougemont G. (Ed.), Recherches Dans Les Cyclades. Résultats des travaux de la RCP 583, Collection de la Maison de l'Orient Méditerranéen No 23, Lyon, pp. 9–57.

Dalongeville, R., Desruelles, S., Fouache, É., Hasenohr, C., Pavlopoulos, K., 2007. Hausse relative du niveau marin à Délos (Cyclades, Grèce): rythme et effets sur les paysages littoraux de la ville hellénistique. Méditerranée 17–28. doi:10.4000/mediterranee.154

Dana, J.D., 1849. Geology. US Exploring Expedition under C. Wilkes (1835–1841), Vol. 10. Putnam, New York, 756pp.

Darwin, C., 1841. On a remarkable bar of sandstone off Pernambuco on the coast of Brazil. The London, Edinburgh and Dublin Philosophical Magazine and Journal of Science 19, 257–260.

de Graauw, A., 2014. The long-term failure of rubble mound breakwaters. Méditerranée, https://mediterranee.revues.org/7078

De Muro, S., Orru, P., 1998. Il contributo delle beach rock nello studio della risalita del mare olocenico. Le beach rock post-glaciali della Sardegna nord-orientale. Il Quaternario 11, 19–39.

Dermitzakis, M., Papanikolaou, D., 1980. The molasse of Paros Island, Aegean Sea. Annalen des Naturhistorischen Museums Wien 83, 59–71.

Desruelles, S., Fouache, E., Ciner, A., Dalongeville, R., Pavlopoulos, K., Kosun, E., Coquinot, Y., Potdevin, J.-L., 2009. Beachrocks and sea level changes since Middle Holocene: comparison between the insular group of Mykonos–Delos–Rhenia (Cyclades, Greece) and the southern coast of Turkey. Global and Planetary Change 66, 19–33.

Doneddu, M., Trainito, E., 2005. Conchiglie del Mediterraneo. Il Castello, Trezzano sul Naviglio.

Doutsos, T., Kokkalas, S., 2001. Stress and deformation patterns in the Aegean region. Journal of Structural Geology, 23(2–3), 455–472.

Dunham, R.J., 1970. Keystone vugs in carbonate beach deposits. American Association of Petroleum Geologists Bulletin 45, 845.

Dürr, St., 1986. Das Attisch-kykladische Kristallin. In: Jacobshagen, V. (Ed.), Geologie von Griechenland, pp. 116-167. Borntraeger, Berlin.

Dürr, S., Altherr, R., Keller, J., Okrusch, M., Seidel, E., 1978. The median Aegean crystal- line belt: stratigraphy, structure, metamorphism, magmatism. In: Closs, H., Rodeder, D., Schmidt, K. (Eds.), Alps, Apennines, Hellenides, pp. 455–477. IUCG Sci. Rep. 38.

Edgren, G., 1993. Expected economic and demographic developments in coastal zones world-wide. In: Beukenkamp, P., Gunther, P., Klein R. (Eds.), Proceedings of World Coast ’93, pp. 367-370. Coastal Zone Management Centre, Noordwijk, the Netherlands.

Ejarque, A., Julià, R., Reed, J.M., Mesquita-Joanes, F., Marco-Barba, J., Riera, S., 2016. Coastal Evolution in a Mediterranean Microtidal Zone: Mid to Late Holocene Natural Dynamics and Human Management of the Castelló Lagoon, NE Spain. PLoS ONE 11(5), e0155446.

Engel, M., Reischmann, T., 1997. Geochronological data on granitoid gneisses from Paros, Greece, obtained by single zircon Pb evaporation. Terra Nova 9, 463.

Engel, M., Reischmann, T., 1998. Single zircon geochronology of orthogneisses from Paros, Greece. Bulletin of the Geological Society of Greece 32, 91–99.

Engelhart, S.E., Horton, B.P., 2012. Holocene sea level database for the Atlantic coast of the United States. Quaternary Science Reviews 54, 12–25.

Erginal, A.E., Kıyak, N.G., Öztürk, B., 2010. Investigation of Beachrock Using Microanalyses and OSL Dating: A Case Study from Bozcaada Island, Turkey. Journal of Coastal Research 262, 350-358.

Evans, J.D., Renfrew, C., 1968. Excavations at Saliagos near Antiparos. Thames & Hudson, Oxford, UK.

Evelpidou, N., 2001. Geomorphological and Environmental study in Naxos Island using remote sensing and GIS technology, Ph.D. thesis, University of Athens, Faculty of Geology and Geoenvironment, 226 pp. (in Greek).

Evelpidou, N., Pirazzoli, P.A., 2014. Holocene relative sea-level changes from submerged tidal notches: a methodological approach. Quaternaire, 25(4), 383–390.

Evelpidou, N., Pirazzoli, P.A., Vassilopoulos, A., Tomasin, A., 2011. Holocene submerged shorelines on Theologos area (Greece). Zeitschrift für Geomorphologie 55, 31-44.

Evelpidou, N., Pirazzoli, P., Vassilopoulos, A., Spada, G., Ruggieri, G., Tomasin, A., 2012a. Late Holocene Sea Level Reconstructions Based on Observations of Roman Fish Tanks, Tyrrhenian Coast of Italy. Geoarchaeology, 27(3), 259–277. https://doi.org/10.1002/gea.21387

Evelpidou, N., Vassilopoulos, A., Pirazzoli, P., 2012b. Submerged notches on the coast of Skyros Island (Greece) as evidence for Holocene subsidence. Geomorphology, 141–142, 81–87. https://doi.org/10.1016/j.geomorph.2011.12.025

Evelpidou, N., Pavlopoulos, K., Vassilopoulos, A., Triantafyllou, M., Vouvalidis, K., Syrides, G., 2012c. Holocene palaeogeographical reconstruction of the western part of Naxos island (Greece). Quaternary International 266, 81-93.

Evelpidou, N., Melini, D., Pirazzoli, P., Vassilopoulos, A., 2012d. Evidence of a recent rapid subsidence in the S-E Cyclades (Greece): an effect of the 1956 Amorgos earthquake? Continental Shelf Research 39–40, 27–40.

Evelpidou, N., Melini, D., Pirazzoli, P. A., Vassilopoulos, A., 2013. Evidence of repeated late Holocene rapid subsidence in the SE Cyclades (Greece) deduced from submerged notches. International Journal of Earth Sciences 103 (1), 381-395.

Evelpidou, N., Melini, D., Pirazzoli, P., Vassilopoulos, A., 2014a. Evidence of repeated late Holocene rapid subsidence in the SE Cyclades (Greece) deduced from submerged notches. International Journal of Earth Sciences, 103(1), 381–395.

Evelpidou, N., Karkani, A., Pirazzoli, P.A., 2014b. Fossil shorelines at Corfu and surrounding islands deduced from erosional notches. The Holocene 24 (11), 1565-1572.

Faivre, S., Fouache, E., Kovačić, V., Glušćević, S., 2010a. Geomorphological and archaeological indicators of Croatian shoreline evolution over the last two thousand years. Geology of the Adriatic area. GeoActa, Special Publication 3, 125-133.

Faivre, S., Bakran-Petricioli, T., Horvatincic, N., 2010b. Relative sea-level change during the Late Holocene on the island of Vis (Croatia) – Issa, harbour archaeological site. Geodinamica Acta, 23(5–6), 209–223.

Flemming, N.C., 1969. Archaeological evidence for eustatic change of sea level and earth movements in the Western Mediterranean in the last 2000 years. Geological Society of America, Special Paper 109, pp. 125.

Fleming, K., Johnston, P., Zwartz, D., Yokoyama, Y., Lambeck, K., Chappell, J., 1998. Refining the eustatic sea-level curve since the Last Glacial Maximum using far- and intermediate-field sites. Earth and Planetary Science Letters 163 (1-4), 327-342.

Fleming, K., 2000. Glacial Rebound and Sea-level Change Constraints on the Greenland Ice Sheet. PhD Thesis, Australian National University, 568 p.

Frechen, M., Neber, A., Tsatskin, A., Boenigk, W., Ronen, A., 2004. Chronology of Pleistocene sedimentary cycles in the Carmel Coastal Plain of Israel. Quaternary International 121(1), 41–52. http://doi.org/10.1016/j.quaint.2004.01.022

Frenzel, P., Boomer, I., 2005. The use of ostracods from marginal marine, brackish waters as bioindicators of modern and Quaternary environmental change. Palaeogeography, Palaeoclimatology, Palaeoecology 225, 68-92.

Furlani, S., Biolchi, S., Cucchi, F., Antonioli, F., Busetti, M., Melis, R., 2011. Tectonic effects on Late Holocene sea level changes in the Gulf of Trieste (NE Adriatic Sea, Italy). Quaternary International 232, 144–157.

Fytikas, M., Innocenti, F., Manetti, P., Mazzuoli, R., Peccerillo, A., Villari, L., 1984. Tertiary to Quaternary evolution of volcanism in the Aegean region. In: Dixon, J.E., Robertson, A.H.F. (Eds.), The Geological Evolution of the Eastern Mediterranean, pp. 687–699. Geological Society of London Special Publication 17.

Galanopoulos, G.A., 1981. The damaging shocks and the earthquake potential of Greece. Annales Geologique de Pays Hellenique 30, 647–724.

Galili, E., Weinstein-Evron, M., Ronen, A., 1988. Holocene sea level changes based on submerged archaeological sites off the Northern Carmel Coast in Israel. Quaternary Research, 29, 36–42.

Gautier, P., Brun, J.-P., 1994. Crustal-scale geometry and kinematics of late-orogenic ex- tension in the central Aegean (Cyclades and Evvia Island). Tectonophysics 238, 399–424.

Gautier, P., Brun, J.-P., Jolivet, L., 1993. Structure and kinematics of upper Cenozoic extensional detachment on Naxos and Paros (Cyclades islands, Greece). Tectonics 12, 1180–1194.

Gautier, P., Brun, J.-P., Moriceau, R., Sokoutis, D., Martinod, J., Jolivet, L., 1999. Timing, kinematics and cause of Aegean extension: a scenario based on a comparison with simple analogue experiments. Tectonophysics 315, 31–72.

Ghilardi, M., Psomiadis, D., Pavlopoulos, K., Çelka, S. M., Fachard, S., Theurillat, T., Verdan, S., Knodell, A.R., Theodoropoulou, T., Bicket, A., Bonneau, A., Doriane Delanghe-Sabatier, D., 2014. Mid- to Late Holocene shoreline reconstruction and human occupation in Ancient Eretria (South Central Euboea, Greece). Geomorphology, 208, 225–237.

Giaime, M., Morhange, C., Cau Ontiveros, M., Fornós, J. J., Vacchi, M., Marriner, N., 2017. In search of Pollentia's southern harbour: Geoarchaeological evidence from the Bay of Alcúdia (Mallorca, Spain). Palaeogeography, Palaeoclimatology, Palaeoecology, 466, 184–201.

Gischler, E., 2007. Beachrock and Intertidal Precipitates. In: Nash, D. J., McLaren, S. J. (Eds.), Geochemical Sediments and Landscapes, pp. 365-390. Blackwell Publishing Ltd, Oxford, UK. doi: 10.1002/9780470712917.ch11

Goudie, A., 1969. A note on Mediterranean beachrock: its history. Atoll Research Bulletin 126 (19), 11–14.

Guerin, G., Mercier, N., Adamiec, G., 2011. Dose - rate conversion factors: update: Ancient TL 29, 5-8.

Guidoboni, E., Comastri, A., Traina, G., 1994. Catalogue of Ancient Earthquakes in the Mediterranean Area Up to 10th Century. ING-SGA, Bologna, p. 504.

Guilcher, A., 1961. Le « beach-rock » ou grès de plage. Annales de Géographie, 70 (378), 113-125. DOI: 10.3406/geo.1961.15487

Hanor, J.S., 1978. Precipitation of beachrock cements: mixing of marine and meteoric waters vs. CO2-degassing. Journal of Sedimentary Petrology 48, 489–501.

Hansom, J., 2001. Coastal sensitivity to environmental change: a view from the beach. CATENA 42 (2), 291–305.

Haslett, S.K., 2000. Coastal Systems. Routledge, New York.

Haslett, S.K., 2002. Quaternary environmental micropalaeontology. Arnold, London.

Hellenic Navy Hydrographic Service, 2012. Statistical data for sea level of the Greek ports. Athens (in Greek).

Hijma, M., Engelhart, S.E., Tornqvist, T.E., Horton, B.P., Hu, P., Hill, D., 2015. A protocol for a Geological Sea-level Database. In: Shennan, I., Long, A., Horton, B.P. (Eds.), Handbook of Sea Level Research, pp. 536–553. John Wiley & Sons, Ltd.

Holmes, J.A., Chivas, A.R. (Eds.), 2002. The Ostracoda: Applications in Quaternary Research. Geophysical Monograph, Volume 131. American Geophysical Union, Washington DC.

Hopley, D., 1986. Beachrock as a sea-level indicator. In: van der Plassche, O. (Ed.), Sea-level Research: a manual for the collection and evaluation of data, pp. 157-173. Geo Books, Norwich.

Huntley, D.J., Lamothe, M., 2001. Ubiquity of anomalous fading in K-feldspars and the measurement and correction for it in optical dating. Can. J. Earth Sci. 38, 1093–1106. doi:10.1139/e01-013

Huntley, D.J., Prescott, J.R., 2001. Improved methodology and new thermoluminescence ages for the dune sequence in south- east South Australia. Quaternary Science Reviews, 20, 687–699.

Jackson, J.A., McKenzie, D., 1984. Active tectonics of the Alpine–Himalayan belt between western Turkey and Pakistan. Geophysical Journal of the Royal Astronomical Society 77, 185–264.

Jansen, J.B.H., 1973. Geological Map of Greece, Island of Naxos (1:50,000). Institute for Geology and Mineral Resources, Athens.

Jansen, J.B.H., Schuiling, R.D., 1976. Metamorphism on Naxos: petrology and geothermal gradients. American Journal of Science 276, 1225-1253.

Jenkins, D.G. (Ed.), 1993. Applied Micropalaeontology. Kluwer Academic Publications, Dordrecht.

Jolivet, L., 2001. A comparison of geodetic and finite strain pattern in the Aegean, geodynamic implications. Earth and Planetary Science Letters 187, 95–104.

Jolivet, L., Brun, J.-P., 2010. Cenozoic geodynamic evolution of the Aegean. International Journal of Earth Sciences 99, 109–138.

Jolivet, L., Lecomte, E., Huet, B., Denèle, Y., Lacombe, O., Labrousse, L., Le Pourhiet, L., Mehl, C., 2010. The North Cycladic detachment system. Earth and Planetary Science Letters 289, 87–104.

Kapsimalis, V., Pavlopoulos, K., Panagiotopoulos, I., Drakopoulou, P., Vandarakis, D., Sakelariou, D., Anagnostou, C., 2009. Geoarchaeological challenges in the

Cyclades continental shelf (Aegean Sea). Zeitschrift Für Geomorphologie, Supplementary Issues, 53(1), 169–190. https://doi.org/10.1127/0372-8854/2009/0053S1-0169

Karagianni, E.E., Papazachos, C.B., Panagiotopoulos, D.G., Suhadolc, P., Vuan, A., Panza, G. F., 2005. Shear velocity structure in the Aegean area obtained by inversion of Rayleigh waves. Geophysical Journal International 160, 127–143.

Karkani, A., Evelpidou, N., Vacchi, M., Morhange, C., Tsukamoto, S., Frechen, M., Maroukian, H., 2017. Using beachrocks to track the millennial shoreline evolution in central Cyclades (Greece). Marine Geology, in review.

Karo, G., 1930. Archäologische Funde aus dem Jahre 1929 und der ersten Hälfte von 1930. Archaeol. Anz. 45, 88–167.

Keay, S., Lister, G.S., Buick, I.S., 2001. The timing of partial melting, Barrovian metamorphism and granite intrusion in the Naxos metamorphic core complex, Cyclades, Aegean Sea, Greece. Tectonophysics 342, 275–312.

Kelletat, D., 1979. Geomorphologische Studien an den Küsten Kretas. Abhandlungen der Akademie der Wissenschaften in Göttingen, Göttingen.

Kelletat, D., 2006. Beachrock as sea-level indicator? Remarks from a geomorphological point of view. Journal of Coastal Research 22 (6), 1555-1564.

Kelletat, D., 2007. Reply to: Knight, J., 2007. Beachrock Reconsidered. Discussion of: Kelletat, D., 2006. Beachrock as Sea-Level Indicator? Remarks from a Geomorphological Point of View, Journal of Coastal Research, 22(6), 1558–1564; Journal of Coastal Research, 23(4), 1074. Journal of Coastal Research, 236, 1605–1606. https://doi.org/10.2112/07A-0020.1

Kemp, A.C., Horton, B.P., Donnelly, J.P., Mann, M.E., Vermeer, M., Rahmstorf, S., 2011. Climate related sea-level variations over the past two millennia. Proceedings of the National Academy of Sciences of the United States of America 108(27), 11017–11022.

Kjerfve, B., 1994. Coastal Lagoons. Elsevier Oceanography Series 60, pp. 1–8.

Knight, J., 2007. Beachrock reconsidered. Discussion of: Kelletat, D., 2006. Beachrock as sea-level indicator? Remarks from a geomorphological point of view. Journal of Coastal Research, 22(6), 1558–1564. Journal of Coastal Research 234, 1074–1078.

Knoblauch, P., 1972. Die Hafenanlagen der Stadt Ägina. Arch Delt 27, 50–85.

Koenigs, W., 1978. Dorische Hallenanlagen auf Paros. Archaeol. Anz. 93, 375–384.

Kolaiti, E., Mourtzas, N. D., 2016. Upper Holocene sea level changes in the West Saronic Gulf, Greece. Quaternary International 401, 71-90.

Kontoleon, N.M., 1958. Excavations of Naxos. Prakt 228–229.

Kontoleon, N.M., 1967a. Excavation of Naxos. Prakt 112–123.

Kontoleon, N.M., 1967b. Excavation of Naxos. Prakt 112–123.

Kontoleon, N.M., 1970. Excavation of Naxos. Prakt 146–155.

Kopp, R.E., Simons, F.J., Mitrovica, J.X., Maloof, A.C., Oppenheimer, M. 2009. Probabilistic assessment of sea level during the last interglacial stage. Nature, 462, 863–868.

Kraounaki, I., Kourkoumelis, D., 2000. Prefecture of Cyclades. Paros, Paroikia. Arch Delt 55, 1213–1215.

Kreutzer, S., Lauer, T., Meszner, S., Krbetschek, M.R., Faust, D., Fuchs, M., 2014. Chronology of the Quaternary profile Zeuchfeld in Saxony-Anhalt /Germany - a preliminary luminescence dating study. Zeitschrift für Geomorphologie 58, 5-26.

Laborel, J., Laborel-Deguen, F., 1994. Biological indicators of relative sea-level variations and of co-seismic displacements in the Mediterranean region. Journal of Coastal Research, 10(2), 395–415.

Laborel, J., Morhange, C., Collina-Girard, J., Laborel-Deguen, F., 1999. Littoral bioerosion, a tool for the study of sea-level variations during the Holocene. Bulletin of the Geological Society of Denmark 45,164–168.

Lambeck, K., Chappell, J., 2001. Sea level change through the last Glacial Cycle. Science 292, 679–686.

Lambeck, K., Purcell, A., 2005. Sea-level change in the Mediterranean Sea since the LGM: model predictions for tectonically stable areas. Quaternary Science Reviews 24, 1969–1988. http://dx.doi.org/10.1016/j.quascirev.2004.06.025.

Lambeck, K., Anzidei, M., Antonioli, F., Benini, A., Esposito, A., 2004. Sea level in Roman time in the Central Mediterranean and implications for recent change. Earth and Planetary Science Letters, 224, 563–575.

Lambeck, K., Purcell, A. Dutton, A. 2012. The anatomy of interglacial sea levels: the relationship between sea levels and ice volumes during the Last Interglacial. Earth Planetary Science Letters, 315-316, 4-11.

Lambrinoudakis, V.K., 1985. Excavation of Naxos. Prakt 144–161.

Lambrinoudakis, V.K., 1988. Excavation of Naxos. Prakt 208–218.

Lambrinoudakis, V.K., Zapheiropoulou, P., 1985. Excavation of Naxos. Cathedral Square (Plateia Metropoleōs). Prakt 162–167.

Land, L.S., 1970. Phreatic vs. vadose meteoric diagenesis of limestones: Evidence from a fossil water table. Sedimentology 14, 175-185.

Larson, M., Kraus, N.C., 2000. Representation of non-erodible (hard) bottoms in beach profile change modeling. Journal of Coastal Research 16 (1), 1–14.

Le Pichon, X. 1982. Land-locked oceanic basins and continental collision. In: Hsü, K. (Ed.), The Eastern Mediterranean as a Case Example, in Mountain Building Processes, pp. 201–211. Academic Press, San Diego, CA.

Le Pichon, X., Angelier, J., 1979. The Hellenic arc and trench system: a key to the evolution of the Eastern Mediterranean area. Tectonophysics 60, 1–42.

Le Pichon, X., Angelier, J., Sibuet, J.-C. 1982. Plate boundaries and extensional tectonics. Tectonophysics, 81, 239–256.

Le Pichon, X., Chamot-Rooke, N., Lallemant, S. L., Noomen, R., Veis, G., 1995. Geodetic determination of the kinematics of Central Greece with respect to Europe: implications for eastern Mediterranean tectonics. Journal of Geophysial Research 100, 12,675–12,690.

Lee, J., Lister, G.S., 1992. Late Miocene ductile extension and detachment faulting, Mykonos, Greece. Geology 20, 121–124.

Lykousis, V., 2009. Sea-level changes and shelf break prograding sequences during the last 400ka in the Aegean margins: Subsidence rates and palaeogeographic implications. Continental Shelf Research, 29(16), 2037–2044.

Lykousis, V., Anagnostou, C., Pavlakis, P., Rousakis, G., Alexandri, M., 1995. Quaternary sedimentary history and neotectonic evolution of the eastern part of Central Aegean Sea, Greece. Marine Geology, 128(1–2), 59–71.

Machaira, V., 1988. Pottery. Prakt 214–218.

Marco-Barba, J., Holmes, J.A., Mesquita-Joanes, F., Miracle, M.R., 2013. The influence of climate and sea-level change on the Holocene evolution of a Mediterranean coastal lagoon: Evidence from ostracod palaeoecology and geochemistry. Geobios 46(5), 409–421.

Marriner, N., 2007. Geoarchaeology of Phoenicia's buried harbours: Beirut, Sidon and Tyre 5000 years of human-environment interactions. Geomorphology. Université de Provence - Aix- Marseille I, English.

Marriner, N., Morhange, C., 2007. Geoscience of ancient Mediterranean harbours. Earth-Science Reviews, 80(3), 137–194. https://doi.org/10.1016/j.earscirev.2006.10.003

Marriner, N., Morhange, C., Faivre, S., Flaux, C., Vacchi, M., Miko, S., Dumas, V., Boetto, G., Radic Rossi, I., 2014. Post-Roman sea-level changes on Pag Island (Adriatic Sea): Dating Croatia's "enigmatic" coastal notch? Geomorphology, 221, 83–94. https://doi.org/10.1016/j.geomorph.2014.06.002

Mascle, J., Martin, L., 1990. Shallow structure and recent evolution of the Aegean Sea: A synthesis based on continuous seismic refection profiles. Marine Geology 94, 271-299.

Mauz, B., 2015. Luminescence, Coastal Sediments. In: Rink, W.J., Thompson, J. W. (Eds.), Encyclopedia of Scientific Dating Methods, pp. 446–450. Dordrecht, Springer Netherlands.

Mauz, B., Baeteman, C., Bungenstock, F. Plater, A.J., 2010. Optical dating of tidal sediments: potentials and limits inferred from the North Sea coast. Quaternary Geochronology 5, 667-678.

Mauz, B., Ruggieri, G., Spada, G., 2015a. Terminal Antarctic melting inferred from a far-field coastal site, Quaternary Science Reviews 116, 122-132. http://dx.doi.org/10.1016/j.quascirev.2015.03.008.

Mauz, B., Vacchi, M., Green, A., Hoffmann, G., Cooper, A., 2015b. Beachrock: A tool for reconstructing relative sea level in the far-field. Marine Geology 362, 1-16. http://dx.doi.org/10.1016/j.margeo.2015.01.009.

Mazzini, I., Anadon, P., Barbieri, M., Castorina, F., Ferreli, L., Gliozzi, E., Mola,M., Vittori, E., 1999. Late Quaternary sea-level changes along the Tyrrhenian coast near Orbetello (Tuscany, central Italy): palaeoenvironmental reconstruction using ostracods. Marine Micropaleontology 37 (3), 289–311.

Mazzini, I., Faranda, C., Giardini, M., Giraudi, C., Sadori, L., 2011. Late Holocene palaeoenvironmental evolution of the Roman harbour of Portus, Italy. Journal of Paleolimnology, 46, 243–256.

McClusky, S., Balassanian, S., Barka, A., Demir, C., Ergintav, S., Georgiev, I., Gurkan, O., Hamburger, M., Hurst, K., Kahle, H., Kastens, K., Keklidze, G., King, R., Kotzev, V., Lenk, O., Mahmoud, S., Mishin, A., Nadariya, M., Ouzonis, A., Paradissis, D., Peter, Y., Prilepin, M., Reilinger, R., Sanli, I., Seeger, H., Tealeb, A., Toksoz, M.N., Veis, G., 2000. Global positioning system constraints on plate kinematics and dynamics in the eastern Mediterranean and Caucasus. Journal of Geophysical Research 105, 5695–5720.

McKenzie, D., 1972. Active tectonics of the Mediterranean region. Geophysical Journal Royal Astronomical Society of London 30, 109–185.

McKenzie, D., 1978. Active tectonics of the Alpine-Himalayan belt: the Aegean Sea and surrounding regions. Geophysical Journal of the Royal Astronomical Society 55, 217–254.

Mendoni, L., Mourtzas, N.D., n.d. Paleogeomorphological representation of Poles bay. A first approach of the harbor of ancient Karthaia. Archaiognosia 4, 127–137.

Mendoni, L.G., Mourtzas, N.D., 1990. An Archaeological Approach to Coastal Sites: The Example of the ancient harbor of Karthaia. Parnassos 32, 387–403.

Mercier, J.-L., Sorel, D., Vergely, P., Simeakis, K., 1989. Extensional tectonic regimes in the Aegean basins during the Cenozoic. Basin Research 2, 49–71.

Meulenkamp, J. E., Wortel, M. J. R., Van Wamel, W. A., Spakman, W., Hoogerduyn Strating, E. 1988. On the Hellenic subduction zone and the geodynamical evolution of Crete since the late Middle Miocene. Tectonophysics, 146, 203–215.

Milliman, J.D., 1974. Marine Carbonates. Springer-Verlag, Berlin, 375 pp.

Milne, G.A., Long, A.J., Bassett, S.E., 2005. Modelling Holocene relative sea-level observations from the Caribbean and South America. Quaternary Science Reviews 24(10), 1183–1202.

Moore, C.H., 1973. Intertidal carbonate cementation in Grand Cayman, West Indies. Journal of Sedimentary Petrology 43, 591–602.

Morelli, C., Pisani, M., Gantar, C., 1975. Geophysical studies in the Aegean Sea and in the Eastern Mediterranean. Bolletino Geofisical Teoritica & Applicata 18, 127–167

Moresby, R., 1835. Extracts from commander Moresby's report on the northern atolls of the Maldives. Journal of the Royal Geography Society of London 5, 398–403.

Morhange, C., Marriner, N., 2010. Paleo-Hazards in the Coastal Mediterranean: A Geoarchaeological Approach. In: Martini, I.P., Chesworth, W. (Eds.), Landscapes and Societies, pp. 223–234. Springer Netherlands, Dordrecht.

Morhange, C., Marriner, N., 2015. Archeological and biological relative sea-level indicators. In: Shennan, I., Long, A.J., Horton, B.P. (Eds.), Handbook of Sea-Level Research, pp. 146-156. John Wiley & Sons, Ltd.

Morhange, C., Laborel, J., Hesnard, A., 2001. Changes of relative sea level during the past 5000 years in the ancient harbour of Marseilles, Southern France. Palaeogeography, Palaeoclimatology, Palaeooecology 166, 319–329.

Morhange, C., Pirazzoli, P.A., Marriner, N., Montaggioni, L.F., Nammour, T., 2006. Late Holocene relative sea level changes in Lebanon, Eastern Mediterranean. Marine Geology 230 (1-2), 99-114.

Morhange, C., Marriner, N., Excoffon, P., Bonnet, S., El-amouri, M., Zibrowius, H., 2013. Relative sea level changes during Roman times in the NW Mediterranean. The 1st century AD fish tank of Forum Julii (Fréjus, France). Geoarchaeology: An International Journal 28, 363–372.

Morhange, C., Marriner, N., Baralis, A., Blot, M. L., Bony, G., Carayon, N., Carmona, P., Flaux, C., Giaime, M., Goiran, J. P., Kouka, M., Lena, A., Oueslati, A., Pasquinucci, M., Porotov, A., 2015. Dynamiques géomorphologiques et typologie géoarcheologique des ports antiques en contextes lagunaires. Quaternaire 26(2), 117–139.

Morhange, C., Giaime, M., Marriner, N., Hamid, A. abu, Bruneton, H., Honnorat, A., Kaniewski, D., Magnin, F., Porotov, A.V., Wante, J., Zviely, D., Artzy, M., 2016. Geoarchaeological evolution of Tel Akko's ancient harbour (Israel). Journal of Archaeological Science: Reports, 7, 71–81.

Mörner, N.A., 1996. Sea level variability. Zeitschrift für Geomorphologie NS 102, 223–232.

Morrison, I.A., 1968. Appendix I. Relative sea-level change in the Saliagos area since Neolithic times. In: Evans, J.D., Renfrew, C. (Eds.), Excavations at Saliagos, pp. 92–98. Thames & Hudson, London.

Mourtzas, N.D., 2010. Sea level changes along the coasts of Kea island and paleogeographical coastal reconstruction of archaeological sites. Bulletin of the Geological Society of Greece XLIII (1), 453-463.

Mourtzas, N.D., 2012. A palaeogeographic reconstruction of the seafront of the ancient city of Delos in relation to Upper Holocene sea level changes in the central Cyclades. Quaternary International 250, 3-18.

Mourtzas, N. D., Kissas, C., Kolaiti, E., 2014. Archaeological and geomorphological indicators of the historical sea level changes and the related palaeogeographical reconstruction of the ancient foreharbour of Lechaion, East Corinth Gulf (Greece). Quaternary International 332, 151–171. http://doi.org/10.1016/j.quaint.2012.12.037

Mourtzas, N., Kolaiti, E., Anzidei, M., 2016. Vertical land movements and sea level changes along the coast of Crete (Greece) since Late Holocene. Quaternary International 401, 43-70. https://doi.org/10.1016/j.quaint.2015.08.008

Murray, A.S., Wintle, A.G., 2000. Luminescence dating of quartz using an improved single aliquot regenerative-dose protocol. Radiation Measurements 32, 57-73.

Murray, A.S., Wintle, A.G., 2003. The single aliquot regenerative dose protocol: potential for improvements in reliability. Radiation Measurements 37, 377-381.

Murray, A.S., Mohanti, M., 2006. Luminescence dating of the barrier spit at Chilika lake, Orissa, India. Radiation Protection Dosimetry 119, 442-445.

Murray, W.M., 1988. The Ancient Harbour Mole at Leukas, Greece. In: A. Raban (Ed.), 1st International Symposium “Cities on the Sea –Past and Present”, pp. 101–118. BAR International Series 404, Oxford, UK.

Négris, P., 1904. Vestiges antiques submergés. Athenische Mitteilungen 29, 340–363.

Negris, P.H., 1915–1919. Roches cristallophylliennes et Tectonique de la Grèce, Athènes.

Neumeier, U., 1998. Le rôle de l' activité microbienne dans la cimentation précoce des beachrocks (sédiments intertidaux). PhD Thesis, University of Geneva, 183 pp.

Neumeier, U., 1999. Experimental modelling of beachrock cementation under microbial influence. Sedimentary Geology 126 (1–4), 35–46.

Nixon, F.C., Reinhardt, E.G., Rothaus, R., 2009. Foraminifera and tidal notches: Dating neotectonic events at Korphos, Greece. Marine Geology 257 (1-4), 41-53.

Nicholls, R.J., Mimura, N., 1998.Regional issues raised by sea-level rise and their policy implications. Climate Research 11, 5–18.

Ozturk, M.Z., Erginal, A.E., Kiyak, N.G., Ozturk, T., 2016. Cement fabrics and optical luminescence ages of beachrock, North Cyprus: Implications for Holocene sea-level changes. Quaternary International 401, 132–140.

Papanikolaou, D., 1980. Contribution of the geology of the Aegean Sea. Annales Géologiques des Pays Helléniques 29, 477–533.

Papanikolaou, D., 1987. Tectonic evolution of the Cycladic blueschist belt (Aegean Sea, Greece). In: Helgeson, H.C. (Ed.), Chemical Transport in Metasomatic Processes, pp. 429–450. Riedel, Dordrecht.

Papanikolaou, D., 1989. Are the medial crystalline massifs of the eastern Mediterranean drifted Gondwanan fragments? Geological Society of Greece Special Publication 1, 63–90.

Papanikolaou, D., 1993. Geotectonic evolution of the Aegean. Bulletin of the Geological Society of Greece 28, 33–48.

Papanikolaou, D., 1996. Geological Map of Paros. IGME.

Papanikolaou, D., 2009. Timing of tectonic emplacement of the ophiolites and terrane paleogeography in the Hellenides. Lithos 108, 262–280.

Papathanassopoulos, G., Schilardi, D., 1981. An underwater survey of Paros, Greece: 1979. The International Journal of Nautical Archaeology and Underwater Exploration 10, 133–144.

Papazachos, B.C., 1990. Seismicity of the Aegean and surrounding area. Tectonophysics 178, 287–308.

Papazachos, B.C., Papazachou, C., 1997. The Earthquakes of Greece. Editions ZITI, Thessaloniki, p. 304.

Pavlidis, S., Caputo, R., 2004. Magnitude versus faults' surface parameters: quantitative relationships from the Aegean Region. Tectonophysics 380, 159–188.

Pavlopoulos, K., Kapsimalis, V., Theodorakopoulou, K., Panagiotopoulos, I.P., 2011. Vertical displacement trends in the Aegean coastal zone (NE Mediterranean) during the Holocene assessed by geo-archaeological data. The Holocene 22(6), 717-728.

Pe-Piper, G., Piper, D.J.W., 2002. The Igneous Rocks of Greece: The Anatomy of an Orogen. Gebrüder Borntraeger, Berlin.

Pe-Piper, G., Kotopouli, C.N., Piper, D.J.W., 1997. Granitoid rocks of Naxos, Greece: regional geology and petrology. Geological Journal 32, 153– 171.

Pérès, J.M., 1982. Zonations and organismic assemblages. In: Kinne, O. (Ed.), Marine Ecology, pp. 9–576. John Wiley & Sons, Chichester.

Peterek, A., Schwarze, J., 2004. Architecture and Late Pliocene to recent evolution of outer-arc basins of the Hellenic subduction zone (south-central Crete, Greece). Journal of Geodynamics 38, 19–55.

Pilarczyk, J.E., Dura, T., Horton, B.P., Engelhart, S.E., Kemp, A.C., Sawai, Y., 2014. Microfossils from coastal environments as indicators of paleo-earthquakes, tsunamis and storms. Palaeogeography, Palaeoclimatology, Palaeoecology 413, 144–157.

Pirazzoli, P., 1976. Sea level variations in the Northwest Mediterranean during Roman times. Science, 194, 519–521.

Pirazzoli, P.A., 1986a. Marine notches. In: Van de Plassche, O. (Ed.), Sea-level research: a manual for the collection and evaluation of data. Geo Books, Norwich, pp. 361–400.

Pirazzoli, P.A., 1986b. The Early Byzantine Tectonic Paroxysm. Zeitschrift für Geomorphologie 62, 31–49.

Pirazzoli, P.A., 1988. Sea-Level Changes and Crustal Movements in the Hellenic Arc (Greece). The Contribution of Archaeological and Historical Data, in: Raban, A. (Ed.), 1st International Symposium “Cities on the Sea –Past and Present”, pp. 157–184. BAR International Series 404, Oxford, UK.

Pirazzoli, P.A., 1991. World Atlas of Holocene Sea-Level Changes. Elsevier, Amsterdam.

Pirazzoli, P.A., 2005. A review of possible eustatic, isostatic and tectonic contributions in eight late-Holocene relative sea-level histories from the Mediterranean area. Quaternary Science Reviews 24 (18-19), 1989-2001.

Pirazzoli, P. A., Ausseil-Badie, J., Giresse, P., Hadjidaki, E., Arnold, M., 1992. Historical environmental changes at Phalasarna harbor, West Crete. Geoarchaeology 7(4), 371–392.

Pirazzoli, P.A., Stiros, S.C., Arnold, M., Laborel, J., Laborel-Deguen, F., Papageorgiou, S., 1994. Episodic uplift deduced from Holocene shorelines in the Perachora Peninsula, Corinth area, Greece. Tectonophysics 229 (3-4), 201-209.

Plater, A.J., Kirby, J.R., 2011. Sea-Level Change and Coastal Geomorphic Response. In: Wolanski, E., McLusky, D.S. (Eds.), Treatise on Estuarine and Coastal

Science. Elsevier (Academic Press), Waltham. doi:10.1016/B978-0-12-374711-2.00304-1

Poulos, S.E., Ghionis, G., Maroukian, H., 2009. Sea-level rise trends in the Attico-Cycladic region (Aegean Sea) during the last 5000 years. Geomorphology 107 (1-2), 10-17.

Prescott, J. R., Hutton, J.T., 1994. Cosmic ray contributions to dose rates for luminescence and ESR dating: large depths and long-term time variations. Radiation Measurements 23, 497-500.

Prescott, J.R., Stephan, L.G., 1982. The contribution of cosmic radiation to the environmental dose for thermoluminescence dating. Latitude, altitude and depth dependences. PACT 6, 17-25.

Primavera, M., Simone, O., Fiorentino, G., Caldara, M., 2011. The palaeoenvironmental study of the Alimini Piccolo lake enables a reconstruction of Holocene sea-level changes in southeast Italy. The Holocene, 21(4), 553–563. https://doi.org/10.1177/0959683610385719

Raban, A. (Ed.), 1985. Harbour archeology. Proceedings of the First International Workshop on Ancient Mediterranean Harbours. BAR International series, 257.

Ranson, G., 1955. La consolidation des sediments calcaires dans les regions tropicales. Comptes Rendus de l'Académie des Sciences, 240, 640–642.

Reimann, T., Tsukamoto, S., 2012. Dating the recent past (<500 years) by post-IR IRSL feldspar e Examples from the North Sea and Baltic Sea coast. Quaternary Geochronology 10, 180-187.

Reimann, T., Tsukamoto, S., Harff, J., Osadczuk, K., Frechen, F., 2011. Reconstruction of Holocene coastal foredune progradation using luminescence dating - An example from the Świna barrier (southern Baltic Sea, NW Poland). Geomorphology 132 (1–2), 1-16. http://dx.doi.org/10.1016/j.geomorph.2011.04.017.

Reimer, P.J., Edouard Bard, B., Alex Bayliss, B., Warren Beck, B.J., Paul Blackwell, B.G., Christopher Bronk Ramsey, B., 2013. Intcal13 and Marine13 Radiocarbon Age Calibration Curves 0–50,000 Years Cal Bp. Radiocarbon 55, 1869–1887. doi:10.1017/S0033822200048864

Reimer, P.J., McCormac, F.G., 2002. Marine radiocarbon reservoir corrections for the Mediterranean and Aegean Seas. Radiocarbon 44, 159–166.

Renfrew, C., 1976. Archaeology and the earth sciences. In: Davidson, A., Shackley, M.L. (Eds.), Geoarchaeology: Earth Science and the Past, pp. 1–5. Duckworth, London.

Robert, E., 1982. Contribution a l'etude geologique des Cyclades (Grece): L'Ile de Paros. Unpublished PhD thesis, Universite de Paris-Sud, France.

Rossi, V., Sammartino, I., Amorosi, A., Sarti, G., De Luca, S., Lena, A., Morhange, C., 2015. New insights into the palaeoenvironmental evolution of Magdala ancient harbour (Sea of Galilee, Israel) from ostracod assemblages, geochemistry and sedimentology. Journal of Archaeological Science, 54, 356–373.

Rovere, A., Antonioli, F., Bianchi, C.N., 2015. Fixed biological indicators. In: Shennan, I., Long, A.J., Horton, B.P. (Eds.), Handbook of Sea-Level Research, pp. 268–280. John Wiley & Sons Ltd.

Rovere, A., Stocchi, P., Vacchi, M., 2016a. Eustatic and Relative Sea Level Changes. Current Climate Change Reports, 2(4), 221–231.

Rovere, A., Raymo, M. E., Vacchi, M., Lorscheid, T., Stocchi, P., Gómez-Pujol, L., Harris, D.L., Casella, E., O'Leary, M.J., Hearty, P. J., 2016b. The analysis of Last Interglacial (MIS 5e) relative sea-level indicators: Reconstructing sea-level in a warmer world. Earth-Science Reviews, 159, 404–427.

Roy, P. S., Cowell, P. J., Ferland, M. A., Thom, B. G., 1994. Wave-dominated coasts. In: Carter, R. W. G., Woodroffe, C. D. (Eds.), Coastal Evolution, pp. 121–186. Cambridge University Press, Cambridge.

Royden, L.H., 1993. Evolution of retreating subduction boundaries formed during continental collision. Tectonics 12, 629–638.

Rubensohn, O., 1901. Paros II. Topographie. Athenische Mitteilungen 26, 157–222.

Rubensohn, O., 1901. Paros II. Topographie. Athenische Mitteilungen 26, 157–222.

Rubensohn, O., 1949. s. Paros. Realenzyklopädie 18, 1781–1872.

Sacchi, M., Molisso, F., Pacifico, A., Vigliotti, M., Sabbarese, C., Ruberti, D., 2014. Late-Holocene to recent evolution of Lake Patria, South Italy: An example of a coastal lagoon within a Mediterranean delta system. Global and Planetary Change, 117, 9-27.

Sakellariou, D., Galanidou, N., 2016. Pleistocene submerged landscapes and Palaeolithic archaeology in the tectonically active Aegean region. Geological Society, London, Special Publications, 411, 145–178.

Sánchez-Gómez, M., Avigad, D., Heimann, A., 2002. Geochronology of clasts in allochthonous Miocene sedimentary sequence on Mykonos and Paros Islands: implications for backarc extension in the Aegean Sea. Journal of the Geological Society of London 159, 45–60.

Sanlaville, P., 1970. Les variations holocènes du niveau de la mer au Liban. Revue de géographie de Lyon 45 (3), 279-304. DOI : 10.3406/geoca.1970.2671

Semeniuk, V., Searle, D.J., 1987. Beach rock ridges/bands along a high-energy coast in Southwestern Australia - their significance and use in coastal history. Journal of Coastal Research 3(3), 331–342.

Schilardi, D., 1973. A fortified acropolis on the Oikonomos island of Paros. AAA 6, 260–265.

Schilardi, D., 1975a. Archaelogical research in Paros. Prakt 197–211.

Schilardi, D., 1975b. Paros, Report II : The 1973 Campaign. Journal of Field Archaeology 2, 83–96.

Schilardi, D., 1979. Excavation in Paros. Prakt 287–294.

Schilardi, D., 2010. Appendix IV: Quarries and Marble of Paros: the decade 2000-2010, in: Schilardi, D., Katsonopoulou, D. (Eds.), Paria Lithos. Athens, pp. 649–661.

Schilardi, D.U., Katsonopoulou, D., 2010. Paria Lithos. Parian Quarries, Marble and Workshops of Sculpture. Athens.

Scholle, P. A., Bebout, D. G., Moore, C. H., 1983. Carbonate Depositional Environments. The American Association of Petroleum Geologists, Tulsa, Oklahoma.

Schuiling, R.D., Kreulen, R., 1979. Are Thermal Domes Heated by CO2-rich Fluids from the Mantle? Earth and Planetary Science Letters 43, 298-302.

Scott, D. S., Medioli, F. S., 1978. Vertical zonations of marsh foraminifera as accurate indicators of former sea-levels. Nature, 272 (5653), 528–531.

Shennan, I., 1982. Interpretation of Flandrian sea-level data from the Fenland, England. Proceedings of the Geologists' Association 93(1), 53–63.

Shennan, I., Horton, B., 2002. Holocene land- and sea-level changes in Great Britain. Journal of Quaternary Science 17, 511–526.

Shennan, I., Long, A.J., Horton, B.P., 2015. Handbook of Sea-Level Research. John Wiley & Sons Ltd.

Simosi, A.G., 2009. The “closed” naval harbor of Samos. Similarities and comparisons with other “closed” naval harbors in the Mediterranean. Cultural Foundation of Samos “Nikolaos Dimitriou.”

Sivan, D., Lambeck, K., Toueg, R., Raban, A., Porath, Y., Shirman, B., 2004. Ancient coastal wells of Caesarea Maritima, Israel, an indicator for relative sea level changes during the last 2000 years. Earth and Planetary Science Letters, 222, 315–330.

Stanley, D. J., Warne, A. G., 1994. Worldwide Initiation of Holocene Marine Deltas by Deceleration of Sea-Level Rise. Science, 265(5169), 228-231.

Stattegger, K., Tjallingii, R., Saito, Y., Michelli, M., Thanh, N.T., Wetzel, A., 2013. Mid to late Holocene sea-level reconstruction of southeast Vietnam using beachrock and beach-ridge deposits. Global and Planetary Change 110, 214–222.

Stiros, S., Marangou, L., Arnold, M., 1994. Quaternary uplift and tilting of Amorgos Island (southern Aegean) and the 1956 earthquake. Earth and Planetary Science Letters 128, 65–76.

Stiros, S.C., Laborel J., Laborel-Deguen, F., Papageorgiou, S., Évin, J., Pirazzoli, P.A., 2000. Seismic coastal uplift in a region of subsidence: Holocene raised shorelines of Samos Island, Aegean Sea. Greece. Marine Geology 170 (1-2), 41-58.

Stiros, S.C., Blackman, D.J., 2014. Seismic coastal uplift and subsidence in Rhodes Island, Aegean Arc: Evidence from an uplifted ancient harbor. Tectonophysics 611, 114-120.

Stoddart, D.R., Cann, J.R., 1965. Nature and origin of beach rock. Journal of Sedimentary Petrology 35, 243–247.

Strasser, A., Davaud, E., 1986. Formation of Holocene limestone sequences by progradation, cementation, and erosion: two examples from the Bahamas. Journal of Sedimentary Petrology 56(3), 422–428.

Stuiver, M., Reimer, P.J., Reimer, R.W., 2016. CALIB 7.1 [WWW program] at http://calib.org, accessed 2016-12-29

Tatumi, S. H., Kowata, E.A., Gozzi, G., Kassab, L.R., Suguio, K., Barreto, A.M., Bezerra, F.H., 2003. Optical dating results of beachrock, eolic dunes and sediments applied to sea-level changes study. Journal of Luminescence 102-103, 562-565.

Taylor, J.C.M., Illing, L.V., 1969. Holocene intertidal calcium carbonate cementation, Qatar, Persian Gulf. Sedimentology 12, 69–107

Taylor, J.C.M., Illing, L.V., 1971. Variation in recent beachrock cements, Quatar, Persian Gulf. In: Bricker, O.P. (Ed.), Carbonate Cements, pp. 32–33. Studies in Geology 19. Johns Hopkins Press, Baltimore.

Taymaz, T., Jackson, J., McKenzie, D., 1991. Active tectonics of the north and central Aegean Sea. Geophysical Journal International 106, 433–490.

Thiel, C., Buylaert, J.-P., Murray, A., Terhorst, B., Hofer, I., Tsukamoto, S., Frechen, M., 2011. Luminescence dating of the Stratzing loess profile (Austria) – testing the potential of an elevated temperature post-IR IRSL protocol. Quaternary International, 234, 23–31.

Thiel, C., Tsukamoto, S., Tokuyasu, K., Buylaert, J.-P., Murray, A.S., Tanaka, K., Shirai, M., 2015. Testing the application of quartz and feldspar luminescence dating to MIS 5 Japanese marine deposits. Quaternary Geochronology 29, 16-29.

Thomas, P.J., 2009. Luminescence Dating of Beachrock in the Southeast Coast of India - Potential for Holocene Shoreline Reconstruction. Journal of Coastal Research 25 (1), 1-7.

Thomas, P.J., Murray, A.S., Granja, H.M., Jain, M., 2008. Optical dating of Late Quaternary coastal deposits in northwest- ern Portugal. Journal of Coastal Research, 24, 134–144.

Tirel, C., Gueydan, F., Tiberi, C., Brun, J.P., 2004. Aegean crustal thickness inferred from gravity inversion. Geodynamical implications. Earth and Planetary Science Letters 228, 267–280.

Tucker, M.E., Wright, V.P., 1990. Carbonate sedimentology. Blackwell Science Ltd., Oxford, https://doi.org/10.1002/9781444314175

Tziligkaki, E.K., 2014. The ancient quarries of Crete. University of Crete.

Vacchi, M., Rovere, A., Zouros, N., Desruelles, S., Caron, V., Firpo, M., 2012. Spatial distribution of sea-level markers on Lesvos Island (NE Aegean Sea): evidence of differential relative sea-level changes and the neotectonic implications. Geomorphology 159-160, 50–62.

Vacchi, M., Ghilardi, M., Spada, G., Currás, A., Robresco, S., 2016a. New insights into the sea-level evolution in Corsica (NW Mediterranean) since the late Neolithic. Journal of Archaeological Science: Reports, 1–12. https://doi.org/10.1016/j.jasrep.2016.07.006

Vacchi, M., Marriner, N., Morhange, C., Spada, G., Fontana, A., Rovere, A., 2016b. Multiproxy assessment of Holocene relative sea-level changes in the western Mediterranean: Sea-level variability and improvements in the definition of the isostatic signal. Earth-Science Reviews, 155, 172–197.

Vamvakaris, D. A., Papazachos, C. B., Papaioannou, C. A., Scordilis, E. M., Karakaisis, G. F., 2016. A detailed seismic zonation model for shallow earthquakes in the broader Aegean area. Natural Hazards and Earth System Sciences, 16(1), 55–84.

Van de Plassche, O., 1986. Introduction. In: Van de Plassche, O. (Ed.), Sea-Level Research: A Manual for the Collection and Evaluation of Data, pp. 1–26. Geobooks, Norwich.

Vella, C., Provensal, M., 2000. Relative sea-level rise and neotectonic events during the last 6,500 yr on the southern eastern Rhone delta, France. Marine Geology 170 (2000) 27-39.

Vieira, M.M., Ros, L.F.D., 2007. Cementation patterns and genetic implications of Holocene beachrocks from northeastern Brazil. Sedimentary Geology 192 (3-4), 207–230.

Vigner, A., 2002. Images sismiques par réflexions verticales et grand-angle de la croûte en contexte extensif: les Cyclades et le Fossé Nord-Egéen. PhD thesis, Institut de Physique du Globe, Paris, 269 pp.

Vis, G.G., Cohen, K.M., Westerhoff, W.E., Veen, J.H., Hijma, M.P., van der Spek, A.J.F., Vos, P.C., 2015. Paleogeography. In: Shennan, I., Long, A.J., Horton, B. (Eds.), Handbook of Sea-Level Research, pp. 514–534. Wiley-Blackwell.

Vlachopoulos, A., 2006. The LH IIIC period in Naxos. Archaiognosia A.

Vött, A., Brückner, H., Handl, M., Schriever, A., 2006. Holocene palaeogeographies of the Astakos coastal plain (Akarnania, NW Greece). Palaeogeography, Palaeoclimatology, Palaeoecology, 239(1–2), 126–146. https://doi.org/10.1016/j.palaeo.2006.01.015

Vousdoukas, M.I., Velegrakis, A.F., Karambas, T., Valais, G., Zarkoyiannis, S., 2005. Morphodynamics of beachrock-infected beaches: Vatera Beach, NE Mediterranean. In: Sanchez-Arcilla, A. (Ed.), 5th International Conference on Coastal Dynamics, pp. 1-12. Barcelona, Spain.

Vousdoukas, M.I., Velegrakis, A.F., Plomaritis, T.A., 2007. Beachrock occurrence, characteristics, formation mechanisms and impacts. Earth-Science Reviews, 85(1–2), 23–46. https://doi.org/10.1016/j.earscirev.2007.07.002

Wallinga, J., Bos, A. J. J., Dorenbos, P., Murray, A. S., Schokker, J., 2007. A test case for anomalous fading correction in IRSL dating. Quaternary Geochronology, 2, 216–221.

Wijbrans, J.R., McDougall, I., 1986. 40Ar/39Ar dating of white micas from an alpine high- pressure metamorphic belt on Naxos (Greece); the resetting of the argon isotopic system. Contributions to Mineralogy and Petrology 93, 187–194.

Wijbrans, J.R., McDougall, I., 1988. Metamorphic evolution of the Attic Cycladic Metamorphic Belt on Naxos (Cyclades, Greece) utilizing 40Ar/39Ar age spectrum measurements. Journal of Metamorphic Geology 6, 571–594.

Winter, E., 1996. Staatliche Baupolitik und Baufürsorge in den römischen Provinzen des kaiserzeitlichen Kleinasien. Asia Minor Stud. Band 20.

Woodroffe, C., 2002. Coasts: Form, Process and Evolution. Cambridge University Press, Cambridge.

Zapheiropoulou, P.N., 1990. Excavation works. Paros. Paroikia. Arch Delt 45, 402–403.

Zapheiropoulou, P.N., 2000. The ancient cemetery of Paros in the Geometric and Archaic period. Archaeol. Ephemer. 283–293.

Zapheiropoulou, P., Lambrinoudakis, V.K., 1982. Excavation of the Cathedral Square (Plateia Metropoleōs) on Naxos. Prakt 260–262.

Zhu, L., Mitchell, B.J., Akyol, N., Cemen, I., Kekovali, K., 2006. Crustal thickness variations in the Aegean region and implications for the extension of continental crust. Journal of Geophysical Research, 111, B01301. doi:10.1029/2005JB003770.

Appendices

Appendix I: Beachrocks of Paros and Naxos (Cyclades, Greece)

General view of the studied beachrocks

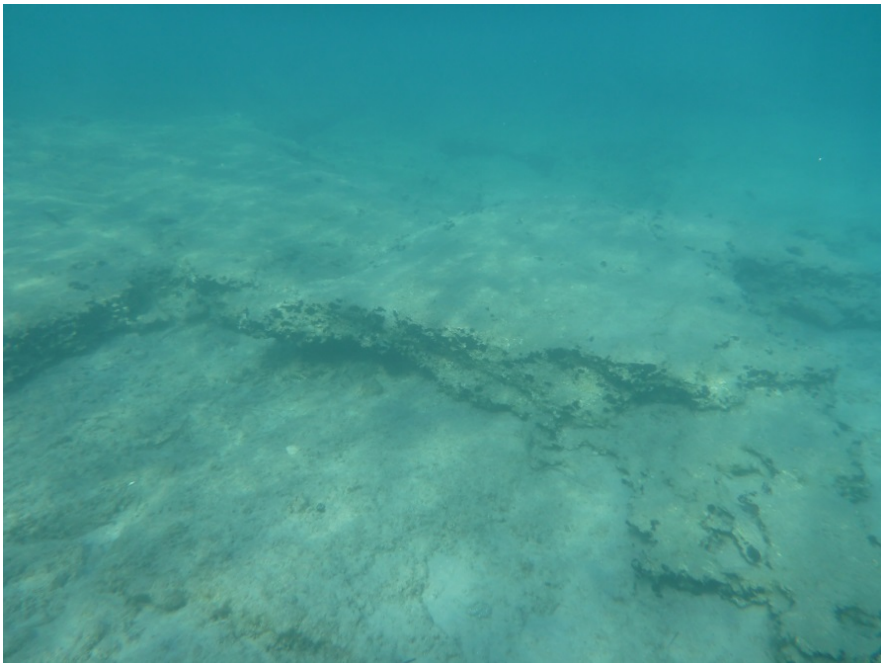

Underwater view of Martselo beachrock at depth -1.8 m, NW Paros

Underwater view of Martselo beachrock at -3.7 m depth, Northwestern Paros

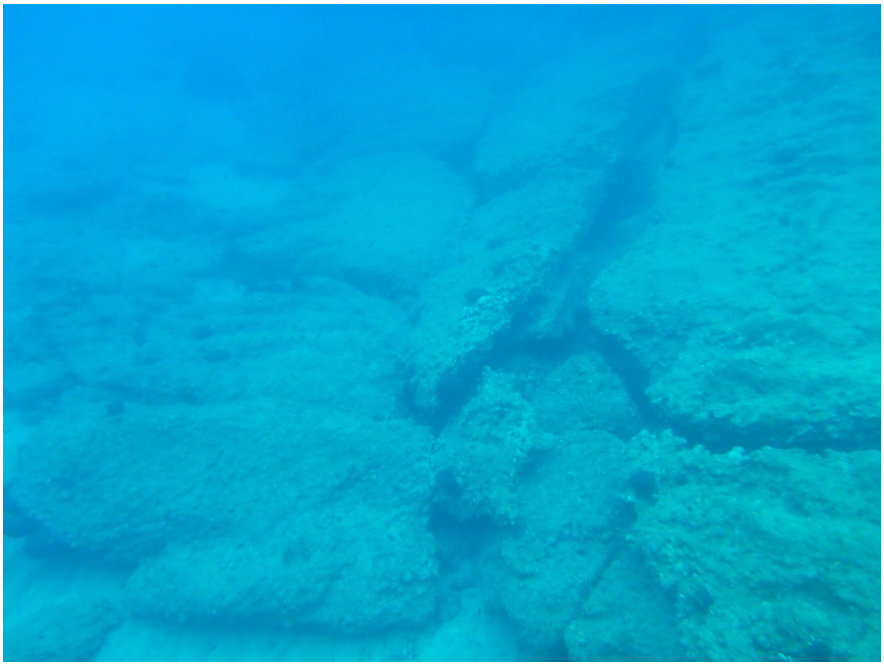

Submerged beachrock at Tsoukalia at a depth of -4 m (Eastern Paros)

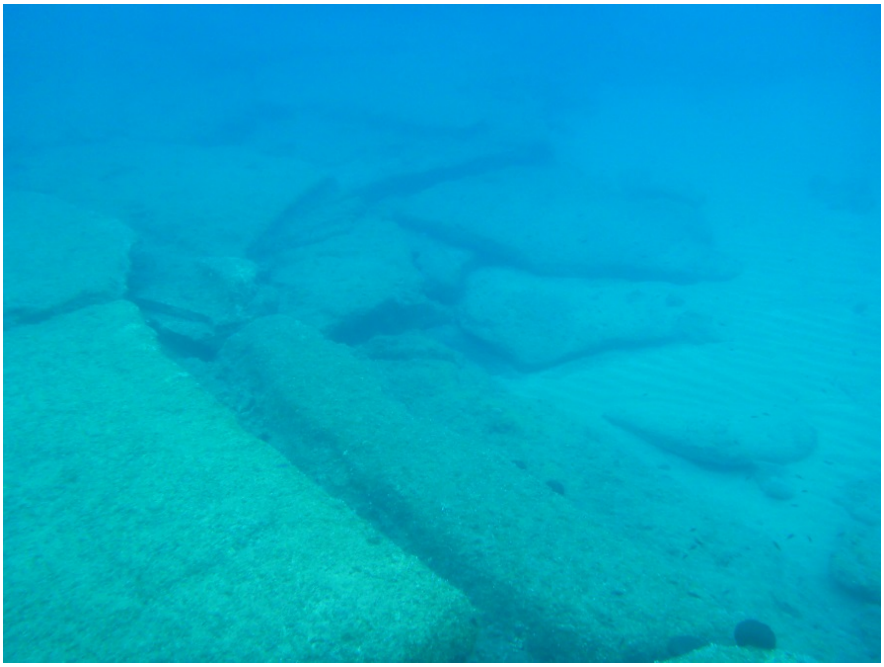

The deepest beachrock slab at Tsoukalia (Eastern Paros), located at -6.2 m

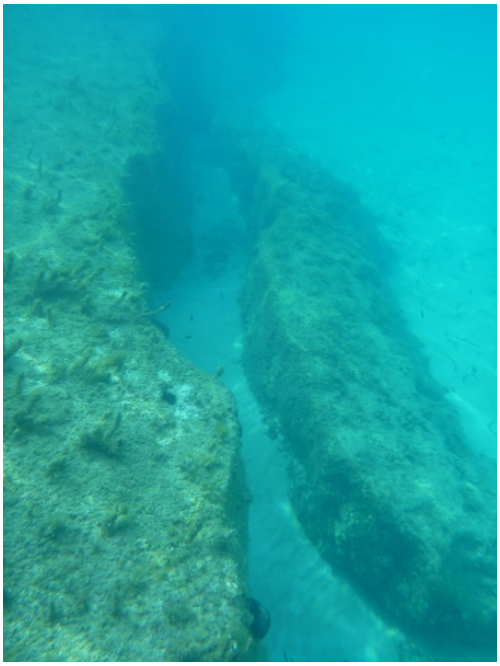

Submerged beachrock slab at Plaka beach (Western Naxos), at a depth of -4.3 m

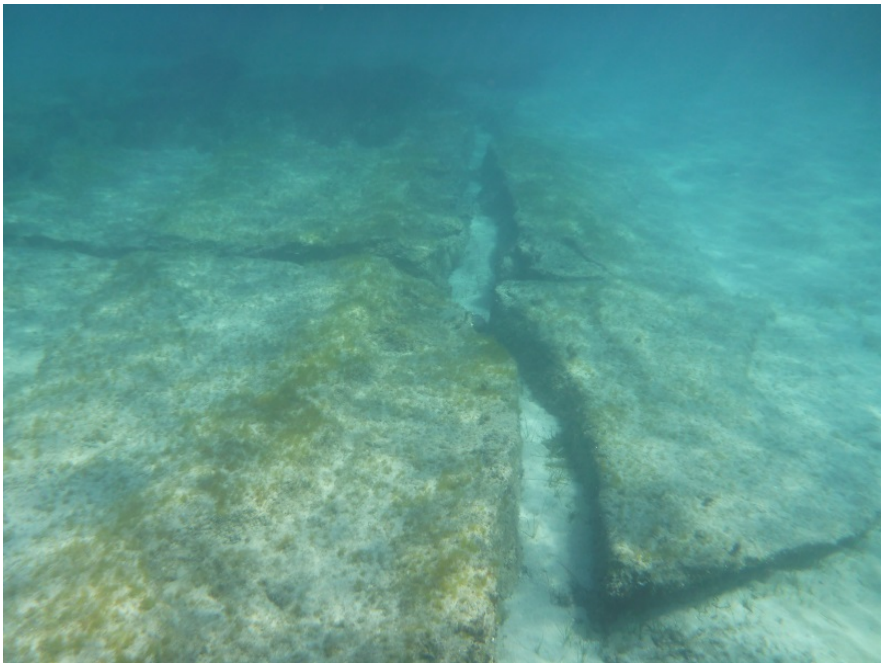

Underwater view of beachrock slabs at Glyfada beach (Western Naxos), located at about -4.4 m

Overview of Agios Georgios deepest beachrock slab at -6.3 m depth (Western Naxos).

Submerged continuous beachrock slab at Glystra (Western Naxos), located between -1.5 and -3.8 m..

Thin sections of studied beachrocks

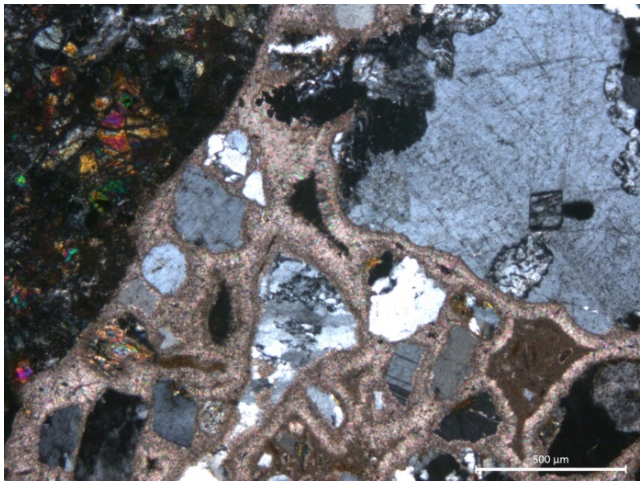

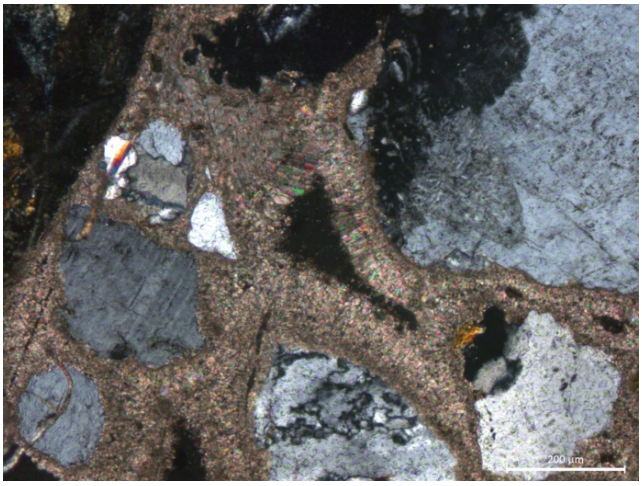

Agios Georgios beachrock at -6.2 m depth (Western Naxos). Well-developed isopachous cement of radiaxial fibrous HCM; Quartz and feldspar grains were mainly observed along with some lithoclasts of various sizes

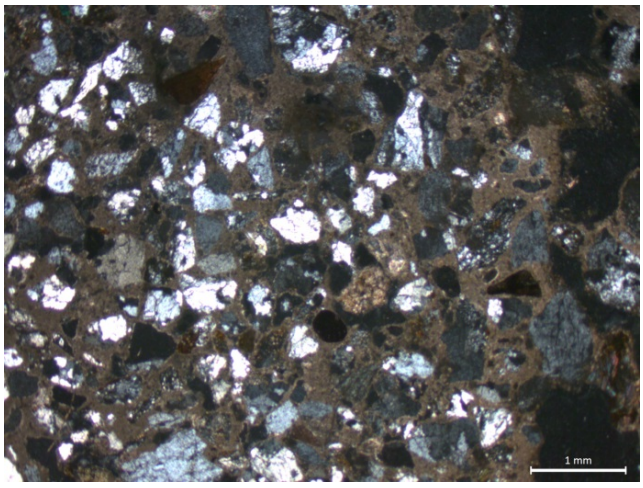

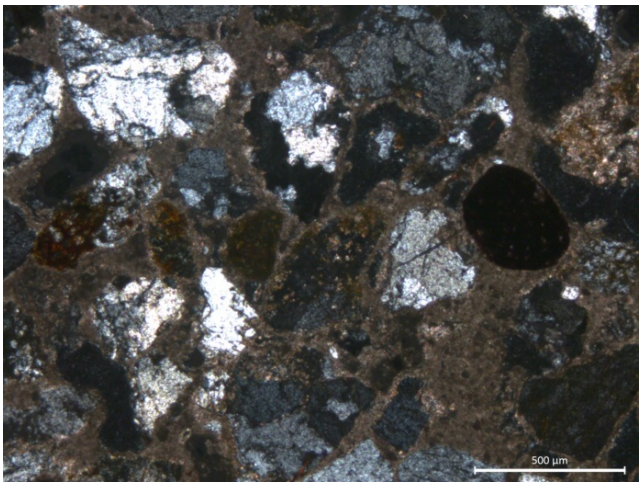

Agios Georgios beachrock at -0.2 m depth (Western Naxos). A fine fringe of isopachous HCM, along with micritization and recrystallization

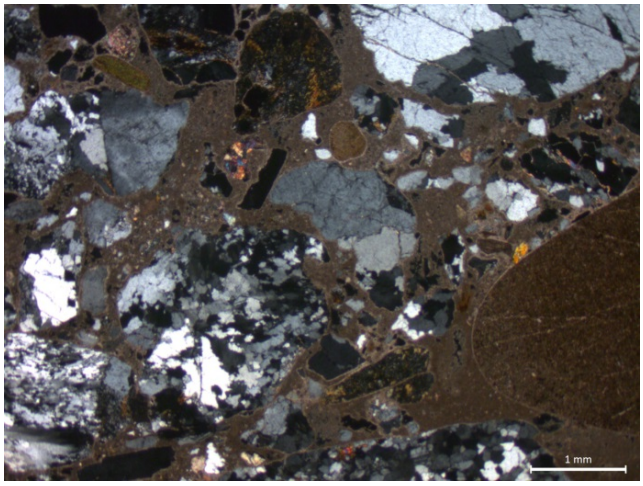

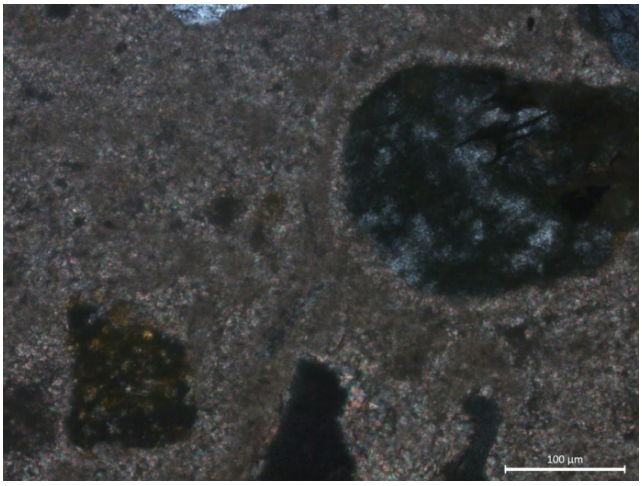

Agios Georgios beachrock at -1.9 m depth (Western Naxos). A fine fringe of isopachous HCM is noted around grains. Peloidal texture is also present. Marine cementation of magnesium calcite around pellets (probably caused by bacterial actions) and recrystallization

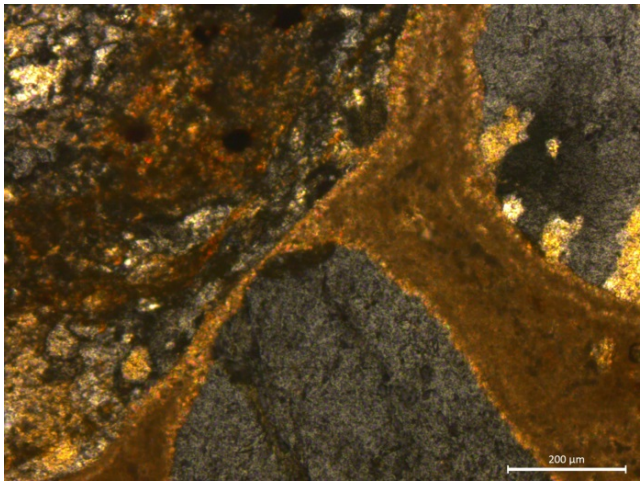

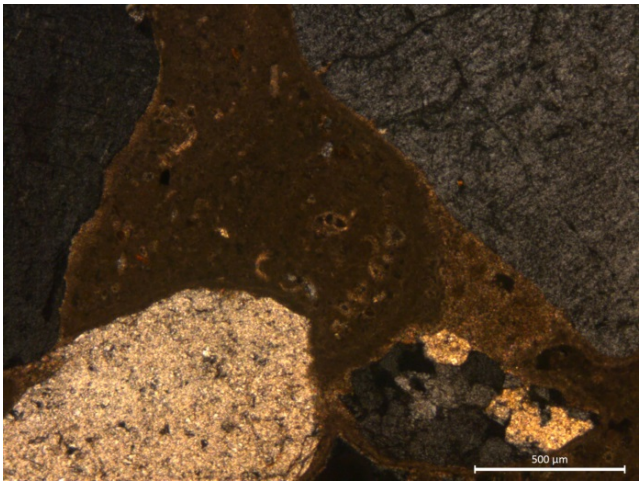

Plaka beachrock at -6.2 m depth (Western Naxos). A fine fringe of isopachous HCM surrounds the grains and meniscus between grains.

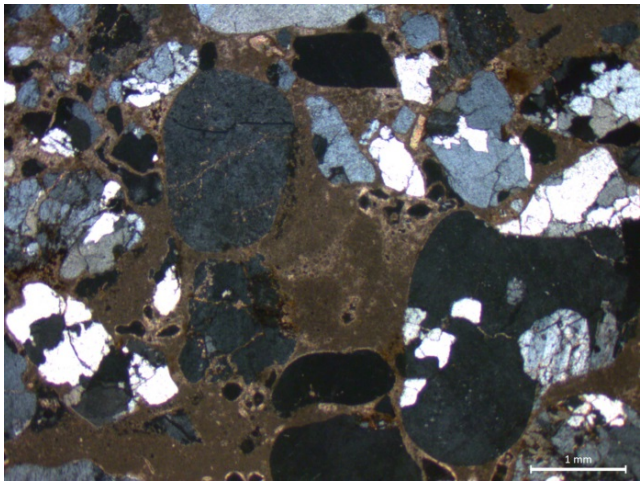

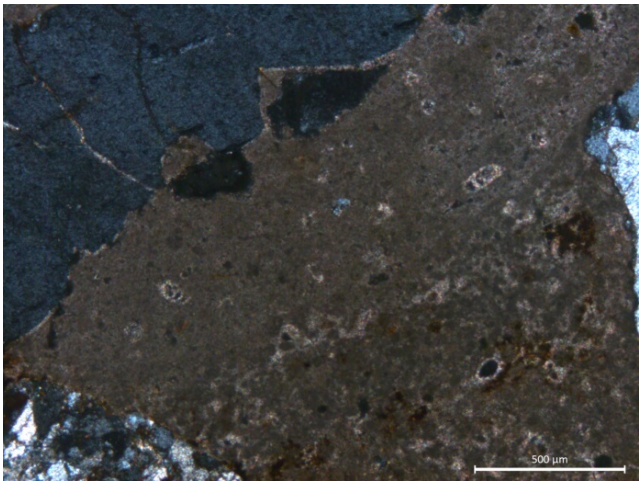

Orkos beachrock at -2.2 m depth (Western Naxos). A fine fringe of isopachous HCM is noted around the grains, along with micritic cement filling pores.

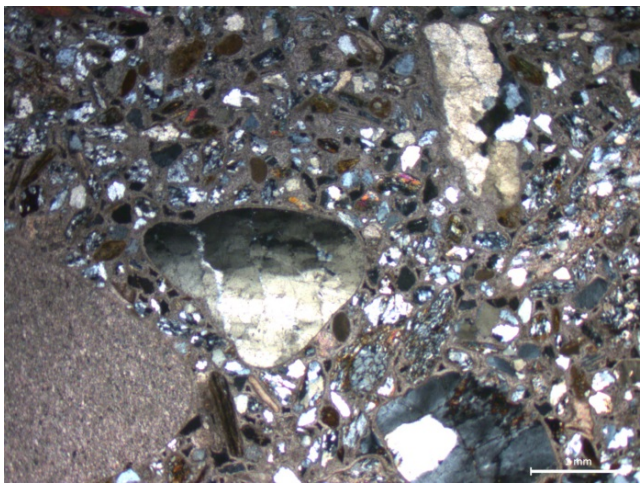

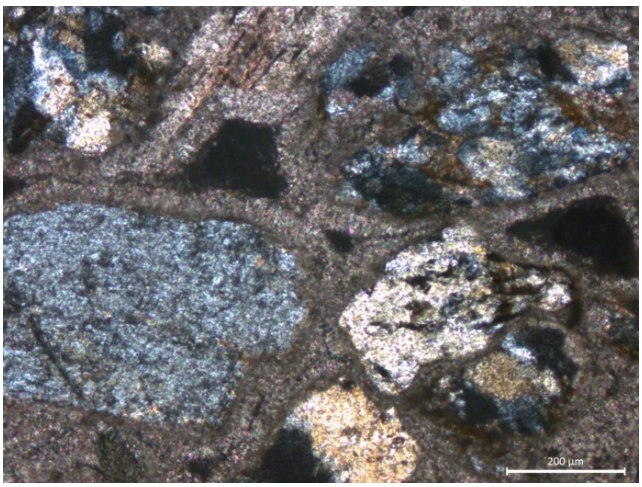

Glystra beachrock at -0.75 m depth (Western Naxos). Well cemented beachrock with bladed isopachous fringe of limpid and contiguous HMC crystals.

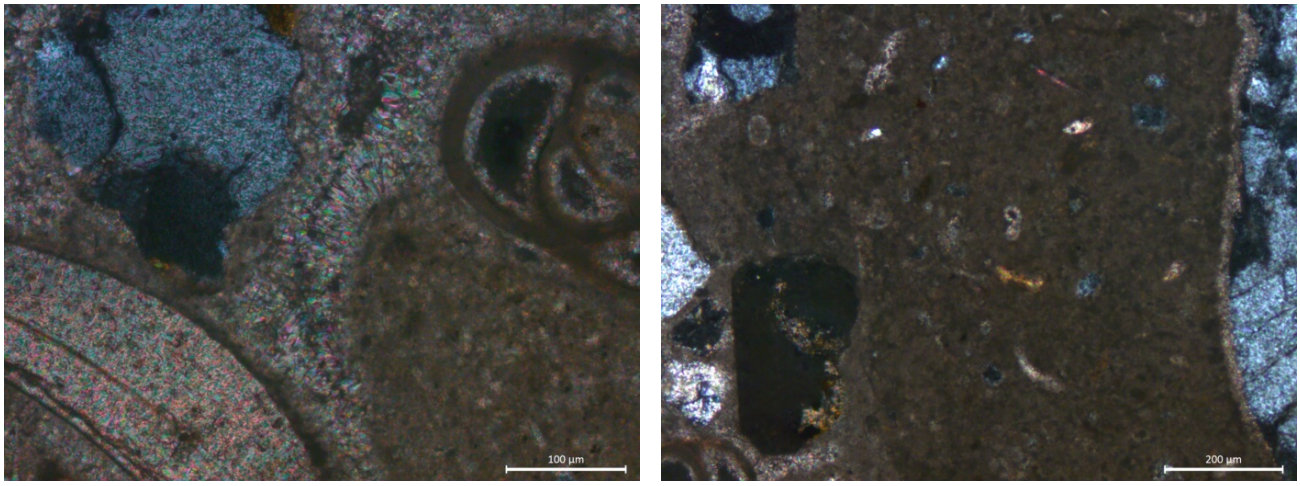

Martselo beachrock at -1.8 m depth (Northwestern Paros). Fringe of acicular cement of aragonite (?) and micritic cement with bioclasts

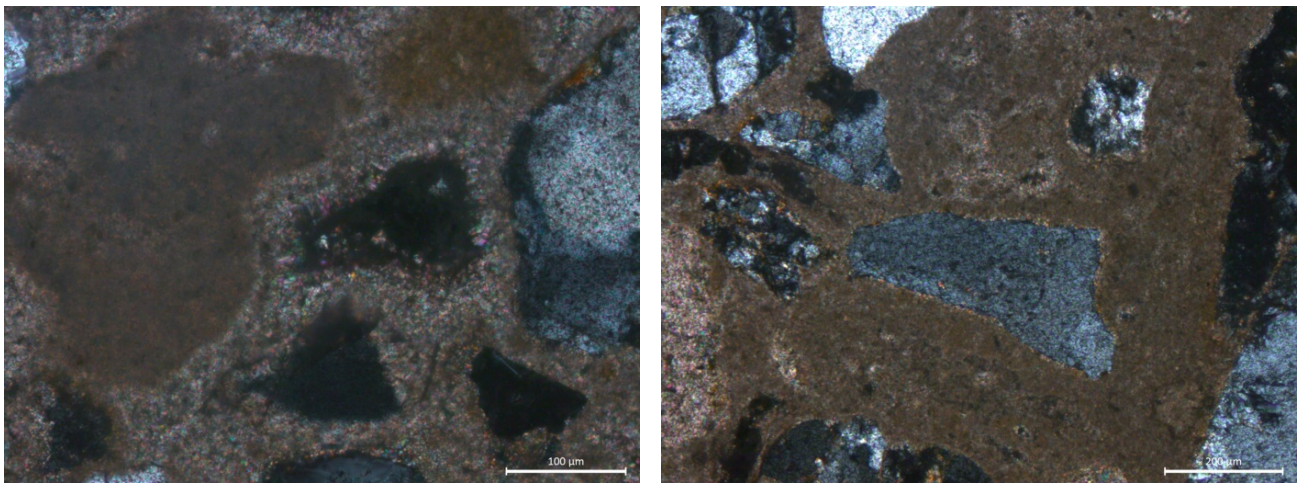

Tsoukalia beachrock at -3.6 m depth (Eastern Paros). A fine fringe of isopachous HCM is noted around grains, micritic filling cement along with micritization and recrystallization.

Appendix II: Scanned cores

Pounta scanned cores (POU2)

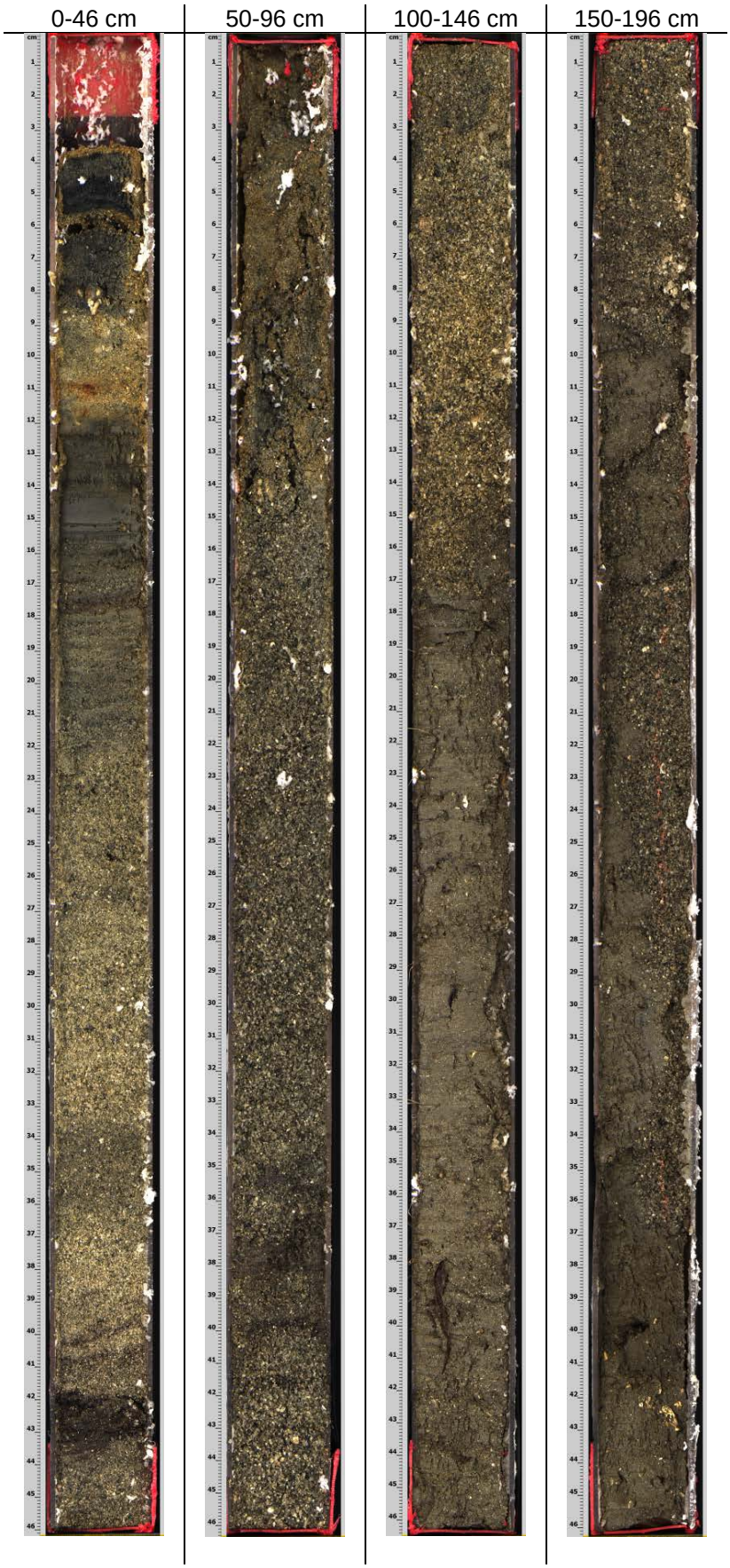


200-246 cm
250-296 cm
300-346 cm
350-396 cm

Livadia scanned cores (LIV1)

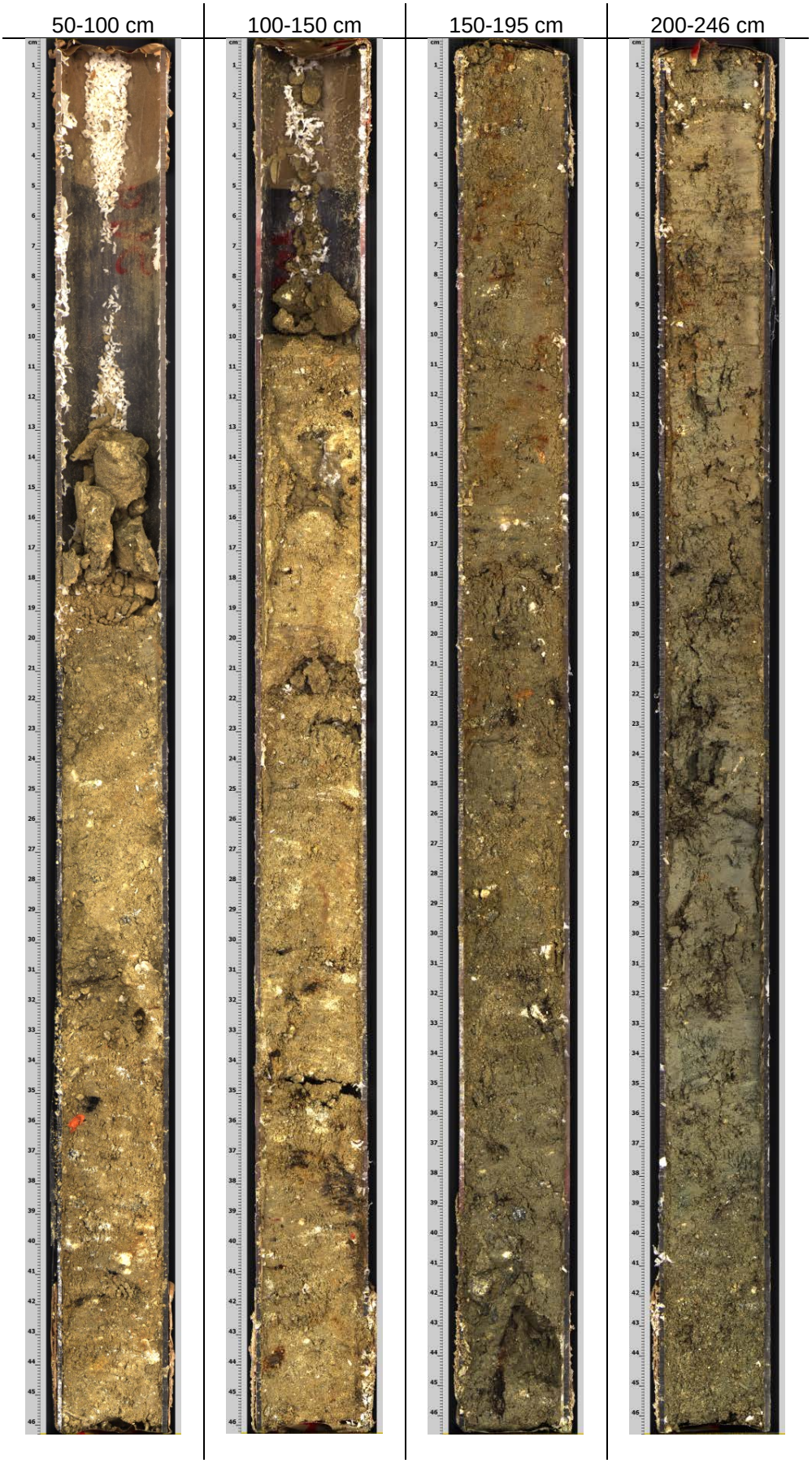

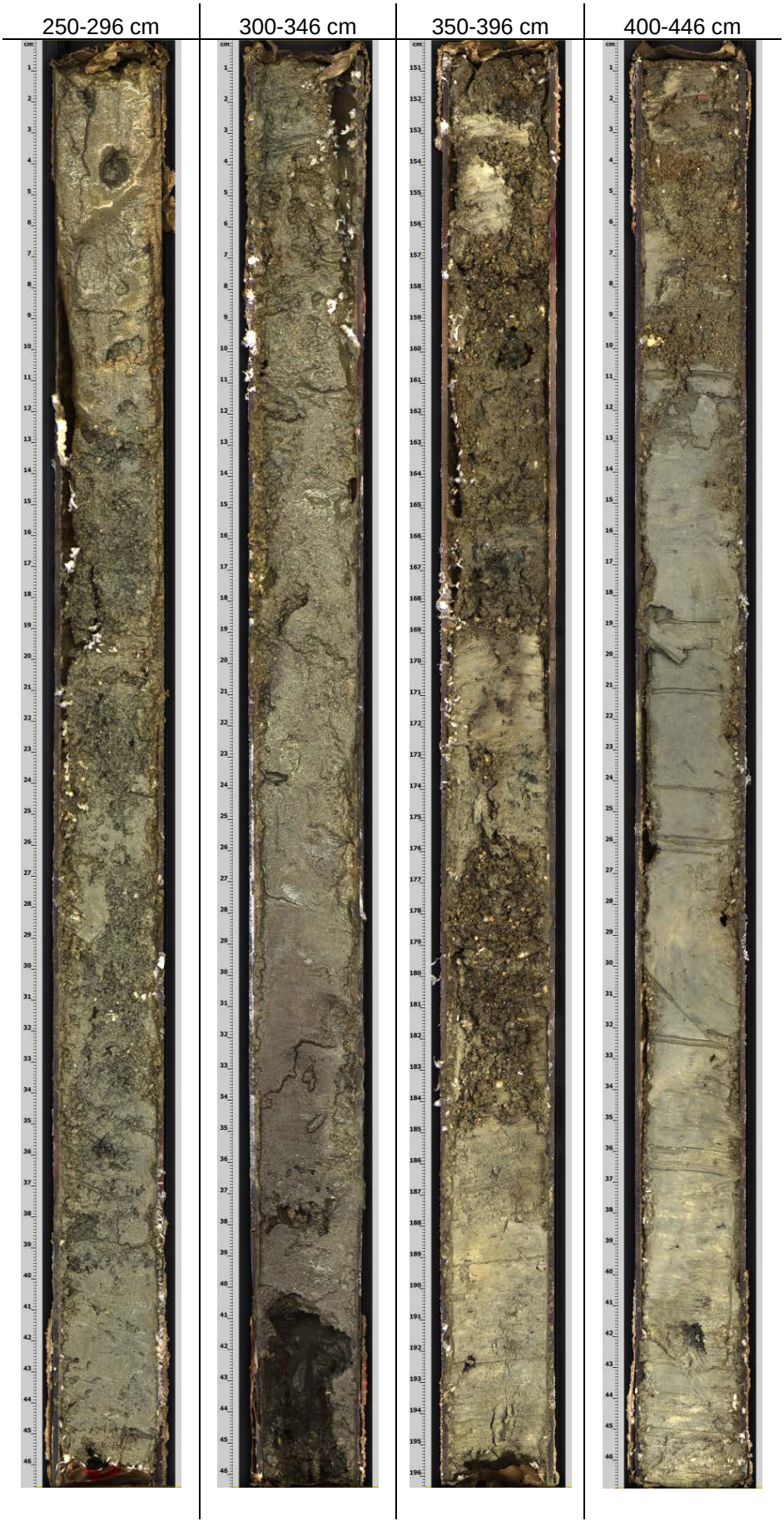
250-296 cm
300-346 cm
350-396 cm
400-446 cm

Kolymbithres cores scanned (KOL1)

237-287 cm	287-327 cm	324-374 cm	374-420 cm